IAEA Nuclear Energy Series

No. NR-T-3.32

Fatigue Assessment in Light Water Reactors for Long Term Operation: Good Practices and Lessons Learned

IAEA
International Atomic Energy Agency

IAEA NUCLEAR ENERGY SERIES PUBLICATIONS

STRUCTURE OF THE IAEA NUCLEAR ENERGY SERIES

Under the terms of Articles III.A.3 and VIII.C of its Statute, the IAEA is authorized to "foster the exchange of scientific and technical information on the peaceful uses of atomic energy". The publications in the **IAEA Nuclear Energy Series** present good practices and advances in technology, as well as practical examples and experience in the areas of nuclear reactors, the nuclear fuel cycle, radioactive waste management and decommissioning, and on general issues relevant to nuclear energy. The **IAEA Nuclear Energy Series** is structured into four levels:

(1) The **Nuclear Energy Basic Principles** publication describes the rationale and vision for the peaceful uses of nuclear energy.
(2) **Nuclear Energy Series Objectives** publications describe what needs to be considered and the specific goals to be achieved in the subject areas at different stages of implementation.
(3) **Nuclear Energy Series Guides and Methodologies** provide high level guidance or methods on how to achieve the objectives related to the various topics and areas involving the peaceful uses of nuclear energy.
(4) **Nuclear Energy Series Technical Reports** provide additional, more detailed information on activities relating to topics explored in the **IAEA Nuclear Energy Series**.

Each publication undergoes internal peer review and is made available to Member States for comment prior to publication.

The IAEA Nuclear Energy Series publications are coded as follows: **NG** – nuclear energy general; **NR** – nuclear reactors (formerly **NP–** nuclear power); **NF** – nuclear fuel cycle; **NW** – radioactive waste management and decommissioning. In addition, the publications are available in English on the IAEA web site:

www.iaea.org/publications

For further information, please contact the IAEA at Vienna International Centre, PO Box 100, 1400 Vienna, Austria.

All users of the IAEA Nuclear Energy Series publications are invited to inform the IAEA of their experience for the purpose of ensuring that they continue to meet user needs. Information may be provided via the IAEA web site, by post, or by email to Official.Mail@iaea.org.

FATIGUE ASSESSMENT IN LIGHT WATER REACTORS FOR LONG TERM OPERATION: GOOD PRACTICES AND LESSONS LEARNED

The following States are Members of the International Atomic Energy Agency:

AFGHANISTAN
ALBANIA
ALGERIA
ANGOLA
ANTIGUA AND BARBUDA
ARGENTINA
ARMENIA
AUSTRALIA
AUSTRIA
AZERBAIJAN
BAHAMAS
BAHRAIN
BANGLADESH
BARBADOS
BELARUS
BELGIUM
BELIZE
BENIN
BOLIVIA, PLURINATIONAL STATE OF
BOSNIA AND HERZEGOVINA
BOTSWANA
BRAZIL
BRUNEI DARUSSALAM
BULGARIA
BURKINA FASO
BURUNDI
CAMBODIA
CAMEROON
CANADA
CENTRAL AFRICAN REPUBLIC
CHAD
CHILE
CHINA
COLOMBIA
COMOROS
CONGO
COSTA RICA
CÔTE D'IVOIRE
CROATIA
CUBA
CYPRUS
CZECH REPUBLIC
DEMOCRATIC REPUBLIC OF THE CONGO
DENMARK
DJIBOUTI
DOMINICA
DOMINICAN REPUBLIC
ECUADOR
EGYPT
EL SALVADOR
ERITREA
ESTONIA
ESWATINI
ETHIOPIA
FIJI
FINLAND
FRANCE
GABON
GEORGIA
GERMANY
GHANA
GREECE
GRENADA
GUATEMALA
GUYANA
HAITI
HOLY SEE
HONDURAS
HUNGARY
ICELAND
INDIA
INDONESIA
IRAN, ISLAMIC REPUBLIC OF
IRAQ
IRELAND
ISRAEL
ITALY
JAMAICA
JAPAN
JORDAN
KAZAKHSTAN
KENYA
KOREA, REPUBLIC OF
KUWAIT
KYRGYZSTAN
LAO PEOPLE'S DEMOCRATIC REPUBLIC
LATVIA
LEBANON
LESOTHO
LIBERIA
LIBYA
LIECHTENSTEIN
LITHUANIA
LUXEMBOURG
MADAGASCAR
MALAWI
MALAYSIA
MALI
MALTA
MARSHALL ISLANDS
MAURITANIA
MAURITIUS
MEXICO
MONACO
MONGOLIA
MONTENEGRO
MOROCCO
MOZAMBIQUE
MYANMAR
NAMIBIA
NEPAL
NETHERLANDS
NEW ZEALAND
NICARAGUA
NIGER
NIGERIA
NORTH MACEDONIA
NORWAY
OMAN
PAKISTAN
PALAU
PANAMA
PAPUA NEW GUINEA
PARAGUAY
PERU
PHILIPPINES
POLAND
PORTUGAL
QATAR
REPUBLIC OF MOLDOVA
ROMANIA
RUSSIAN FEDERATION
RWANDA
SAINT KITTS AND NEVIS
SAINT LUCIA
SAINT VINCENT AND THE GRENADINES
SAMOA
SAN MARINO
SAUDI ARABIA
SENEGAL
SERBIA
SEYCHELLES
SIERRA LEONE
SINGAPORE
SLOVAKIA
SLOVENIA
SOUTH AFRICA
SPAIN
SRI LANKA
SUDAN
SWEDEN
SWITZERLAND
SYRIAN ARAB REPUBLIC
TAJIKISTAN
THAILAND
TOGO
TONGA
TRINIDAD AND TOBAGO
TUNISIA
TÜRKİYE
TURKMENISTAN
UGANDA
UKRAINE
UNITED ARAB EMIRATES
UNITED KINGDOM OF GREAT BRITAIN AND NORTHERN IRELAND
UNITED REPUBLIC OF TANZANIA
UNITED STATES OF AMERICA
URUGUAY
UZBEKISTAN
VANUATU
VENEZUELA, BOLIVARIAN REPUBLIC OF
VIET NAM
YEMEN
ZAMBIA
ZIMBABWE

The Agency's Statute was approved on 23 October 1956 by the Conference on the Statute of the IAEA held at United Nations Headquarters, New York; it entered into force on 29 July 1957. The Headquarters of the Agency are situated in Vienna. Its principal objective is "to accelerate and enlarge the contribution of atomic energy to peace, health and prosperity throughout the world''.

IAEA NUCLEAR ENERGY SERIES No. NR-T-3.32

FATIGUE ASSESSMENT IN LIGHT WATER REACTORS FOR LONG TERM OPERATION: GOOD PRACTICES AND LESSONS LEARNED

INTERNATIONAL ATOMIC ENERGY AGENCY
VIENNA, 2023

COPYRIGHT NOTICE

Marketing and Sales Unit, Publishing Section
International Atomic Energy Agency
Vienna International Centre
PO Box 100
1400 Vienna, Austria
fax: +43 1 26007 22529
tel.: +43 1 2600 22417
email: sales.publications@iaea.org
www.iaea.org/publications

Printed by the IAEA in Austria
April 2023
STI/PUB/2017

IAEA Library Cataloguing in Publication Data

Names: International Atomic Energy Agency.
Title: Fatigue assessment in light water reactors for long term operation : good practices and lessons learned / International Atomic Energy Agency.
Description: Vienna : International Atomic Energy Agency, 2023. | Series: IAEA nuclear energy series, ISSN 1995–7807 ; no. NR-T-3.32 | Includes bibliographical references.
Identifiers: IAEAL 22-01523 | ISBN 978–92–0–128222–4 (paperback : alk. paper) | ISBN 978–92–0–128322–1 (pdf) | ISBN 978–92–0–128422–8 (epub)
Subjects: LCSH: Light water reactors. | Nuclear power plants | Fatigue | Evaluation. | Nuclear reactors. | Light water reactors | Safety measures.
Classification: UDC 621.039.524.44 | STI/PUB/2017

FOREWORD

The IAEA's statutory role is to "seek to accelerate and enlarge the contribution of atomic energy to peace, health and prosperity throughout the world". Among other functions, the IAEA is authorized to "foster the exchange of scientific and technical information on peaceful uses of atomic energy". One way this is achieved is through a range of technical publications including the IAEA Nuclear Energy Series.

The IAEA Nuclear Energy Series comprises publications designed to further the use of nuclear technologies in support of sustainable development, to advance nuclear science and technology, catalyse innovation and build capacity to support the existing and expanded use of nuclear power and nuclear science applications. The publications include information covering all policy, technological and management aspects of the definition and implementation of activities involving the peaceful use of nuclear technology. While the guidance provided in IAEA Nuclear Energy Series publications does not constitute Member States' consensus, it has undergone internal peer review and been made available to Member States for comment prior to publication.

The IAEA safety standards establish fundamental principles, requirements and recommendations to ensure nuclear safety and serve as a global reference for protecting people and the environment from harmful effects of ionizing radiation.

When IAEA Nuclear Energy Series publications address safety, it is ensured that the IAEA safety standards are referred to as the current boundary conditions for the application of nuclear technology.

Fatigue is one of the major elements in time limited ageing analysis for the long term operation of nuclear power plants. The characteristic of fatigue strength of material is represented by the relationship between stress or strain amplitude and the number of cycles to failure of the material. Structural deterioration can occur as a result of repeated stress/strain cycles caused by fluctuating loads or temperatures. Fatigue failure does not depend on the time to failure, but on the number of cyclic loadings. To prevent fatigue failure, it is essential to keep the stress in the component below the fatigue limit or target the stress amplitude corresponding to the expected number of loading cycles.

In the design and operating phases of nuclear power plants, it is essential to consider the concurrent loadings associated with the design transients, thermal stratification, seismically induced stress cycles and all relevant loads due to the various operational modes to ensure structural integrity against fatigue damage according to structural design codes and standards.

Many experiments have been carried out on this phenomenon, as a result there is now a great deal of experimental data which clearly demonstrate the reduction of fatigue lives in high temperature water environments of light water reactors compared with fatigue lives in the normal air atmosphere at the same stress/strain range and temperature. All the materials that constitute the pressure boundary, including austenitic and ferritic steels, were found to be susceptible to some extent to this environmental effect.

This publication documents the revalidation of safety analyses for the long term operation of nuclear power plants to demonstrate structural integrity against thermal and mechanical fatigue and to assess the structure and components from the point of view of fatigue damage. The methodology of fatigue assessment for nuclear power plant components is summarized and the differences of the fatigue design requirements between different national structural design codes and standards are discussed.

The IAEA is grateful for the valuable contributions from Member State experts in preparing this publication. In addition, the IAEA wishes to express its gratitude to the experts who supported the drafting and review of the publication, in particular those who contributed to the specific technical data on fatigue assessment. The IAEA officers responsible for this publication were Ki Sig Kang and H.T. Varjonen of the Division of Nuclear Power.

EDITORIAL NOTE

This publication has been edited by the editorial staff of the IAEA to the extent considered necessary for the reader's assistance. It does not address questions of responsibility, legal or otherwise, for acts or omissions on the part of any person.

Guidance and recommendations provided here in relation to identified good practices represent experts' opinions but are not made on the basis of a consensus of all Member States.

Although great care has been taken to maintain the accuracy of information contained in this publication, neither the IAEA nor its Member States assume any responsibility for consequences which may arise from its use.

The use of particular designations of countries or territories does not imply any judgement by the publisher, the IAEA, as to the legal status of such countries or territories, of their authorities and institutions or of the delimitation of their boundaries.

The mention of names of specific companies or products (whether or not indicated as registered) does not imply any intention to infringe proprietary rights, nor should it be construed as an endorsement or recommendation on the part of the IAEA.

The IAEA has no responsibility for the persistence or accuracy of URLs for external or third party Internet web sites referred to in this publication and does not guarantee that any content on such web sites is, or will remain, accurate or appropriate.

CONTENTS

1. INTRODUCTION

1.1. BACKGROUND

The IAEA Nuclear Energy Series includes a large number of engineering publications dealing with ageing management as well as with degradation mechanisms, failure prevention and mitigation programmes. These publications contain elements of materials science and techniques as applied to ageing systems, structures and components (SSCs).

Fatigue is one major element in time limited ageing analysis for long term operation of nuclear power plants (NPPs). Fatigue is the structural deterioration that can occur as a result of repeated stress/strain cycles caused by fluctuating loads or temperatures. After repeated cyclic loading, crack initiation can occur at the most highly affected locations if sufficient localized microstructural damage has accumulated. It is important to understand how cracks occur and grow as a result of fatigue, and then assess fatigue failure bearing in mind the following potential causes:

— Design configuration: This type of failure occurs when the design of a component or system has not been adequately evaluated for steady state vibration.
— Manufacture: This type of failure occurs when the manufacturing of the component or system has a defect (e.g. a weld defect).
— System/plant operation: This type of failure occurs when a component or system is operated in a manner such that a fatigue failure occurs. System operation includes, for example, low flow conditions that may cause cavitation or mixing of fluids exhibiting a significant temperature difference.
— Maintenance: This type of failure occurs when a system or component fails after refurbishment or testing.

Fatigue crack initiation and growth resistance are governed by a number of materials, structural and environmental factors, such as stress range, temperature, fluid oxygen content, mean stress, loading frequency (strain rate), surface roughness and number of cycles. Cracks typically begin at local geometrical stress concentrations, such as welds, notches, other surface defects and structural discontinuities. The presence of an oxidizing environment or other deleterious chemical processes can accelerate the fatigue crack initiation and propagation process. The relevant fatigue related degradation mechanisms include the following:

— Low cycle fatigue: The stress cycling that contributes to low cycle fatigue is generally due to the combined effects of pressure, attached component loadings (e.g. piping moments) and local thermal stresses that result during normal operation.
— High cycle fatigue: The most classical fatigue related degradation mechanism is high cycle fatigue. This involves a large number of stress cycles at relatively low stress amplitude. High cycle fatigue may come from the following types of cause:
    • Thermal, due to cyclic stresses that result in changing temperature conditions in a component or in the piping attached to the component;
    • Mechanical, due to vibration, pressure pulsation, flow induced vibration (FIV) or combinations of thermal and high cycle mechanical loads such as might occur on pump shafts in the thermal barrier region;
    • Thermally induced, due to the mixing of cold and hot fluids where local instabilities of mixing lead to low amplitude thermal stresses at the component surface exposed to the fluid.
— Environmental effects: Environmentally enhanced fatigue concerns the reduction in fatigue life in the reactor water environment as compared with that in a room temperature air environment.

Fatigue damage for existing components is mitigated by reducing the magnitude of the applied loads or thermal conditions, or by reducing the number of loading cycles.

1.2. OBJECTIVE

An objective of this publication is to provide guidelines on how to manage fatigue based on recent insights and experiences, with a focus on providing industry assessment methods for fatigue failures as well as the latest information on the root causes of plant fatigue failures. Another objective is to summarize the related work on identifying where fatigue failures may occur in the future to determine the need for additional research. Guidance and recommendations provided here in relation to identified good practices represent experts' opinions but are not made on the basis of a consensus of all Member States.

1.3. SCOPE

This publication provides practical guidelines on how to identify and manage fatigue issues in NPPs. It explains the mechanism of fatigue, identifies which elements are the major contributors and describes how fatigue can be minimized in the design phase for new NPPs. This publication is intended to be used by:

— Bodies responsible for designing SSCs;
— Construction vendors and suppliers;
— Regulatory authorities and support organizations;
— Present and future owners/operators;
— Technical service organizations.

1.4. STRUCTURE

Fatigue lives are influenced by a number of factors and thus their effects need to be taken into account in evaluating the structural integrity of the susceptible components. The complex mechanisms of the major contributors to fatigue are described in Section 2, as are the influence factors to help understand these complex phenomena.

Section 3 provides the methodology of fatigue assessment for new NPP design. With reference to the design and construction of NPP components for pressure retaining components and piping, the international and national codes are reviewed and discussed in terms of the differences between codes in the fatigue design requirements. The description is based mainly on American Society of Mechanical Engineers (ASME) Boiler and Pressure Vessel Code (BPVC) Section III, Subsection NB, though other codes are also cited.

In Section 4, the approaches for fatigue assessment in operating NPPs are described using operating experience. An overview of the current national situation, fatigue damage mechanisms and country experience with fatigue assessment in operating NPPs is given, followed by a summary of experience with fatigue failure and root causes.

In Section 5, environmentally assisted fatigue is explained. It is now common to take environmental effects into account in evaluating structural integrity against fatigue mechanisms. In this section, the methods for estimating environmental effects, application to arbitrary loading conditions, code development, regulatory status and environmental effects on fatigue crack growth are discussed based on a variety of experimental results.

In Section 6, the principles of fatigue monitoring are explained and the commercial fatigue monitoring systems on the market are described. Plant cycle counting and fatigue monitoring in NPPs are extremely useful for tracking design life as well as minimizing damage to important components, thereby

increasing safety. Fatigue monitoring strategies and technologies, monitoring locations and general steps for implementation are introduced.

Appendix I addresses the sample fatigue evaluation of vessel and piping based on design experience at NPPs of Member States. Fatigue evaluations of the reactor pressure vessel are conducted for the direct vessel injection nozzle of the reactor pressure vessel. Appendix II lists activities that have been supporting research on the management of fatigue assessment. Appendix III introduces survey results on fatigue monitoring and assessment in operating NPPs.

2. MECHANISMS AND MAJOR CONTRIBUTIONS TO FATIGUE

2.1. BASIC MECHANISM OF FATIGUE

2.1.1. Stress/strain versus life diagram

Various cyclic loadings are applied to components and equipment in NPPs. Figure 1 shows typical cyclic loadings with the same tensile and compressive stress (or strain). Such loadings, even if the maximum stress is smaller than the yield stress of the materials, can lead to the failure of the metallic component. This phenomenon is called fatigue.

The most fundamental characteristic of the fatigue of material is the S–N curve. This is the relationship between stress or strain amplitude and the number of cycles to failure (life) of the material. The basis of the stress-life method is the S–N diagram, shown schematically for two materials in Fig. 2. The S–N diagram plots nominal stress amplitude *S* versus cycles to failure *N*. There are numerous testing procedures to generate the required data for a proper S-N diagram. S-N test data are usually displayed on a log-log plot, with the actual S-N line representing the mean of the data from several tests.

In general, a fatigue test is conducted using small size specimens instead of actual components in NPPs because of size and handling issues. The basic concept of the S–N curve, however, is the same for small size test specimens and actual components. The curve is usually obtained by constant cyclic loading fatigue tests performed at room temperature, in air. Fatigue failure depends not on the time to the failure but the number of cyclic loadings, excluding time dependent fatigue phenomena such as corrosion or environmental fatigue and high temperature fatigue.

As can be seen from Fig. 2, the allowable number of cycles decreases as the stress amplitude increases. Though the shape of the S–N curve depends on the material, the S–N curve for carbon steel typically has a distinct ‘knee point’ around 10^6 to 10^7 cycles, and the S–N curve approaches to the horizontal line asymptotically in the range of cycle numbers higher than 10^7. The stress amplitude at the knee point is called the fatigue limit or endurance limit; components can withstand fatigue failure for indefinitely continuing cyclic loadings if the stress level is below the fatigue limit. On the other hand,

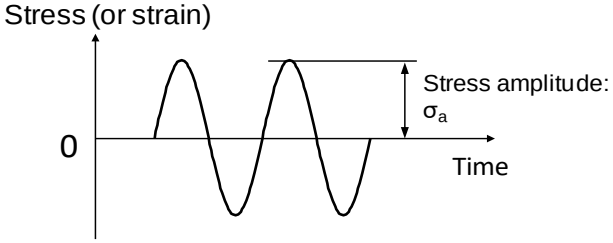

FIG. 1. Typical cyclic loading.

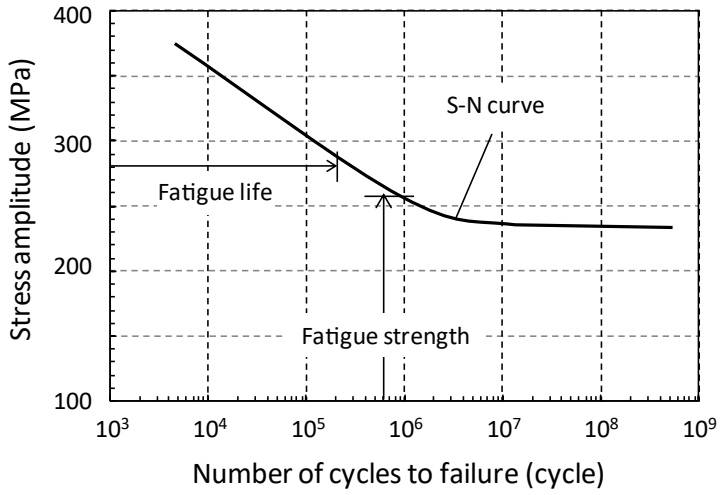

FIG. 2. Schematic example of the S–N curve.

the S–N curve of many materials does not show a distinct knee point, so a stress amplitude at around 10^7 to10^8 cycles is assumed to be a target of fatigue design for the components of those materials. Obviously, the allowable stress amplitude of the component depends on the material and expected number of cycles during operation.

To prevent fatigue failure, it is essential to maintain the stress in the component lower than the fatigue limit or target stress amplitude corresponding to the expected number of loading cycles.

2.1.2. Initiation of fatigue crack and crack propagation

The basic process of fatigue failure is illustrated in Fig. 3. The process can be divided into two different mechanisms:

— Crack initiation;
— Crack propagation.

Fatigue crack initiation can be defined both from a physical and a technical perspective, as shown in Fig. 4.

Cyclic loading on material causes slip bands on the surface as a result of shear stress. These slip bands grow with cycles, and a microscopic convex–concave pattern is formed on the surface of the material as a result of the intrusion and extrusion of the slip bands. Then, crack initiation takes place at the bottom of the concave of the surface.

Once a crack is initiated, it propagates towards the inside of the material along the plane inclined by about 45 degrees against the surface, after which it turns to the direction perpendicular to the maximum tensile stress. The crack then grows at an accelerated rate, and finally the structure fails in the ductile mode when the ligaments of the structure become unable to withstand the maximum load.

Figure 5 shows a typical S–N curve and fatigue crack initiation life. In the low cycle region of the S–N curve, crack initiation occurs in an early phase in the total life, and the fatigue life of the material is governed almost entirely by crack propagation. On the other hand, in the high cycle region of the curve, the crack initiation life almost coincides with the total failure life, and it can be understood that crack initiation dominates the fatigue life in high cycle regions.

The technical definition of crack initiation is difficult to formulate. Nevertheless, it is commonly recognized that the fatigue curves developed based on small specimen test data correspond to the formation of an engineering size crack of around 3 mm when using a 25% maximum load drop criterion

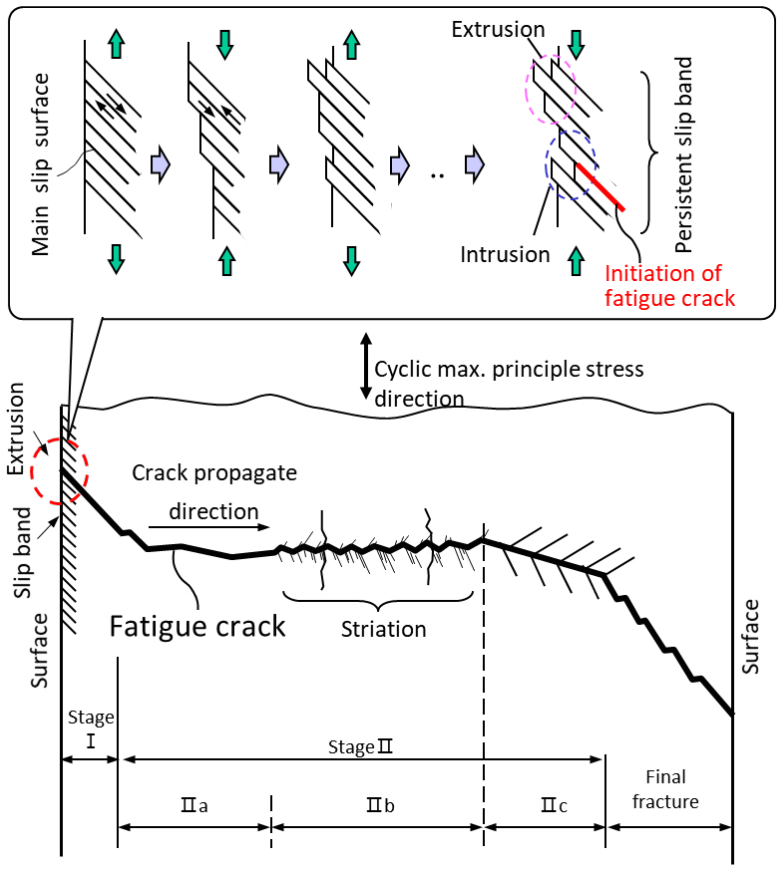

FIG. 3. Fatigue crack initiation and propagation [1].

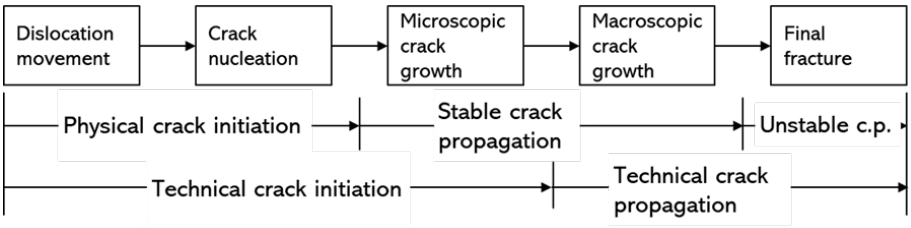

FIG. 4. Block diagram of fatigue crack initiation and propagation [1]. c.p — crack propagation.

to define life. This means that the formation of an approximately 3 mm crack is defined as crack initiation in a component when the fatigue curves are used for predicting the crack initiation life. Therefore, fatigue analysis is carried out to confirm a fatigue cumulative usage factor (CUF) < 1 with the fatigue curve first, and then, if the CUF > 1, the fracture mechanics approach presented in the following section is used to assess the tolerance of the components against fatigue failure. Note that the CUF is the ratio of cumulative fatigue damage of the materials against the target fatigue curve.

2.2. CATEGORIES OF FATIGUE

2.2.1. High cycle fatigue

High cycle fatigue (HCF) [2] is due to low amplitude, linear, elastic, cyclic material behaviour or elastic stress, and numbers of cycles in over the millions. HCF concerns in NPPs are generally associated

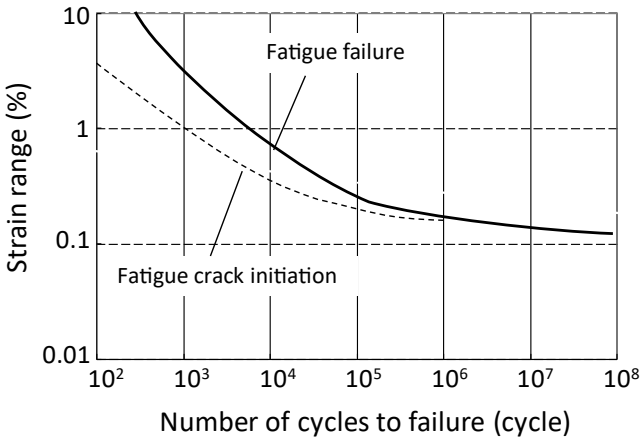

FIG. 5. Typical S–N and fatigue crack initiate life curve.

with high speed rotating or reciprocating components or with vibration. In addition, local thermal cycling due to hot and cold fluid mixing is also of concern. A large number of the fatigue failures occurring in NPPs is attributable to HCF. The very high cycle range in the S–N curve shown in Fig. 2 indicates that the fatigue strength of the material asymptotically approaches a horizontal line. This is generally taken to be the material fatigue limit.

Since cycles change rapidly, the fatigue design for high cycle equipment such as pumps or turbines generally seeks to keep all cyclic stresses or strains below the fatigue limit. Conversely, if stresses are above the fatigue limit, fatigue lives will be reduced because of the high frequency of the loading.

Very high cycle fatigue (VHCF), which occurs after more than 10^9 cycles and amplitudes lower than the endurance limit, is a special category of HCF. Crack initiation in VHCF takes place usually as a result of defects inside the volume, not on the surface; this fracture surface is called ‘fish-eye’. Usually, VHCF can be observed in very high strength materials [3].

2.2.2. Low cycle fatigue

Low cycle fatigue (LCF) is generally associated with many instances of cyclic plastic deformation and is characterized in terms of the cyclic strain range rather than the stress amplitude.

The total strain range $\Delta\varepsilon_t$ under tension and compression strain-controlled fatigue tests can be described by the sum of the elastic strain range $\Delta\varepsilon_e$ and the plastic strain range $\Delta\varepsilon_p$ in Eq (1).

$$\Delta\varepsilon_t = \Delta\varepsilon_e + \Delta\varepsilon_p \quad (1)$$

where

$\Delta\varepsilon_t$ is the total strain range;

$\Delta\varepsilon_e$ is the elastic strain range;

and $\Delta\varepsilon_p$ is the plastic strain range.

Figure 6 shows the S–N curves for elastic, plastic and total strain range. The elastic strain range $\Delta\varepsilon_e$ is known to have a linear relationship with the number of load reversals to failure $2N_f$ on a double logarithmic chart in Eq. (2).

$$\Delta\varepsilon_e = C_e (2N_f)^{-a} \quad (2)$$

where

N_f is the number of cycles to failure;

and C_e and a are constants.

This relationship is called Basquin's law of fatigue. A similar relationship between the plastic range $\Delta\varepsilon_p$ and fatigue life N_f is known as Coffin's law and is expressed in Eq. (3).

$$\Delta\varepsilon_p = C_p (2N_f)^{-b} \tag{3}$$

where C_p and b are constants.

The relationship between the total strain range and fatigue life can be obtained by substituting Eqs (2) and (3) by with Eq. (1). This relationship is known as Coffin–Manson's law and is expressed in Eq. (4) [4, 5].

$$\Delta\varepsilon_t = C_e (2N_f)^{-a} + C_p (2N_f)^{b} \tag{4}$$

The S–N curve for the total strain range asymptotically approaches the plastic strain range curve in the low cycle region. The S–N curve for the total strain range asymptotically approaches the elastic strain range curve in the high cycle region. These results suggest that the LCF of materials is governed by the plastic strain range, and HCF is governed by the elastic strain range.

The other type of S–N curve was also proposed by Langer [6], who assumed that the plastic portion of the S–N curve has a negative slope of −1/2, and is expressed in Eq (5).

$$\Delta\varepsilon_p = \frac{C}{\sqrt{N_f}} \tag{5}$$

where C is a constant.

When a tensile test is regarded as a quarter of a cycle (N_f = 1/4), the cyclic plastic strain of Eq. (5) can be related to the true failure strain calculated from the reduction of area (*RA*) as $\Delta\varepsilon_p = \ln\{100 / (100 - RA)\}$, and Eq. (5) can be converted into Eq. (6).

$$\Delta\varepsilon_p = \frac{C}{2\sqrt{N_f}} \ln\frac{100}{100 - RA} \tag{6}$$

Noting that the alternating component (amplitude) of plastic strain is half of Eq. (6), and assuming that the elastic strain amplitude can be obtained by dividing the fatigue limit S_e by Young's modulus, then the total alternating stress amplitude S_a defined by total strain amplitude times Young's modulus is given in Eq. (7).

$$S_a = \frac{E}{4\sqrt{N}} \ln\frac{100}{100 - RA} + S_e \tag{7}$$

This equation is called the Langer curve [6] and is widely used in the nuclear industry through international codes and standards.

Usually, the designer does not perform elastic–plastic analysis to estimate the strain at the locations of concern. A half of the cyclic strain ranges is simply multiplied by the elastic modulus to obtain a large hypothetical elastic stress amplitude versus the cycle to failure curve, and the stress obtained from elastic analysis is compared with this hypothetical S–N curve. The LCF design also commonly uses the

concept of linear cumulative damage, Miner's law[1], to estimate fatigue damage associated with cycling at different amplitudes.

Generally, the local strain used for the fatigue evaluation should be estimated by elastic–plastic analysis, instead of purely elastic analysis, when the range of stress intensity exceeds a limit such as design yield stress and plastic strain is generated. However, the elastic–plastic strain can be conservatively predicted from elastic analysis in a simplified way under certain conditions, and such a simplified approach is very convenient for designers. Therefore, several international codes and standards [7–10] prescribe the simplified elastic–plastic analysis methods to evaluate elastic–plastic strain (or corresponding stress) by multiplying the strain enhancement factor K_e. For example, the alternating stress amplitude S_a can be estimated from the stress amplitude calculated by elastic analysis, S_e and K_e and is expressed in Eq. (8).

$$S_a = K_e S_e \tag{8}$$

where

S_a is the alternating stress amplitude;

S_e is the estimated stress amplitude;

and K_e is characterized by the role of converting elastic strain (ε_e) to elastic–plastic strain (ε_{ep}). K_e is expressed in Eq. (9).

$$K_e = \frac{\varepsilon_{ep}}{\varepsilon_e} \tag{9}$$

Details of the K_e factor are specified in each code and standard and an example is presented in Section 3.1.2.5.

One important point in evaluating fatigue damage for the component is to decide what kind of equivalent stress or strain is adopted under multiaxial stress status. Several types of equivalent stress or strain, such as maximum shear stress, for example, the Tresca criterion[2], von Mises stress[3] or effective strain, can be used to determine the peak stress range responsible for fatigue damage of the component. The codes and standards for nuclear components or pressure vessel design stipulate possible options for equivalent stress and strain.

The difference for other aspects of stress multiaxiality does not affect the fatigue life as much, but the fatigue life under complex non-proportional (out of phase) cyclic loading which leads to the rotation of the principal direction of stress can be much shorter than the under the uniaxial cyclic loading condition even if the same equivalent strain range is applied [11]. Further information can be found in Refs [12–14].

---

[1] In 1945, M.A. Miner popularized a rule that had first been proposed by A. Palmgren in 1924. The rule is variously called Miner's rule or the Palmgren–Miner linear damage hypothesis.

[2] The Tresca criterion is equivalent to saying that yielding will occur at a critical value of the maximum shear stress, consistent with micromechanical behaviour of crystals, involving slip and dislocation motion.

[3] The von Mises stress is often used in determining whether an isotropic and ductile metal will yield when subjected to a complex loading condition.

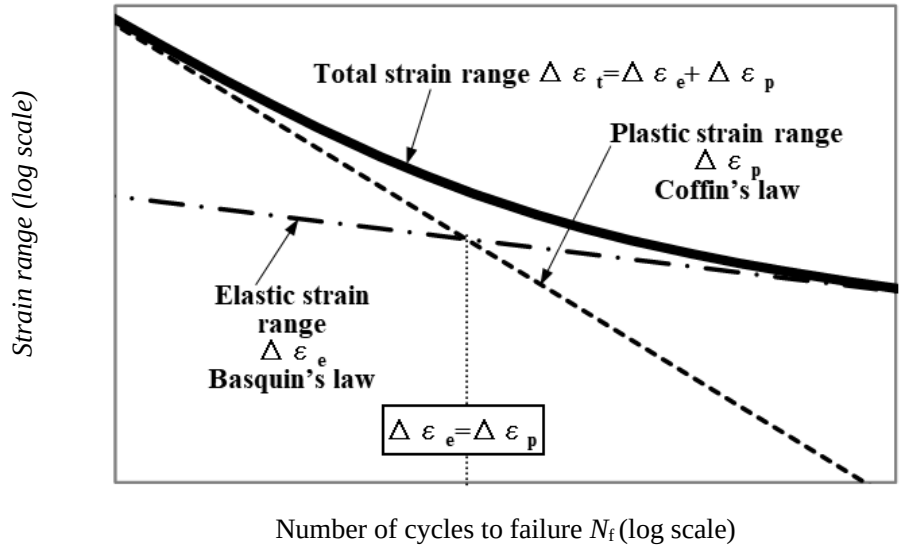

FIG. 6. S–N curves for elastic, plastic total strain range [6].

2.3. INFLUENTIAL FACTOR

2.3.1. Mean stress

While cyclic loading with the same tensile and compressive stress amplitude are applied to the specimen in ordinary fatigue tests, some sustained stress is often superimposed on cyclic loadings in the actual engineering application. For example, in the piping system, internal pressure with pulsation is regarded as the combination of stresses of constant internal pressure and its fluctuations. These sustained stresses are called mean stress in the fatigue analysis. The concept of mean stress is illustrated in Fig. 7. It is a well-known influence factor to reduce the fatigue strength of materials. The effect of mean stress on fatigue life is usually expressed by a fatigue limit diagram, as shown in Fig. 8. Several equations to estimate the relationship between the mean stress and the fatigue limit are proposed, and a modified Goodman diagram expressed by Eq. (10) is shown in Fig. 8.

$$\sigma_{wa} = \sigma_{w0}\left(1 - \frac{\sigma_m}{\sigma_B}\right) \tag{10}$$

Where

σ_B is the tensile strength of the material;

σ_m is the mean stress;

σ_{w0} is the fatigue limit under fully reversed loading;

and σ_{wa} is the fatigue limit under the mean stress, σ_m.

This equation demonstrates that the fatigue limit under the mean stress decreases linearly with increasing mean stress σ_m. Consequently, the stress amplitude of components subjected to mean stress should be maintained below σ_{wa} instead of σ_{w0} if using the fatigue limit design.

The basic design concept of NPP components is that the mechanical behaviour of the component under static loading should be restricted within the elastic range. Therefore, the design target is the area of ADFC in Fig. 8, because stress in this area does not cause the fatigue failure and the yield of the materials.

Usually, mean stress effects are an issue only for high cycle regions in which the alternating stress amplitude is less than the yield stress of the material. The well-known mean stress correction models, including the Sorderberg, Gerber and Morrow models and the Smith–Watson–Topper (SWT) correction model, are described as follows:

— Sorderberg $\sigma_{wa} = \sigma_{w0}\left(1-\sigma_m / \sigma_Y\right)$;
— Gerber $\sigma_{wa} = \sigma_{w0}\left(1-\sigma_m / \sigma_B\right)^2$;
— Morrow $\sigma_{wa} = \sigma_{w0}\left(1-\sigma_m / \sigma_T\right)$;
— Smith-Watson-Topper $\sigma_{w0} = \sqrt{\sigma_{max}\sigma_{wa}}$ or $\sigma_{wa} = \sigma_{w0}^2 / \sigma_{max}$.

where σ_Y is the yield stress and σ_T is the true fracture strength.

The Sorderberg model is very conservative and most actual fatigue data for metals tend to fall between the modified Goodman and the Gerber models. The Morrow model assumes that the mean stress has a significant effect on fatigue life. The Smith–Watson–Topper model predicts the mean stress effect in high cycle regions accurately but gives conservative results in the low cycle regime.

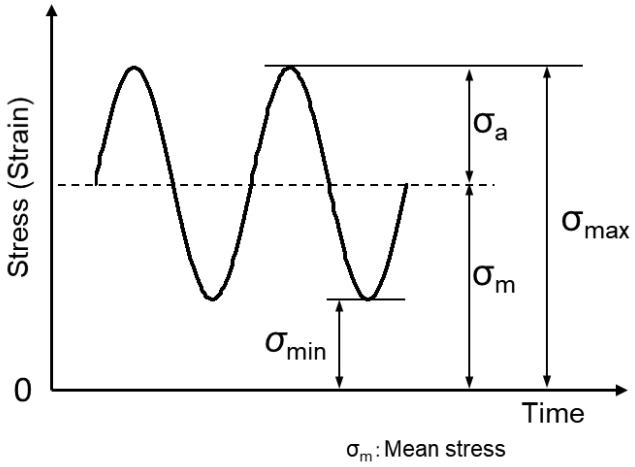

FIG. 7. Illustration of mean stress.

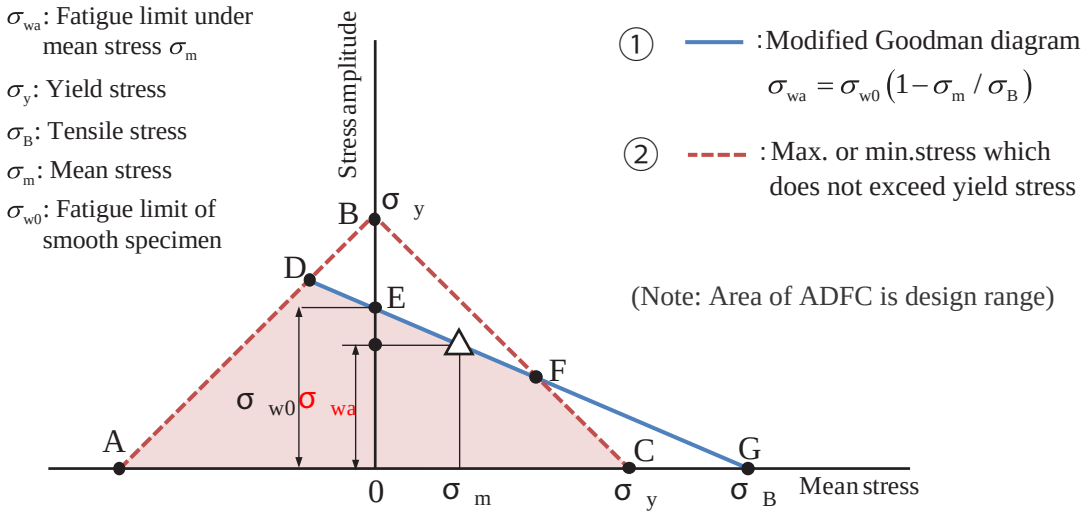

FIG. 8. Fatigue limit diagram.

2.3.2. Stress concentration effects

Many components have various locations with geometrical discontinuities. A study of NPPs has shown that many fatigue failures are initiated at such locations of components. In terms of stress concentration, weld regions are also the subject of concern in pressure vessels and piping. The typical stress distribution around a notch is shown in Fig. 9, where the ratio between the maximum stress, σ_{max}, at the notched root and the nominal stress, σ_0, is expressed in Eq. (11).

$$\alpha = \frac{\sigma_{max}}{\sigma_0} \tag{11}$$

where α is the stress concentration factor.

Figure 9 indicates that the stress at a discontinuity region is much higher than the nominal stress, and the theoretical elastic stress concentration factor for a semi-circle notch is α = 3 when b a in Fig. 9. In this case, the stress on the material surface at the notch root is three times bigger than the nominal stress, and this stress concentration decreases the fatigue strength of materials. It is important, therefore, to recognize the effects of stress concentration on the fatigue strength of materials.

The fatigue strength reduction factor β is defined by the ratio of the fatigue limit of notched and smooth specimens, and is expressed in Eq. (12).

$$\beta = \frac{\sigma_{w0}}{\sigma_{wn}} \tag{12}$$

where σ_{wn} and σ_{w0} are the fatigue limit for smooth specimens and for the notched specimen, respectively.

Experimental data for the effect of stress concentration on the fatigue strength of several strength of materials are shown in Fig. 10 using β and α [15]. The increase of stress concentration decreases the fatigue strength of the materials. The predicted reduction of fatigue strength using the stress concentration factor α is conservative because β is always less than α due to the stress gradients at the notch root. Also, the difference between β and α increases with decreasing notch root radius and decreasing tensile strength of the material.

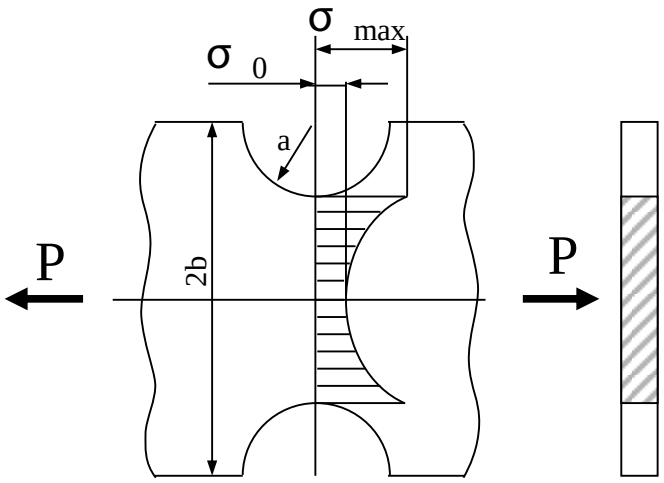

FIG. 9. Stress at the notched part. σ_{max} — maximum stress at the notched root; σ_0 — nominal stress.

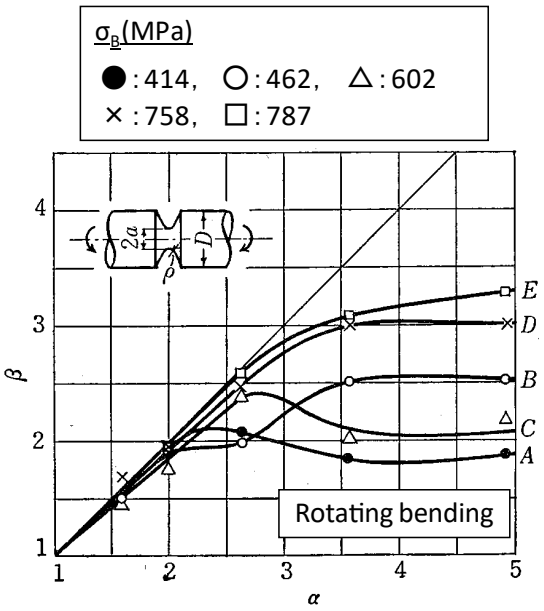

FIG. 10. Fatigue strength reduction factor versus the stress concentration factor [15].

2.3.3. Size effects

The fatigue strength of a larger specimen is generally equal to or less than that of a geometrically similar small specimen due to the size effect. The cause of the size effect is explained by the following two reasons:

— Mechanical factors related to the stress gradient in the material;
— Statistical factors related to risk volume or risk surface.

The stress distribution for large and small specimens subjected to bending moment is shown in Fig. 11. Compared with a small specimen, the stress gradient in a large specimen is small and the stress changes moderately. This means that the fatigue strength of a larger specimen is lower than that of a smaller specimen because a larger specimen has more high stress region volume.

On the other hand, statistical reasons, such as variability of strength or the characteristics inside the material, are also considered to contribute to the size effect. When the size of a test specimen becomes larger, the risk volume or surface which contains the weak portion enlarges, bringing with it a reduction of fatigue strength. However, as shown in Fig. 12, fatigue limits derived from the tension compression test do not depend on the size of the specimen in materials of various strength levels, so consideration of the size effect may not be necessary.

2.3.4. Surface finish

The condition of the surface is an important factor affecting the fatigue strength of components, since most of the fatigue cracks begin at the surface of the material, except in cases of VHCF. Figure 13 shows the relationship between 10^7 fatigue strength and hardness of the material [18]. As can be seen in this figure, the fatigue limit correlates well with the hardness of the material. Hence, the HCF strength can be improved by enhancing the hardness of the component's surface using heat treatment. Also, asperity (roughness or unevenness) of the surface plays the same role as a notch in causing stress concentration and reducing fatigue strength, so surface smoothing is an effective method to prevent fatigue failure. Note that notch sensitivity in the high cycle regime increases when the material surface is hardened, so that the harder the material becomes, the bigger the influence of surface roughness on the fatigue life.

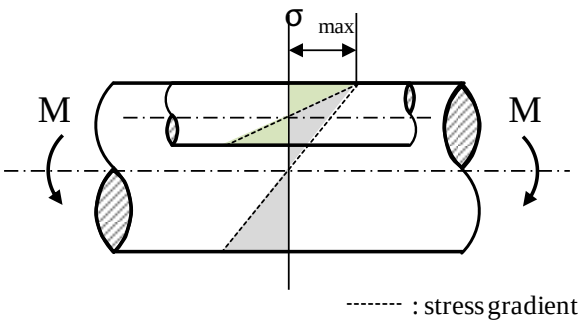

FIG. 11. Stress gradient of a large and small smooth specimen. M — bending moment.

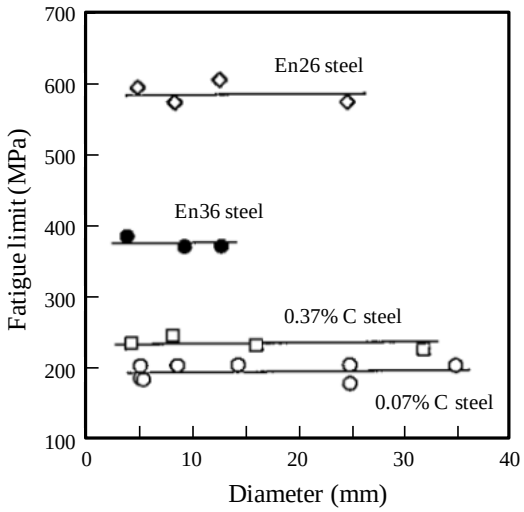

FIG. 12. Relationship between fatigue limit and the diameter of the specimen (tension compression) [16, 17].

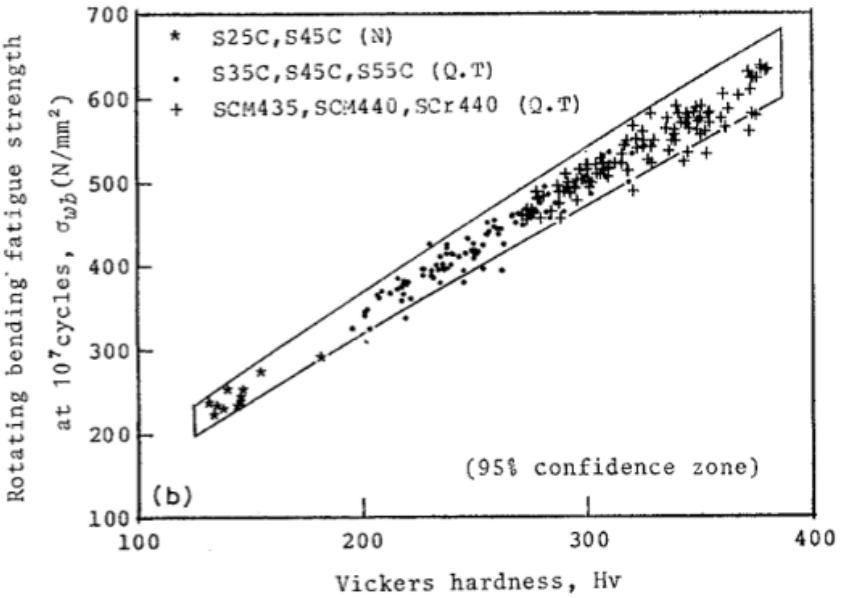

FIG. 13. Fatigue strength versus Vickers hardness [18].

The influence of the ground surface finish in the LCF regime has been investigated in various environments and strain waveforms [19–21]. It has been shown that the combined effects of the ground surface finish and pressurized water reactor (PWR) water environment are highly dependent on the strain waveform. More generally, it was demonstrated that the fatigue life cannot be predicted by means of a simple multiplication of factors accounting for each isolated effect. This work, which started in 2005, was at the origin of the RCC-M 2016[4] evolutions (Rules in Probationary Phase No. 3) and is still ongoing.

2.3.5. Temperature

It is well known that the fatigue strength in air changes with temperature: generally, it decreases as the temperature rises. The difference between fatigue characteristics at room temperature and at high temperature is that the former depends only on the number of cycles, while the latter depends not only on the number of cycles but also on the time if the temperature is sufficiently high. In addition, the fatigue limit of some materials disappears in the high temperature region. The loading frequency thus influences the fatigue strength at elevated temperature in air in a way that the lower loading frequency gives a higher fatigue crack growth rate (CGR) and lower fatigue strength. However, the dominant fatigue CGR under an inert gas environment at elevated temperature is almost the same as the CGR at room temperature. Therefore, it can be considered that fatigue strength at elevated temperature is related strongly to the oxidization of the materials.

In terms of LCF at elevated temperatures without creep effect, the fatigue strength and fatigue life of the materials can be predicted by Coffin–Manson's law, shown in Eq. (4). However, if the creep behaviour cannot be ignored, the creep–fatigue interaction should be considered in the damage analysis[5].

The variation in temperature may also cause fatigue failure when the thermal expansion of the material is constrained. This phenomenon is called thermal fatigue. Obviously, the temperature of the components is not constant during operation and the temperature difference which causes thermal fatigue may vary. The transient temperature distribution is a matter of concern for the prediction of fatigue life.

2.3.6. Corrosion fatigue due to environmental effects

Machines and structural components may be affected by corrosion due to changes in temperature, humidity, etc. The surface of a component is roughened by corrosion, which induces stress concentration and reduces fatigue strength. Predicted fatigue lives for corrosive materials are, however, much lower than estimated lives when considering only the effect of stress concentration. Corrosion fatigue failure under aqueous solution or corrosive gas environments cannot generally be assessed by superimposing the influence of cyclic loading and corrosion. In addition, in certain materials such as iron and steel, corrosion fatigue may not have a fatigue limit even if the material has a fatigue limit in air. Accordingly, prevention or mitigation of corrosion is very important to avoid fatigue failure of the component under certain environmental conditions. Extensive studies have been performed to clarify the effect of light water reactor (LWR) coolant on fatigue strength, as shown in Section 5 on environmental effects on fatigue life.

2.3.7. Loading history effect

The loading sequence is also a matter of concern for fatigue. The literature indicates that the fatigue life at a low strain level for type 304 stainless steel decreased by a factor of 2 to 4 under the decreasing strain sequence [22]. Also, strain-controlled fatigue tests in air and the LWR environment indicate a decrease by a factor of 3 or more in fatigue life under variable amplitude loading as compared with constant amplitude [23]. On the other hand, some experimental results suggest that this effect: (a) is not systematically observed in 304L and 316L; and (b) is not visible in the ferritic steel tested [11].

---

[4] See RCC-M 2016, Design and Construction Rules for Mechanical Components of PWR Nuclear Islands.

[5] See Section III of the ASME Boiler and Pressure Vessel (BPV) Code, Division 5.

Furthermore, operational experience seems to indicate that a possible effect of load history is covered by code conservatism, for example in the determination of the fatigue design curve transference factor [24].

2.4. LOADING AS A CAUSE OF FATIGUE FAILURE

2.4.1. Vibration fatigue

Vibration fatigue is one of the main mechanical fatigue elements in NPPs of all ages and occurs primarily in small diameter piping. The failures have occurred mainly at weldolets and socket welds in small diameter pipelines. These failures resulted from high cycle mechanical fatigue due to low amplitude cyclic stress.

One of the main contributing factors is mechanical excitation mechanisms such as pump induced pressure pulsations occurring at frequencies, usually of the multiple of the pump speed. When pressure pulsations coincide with a natural frequency of the piping system, severe vibratory fatigue damage may take place.

Another element is cavitation, which occurs when the fluid pressure approaches its vapour pressure. The resulting pressure pulsation can cause severe vibration of piping downstream such as a multistage high energy orifice. The frequency content of the excitation is one of the main differences between cavitation and pump induced pressure pulsation. In addition to severe vibrations, the collapse of the cavities on a solid surface removes material by mechanical erosion, damaging piping and other components. The other is flashing that occurs when the water temperature is higher than its saturation temperature at a given pressure and the water flashes into steam. This also results in broadband pressure pulsations causing vibration of piping downstream of the flashing component.

2.4.2. Thermal fatigue

When the thermal cycle is applied to the components, thermal stresses occur by constraining the thermal expansion or contraction resulting from temperature changes. The constraints that prevent thermal expansion or contraction can either be externally applied or self-imposed due to the configuration of the body and the temperature distribution [2].

Thermal fatigue is the major ageing mechanism for surge, spray and branch lines and their nozzles that are subject to thermal stratification, thermal shock, turbulent penetration and thermal cycling including during power manoeuvring and plant startup and shutdown. The original fatigue analysis of these components considered the design basis transients with high conservatism and did not take into account of the phenomena such as thermal stratification present in the surge and spray lines and thermal cycling present in the branch lines; these phenomena were discovered after the plants were put into operation. The design margin of components will be used to cope with these phenomena.

2.4.3. Fretting fatigue

Fretting fatigue occurs as a result of very small relative sliding motions between the metal contact areas under cyclic loading. It is associated with the generation of oxide abrasion powder at the edge of the contact area which induces fretting corrosion and decreases the fatigue limit of the material significantly. Therefore, fretting fatigue is sometimes categorized as corrosion fatigue. Also, one of the features of fretting fatigue is that the fatigue failure is initiated at the edge of the contact area by nucleation of very shallow Mode II cracks[6] due to the maximum shear stress. These basic mechanisms of fretting are illustrated in Fig. 14.

Fretting fatigue can occur in components using fitting structures such as a press fitting shafts, wire ropes, bolted or riveted joint plates, and steam turbine blades.

---

[6] Mode II crack: crack surfaces move over each along the x axis, that is, perpendicular to the crack tip.

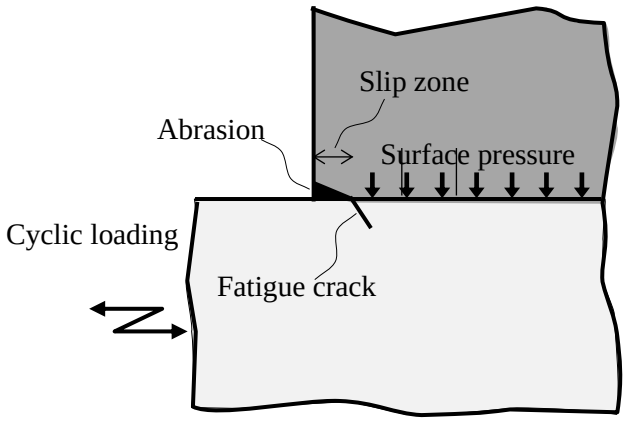

FIG. 14. Basic mechanism of fretting fatigue.

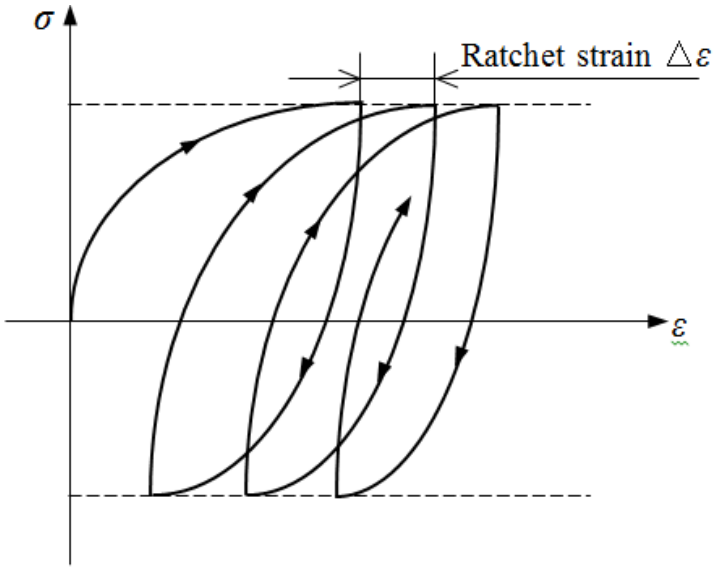

FIG. 15. An example of a cyclic stress–strain diagram for ratcheting (constant stress amplitude).

2.4.4. Ratcheting

Ratcheting is the accumulation of progressive plastic strain in the direction of mean stress associated with cyclic loading. A typical cyclic stress–strain diagram for ratcheting under constant stress amplitude is shown in Fig. 15. For example, the excessive load-controlled ratcheting fatigue described in Fig. 15 can be caused by seismic events.

When designing NPP components, primary stress of the components should remain in the elastic region to avoid plastic collapse. However, when the primary stress is acting on the component with repeated inelastic secondary stress, such as thermal stress, ratcheting deformation can be observed even if the primary stress is limited within the elastic regime. This type of ratcheting, by the combination of primary and secondary stress, for example, could occur in the piping system because the pipe could be subjected simultaneously to the primary stress due to the inner pressure and cyclic secondary stress due to the thermal stress.

Ratcheting decreases the ductility of the materials and accelerates the fatigue damage. Therefore, it is important to take into account not only the usual fatigue damage, but also the damage caused by ductility exhaustion when predicting fatigue life under ratcheting.

2.5. FRACTURE MECHANICS APPROACH TO FATIGUE

As mentioned in the previous section, fatigue life can be divided into two phases: fatigue crack initiation and fatigue crack propagation. Fracture mechanics is a tool dealing with crack propagation in materials. A fracture mechanics approach for new NPPs, where in the design stage the CUF should be less than 1, is of low priority. However, once a fatigue crack is initiated, it is important to evaluate the fatigue strength of the structures with a crack to manage the safety or residual life of the component appropriately.

The basis of fracture mechanics is the stress intensity factor K, which represents the asymptotic stress field near the crack tip. For example, the stress intensity factor for a crack in an infinite plate subjected stress σ as shown in Fig. 16, is expressed in Eq. (13).

$$K = \sigma\sqrt{\pi a} \tag{13}$$

where 2a is the crack length.

The concept of stress intensity factor is applicable only for a small scale yielding condition at the crack tip. When the applied stress changes cyclically between the maximum stress, σ_{max}, and minimum stress, σ_{min}, the stress intensity factor at these stresses can be expressed by Eq. (14).

$$K_{max} = \sigma_{max}\sqrt{\pi a},\ K_{min} = \sigma_{min}\sqrt{\pi a} \tag{14}$$

The stress intensity factor range ΔK is expressed by Eq. (15).

$$\Delta K = K_{max} - K_{min} = \Delta\sigma\sqrt{\pi a} \tag{15}$$

where $\Delta\sigma = \sigma_{max} - \sigma_{min}$

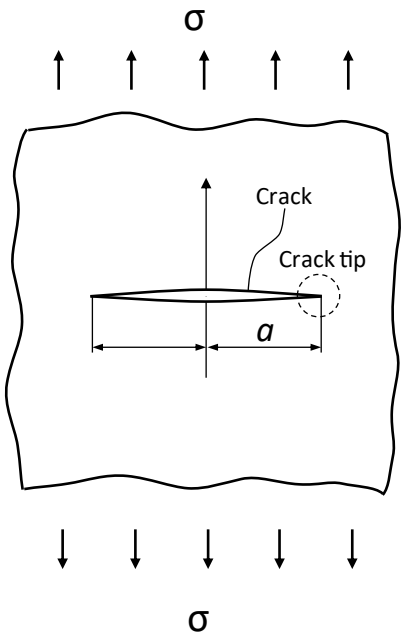

FIG. 16. Infinite plate with crack.

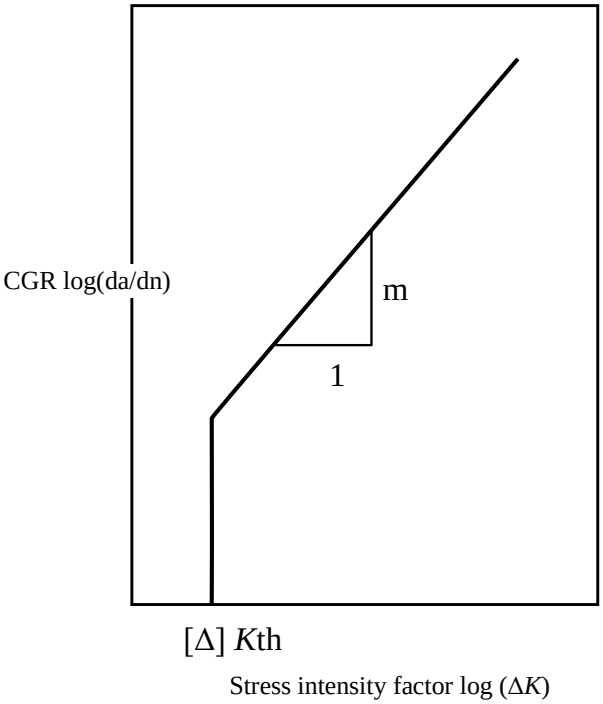

FIG. 17. Typical image of CGR versus the stress intensity factor.

Paris and Erdogan [25] found that the CGR *da*/*dn* has a linear relationship with the stress intensity factor range *ΔK* in a double logarithm chart and can be expressed by Eq. (16). This equation is called as Paris Law. The material coefficients *C* and *m* are obtained experimentally and also depend on the environment, frequency, temperature and stress ratios.

$$\frac{da}{dn} = C(\Delta K)^m \tag{16}$$

where

a is the crack length;

and *da/dn* is the fatigue crack growth for a load cycle *N*.

The typical shape of the CGR versus *ΔK* for carbon and low alloy ferritic steels is illustrated in Fig. 17. At very low *ΔK* levels, the material shows almost no crack growth. This indicates that the fatigue crack growth threshold is similar to the fatigue limit at the high cycle of the S–N curve. The fatigue CGR curves of this type are provided in many codes and standards. When a crack is detected, or assumed to exist in the actual component, it is possible to predict the growth of the crack during operation and calculate the residual fatigue life of the components by the fracture mechanics approach presented here.

The *ΔK* based discussion mentioned above is only applicable to the small scale yielding condition. Once the higher loading is applied and the crack tip condition exceeds the small scale yielding regime, it is necessary to apply another approach for fatigue crack evaluation. Elastic–plastic fracture mechanics using crack tip parameters such as the cyclic J-integral (*ΔJ*) or the range of crack tip opening displacement (*ΔCTOD*) can successfully predict fatigue crack behaviour under the large scale yielding condition.

3. FATIGUE ASSESSMENT IN NEW NUCLEAR POWER PLANT DESIGNS

3.1. CODES FOR FATIGUE DESIGN

3.1.1. Overview of design codes for nuclear power plants

The following codes provide rules for the construction of NPP components, which include detailed fatigue design and analysis requirements for pressure retaining components. Some important differences exist in the fatigue design requirements in these codes and these differences are discussed in Ref. [26], as summarized in the following.

3.1.1.1. ASME Boiler and Pressure Vessel Code

ASME has published multiple sections and subsections for nuclear applications. The ASME BPVC for Class 1 components is discussed in this publication, focusing on construction rules for mechanical components of the reactor pressure boundary.

The rules for fatigue design are contained in Article NB-3000 of Section III Division 1, Subsection NB of the ASME Code [27], which is divided into four sub articles:

(a) NB-3100, General Design Rules;
(b) NB-3200, Design by Analysis;
(c) NB-3300, Vessel Design;
(d) NB-3600, Piping Design.

Subarticle NB-3100 deals with loading conditions specified by the owner in the form of equipment specifications. The methods of analysis and stress limits depend upon the category of loading conditions. Subarticle NB-3300 gives special requirements that have to be met by Class 1 vessels. Subarticle NB-3600 contains design rules for Class 1 piping systems. These rules represent a simplification of the design by analysis, as specified in NB-3200.

3.1.1.2. AFCEN RCC-M

AFCEN was founded in October 1978 by Électricité de France (EdF) and Framatome. The first RCC-M specification was issued in 1980 and the first official issue was released in 1984. At that time, it was based on a combination of the ASME BPVC Section III Code, Westinghouse type PWR design specifications and French construction practices. Over time, it was developed further to include the provisions and experiences from the French regulatory requirements, from German and French utilities, and from the European standard practice.

The rules for fatigue design are contained in the following articles in RCC-M section 1, volume B [28]:

(a) B-3100, General Design Rules;
(b) B-3200, General Rule for Analysing Components Behaviour;
(c) B-3300, General Vessel Design;
(d) B-3600, Piping Design.

Some similarities with the ASME BPVC are obvious. For instance, the general stress analysis philosophy is the same: both are based on stresses calculated using elastic calculations and the Tresca stress intensity as a yield criterion. There are differences between the RCC-M code and ASME Code:

— Differences in allowable stresses, in particular associated with non-linear analysis.
— Differences in fatigue analysis, such as differences in the strain correction factor, K_e, or crack-like defect analysis. For crack-like defects, the RCC-M code offers a method that is a hybrid between initiation and propagation.
— The RCC-M 2016 edition has seen the implementation of several major measures regarding fatigue assessment:
    • The austenitic stainless-steel fatigue design curve was revised as follows:
        — The ASME curve was evaluated to fit RCC-M materials;
        — Transference factors were evaluated, as the result of a statistical analysis: A factor of 10 is imposed on cycles and 1.4 on strain;
    • Revision is introduced as a code case (rule in probation phase No. 2), included in the RCC-M version in 2018.
— Rules to integrate environmental fatigue in the calculation. Environmental effects were defined in another code case (rule in probation phase No. 3), which included in the RCC-M version in 2018:
    • This code case introduces a factor, Fen-integrated, which allows quantification of the portion of environmental effects which are already covered by the fatigue curve.
— An analysis method to assess mixing zones type phenomena was introduced as an appendix in the 2018 version.

3.1.1.3. Japan Society of Mechanical Engineers (JSME) Code

The Committee on Power Generation Facility Code was established by the Japan Society of Mechanical Engineers (JSME) in October 1997 and has issued a number of codes in the fields of thermal power as well as nuclear and fusion power. The first edition of Rules on Design and Construction for NPPs, which is a counterpart of ASME BPVC section III, was published in 2001.

ASME BPVC section III is organized by component Class, whereas the JSME code is organized by component type. JSME S-NC1 [29] covers the general aspects for the design and construction of nuclear components, including material, design, fabrication, examination, testing and overpressure protection. The rules given in the above ASME BPVC Code are specified in Subsections PVB-3000 (Design of Class 1 Vessels) and PPB-3000 (Design of Class 1 Piping) of JSME S-NC1.

Generally, requirements for the design rules for Class 1 vessels are almost the same as those in NB-3000 in the ASME Code. In particular, the basic design allowable limits for the failure modes that should be considered in the design and for every operating condition are identical. However, there are some differences between the JSME code and the ASME Code, as described below:

— *Plastic analysis:* ASME BPVC NB-3228 specifies limit, experimental and plastic analyses as primary stress evaluation methods. Shakedown analysis is also specified in ASME. JSME PVB-3160, however, only specifies limit analysis as a primary stress evaluation method. Instead, JSME has a code case specifying evaluations for primary stress, primary plus secondary stress and shakedown assessment by direct use of inelastic finite element (FE) analysis results.
— *K_e factor*: The K_e factor specified in ASME NB-3228.5 and JSME PVB-3300 specifies original K_e factors that are formulated based on the elastic follow-up model for local plasticity, reflecting Japanese R&D results. The JSME code gives more realistic values.

— *ASME*: The piping stress limits against seismic loads (stress due to inertial reversing dynamic loads, Level D service limits) are given by $3S_m$ with a reduced B_2 index. In Japan, JEAC 4601[7] requires fatigue analysis for seismic loading.

Where S_m is material allowable stress and B_2 is stress indices applicable respectively to pressure P.

3.1.1.4. Korea Electric Association (KEA) Korea Electric Power Industry Code (KEPIC)

The Korea Electric Association (KEA) is the exclusive review organization for new electric power technologies in the Republic of Korea. It maintains and develops technical standards in the power industry. In 2001, KEA was registered as a private collective standards development organization at the ISO/IEC information centre. The association's goal is to improve domestic technical power in the Republic of Korea's power industry, continuously reflect power plant construction and operating experience, and improve standardization by continuously maintaining and managing the Korea Electric Power Industry Code (KEPIC).

The machinery parts of KEPIC [24] were developed to conform to the ASME BPVC Code. The technical contents and composition systems are also the same as those of the ASME Code. The following list shows the articles of KEPIC MN that correspond to ASME BPVC:

(a) MNB-3100, General Design Rules;
(b) MNB-3200, Design by Analysis;
(c) MNB-3300, Vessel Design;
(d) MNB-3600, Piping Design.

3.1.1.5. Canadian Standards Association (CSA) standard

The Canadian Standards Association (CSA) is an independent private organization that develops standards in the field of boilers and pressure vessels. Nuclear standards are designated by the letter N (e.g. N285.0).

ASME BPVC is used in various Canadian provinces and N285.0 has been provided to define how ASME BPVC section III is adapted to fit Canadian laws. N285.0 provides for classification of the various components. Once classification is complete, the relevant ASME BPVC section III part can be used.

The ASME technical requirements for design are directly referenced by the CSA N285.0 standard [30], as shown in the following: Class 1 systems and components are designed to comply with the requirements of ASME BPVC, section III, division 1, NB-3000. However, CSA has developed a series of standards, the N289 Series, which identifies the Canadian requirements for considering the evaluation and impact of seismic loadings on the pressure boundary items.

In particular, CSA N289.3 [31] is the requirement on seismic fatigue. The standard states that seismic fatigue analysis of ASME Class 1 components and supports is not required when the range of primary plus secondary stresses due to the seismic load alone are limited to $3S_m$ or equivalent.

3.1.1.6. Research and Design Institution for Energy Technology (NIKIET) PNAE G-7 code

In 1978, an interdepartmental commission headed by the Research and Design Institution for Energy Technology (NIKIET) was organized in the former Union of Soviet Socialist Republics (USSR). Its main task was to revise previous codes and create a new series, PNAE G-7 (Rules and Norms in Nuclear Energy). Experts from all nuclear power organizations of the former USSR were involved. Specialists from the Central Boiler and Turbine Institution (CKTI) and the Central Research Institute of Structural

[7] JEAC 4601 : Technical code for seismic design of nuclear power plant, Japan Electric Association, 2008.

Materials (CRISM) (Prometey) made significant contributions to the development of the PNAE G-7 series of documents.

The structure of the PNAE G-7 series [32] differs substantially from the structure of the ASME Code. In most cases, it is difficult to define a clear correspondence between the ASME Code and the documents within the PNAE G-7 series. PNAE G-7-002-86 corresponds to ASME NB-3000. Along with the PNAE G-7 series of documents, other government and industry standards are typically used in the Russian nuclear industry as approved by the owner and regulatory body. The number of governing documents from various Russian Federation State and industry organizations, such as GOST standards, is expanding and, in some cases, is being updated for inclusion in the PNAE G-7 series for specific equipment at various stages of the plant life cycle.

3.1.2. ASME Code rules for fatigue design

Detailed fatigue evaluations are required for Class 1 components in accordance with the requirements of ASME BPVC Section III, Subsection NB. This code's approach to fatigue design is discussed below. Fatigue analysis requirements for Class 2 and 3 components are less explicit but are also discussed in Section 3.1.2.8.

3.1.2.1. Consideration of plant and system operating and test conditions

The design specification identifies the loadings and combinations of loadings considering all plant or system operating and test conditions anticipated or postulated to occur during the intended service life of the component. These conditions are classified into the following categories:

— Normal conditions;
— Upset conditions;
— Emergency conditions;
— Faulted conditions;
— Testing conditions.

3.1.2.2. Stress and stress categories

Different types of stress require different limits, and before establishing these limits, it is necessary to choose the stress categories to which limits should be applied. The categories and subcategories chosen are as follows:

— Primary stress:
  - General primary membrane stress P_m;
  - Local primary membrane stress P_l;
  - Primary bending stress P_b;
— Secondary stress Q;
— Peak stress F.

Primary stress is the result of the imposed loading, which occurs because the laws of equilibrium between external and internal forces and moments. The basic characteristic of primary stress is that it is not self-limiting. If a primary stress exceeds the yield strength of the material through the entire thickness, the prevention of failure is entirely dependent on the strain-hardening properties of the material.

Secondary stress develops from the internal constraint of a structure. It is the result of an internal strain pattern rather than equilibrium with an external load. The basic characteristic of a secondary stress is that it is self-limiting. These stresses are caused by thermal expansion or discontinuity conditions. The main concern with secondary stresses is that they may result in localized yielding or distortion.

Peak stress is the increment of the stress superimposed on primary and secondary stresses for the region where the total stress is larger than the sum of primary and secondary stresses. The basic characteristic of a peak stress is that it causes no significant distortion and is considered mostly as a possible source of fatigue failure.

3.1.2.3. Stress intensity limits

The choice of the basic stress intensity limits for the stress categories described above is accomplished by the application of limit design theory tempered by engineering judgement and some conservative simplifications.

The primary stress limits are intended to prevent plastic deformation and to provide a nominal factor of safety on the ductile burst pressure. The primary plus secondary stress limits are intended to prevent excessive plastic deformation leading to incremental collapse, and to validate the application of elastic analysis when performing the fatigue evaluation. The peak stress limit is intended to prevent fatigue failure as a result of cyclic loadings. Special stress limits are provided for elastic and inelastic instability.

The stress limits change for different service levels. Stress limits are established for Design, Level A, Level B, Level C, Level D and test loadings. Under Level A and B service limits, a fatigue analysis is required. The stress limits for Level A and B service and potential failure mode for each type of stress category are shown in Table 1.

3.1.2.4. Analysis for cyclic operation (fatigue analysis)

If the specified service loadings for a component do not meet the conditions of NB-3222.4(d) [12], a fatigue analysis is required. The conditions and procedures of fatigue analysis are based on a comparison of peak stress intensity with strain cycling fatigue data. The strain cycling fatigue data are represented by design fatigue curves described in Section 3.1.2.7. These curves show the allowable amplitude, S_a, of the alternating stress intensity (one half of the alternating stress intensity range) plotted against the number of cycles. This stress intensity amplitude is calculated on the assumption of elastic behaviour and, hence, has the dimensions of stress, but it does not represent a real stress when the elastic range is exceeded.

TABLE 1. LIMITS OF STRESS INTENSITY FOR LEVEL A AND B SERVICES AND THE POTENTIAL FAILURE MODE FOR EACH TYPE OF STRESS CATEGORY [33]

Stress category		Stress intensity limit	Potential failure mode
Primary stress	General membrane	110% S_m for Level B*	Ductile bursting and plastic deformation from a single load application.
	Local membrane + Primary bending	110% ($1.5S_m$) for Level B*	
Primary and secondary		$3.0S_m$**	Excessive plastic deformation leading to incremental collapse; used for validating the fatigue evaluation.
Peak		CUF ≤ 1	Crack initiation

***** There are no specific limits in the Level A limits.

****** The $3.0S_m$ limit may be exceeded if the simplified elastic–plastic analysis rules are satisfied.

The analysis is made on the basis of the stresses at a point, and the allowable stress cycles are adequate for the specified service loadings at every point. Only the stress differences due to service cycles as specified in the design specifications are considered. The requirements for fatigue evaluation of Class 1 components and the specific steps required for calculating partial and CUFs are as follows:

When determining the stress differences and the alternating stress intensity, S_{alt}, ASME Code NB-3216 gives two procedures for calculating the stress differences (constant principal stress direction and varying principal stress direction). The stress differences are defined in Eq. (17).

$$S_{12} = S_1 - S_2,\ S_{23} = S_2 - S_3,\ S_{31} = S_3 - S_1 \tag{17}$$

where S_1, S_2, S_3 are the principal stresses.

The maximum of the stress difference ranges is used in fatigue analysis and the alternating stress intensity (S_{alt}) is one half of this maximum range.

Adjust the alternating stress intensity (S_{alt}) and produce the alternating stress intensity (S_a) to be used in the S–N curve. (S_{alt}) is multiplied by the following adjustment factor when these factors are appropriate:

— The ratio of the modulus of elasticity given on the design fatigue curve to the value of the modulus of elasticity used in the analysis;
— K_e (discussed in Section 3.1.2.5) when the $3S_m$ limit on the range of primary plus secondary stress intensity is not met;
— The fatigue strength reduction factor defined in ASME NB-3213.17, when this factor is applied to address stress concentrations.

The cumulative effect of various stress cycles is evaluated, as stipulated in steps 1–6 below (NB-3222.4 (5)) [12]:

— *Step 1*: Designate the specified number of times each type of stress cycle of types 1, 2, 3,..., *n*, will be repeated during the life of the component as n_1, n_2, n_3,..., n_n, respectively;
— *Step 2*: For each type of stress cycle, determine the alternating stress intensity S_{alt} by means of points (1) and (2) above. Label these quantities $S_{alt\,1}$, $S_{alt\,2}$, $S_{alt\,3}$, $S_{alt\,n}$;
— *Step 3*: For each value $S_{alt\,1}$, $S_{alt\,2}$, $S_{alt\,3}$,..., $S_{alt\,n}$, use the applicable design fatigue curve to determine the maximum number of repetitions which would be allowable if this type of cycle was the only one. Label these values N_1, N_2, N_3,..., N_n;
— *Step 4*: For each type of stress cycle, calculate the usage factors U_1, U_2, U_3,..., U_n, from $U_1 = n_1/N_1$, $U_2 = n_2/N_2$, $U_3 = n_3/N_3$,..., $U_n = n_n/\underline{N}_n$;
— *Step 5*: Calculate the CUF *U* from $U = U_1 + U_2 + U_3 + \ldots + U_n$;
— *Step 6*: The CUF *U* is not to exceed 1.0.

3.1.2.5. Simplified elastic–plastic analysis

ASME Code section III allows membrane-plus-bending stresses to exceed the yield stress, which can cause a strain concentration that is not included in an elastic analysis. ASME Code NB-3228.5 [7] states that the $3S_m$ limit on the range of primary plus secondary stress intensity may be exceeded provided that requirements (1)–(6) below are met.

(1) The range of primary plus secondary membrane-plus-bending stress intensity, excluding thermal bending stresses, should be $\leq 3S_m$.

(2) The value of S_a used for entering the design fatigue curve is multiplied by the factor K_e expressed in Eq. (18):

$$\begin{aligned} K_e &= 1.0 \text{ for } S_n \le 3S_m \\ &= 1.0 + \left[\frac{1-n}{n(m-1)}\right]\left[\frac{S_n}{3S_m} - 1\right] \text{ for } 3S_m < S_n < 3mS_m \\ &= \frac{1}{n} \text{ for } S_n \ge 3mS_m \end{aligned} \tag{18}$$

where S_n is the range of primary plus secondary stress intensity.

The values of the material parameters m and n for the various classes of permitted materials are given in Table NB-3228.5(b)-1 of ASME Code NB-3200.

(3) The rest of the fatigue evaluation stays the same, as required in NB-3222.4, except that the procedure of NB-3227.6 (Applications of elastic analysis for stresses beyond the yield strength).
(4) The component meets the thermal ratcheting requirement of NB-3222.5 (Thermal stress ratchet).
(5) The temperature does not exceed that listed in table NB-3228.5(b)-1 for the various classes of materials.
(6) The material has the specified minimum yield strength to specified minimum tensile strength ratio of less than 0.80.

3.1.2.6. Rules for the evaluation of Class 1 piping

The rules in ASME Code section III for the evaluation of Class 1 piping components is presented in NB-3650. In this code, there is no discussion of stress characteristics, categories, allowable and criteria, but equations are provided to calculate the required stresses for comparison with the allowable.

The requirements for fatigue are provided in NB-3653 (Consideration of level A service limits) and NB-3654 (Consideration of level B service limits). The fatigue rules for piping require a determination of whether the piping is cycling elastically or if some elastic–plastic cycling is occurring. This is accomplished in NB-3653.1 using Eq. (19) (in ASME Code section III) by considering every loading condition listed in the design specification as a Level A, Level B or as test conditions. This calculation is based upon the effect of changes that occur in mechanical or thermal loadings that take place as the system goes from one load set, such as pressure, temperature, moment and force loading, to any other load set that follows it in time. It is the range of pressure, temperature and moment between two load sets which is to be used in the calculations expressed by Eq. (19).

$$C_1 \frac{P_O D_O}{2t} + C_2 \frac{D_O M_i}{2I} + C_3 C E_{ab} \left|\alpha_a T_a - \alpha_b T_b\right| \le 3S_m \tag{19}$$

where

C_1, C_2, C_3 are the secondary stress indices for the specific product under investigation (NB-3680);

P_o is the range of service pressure;

D_o, t, I are the outside diameter of the pipe, the nominal wall thickness of the product, and the moment of inertia;

M_i is the resultant range of moment which occurs when the system goes from one service load set to another;

E_{ab} is the average modulus of elasticity of the two sides of a gross structural discontinuity or material discontinuity at room temperature;

α_a, α_b are the coefficients of thermal expansion on side (a) and side (b) of a structural material discontinuity;

and T_a, T_b are the range of the average temperatures on side (a) and side (b) of a structural discontinuity when the system goes from one service load to another.

For every pair of load sets, the range of peak stress intensity (S_p) is calculated using Eq. (20) in NB-3653.2.

$$S_P = K_1 C_1 \frac{P_0 D_0}{2t} + K_2 C_2 \frac{D_0}{2t} M_i + K_3 C_3 E_{ab} \left|\alpha_a T_a - \alpha_b T_b\right| + \frac{1}{2(1-v)} K_3 E\alpha \left|\Delta T_1\right| \quad (20)$$
$$+ \frac{1}{(1-v)} E\alpha \left|\Delta T_1\right|$$

where

$E\alpha$ is the modulus of elasticity (E) times the mean coefficient of thermal expansion (α);

K_1, K_2, K_3 are the local stress indices for the specific product under investigation (NB-3680);

$\left|T_1\right|$ is the absolute value of the range of the temperature difference between the temperature of the outside surface and the temperature of the inside surface of the piping product;

and $\left|T_2\right|$ is the absolute value of the range for that portion of the non-linear thermal gradient through the wall thickness not included in ΔT_1.

For a pair of load sets that satisfy Eq. (19), the alternating stress intensity (S_a) is equal to one half the value of S_p ($S_{alt} = S_p/2$) calculated in Eq. (20) above. But, if Eq. (19) cannot be satisfied for all load-set pairs, Eqs (21) and (22)(of section III, NB-3653.6) are met and the value of S_{alt} can be calculated using Eq. (23)(of section III, NB-3653.6). The cumulative damage is evaluated in accordance with NB-3222.4 I (5).

$$S_e = C_2 \frac{D_o}{2I} M_i^* \le 3S_m \quad (21)$$

where

S_e is the nominal value of expansion stress;

M_i^* is the same as M_i in Eq. (19) (of section III, NB-3653.6), except that it includes only moments due to thermal expansion and thermal anchor movement.

$$C_1 \frac{P_O D_O}{2t} + C_2 \frac{D_O M_i}{2I} + C_3' E_{ab} \left|\alpha_a T_a - \alpha_b T_b\right| \le 3S_m \quad (22)$$

where

C_3 are the values in table ASME Code NB-3681(a)-1;

M_i is defined in NB-3652;

and all other variables are as defined in NB-365.3.

$$S_{alt} = K_e \frac{S_p}{2} \tag{23}$$

where

S_{alt} alternating is the stress intensity;

S_p peak stress is the intensity value calculated by Eq. (20);

and K_e as discussed in Section 3.1.2.5

For all load-set pairs the value of the range of ΔT_1 cannot exceed that calculated per NB-3653.7 and expressed in Eq. (24).

$$\Delta T_1 range \leq \frac{y' S_y}{0.7 E\alpha} C_4 \tag{24}$$

where

C_4 is 1.1 for ferritic material, 1.3 for austenitic material;

$E\alpha$ is as defined for Eq. (20);

P is the maximum pressure for the set of conditions under consideration;

S_y is the yield strength value taken at average fluid temperature of the transient under consideration;

X is $(PD_o/2t)(1/S_y)$

and y' is 3.33, 2.00, 1.20, and 0.80 for x = 0.3, 0.5, 0.7, and 0.8, respectively.

The above requirements are applied to all Class 1 piping except for piping exempted under points (1) or (2) below:

(1) Piping of NPS 1 or less which has been classified as Class 1;
(2) The specified service loads for which Level A and B service limits are designated that meet all of the requirements stipulated in NB-3630 (d) (e) (2).

A detailed description of reversing and non-reversing dynamic loading is provided in NB-3622. Reversing load and acting without non-reversing loads are considered to be a concern for fatigue and fatigue ratchet only. All of the requirements for reversing dynamic loading under service limits C and D are provided in NB-3655 (Consideration of level C service limits) and NB–3656 (consideration of level D service limits).

3.1.2.7. Design fatigue curves

The design fatigue curves for use with the above fatigue analysis procedures are given in ASME Code figs I-9.0[8]. The curves of figs I-9.0 are defined over a cyclic range of 10 to 10^6 cycles, except for austenitic steels, nickel–chromium–iron alloys, nickel–iron–chromium alloys, nickel–chromium–molybdenum–iron alloys and nickel–copper alloys, for which the design fatigue curve is extended to 10^{11} cycles in figs I-9.2.2 and I-9.5. The code design fatigue curves were developed from uniaxial tests, where displacements were imposed at room temperature and adjusted for mean stress. The stress amplitude values shown on the ordinates of the curves were obtained from the best-fit curves by applying a factor of 2 on stress or a factor of 20 on cycles, whichever was more conservative at each point to account for scatter of data, size effects, surface roughness and industrial environment.

ASME modified the above fatigue design curves for carbon, low alloy, austenitic steels and nickel–chromium–iron alloys in the 2009 Addenda of the ASME Code:

— The curve for carbon and low alloy steels is extended to 10^{11} cycles;
— The curve for austenitic steels and nickel–chromium–iron alloy steels are developed by using margins of 12 for cyclic life and 2 for strain (whichever is more conservative).

3.1.2.8. Fatigue evaluation for Class 2 and Class 3 components

Fatigue evaluation is not performed for Class 2 and Class 3 pressure vessels, unless the designer optionally invokes the alternative rules of NC-3200. The fatigue evaluation rules for Class 2 vessels are described in NC-3219 of section III, division 1, subsection NC of the ASME Code [27]. The need for a fatigue analysis is determined based on NC-3219.1 to NC-3219.3. If a fatigue analysis is needed, one can be made in accordance with the rules of Section III appendices, Mandatory appendices XIII (Design Based on Stress Analysis) and XIV (Design Based on Fatigue Analysis).

Class 2 and Class 3 piping are evaluated following the requirements of NC/ND-3611.2. The only consideration is to evaluate cycling moment loading. This is accomplished by satisfying the thermal expansion requirements. The thermal expansion stress S_E is determined and bounded and is expressed in Eq. (25).

$$S_E = \frac{iM}{Z} \leq S_A \tag{25}$$

where

M is the maximum range of moment;

I is the stress intensification factor;

and Z is the section of pipe.

The allowable stress range for expansion stress, S_A, is defined in Eq. (26).

$$S_A = f\left(1.25S_c + 0.25S_h\right) \tag{26}$$

where

[8] See KEISLER, J., CHOPRA, O.K., SHACK, W.J., Fatigue Strain-Life Behavior of Carbon and Low-Alloy Steels, Austenitic Stainless Steels, and Alloy 600 in LWR Environments, NUREG/CR-6335, Argonne National Laboratory, Argonne, IL (1995).

S_c is the basic material allowable stress at minimum (cold) temperature;

S_h is the basic material allowable stress at maximum (hot) temperature;

and f is the stress range reduction factor as determined in table NC/ND-3611.2(e)-1.

3.2. FATIGUE DESIGN LOADINGS

3.2.1. Design transients

The set of design basis events consists of events that the components may potentially experience. The component specifications should consider all of the events. The events are divided into five categories — normal, upset, emergency, faulted and test — based on the frequency of occurrence. The normal and test events are planned operations that will occur during the life of the plant. Upset events are those that may occur during the life of the plant (i.e. anticipated operational occurrences). Emergency and faulted events are not expected to occur (i.e. they are accidents), but these events are included in the design basis for additional design margin. The design frequencies of occurrences are determined in two ways. The unplanned event frequencies are conservatively determined by reviewing previous historical data. The planned event frequencies are conservatively determined from operational philosophies or conservatively determined to reflect estimate of the yearly, monthly, weekly and daily frequency over plant life.

Design transients are time history plots of fluid temperature, pressure and flow rate during plant events and are detailed in the design specifications. The thermal-hydraulic transient data presented in the design specifications is intended for component design, and the eventual use of these data is to calculate fatigue usage factors for each component. A listing of the transients, categories and number of occurrences contained in a typical specification is shown in Table 2.

3.2.2. Thermal stratification

Piping systems subjected to stratified flow are evaluated for additional thermal stresses due to thermal stratification. Stratified flow exists when a hotter fluid flows over a colder one.

This condition induces a vertical thermal gradient, resulting in increased overall bending stresses and localized thermal gradient stresses. Stratified flow effects consist of:

— Local stresses due to temperature gradients in the pipe wall;
— Additional thermal pipe bending moments generated by the restraining effect of supports on the stratified flow induced curvature of the piping.

The extent of stratification is reduced by sloping generally horizontal pipe runs and is mitigated by carefully selecting designs and operating procedures. As the magnitude of thermal stratification is not easily predictable via fluid flow computation, its estimation usually relies on in situ measurements derived with thermocouples positioned on the outside wall of instrumented pipes.

3.2.3. Earthquake loads

Earthquake associated loads are caused by the inertial response of the SSC to earthquake induced motion of the SSC supports or the foundations of the supports. Seismic loads are identified as seismic anchor motion loads and seismic inertia loads. The seismic anchor motion loads represent the static

TABLE 2. TYPE OF TRANSIENT, NUMBER OF OCCURRENCES AND TRANSIENT CLASSIFICATION IN A TYPICAL PWR DESIGN SPECIFICATION [33]

Type of transient	Occurrences	Classification
Plant heat-up at 55°C/h	200	Normal
Plant cooldown at 55°C/h	200	Normal
Plant loading at 5% of full power per minute	18 300	Normal
Plant unloading at 5% of full power per minute	18 300	Normal
Step load increase of 10% of full power	2000	Normal
Step load decrease of 10% of full power	2000	Normal
Large step load decrease (with steam dump)	200	Normal
Steady state fluctuation	Infinite	Normal
Loss of load (without immediate turbine or reactor trip)	80	Upset
Loss of power (blackout with natural circulation in reactor coolant system (RCS))	40	Upset
Loss of flow (partial loss of flow — one pump only)	80	Upset
Reactor trip from full power	400	Upset
Inadvertent auxiliary spray	10	Upset
Turbine roll test	10	Test
Primary side hydrostatic test before startup at 3105 psig	5	Test
Primary side leak test at 2485 psig	50	Test
Steam pipe break	1	Faulted
Reactor coolant pipe break	1	Faulted

portion, and the inertia loads represent the dynamic portion of the response. Earthquake associated loads are determined by seismic analysis. The seismic analysis is performed using one of the following methods:

— Equivalent static load analysis;
— Response spectrum analysis;
— Time history analysis.

An NPP is designed for maximum ground acceleration, with certain SSCs designed to remain functional and within applicable stress, strain, and deformation limits (safe shutdown earthquake (SSE)). It is also designed for the magnitude of ground acceleration for which those features of the plant necessary for continued operation without undue risk to the health and safety of the public will remain

functional (operating basis earthquake (OBE)). The fatigue effects of such seismic induced stress cycles are considered in the fatigue evaluation of components and piping.

3.2.4. Vibratory loads

Vibratory loads in mechanical systems and components are cyclic and usually arise from the operating environment of the system or component. The following operating conditions may lead to vibratory loads: response to rotating or reciprocal pumps, fluid pulsation, cavitation and flashing, vortex shedding and FIV.

Both steady state vibrations and transient induced vibrations can occur within plant operational conditions. Transient induced vibrations occur during relatively short periods of time and result in less than 10^6 stress cycles. Examples of transient sources of vibration are pump actuation and pump switching, rapid valve opening or closing, and safety relief valve operation. Steady state vibrations are repetitive vibrations that occur for relatively long periods of time during normal plant operation [34].

There is not much information on vibratory loads in codes. However, section B3622.5 of RCC-M [9] provides the following recommendation for preventing failure caused by piping vibration. Piping should be arranged and supported to reduce vibration. The manufacturer is responsible for ensuring and demonstrating that system vibration is within acceptable levels by taking the necessary design measures, by monitoring as necessary and by taking measurements under startup or initial service conditions.

Additions to annex A of EN13480[9] dealing with piping vibration were addressed in 2017. The additions proposed a guideline that may be used to obtain a reduction in the number of pipework circuits that exceed vibratory acceptance criteria. Three issues needed to be resolved to optimize the vibratory behaviour of the piping systems:

— The definition of the operation of circuits;
— The recommendation for pumps, valves and orifice plates;
— The installation of piping and their supports.

3.2.5. Thermal oscillations in piping

3.2.5.1. Thermal oscillations in piping connected to the RCS

Normally, stagnant lines connected to the RCS can be subjected to stresses from thermal stratification caused by valve leakages or turbulent penetrations. As required by US NRC Bulletin 88-08 [35], such lines need to be reviewed to ensure their structural integrity. Thermal stratification and oscillation should be evaluated to review the conformity with the requirements in Bulletin 88-08 for all piping connected to the RCS.

3.2.5.2. Thermal oscillations in a mixing zone

A cyclic mixing of fluids with significantly different temperatures in a mixing zone may result in thermal fluctuations, stratification or vortex phenomena. The designer is recommended to take the necessary measures to prevent fatigue failure induced by these local thermo-hydraulic phenomena. These phenomena should be taken into consideration when the temperature difference between the fluids exceeds 44°C for austenitic stainless pipes and 28°C for unalloyed or low alloy steel pipes, where the cumulative usage period is more than 30 hours (B 3624.3 of section 1, volume B of RCC-M [28]).

[9] EN 13480, Metallic industrial piping, Standard by DIN-adopted European Standard (2017).

3.2.6. Other loadings

Other loadings are considered, as follows: dead weight, vibratory excitation by pump, in-containment refuelling water storage tank (IRWST) discharge, fluid transient loadings such as valve thrust, pressure forces on unbalanced expansion joints and hydrostatic test pressure.

3.2.7. Loading combinations

The vessels and piping are designed to withstand any combination of loading that is postulated to occur simultaneously. The loading combinations specified for the design of the vessels and piping are categorized as design, Level A (normal), Level B (upset), Level C (emergency), Level D (faulted), and test conditions. The loading combinations of Level A and B and test conditions are used for fatigue analysis. An example of load combinations for fatigue analysis of reactor coolant pipe is as follows:

— Level A condition: Normal operation loads, including dead weight + normal transients + pump vibratory excitations;
— Level B condition: Normal operation loads, including dead weight + upset transients + IRWST discharge + fatigue effects of seismic induced stress cycles;
— Test condition: Hydrostatic test and leak test.

3.2.7.1. Consideration of fatigue effects due to safe shutdown earthquake loading for piping

SSE is assigned as Level D and is required to meet the Level D limit related to fatigue and fatigue ratchet as provided in NB-3656 (Consideration of Level D Service Limits). For some NPPs, SSE is evaluated differently:

— JEAC 4601 [36] requires additional fatigue analysis using elastically dynamic design earthquake ground motion and design basis earthquake ground motion under levels C_s and D_s;
— In Canada, only one seismic event is considered in design under Level C and, in addition, requires evaluation of the fatigue effects of the cycling loading.

3.3. DESIGN CONSIDERATIONS FOR AVOIDING POSSIBLE FATIGUE FAILURE

NPP components are designed to the requirements of codes for fatigue design listed in Section 3.1. All codes address structural design limits for pressure vessel and piping components that ensure safe plant operation with the highest reliability and little threat to public health and safety. However, structural analysis is one of the elements of good design that is a major part of the construction code design process. The role of analysis is to alert the designer to design deficiencies that can be fixed before construction. The experience of many years of successful pressure vessel operation is a positive condition for obtaining good design. This section addresses key factors from the standpoint of fatigue resistance.

3.3.1. Design consideration for vibration fatigue

3.3.1.1. Code requirements for piping vibration

There is little information in codes on vibratory loads. However, section B3622.5 of RCC-M [28] provides the following recommendation for piping vibration failure prevention (ASME Code NB-3622.3[10]

[10] AMERICAN SOCIETY OF MECHANICAL ENGINEERS, Boiler and Pressure Vessel Code Sec III Div. 1, Subsection NB, NB-3622.3, ASME, New York.

uses similar wording). Piping should be arranged and supported to reduce vibration. The manufacturer is responsible for demonstrating that system vibration is within acceptable levels by taking the necessary design measures, by monitoring as necessary and by taking measurements under startup or initial service conditions.

Additions to Annex A of EN13480 dealing with piping vibration were released in the fall of 2017. These proposed a guideline that may be used to obtain a reduction in the number of pipework circuits that exceed vibratory acceptance criteria. Three issues need to be addressed to optimize the vibratory behaviour of the piping systems:

— The definition of the operation of circuits;
— The recommendation for pumps, valves and orifice plates;
— The installation of piping and their supports.

3.3.1.2. Butt welded joints

Socket welded piping joints are allowed for branch connections with pipe sizes of 50.8 mm and less in accordance with ASME NB-3661.2 [7]. However, the major cause of vibrational fatigue failures in small-bore piping systems in NPPs have been poor quality socket welds. The fillet weld may contain root defects, which are undetectable by normal code inspection processes, and which greatly reduce its fatigue resistance. Most of the failures occur in the root of fillet weld (generally associated with weld defects such as lack of penetration), rather than at its toe. Lack of penetration at the weld root was found to have a very significant effect on failure initiation at the weld root.

The deleterious effect of fillet welds on fatigue life can be eliminated by replacing fillet welded joints with full penetration welds using butt welding fittings or integrally reinforced outlet fittings (e.g. Sweepolet) (see Fig. 18 and Fig. 19). The butt welds also have a lower level of stresses from the viewpoint of stress concentration as compared with fillet welds. Considering these merits, butt welded joints are recommended instead of fillet welded joints in the design of construction plants.

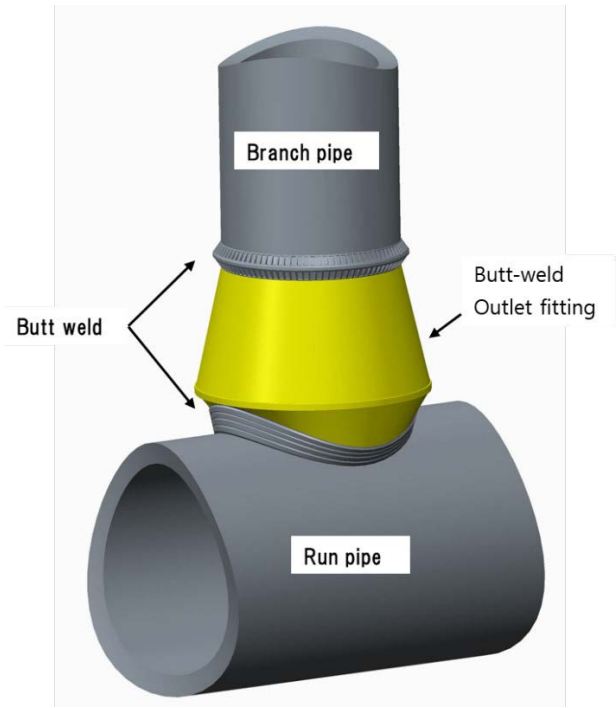

FIG. 18. Butt weld outlet fitting.

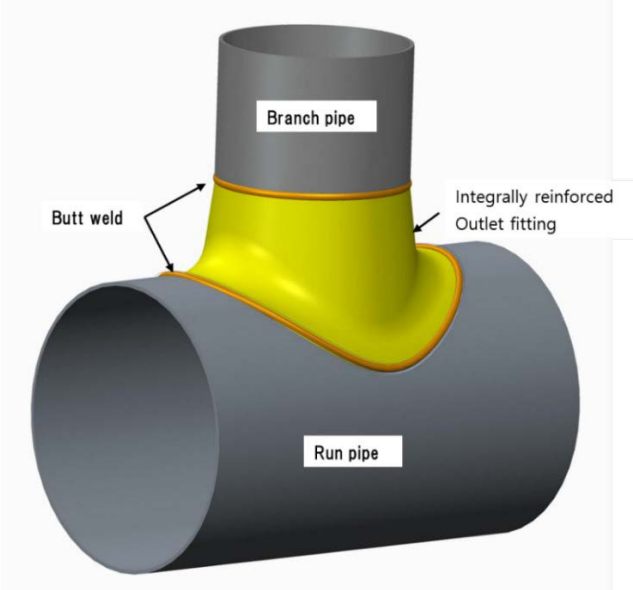

FIG. 19. Integrally reinforced outlet fitting.

3.3.1.3. Piping design practice

Some design practices for addressing vibration are given in the following list [37]:

— In the initial layout of the piping, the number of pipe bends should be minimized and a reasonable number of spring or constant support hangers and rigid supports should be used in system design.
— Pulsation dampers on the discharge piping and suction stabilizers on the suction piping may be used for pumps that produce large pressure pulses, such as reciprocating charging pumps.
— Large lumped masses such as valves and small branch lines should be supported to obtain vibration resistant designs.
— The use of fast closing valves should be minimized, and operating procedures should be written to avoid unnecessary pump trips or rapid opening and closing of control valves and cavitation of regulating/control devices.

3.3.2. Design consideration for thermal fatigue

3.3.2.1. Thermal sleeves

Thermal sleeves have been used in the design of component nozzles to protect critical pressure boundary components from the adverse effects of severe thermal transients. The high stress, pressure boundary nozzle is insulated from the different temperatures of fluid. There are several different attachment techniques for thermal sleeves such as nominally tight fit, interference fit, pressure fit, partial penetration weld, full penetration weld and so on. However, the attachment techniques should take account of the loading conditions to prevent the failure of the thermal sleeves. Figure 20 shows a typical thermal sleeve at a nozzle intersection between a branch pipe and PWR RCS piping.

3.3.2.2. Reduction or elimination of discontinuities

A notch is defined as any geometrical or material discontinuity that causes a stress or strain concentration that decreases the fatigue life. Two approaches fo addressing stress concentrations are discussed in Section 2.3.2: the stress concentration factor and the fatigue strength reduction factor. Table

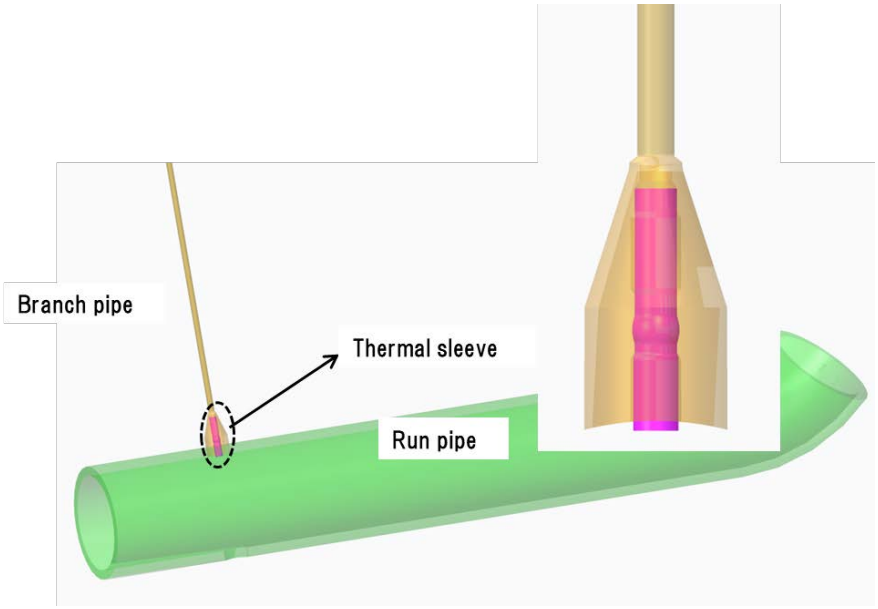

FIG. 20. Typical thermal sleeve connection on RCS piping.

TABLE 3. SOURCE OF NOTCHES [37]

Type of notch	Description	Examples
Design notch	A planned design condition based on the nature of the product or material requirements (e.g. blend radius and bimetal interface)	Changes in shell thickness, shell penetrations, and blend/fillet radii at discontinuities
Fabrication notch	Geometrical local discontinuities caused by manufacturing requirements or processes	Partial penetration welds, non-removed backing straps, as-welded condition, tooling marks and exposed porosity
Operation notch	Surface geometry discontinuities caused by load cycling or aggressive environment or not detected by shop non-destructive examination (NDE)	Corrosion pitting, head cracking, fretting or NDE indications found in-service

3 categorizes notches according to whether they are based on design, fabrication or operation. Effort should be focused on reducing or eliminating component discontinuities to the extent possible. Examples of reducing or eliminating discontinuities are as follows:

— Using bent piping with a larger bending radius instead of installing welded elbows;
— Application of full penetration welds instead of partial penetration welds;
— Flush welded condition;
— Notches remote from welds or geometric discontinuities.

3.3.2.3. Sloped routing for reduction of stratification

As described in Section 3.2.2, stratification occurs in horizontal sections of piping that contain fluids of at least two different temperatures, and in which at least one of the fluids is flowing at relatively low flow rates. To reduce the magnitude of stresses due to thermal stratification, the horizontal routing of piping can be changed to the sloped routing in the design of piping arrangement.

3.3.2.4. Material considerations

According to an Argonne National Laboratory (ANL) review on corrosion [38], the extent of the effects of the environment is considerably less for Ni–Cr–Fe alloys than for austenitic stainless steels. It can be beneficial to use an Ni–Cr–Fe alloy such as Inconel 690 for reducing the effect of environmental fatigue instead of stainless steel in fatigue susceptible locations.

The effect of the residual sulphur content on fatigue life in carbon and low alloy steels decreases in low sulphur content. It is recommended that low sulphur content (wt% < 0.005) be specified, if necessary, in fatigue design.

3.3.2.5. Provisions for possible thermal oscillations in piping

Temperature oscillations happen at normally stagnant lines connected to the RCS resulting from a swirling turbulent flow. Electric Power Research Institute (EPRI) reports [39, 40] will be used for the assessment of thermal oscillations. According to the EPRI reports, thermal fatigue will not occur, and no further evaluation is required if any of the following conditions are met:

— For top connected piping, the vertical leg is long enough such that swirl penetration cannot reach the upper horizontal sections;
— Up-horizontal lines are 50.8 mm nominal pipe size or less;
— The in-leakage path includes pressure relief or other pressure control devices;
— The vertical length between the RCS piping and down horizontal lines is long enough such that swirl penetration is not expected to extend to the down horizontal sections;
— The vertical length between the RCS piping and down horizontal lines is short enough that such swirl penetration is always expected to keep the down horizontal sections hot.

For thermal oscillations in the mixing zone, EdF has embarked on several research programmes to understand the cracking that has occurred in the operating plant and to develop acceptance criteria. According to the results, some of the corrective actions for addressing thermal oscillations in the mixing zone are required by RCC-M, B 3624.3 [28] and given in the following list:

— Eliminate, or at least grind flush, the weld;
— Reduce the surface roughness and residual stress of the internal surface;
— Implement an in-service inspection programme;
— Smooth operating procedures (low temperature differences);
— Reduce the risk of damage in these zones, e.g. by adding mixers, tapping off leaks from isolating valves or altering the route of the line to move the hot/cold mix zone to a straight section with no discontinuity.

3.4. APPROACH TO FATIGUE ASSESSMENT

3.4.1. Design fatigue analysis

The purpose of the fatigue analysis is to demonstrate that fatigue failure will not occur when the components are subjected to typical cyclic events that may occur during the life of the plant. All applied loads on the vessels and piping are considered when performing a fatigue analysis. An overview of the fatigue loading that is considered in a design is discussed in Section 3.2. Loading combinations for the design are discussed in Section 3.2.6 and Level A and B conditions, including test conditions, are considered in the analysis. For the component design to be acceptable, the CUF at the end of plant life should not exceed 1.0.

3.4.1.1. Fatigue evaluation for vessels

For vessels, the code requirements for fatigue analysis are discussed in Section 3.1.2.4. The following procedure can be used to evaluate fatigue failure due to service levels A and Level B loading, including test conditions:

— *Step 1:* Determine all loading conditions and transient events based on the information in the design specification. Those loadings should include all operating loads and events that are applied to the component, including the number of cyclic occurrences for each transient.
— *Step 2:* Calculate the total stress component for each type of loading such as pressures, mechanical loads and thermal loadings, taking into account both gross and local structural discontinuities.
— *Step 3:* Calculate the total stress from the algebraic sum of the stress components which result from the different types of loadings.
— *Step 4:* Determine the stress differences and designate the specified number of times for the complete cycle.
— *Step 5:* The cumulative effect of various stress cycles is evaluated as stipulated in steps 1 to 6 in Section 3.1.2.4.

The sample fatigue analysis for a vessel is provided in Appendix I to illustrate the application of code rules to a specific vessel, and to explain how they are applied.

3.4.1.2. Fatigue evaluation for piping

For piping, the code requirements for fatigue analysis are discussed in Section 3.1.2.6 and follow the requirements for vessels. The procedure for evaluating fatigue damage is as follows:

— *Step 1:* Determine all loading conditions and transient events based on the information in the design specification. Those loadings should include all operating loads and events that are applied to the piping, including the number of cyclic occurrences for each transient.
— *Step 2:* Calculate the peak stress intensity (S_p).
— *Step 3:* Calculate the alternating stress intensity (S_{alt}).
— *Step 4:* Determine the allowable number of cycles (N) for the S_{alt} value by entering the fatigue curve.
— *Step 5:* Determine the partial usage factor by dividing the allowable number of cycles by the imposed cycles for the set of conditions.
— *Step 6:* Calculate the CUF by summing the partial usage factor for each set of conditions.

The sample fatigue analysis for piping is provided in Appendix I to illustrate the application of the code rules to a specific system, and to explain how they are applied.

3.4.2. Environmentally assisted fatigue analysis

The effect of LWR environments on fatigue behaviour in RCS structural materials has been an issue for decades among nuclear industries and safety regulators, particularly for the 60 years design life of advanced light water reactors. In 2007, the United States NRC issued Regulatory Guide (RG) 1.207 [41] for use in the design analyses of new reactors, incorporating the fatigue life reduction of pressure boundary components due to the effects of the LWR environment. Therefore, fatigue analysis is performed considering the effects of LWR environments on carbon and low alloy steels, austenitic stainless steels and Ni–Cr–Fe alloys.

R&D programmes are continuing around the world on environmentally assisted fatigue (EAF). For example, 16 organizations from 9 European countries joined efforts in the European Commission

Horizon 2020 funded project INCEFA+[11] to obtain environmental fatigue experimental data points and derive an industrial methodology based on these results. Methods for estimating environmental effects are described in detail in Section 5.

3.4.3. Piping vibration testing

Piping vibration for high and moderate energy piping is tested during the initial test programme to confirm that the piping has been designed to withstand the dynamic effects of transient and steady state, FIV and anticipated operational transient conditions. Specific vibration testing requirements are defined in ASME OM-S/G [34]. Part 3 of this standard addresses testing requirements, acceptance criteria, qualification methods, instrumentation and vibration measurement requirements, and corrective action. For the purpose of piping design and monitoring, vibration is typically divided into two types: steady state and dynamic transient vibrations.

3.4.3.1. Steady state vibration

The piping is visually inspected, and vibration movements are measured at locations where the vibration is judged to be the most severe. The measured piping displacements are compared with allowable displacement limits that are based on the allowable stress amplitudes. If the measured piping displacements exceed allowable limits, actions are taken so that the vibration can be qualified.

3.4.3.2. Transient vibration

The piping is instrumented to measure the system response during the transient events. The measured responses are compared with analytically predicted values from the piping stress reports. If the predicted values are exceeded, the measured response is made to reduce the system response to acceptable levels.

3.4.4. Transient and fatigue monitoring

As the design life of advanced light water reactors (ALWRs) is increased to 60 years, plant fatigue monitoring is implemented to effectively monitor and manage the component fatigue usages during the plant lifetime. A monitoring of actual operation transients will make it possible to effectively eliminate various conservatisms inherent in the design basis fatigue evaluation. In general, fatigue monitoring systems utilize inputs of the on-line signals transmitted from the reactor process instruments that are already provided for evaluating the system thermal-hydraulic performance during plant operation and evaluate actual transient cycles and fatigue usages based on load-time histories at the monitoring locations. The fatigue monitoring strategies and technologies are described in Section 6 in detail.

3.4.5. Vibration monitoring

The vibration monitoring system (VMS) monitors changes in the vibration behaviour of a structure or of components, such as the reactor coolant pump, turbine generator or reactor vessel internal, and provides an alarm to plant operators if the vibration levels exceed the pre-determined set points. It has as an input the monitored variable (i.e. displacement, velocity or acceleration) at the measurement location. The system output is a signal analogous to the measured variable and is readily convertible to the appropriate physical units. A typical VMS for the reactor coolant pump is shown in Fig. 21. The reactor coolant pump VMS monitors the vibration characteristics of the pump and motor and provides diagnostic

[11] See INcreasing Safety in NPPs by Covering gaps in Environmental Fatigue Assessment, https://cordis.europa.eu/project/id/662320.

information to assist in adjusting shaft alignment, rotor balancing and in detecting shaft cracks. Part 14 of ASME OM-S/G [34] provides guides for the vibration monitoring of rotating equipment in NPPs.

3.4.1. Current regulatory fatigue issues: EAF evaluation methods

Because of the additional conservatisms required for the EAF evaluation using the F_{en} method through RG 1.207[12], backfitting environmental fatigue into the ALWR design is not feasible or cost effective without removing conservatisms inherent in the code design and analysis methods. More research and code developments are needed to bridge the gap between the required and the available technologies to explicitly consider the environmental effects as design basis requirements. The ASME Codes and Standards Committees are planning a research programme to revise fatigue design criteria for the construction of nuclear components: Section III, ASME BPVC. In the interim, two alternative approaches are considered to manage the fatigue life for ALWR components, including the combined design and operation programme, as summarized below.

3.4.1.1. Fatigue monitoring

Fatigue monitoring is carried out in the following steps:

— Perform the EAF evaluations for Code Class 1 components in accordance with the requirements of RG 1.207, and select representative monitoring locations based on results of EAF evaluations;
— Establish the plant operation programme, including fatigue monitoring and enhanced in-service inspection programmes to reassess the fatigue life of critical components, by applying the real operation transients that have occurred during the plant's lifetime;
— Implement the fatigue monitoring programme from the beginning of the plant's lifetime and include cycle counting of plant operation transients and stress based monitoring of fatigue usage factors in critical components while considering NPPs environment.

3.4.1.2. Applying the $F_{en\text{-}integrated}$ factor

Another alternative approach was developed in the framework of RCC-M, as an evaluation method for the 900 MW(e) EdF plants, as the LTO of French NPPs is governed by the consideration of EAF in their fatigue analysis.

This alternative method is based on the work presented in NUREG/CR-6909 [42]. This experimental work, which is still continuing today, has demonstrated that there is a clear interaction between the

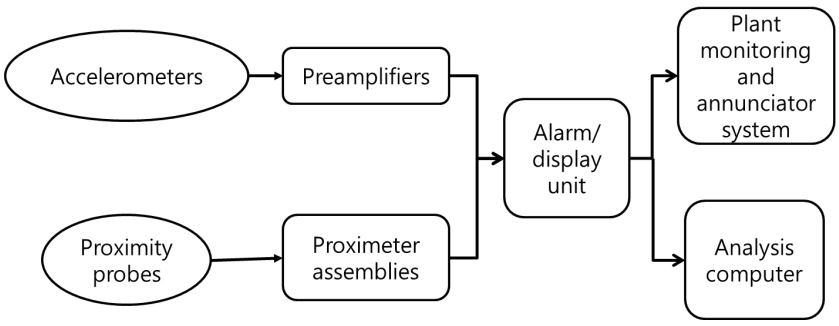

FIG. 21. Typical components of a reactor coolant pump VMS.

[12] NUCLEAR REGULATORY COMMISSION, Guidelines for Evaluating the Effects of Light-Water Reactor Water Environments in Fatigue Analyses of Metal Components, NUREG 1.207, Revision 1, NRC, Washington, DC (2018)

two aggravating effects of surface finish and PWR environment in fatigue damage. This interaction has also been highlighted independently by testing carried out in the United Kingdom by Rolls-Royce and AMEC FW [43].

The key conclusion for fatigue analyses was that there is a level of conservatism included in the estimation of F_{en} proposed in NUREG/CR-6909 [42] when the testing conditions are more severe than the plant in normal operation. As a result, it was concluded that the direct multiplication of all the aggravating effects involved in the fatigue degradation mechanisms was not accurate and it was considered acceptable to introduce a factor, $F_{\text{en-integrated}}$, which permitted the quantification of the interaction between surface finish and the PWR environment by acknowledging that the fatigue curves already cover part of the environmental effects through the factor on surface roughness.

$F_{\text{en-integrated}}$ is the explicit quantification of the mismatch between these two life estimations using two separate methods. It quantifies the margin already included in the overall fatigue model and, more specifically, the design curve in relation to covering EAF and the surface finish. As an example, for RCC-M austenitic stainless steels and cast stainless steels materials, the minimum value of $F_{\text{en-integrated}}$ is 3 based on the fatigue curve of these materials.

This method has been codified as a Rule in Probation Phase (i.e. a code case) in the 2016 version of the RCC-M [44] and has been proposed as a code case for the ASME Code (item No. 16-2731).

4. FATIGUE ASSESSMENT IN OPERATING NUCLEAR POWER PLANTS

4.1. OPERATING EXPERIENCE: GENERAL TRENDS AND ISSUES

Operating experience is useful to understand the fatigue failure mechanisms that pose a threat to various types of NPP equipment, identify the specific components and locations susceptible to each fatigue mechanism (vibrational fatigue, thermal fatigue), take cost effective measures to monitor and correct fatigue problems before they lead to forced outages, and provide feedback to plant operations and maintenance personnel on how to avoid such problems in the future.

The state of the art of transient and fatigue monitoring can help the operator understand the available options and how to operate NPPs more effectively to lessen fatigue damage. NPP operation has changed over the years as outage time is reduced and NPPs perform more on-line testing.

As NPP personnel retire, historical knowledge may be lost, which can affect the available information on fatigue failures due to system or operation. Lessons learned during initial startup and normal operation may be lost and failures that were solved in the past may occur again. Fatigue failures that have occurred at plants are typically reported through an incident report system so that other plants can review similar occurrences at their plants, through the sharing of information between utilities.

Industry experience, based on selected plant interviews, reflect the materials reliability programme (MRP) described in Ref. [45]. It addresses key issues related to fatigue damage in operating NPP piping systems and components. Vibrational fatigue failures in small-bore piping and thermal fatigue failures due to thermal stratification, stratification cycling and striping represent the most common fatigue related problems appearing in NPP equipment [45]. While less pervasive, thermal fatigue failures tend to entail greater per incident costs in areas such as weld repair and bypass leakage, and sometimes result in forced outages. Fatigue management enables utilities to identify locations susceptible to various fatigue failure mechanisms and proactively implement cost effective monitoring and corrective actions to prevent fatigue related failures.

With a few exceptions, fatigue failures in safety related systems and components continue to be rare. Fatigue in pressure retaining equipment, safety related or not, is generally detected as small cracks

or leaks; they are caught before they reach a size that could cause a major pressure boundary rupture. In these circumstances where the consequences are tolerable, fatigue is considered less of a safety issue. The fatigue failures that have occurred during service have mostly been in non-safety-related systems or in small components in safety related systems, which were exempt from detailed fatigue design requirements because reactor coolant losses from their failure would be within the capacity of normal make-up systems. Operating NPP fatigue surveys and a database of fatigue related failures at all NPPs in the United States of American (USA), in addition to a sampling of available data from overseas reactors, are included in volume 2, appendix B of Ref. [45]. The documented failures include those in pressure boundary components and related equipment, which includes reactor pressure vessel internal components. However, it excluded any rotating equipment (e.g. RCP shafts).

Another very important source of information is the current project CODAP (Component Operational Experience, Degradation & Ageing Program), which deals with operating experience insights related to fatigue mechanisms. CODAP is a continuation of the 2002–2011 Pipe Failure Data Exchange project and 2006–2010 SCAP-SCC (Stress Corrosion Cracking & Cable Ageing) project. CODAP's objective is to encourage multilateral cooperation in the collection and analysis of service experience relating to degradation and failure of metallic piping and non-piping passive components. CODAP has also established a knowledge base on metallic passive component degradation, national codes and standards addressing mechanical integrity, non-destructive examination and related R&D [46]. This project has created a basis for the exchange of international service experience and a platform for applications, including trends, patterns and risk significance determinations[13].

The risk of failure from the fatigue of various RCS components over 40 years of plant life was studied by the U.S. Nuclear Regulatory Commission (US NRC)under Generic Issue 78[14] and later integrated into the NRC fatigue action plan, which was completed and documented in SECY-95-245[15]. The impact of an additional 20 years of plant life was studied separately under Generic Issue 190[16]. The NRC concluded in NUREG/CR-6674[17] that fatigue was not a safety issue for operating plants in the first 40 years of their lives because the design and fabrication procedures for safety related NPP equipment have been quite successful in producing fatigue resistant designs.

With a number of NPPs approaching the end of their original design lives, a lot of modification to cope with fatigue failure has been carried out during the design lifetime. Thus, the number of fatigue failures in systems has been relatively low, and none have resulted in safety concerns. New knowledge regarding operating NPP service, which is gained during plant operation, reflects a wide range of options available to manage fatigue concerns in operating plants, including screening criteria to identify locations of fatigue concern, new ASME Section XI Code[18] requirements for operating plant fatigue assessments, fatigue monitoring technology and recommended practices for repairs and corrective actions when fatigue problems occur.

---

[13] See Component Operational Experience, Degradation and Ageing Programme (CODAP), https://www.oecd-nea.org/jointproj/codap.html

[14] See Resolution of Generic Safety Issues: Issue 78: Monitoring of Fatigue Transient Limits for Reactor Coolant System (Rev. 3), NUREG-0933, https://www.nrc.gov/sr0933/Section%203.%20New%20Generic%20Issues/078r3.html.

[15] See Completion of the Fatigue Action Plan, SECY–95–245, https://www.nrc.gov/docs/ML0314/ML031480210.pdf.

[16] See Resolution of Generic Safety Issues: Issue 190: Fatigue Evaluation of Metal Components for 60-Year Plant Life (Rev. 2) (NUREG-0933, Main Report with Supplements 1–34), https://www.nrc.gov/sr0933/Section%203.%20New%20Generic%20Issues/190r2.html/.

[17] See Fatigue Analysis of Components for 60-Year Plant Life, NUREG/CR–6674, https://www.nrc.gov/docs/ML0037/ML003724215.pdf.

[18] See Section XI: Rules for Inservice Inspection and Tests of Nuclear Power Plant Components, https://doi.org/10.1115/1.861981_ch29.

Industry efforts have demonstrated that most issues, including evaluation of environmental fatigue effects, are typically resolved if more accurate tracking of plant transients is performed. Such tracking needs to consider the strain rate effect and detailed temperature and oxygen measurements during transient conditions for those locations being monitored for the environmental effects of LWR coolant on their fatigue life.

4.1.1. Summary of Member State experiences

Significant attention was devoted to metal fatigue and its impact on the serviceability of operating NPP components. The survey of fatigue problems in operating NPPs contains data gathered from NPP engineers dealing with fatigue issues to:

— Obtain information on fatigue failures that might have occurred at each NPP;
— Collect industry data to determine if there are any new trends in fatigue assessment and fatigue monitoring; and
— Analyse other recent related fatigue experience.

4.1.1.1. Catalogue of questionnaires

Catalogue of questionnaires and possible answers are shown in Appendix III. Exceptions are questions for which there are only two possible responses (yes or no), and the number of individual responses is reported. Additional and more detailed processing of survey results is contained in Appendix III (survey results on fatigue monitoring and assessment), including the graphical representation of survey results for questionnaires with different options of responses. The following catalogue of questionnaires was developed and sent to experts representing Member States. Table 4 shows the summary of region country experience with fatigue assessment in operating NPPs.

4.1.2. Evaluation of survey results

The survey contains a total of 28 questionnaires, of which 20 were fully completed and 8 were incomplete and anonymous. Completed questionnaires were received from 11 countries (Brazil, Canada, China, Finland, Japan, Republic of Korea, South Africa, Russian Federation, Slovakia, Sweden and USA). The most responses were received from the North America region, represented mainly by the USA. The second most active participant in the survey was the Far East Asia region, which was represented by countries such as China, Japan and the Republic of Korea (see Table 4).

Table 4 contains the most frequent responses for the above catalogue of questions. The reason for selecting the most frequent answer was that the responses of some countries belonging to the same region could be different. The evaluation of survey results without considering the classification of survey participants in a particular Member State is given in Appendix III.

The results of our survey can be compared with the survey based on an EPRI document [47] and the OECD CODAP project [46]. The dominant fatigue failure mechanism based on the EPRI document is mechanical vibrations, as shown in Fig. 22, while the CODAP project identifies vibration fatigue as the dominant fatigue failure mechanism, as shown in Fig. 23. However, based on Fig. 23, the dominant fatigue failure mechanism is thermal fatigue.

TABLE 4. SUMMARY OF REGION COUNTRY EXPERIENCE WITH FATIGUE ASSESSMENT IN OPERATING NPPs

Fatigue assessment issue	Region					
	Africa frequent response	Latin America frequent response	North America frequent response	Central and Eastern Europe frequent response	Western Europe frequent response	Far East (Asia) Frequent response
Selection of fatigue relevant NPP components	Implementation of: plant life management, design fatigue, usage screening	Design fatigue usage screening, NUREG/CR-6260 recommendation	Design fatigue usage screening	Implementation of: plant life management, design fatigue usage screening	Design fatigue usage screening	design fatigue usage screening
Standards used for assessment of fatigue and crack growth due to fatigue	ASME, RCC-M	ASME (KTA)	ASME	PNAE G (ASME)	ASME (RCC-M, KTA, PNAE G, Swedish Guidelines with respect to CGRs)	ASME (KEPIC, RCC-M, JSME)
Data of loads for evaluation of CUF	Design loads: design transient	Combination of design and operating transient	Design loads: design transient	Realistic loads: real transients	Design loads: design transient	Combination of design and operating transient
Monitoring system of operational load data	Installed	Installed (2) Not installed (0)	Installed (3) Not installed (3)	Installed (3) Not installed (0)	Installed (2) Not installed (1)	Installed (4) Not installed (1)
Monitoring of local loads at the fatigue relevant components	None used	Permanent thermocouples	None used	Permanent thermocouples	Permanent thermocouples	Permanent thermocouples
Periodicity of fatigue evaluation	Yearly	Yearly	Other (refuelling cycle)	Yearly	Yearly	Yearly or other (from time to time)
Consideration of EAF	Yes	Yes (2) No (0)	Yes (5) No (1)	Yes (1) No (2)	Yes (3) No (0)	Yes (5) No (0)
Incident reporting system	Implemented	Implemented (2) Not implemented (0)	Implemented (6) not implemented (0)	Implemented (3) not implemented (0)	Implemented (3) Not implemented (0)	Implemented (2) Not implemented (3)

TABLE 4. SUMMARY OF REGION COUNTRY EXPERIENCE WITH FATIGUE ASSESSMENT IN OPERATING NPPs (cont.)

Fatigue assessment issue	Region					
	Africa frequent response	Latin America frequent response	North America frequent response	Central and Eastern Europe frequent response	Western Europe frequent response	Far East (Asia) Frequent response
Dominant fatigue failure mechanism	Thermal fatigue	Mechanical vibrations, thermal fatigue	Mechanical vibrations, FIVs, thermal fatigue	Thermal fatigue	Thermal fatigue	Thermal fatigue
Components with fatigue failure occurrence	Heat exchangers/ coolers, turbines, nozzles	Other or none identified	Nozzles	Other or none identified	Pipe, valves	Pipe, heat exchangers/ coolers, nozzles
Country	1 South Africa	2 Brazil	5 USA 1 Canada	2 Slovakia 1 Russian Fed.	2 Finland 1 Sweden	2 China 2 Korea, Rep. of 1 Japan

4.2. EXPERIENCES OF FATIGUE FAILURE AND ROOT CAUSES

4.2.1. Fatigue failure

As mentioned earlier, fatigue is an ageing degradation mechanism that can affect a number of components throughout the reactor coolant pressure boundary of both PWRs and boiling water reactors (BWRs). Fatigue failures have occurred at all NPPs and have caused unplanned shutdowns in some cases. The assessment of fatigue failures that have occurred in NPPs from 1990 through July 2004, along with a discussion of related issues, can be found in Ref. [47]. This document contains the results of the industry survey and review of industry databases on fatigue failures and, in addition, summarizes areas of future potential fatigue related component degradation. It also minimizes or addresses the main causes of fatigue failures. The information summarized in this publication has identified fatigue as one of the issues that may become more significant as plants age.

From a review of the EPRI work [47], it was concluded that the combined effects of adverse loadings and environmental effects might lead to more cracking than has been observed in the past with longer term operation and inspection of areas which would previously have been deemed unnecessary. In addition, the effects of power uprates have increased the occurrences of failures due to FIV and related damage to component supports. A number of cases have confirmed that FIV and acoustic loadings result in piping and component wear and failure.

In France, several incidences of cracking have been led by EdF to embark on research programmes on HCF effects due to hot- and cold-water mixing [48]. Following the incident (through-wall crack and crazing zones) in May 1998 on the principal mixing zone of the residual heat removal system at the Civaux NPP, EdF has initiated an R&D programme to understand the incident and assess the risks of damage in other mixing zones. The programme includes different sectors of developments: assessment of temperature fluctuations in mixing zones, study of high cycle thermal fatigue behaviour of austenitic steel, and development of mechanical methodologies for damage assessment and propagation of crazing zones (thermal striping).

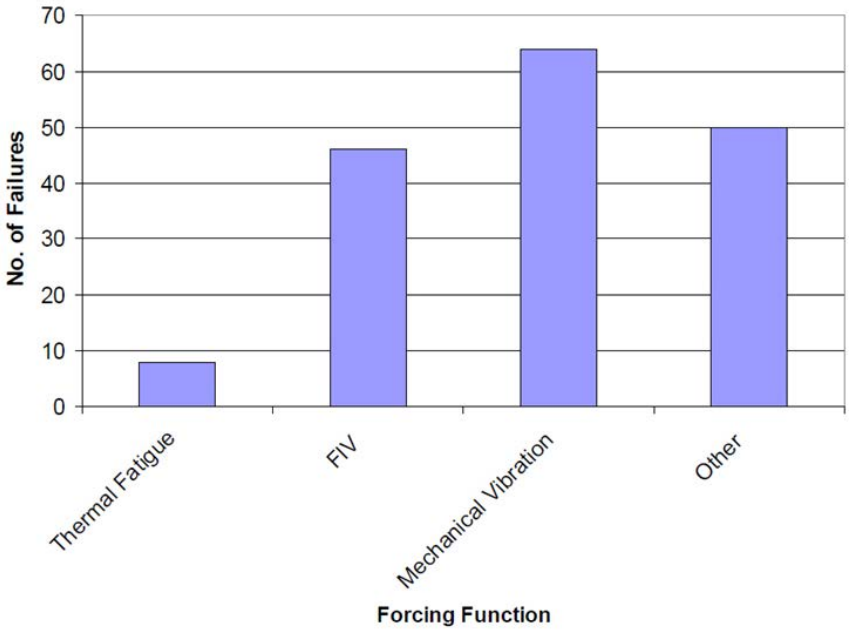

FIG. 22. Fatigue failures sorted by forcing function (FIV — flow induced vibration) [47].

4.2.2. Flow induced vibration and acoustically induced vibration

Understanding the trends in the causes of fatigue failures assists plant personnel in maximizing plant safety and availability. In addition, it allows industry to focus efforts on minimizing fatigue failures due to main causes. Based on the survey responses, database searches [47] and operating experience, the root causes of fatigue related failures can be divided into the following broad categories:

— System/plant operation;
— Design configuration;
— Other.

The causes of fatigue failures were classified into a single category, when in reality more than one cause may be responsible, but the primary cause was applied to each fatigue failure. Fatigue failures, in particular due to vibration, are typically HCF failures that occur in a short time. During initial plant startup, failures due to vibration can occur during startup testing or soon thereafter, since systems are new and may experience vibration and HCF. After the initial plant fatigue failures, there is a period of plant operation when the number of vibration failures should be fairly low and constant. The theoretical expectation for an increase in the number of vibration failures would be at some point in time, as plants approach the end of their design lives.

Figure 22, which is taken from Ref. [47], schematically illustrates the failures sorted by forcing function. The main forcing functions of fatigue failures are mechanical vibration and FIV loads. Other forcing functions include torsional vibration, water hammer loads, cavitation loads and forcing functions that otherwise cannot be identified. The major occurrence of leakage has been due to mechanical vibration induced cracking of small attached lines (primarily socket welded instrument lines of RCS piping). The FIV of the BWR steam dryer has led to cracking of the vessel attached support brackets in several plants. Also, BWR jet pumps and related components have experienced damage due to vibration.

A database such as CODAP [46] provides a strong basis for operating experience feedback concerning fatigue and many other degradation mechanisms. Figure 23 schematically illustrates the fatigue mechanisms in the CODAP database. The main fatigue mechanism with the largest number of pipe failures is low/high cycle vibration fatigue, and the second most significant is thermal fatigue. CODAP focuses attention on the following types of degradation and failure: service induced wall thinning, part through-wall cracks, through-wall cracks with and without active leakage, and significant degradation, including structural failures.

Review of the operating plant fatigue database [45] reveals that a far more common source of thermal fatigue failures is the occurrence of thermal fatigue mechanisms that were not anticipated, and therefore not addressed in the plant design process. Thermal fatigue has caused cracking in normal flowing lines where relatively colder water is injected into flowing RCS lines. Thermal fatigue has also occurred in a number of normally stagnant branch lines attached to flowing RCS lines. The source has been thermal stratification, striping and unanticipated thermal cycling [49] due to valve in-leakage in up-horizontal running safety injection line configurations and swirl penetration thermal cycling (cavity flow type thermal stratification [50]) in down–horizontal drain/excess letdown lines.

Mitigation of fatigue damage for existing components is accomplished by reducing the magnitude of the applied loads or thermal conditions, or by reducing the number of loading cycles. For thermal transients, a reduction in the rate of temperature change for extreme temperature cycles can be effective. However, the normal operating cycles are not generally the source of significant fatigue damage in NPPs. The observed fatigue cracking has generally been due to LCF or HCF as a result of operating conditions (component loading) that were not anticipated during plant design but were discovered after the plants were placed in the unspecified loading condition during operation. A typical example is BWR feedwater nozzles and control rod drive nozzles, where the effects of cold-water injection caused cracking early in the plant life.

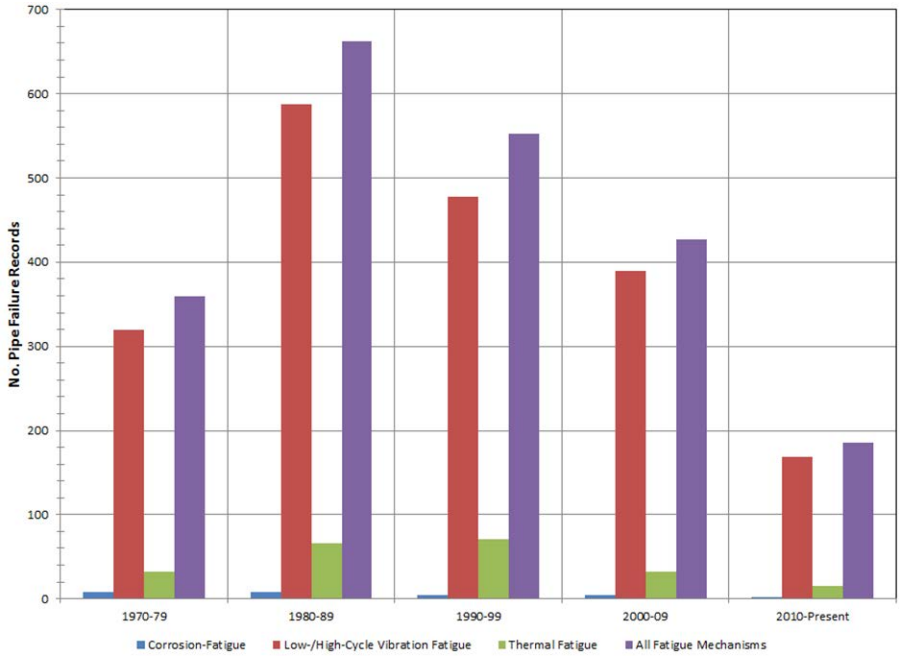

FIG. 23. Fatigue mechanisms in the CODAP database [46].

4.2.2.1. System/plant operation

System and/or plant operation is a cause of fatigue failure that occurs when a component or system is operated in such a manner that a fatigue failure occurs. Some of the typical fatigue failures that are attributed to system and/or plant operation are listed and discussed with corresponding examples here:

— Vibration;
— LCF;
— High cycle thermal fatigue;
— Thermal striping;
— Turbulence penetration;
— Environmental effects/corrosion fatigue.

4.2.2.2. Fatigue failure induced by vibration

The following fatigue failures induced by vibration have been observed [47]:

— Feedwater sample probe failure led to damage of the feedwater sparger due to foreign material intrusion into the reactor pressure vessel. The sample probe failed due to fatigue and the most likely mode of failure was mechanical HCF due to FIV, because the probe design was susceptible to vortex shedding and one of its natural frequencies coincided with the vortex shedding frequency.
— A small pressure boundary leak in a drain valve located in the high pressure safety injection system occurred at a socket weld connection on the upstream side of the drain valve. The socket weld failure was attributed to HCF.
— A review of the pump operating history showed a correspondence between the failure (leak) of the pipe and startup of the pump. The subsequent evaluation determined that resonant vibration occurred during startup and shutdown. The cumulative effects of starting up and shutting down the pump over a 13 year period appear to have exceeded the fatigue life of the drain line.

— Six failed tubes in the component cooling (CC) heat exchanger were observed to be the cause of the high CC leak rate. Two CC pumps were operated through a single CC heat exchanger. This high flow was sufficient to overexcite the tube bundle into resonance at tubes along a baffle cut, which had very long unsupported spans. These tubes failed due to fatigue due to excessive flow with cracking initiating at pre-existing stress risers.
— During an outage with water level at the reactor vessel upper flange, two small-bore pipe failures occurred on one of the residual heat removal (RHR) system loops due to HCF. The causes of the piping failures were system operation that was not compatible with the design and a design analysis deficiency. To reduce shutdown cooling flow, the RHR heat exchanger outlet valve was throttled. This mode of operation caused the flow velocity to increase at the valve outlet, creating cavitation across the valve. This condition caused excessive vibration that led to the small-bore piping failure near this valve.
— The damaged steam dryer cover plate of BWR had broken into several pieces. The root cause of the steam dryer failure was lack of industry experience and knowledge of FIV steam dryer failures. The failure of the cover plate was attributed to HCF, as a result of conditions established by the implementation of the emergency power uprate. Specifically, the higher steam flow rate increased vortex effects in the area adjacent to the cover plate. This vortex set up a standing wave of 180 Hz, which matched the natural frequency of the cover plate.
— During an outage, maintenance workers identified damage to the electromagnetic relief valve (ERV) solenoid actuator. A test laboratory for failure analysis identified mechanical indentations in the pipe caused by a chipping hammer, which is routinely used to remove slag during welding activities. The laboratory further identified weld voids within the same area at the site of the failure. ERV was dynamically tested on a shake table to confirm the proposed design modifications. Shake table testing showed that a local mode of the plunger caused the excessive bushing wear. The excessive wear was attributed to increased vibration following implementation of the extended power uprate.

Implementation of extended power uprates at BWRs has resulted in vibration fatigue failures that are mainly attributed to FIV or acoustic loadings on piping components that have led to vibration. The power uprates can also increase flow, may change the acoustical characteristics of the system and may excite a high cycle mode where resonant frequency is achieved.

4.2.2.3. Low cycle thermal fatigue (LCF)

Thermal fatigue is due to cycling stresses caused by changing temperature conditions in a component, or in the piping attached to the component. Thermal fatigue can occur for a variety of reasons in NPP pressure retaining piping and components. The original design bases for Class 1 components generally included lists of thermal transients associated with various expected plant operating conditions. Such operating transients represent a source of thermal fatigue, although it is generally not severe enough to cause fatigue failures during operation. In some cases, the number or severity of operating transients have exceeded those accounted for in the design process, and plant operating transients have become a cause for thermal fatigue concern. However, such cases are very rare.

The stress cycling that contributes to LCF is generally due to the combined effects of pressure, attached component loadings (e.g. piping moments) and local thermal stresses that result during normal operation. High thermal fatigue usage will only occur at components experiencing significant thermal transients. Step changes due to on/off flow, stratification and local thermal cycling effects are the primary causes of significant thermal transients.

Low cycle transients due to heat-up/cooldown operation are often responsible for excessive fatigue usage factor (UF). Modification of operating procedures to reduce heat-up/cooldown and flow transients are suitable mitigating actions, because a large part of UF is due to thermal loads during these operations. To reduce thermal stratification, for example in surge lines, and thus the rate of thermal fatigue, changes in operating procedures can be implemented, such as limiting the differences in pressurizer and RCS

temperatures during heatups and cooldowns. An important controlling parameter in limiting this temperature difference is the method used to form the bubble in the pressurizer [51].

Thermal stratification is famous for the unexpected thermal movement and interference with the whip restraints of the pressurizer surge line. This phenomenon in piping systems can produce LCF due to cycling between stratified and non-stratified conditions. The density of water varies significantly with temperature. When streams of water at different temperatures meet, the warmer fluid, which is less dense, tends to seek the upper portion of the pipe, while the cooler fluid remains at the bottom. The two layers can remain in thermal equilibrium without mixing under a wide range of flow conditions. Thermal stratification effects can be considered an unspecified loading condition and may occur in the horizontal portion of the long line section when the flow rate in the line is low. It generates non-axisymmetric loading that produces three effects:

— Global bending effects in the piping system that can produce modified piping thermal expansion moments remote from the regions affected by the stratification;
— Local stresses at the region of stratification temperature interface related to the temperature distribution from top to bottom being non-linear;
— Transient through-wall thermal stresses that are not uniform around the pipe circumference for stratified conditions (if the stratification occurs concurrently with thermal transient conditions).

Figure 24 shows a typical thermal stress profile at a pipe cross-section which also illustrates top to bottom bending stresses due to flow stratification (stratification Level A and Level B). Stratification can also occur in non-stagnant piping systems with low flow rates for at least some modes of operation, for example, in systems such as feedwater piping, pressurizer surge piping and pressurizer spray piping.

Although no occurrences of leakage have been identified, an issue related to surge-line stratification was identified in 1988 [52]. The issue was resolved by analysis; however, the CUFs were quite high. Environmental fatigue effects may be significant for these lines. Steam generator feedwater nozzles have exhibited cracking as a result of thermal stratification and cycling, but the high oxygen content of the feedwater for low power conditions may also have increased environmental effects.

In case of PWRs, the auxiliary spray systems draw from the charging systems and are stagnant during normal operation. If the isolation valve leaks, charging system pressure can produce flow toward the tee with the main spray system. The fluid in the auxiliary spray system is typically cold because the piping length is long enough to cool to ambient temperature. The main spray comes from the reactor coolant loop cold legs; thus, there is a potential for a significant temperature difference between the main and auxiliary spray near the tee. One potential concern is whether thermal stratification cycling could result if there is turbulence penetration from the main spray line interacting with the cold leakage flow in the auxiliary spray line.

In-leakage can occur in reactor systems. Figure 25 illustrates the phenomenon. Two conditions need to be present for in-leakage to occur: the isolation valve should leak, and a pressure gradient from the upstream to the downstream side of the valve should exist. The high-pressure safety injection system in a PWR, as an example, is driven by charging pump discharge pressure, which is higher than the RCS pressure [53].

The cause of concern is when the leakage is into normally stagnant portion of the piping system which cannot be isolated, where the leakage can interact with the hot water from the RCS. The colder leakage fluid can interact with turbulence penetration from the RCS and cause cycling at a high frequency, depending on the distance from the leaking valve to the RCS pipe. This is illustrated in Fig. 26.

Out-leakage is illustrated in Fig. 27. The leak path is from the reactor coolant loop, through an unisolable branch line, to a lower pressure system. The leak could be either past the isolation valve seat or past the valve stem packing and out of the leakoff line if one exists. Out-leakage stratification is generally steady with a limited number of cycles.

Heating and thermal stratification can also occur without valve leakage. In a long, stagnant section of pipe with a source of heat at one end, through a combination of conduction and convection, the hot water travels to the upper portion of the pipe, while losses to the ambient environment cool the fluid in the lower portion of the pipe. This is illustrated in Fig. 28.

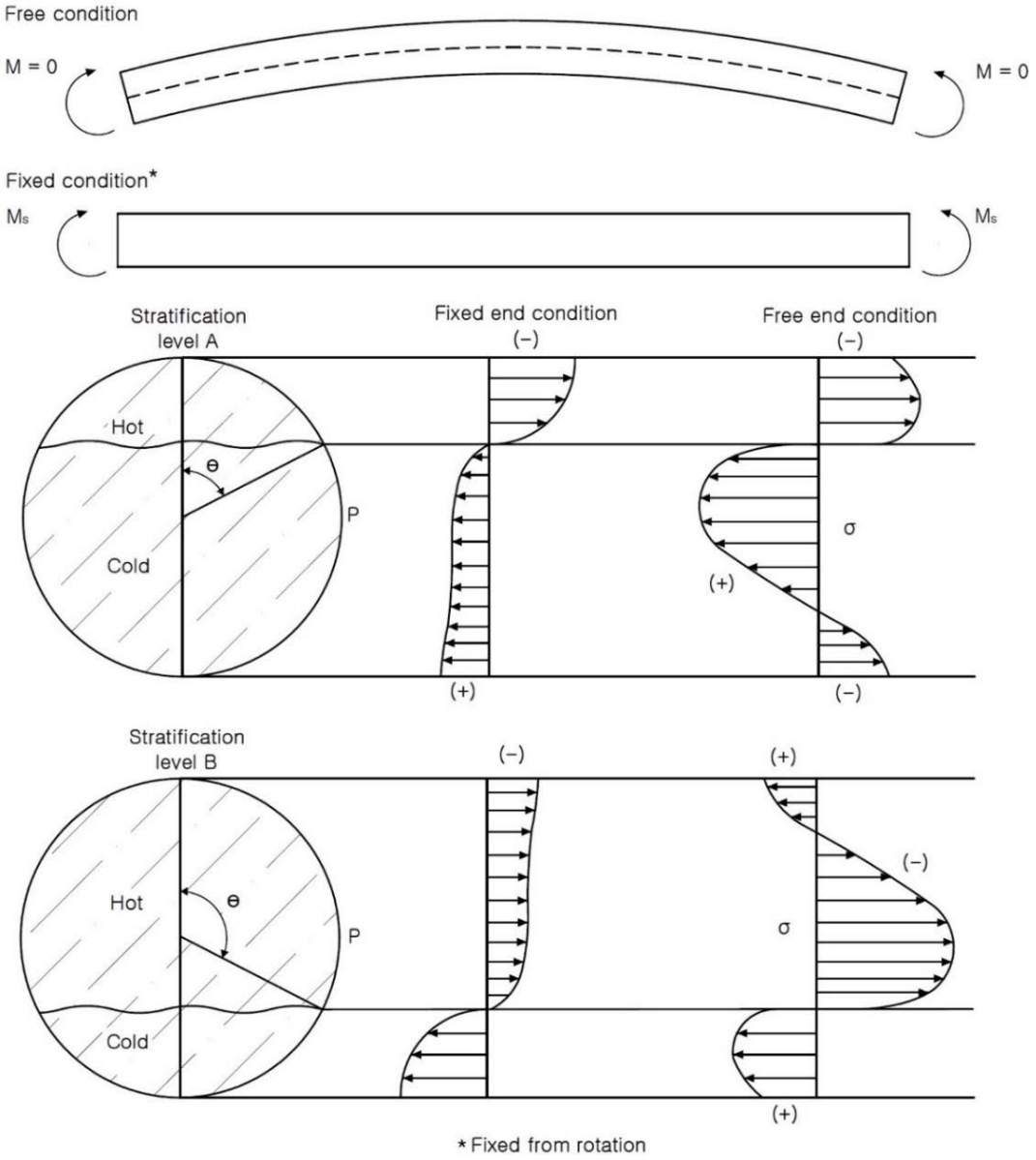

FIG. 24. Thermal stratification stress distribution (M: bending momentum) [52].

4.2.2.4. High cycle thermal fatigue

HCF concerns are generally associated with high speed rotating or reciprocating equipment, or vibrational or local thermal cycling due to hot and cold fluid mix. HCF may be thermally induced by the mixing of cold and hot fluids, where local instabilities of mixing lead to low amplitude thermal stresses at the component surface exposed to the fluid. Thermal fatigue occurs at mixing tees, where the temperature of the injected fluid is different from that of the flowing fluid. There is a number of research programmes under way in France [48, 54] to investigate the phenomena associated with mixing tee fatigue initiated after the Civaux NPP's RHR piping leakage [55]. An engineering method was developed to screen mixing zones risking thermal fatigue failures. The main outcome was the identification of several other areas at risk. The result of the research programme was the elimination of further mixing zone type failures in the EdF fleet following the Civaux NPP incident in 1998.

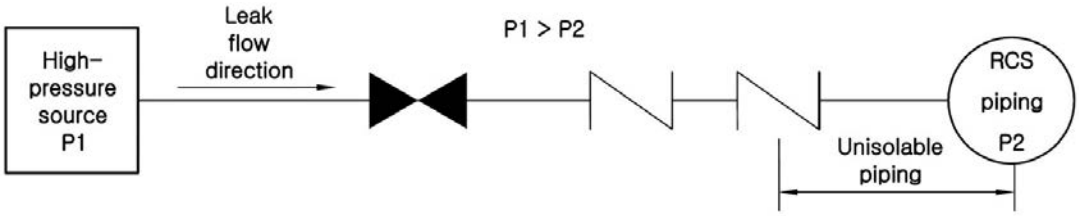

FIG. 25. In-leakage [53].

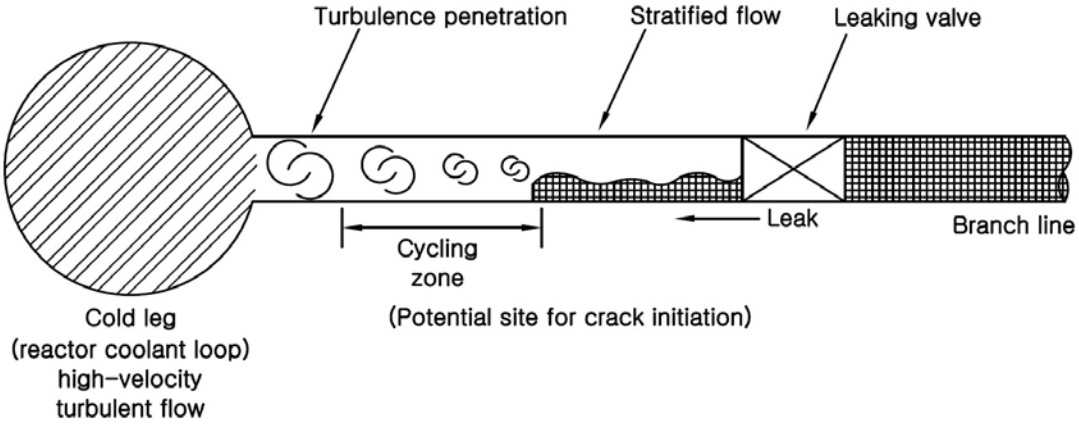

FIG. 26. Turbulence penetration and in-leakage [53].

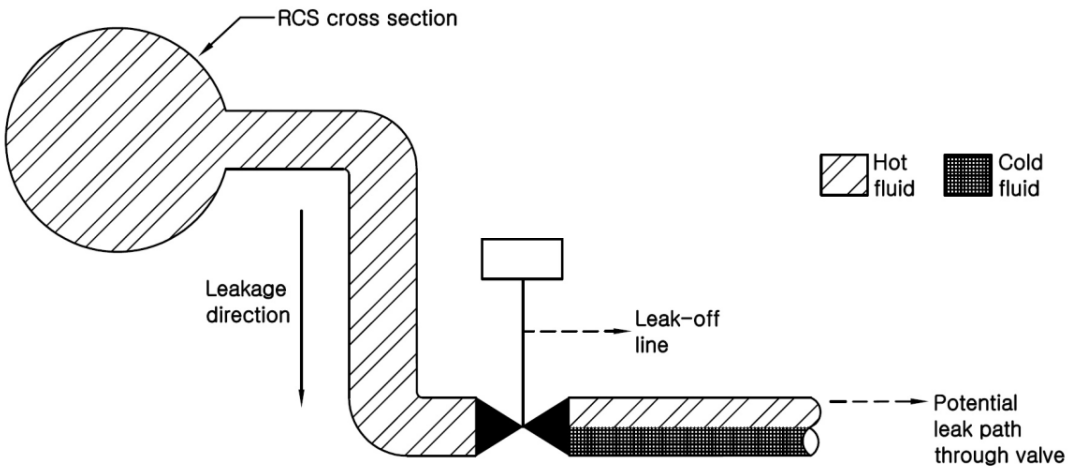

FIG. 27. Thermal stratification from out-leakage [53].

Bypass at thermal sleeves can cause a similar effect. Other potentially susceptible locations include PWR charging nozzles and BWR RHR tees, where significant thermal transients can occur in some plants and where thermal mixing occurs during normal operation or other plant operational modes.

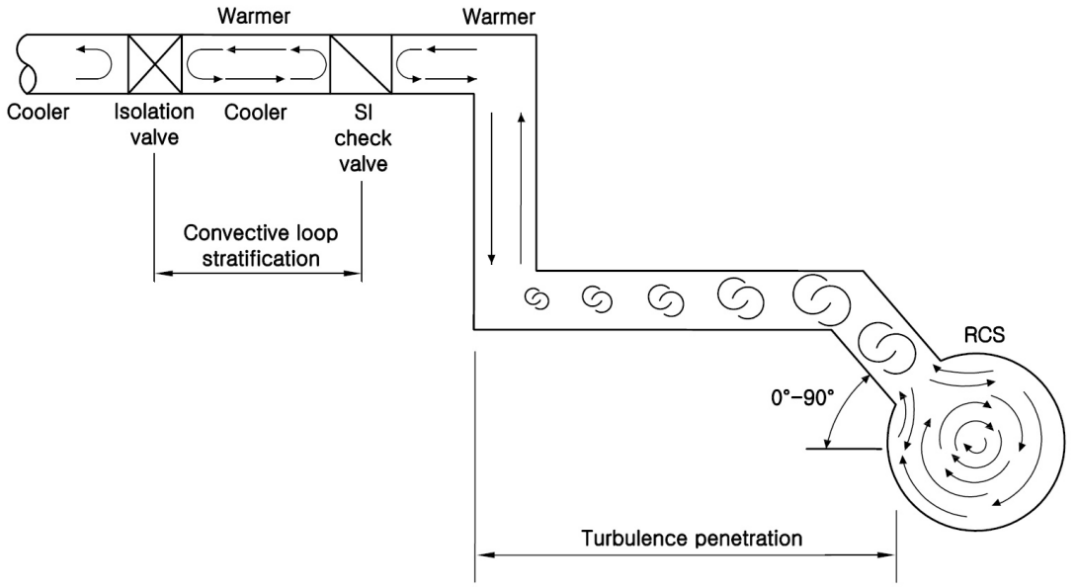

FIG. 28. Natural convection [53].

4.2.2.5. Turbulence penetration

Turbulence penetration is secondary turbulence in branch lines caused by flow turbulence from high velocity fluid in the run pipe. Figure 29 illustrates this phenomenon. Hot turbulence (vortex) penetrates from the main coolant pipe to a small-bore branch line downward, and when it reaches a horizontal portion of the branch line, the hot water is stratified with the cold water in the horizontal line. The cavity flow front (stratified plane) fluctuates due to the interference between the hot turbulence and cold-water natural convection in the horizontal line. The case illustrated in Fig. 29 is typical of drain lines in the absence of any valve leakage. The length that the turbulence penetrates the branch varies with flow conditions, temperature and the randomness of the fluid dynamics.

The phenomena are not yet fully understood, but the range of turbulence penetration cycling length is approximately 5–25 branch pipe inside diameters [49]. The latest information can be found in Ref. [56], which provides improved assessment criteria that will allow utilities to determine if normally stagnant non-isolable branch lines attached to RCS piping might be affected by thermal fatigue, resulting from turbulence/swirl penetration effects, including interaction with valve in-leakage. Based on this assessment, lines may be shown to be unaffected, or specific locations may be identified for examination or further evaluation. Effective non-destructive examinations, monitoring and other actions can be taken to manage thermal fatigue at susceptible locations.

Leakage has been reported at Mihama-2 NPP in Japan and at TMI-1 and Oconee-1 NPPs in the USA. No leakage has been reported at Angra NPP in Brazil, but there has been significant temperature fluctuation based on temperature measurements on the outer surface of the RHR branch line [50].

4.2.2.6. Thermal striping

Thermal stratification can induce local cyclic stresses in the portion of the pipe near the inside surface and adjacent to the interface between the hot and cold coolant layers, if the flow rates are sufficiently high. These stresses are caused by oscillations of the fluid temperature at the interface resulting from interfacial mixing of the hot and cold fluid layers. Such interfacial mixing results in a phenomenon called ‘thermal striping’. The magnitude of the thermal striping stresses is the highest on the inside surface and reduces rapidly through the thickness. The HCF damage caused by these stresses is limited to the pipe

inside surface adjacent to the fluid interface, so it is unlikely to cause the crack to grow through the wall in the absence of other loadings.

4.2.2.7. Environmental effects/corrosion fatigue

Corrosion effects remain an important concern in NPP fatigue. Corrosion fatigue refers to the interaction between a corrosive environment and cyclic stress. The combination of the two acting together can be more detrimental than either acting separately. That is, cyclic stress accelerates the corrosive action, and corrosive action accelerates the mechanical fatigue process [55].

Figure 30, from Ref. [45], illustrates the S–N behaviour of a typical engineering material in various environments. As expected, the vacuum and air curves are very close. If the specimen is 'pre-soaked' in a corrosive environment, a moderate detrimental effect is observed, especially at the HC end of the curve. Finally, if the corrosive environment is maintained throughout the test, the most drastic effect is observed. The significance of the corrosive effect also depends on how the environment is applied. For example, specimens submerged in water have better corrosion resistance than those subjected to water spray, drip or wicking action or to those submerged in continuously aerated water. This is due to the great importance of oxygen and the formation of oxide films in the corrosion fatigue process.

4.2.2.8. Environmentally assisted fatigue

The code fatigue design curves were based on room temperature testing in air, so they do not explicitly address environmental effects associated with LWR coolant. Laboratory data indicate that the reactor environment leads to less fatigue resistance of materials than is represented by room temperature testing in an air environment. Environmental fatigue involves two primary elements:

— The effects of a reactor water environment on the overall fatigue life of reactor components;

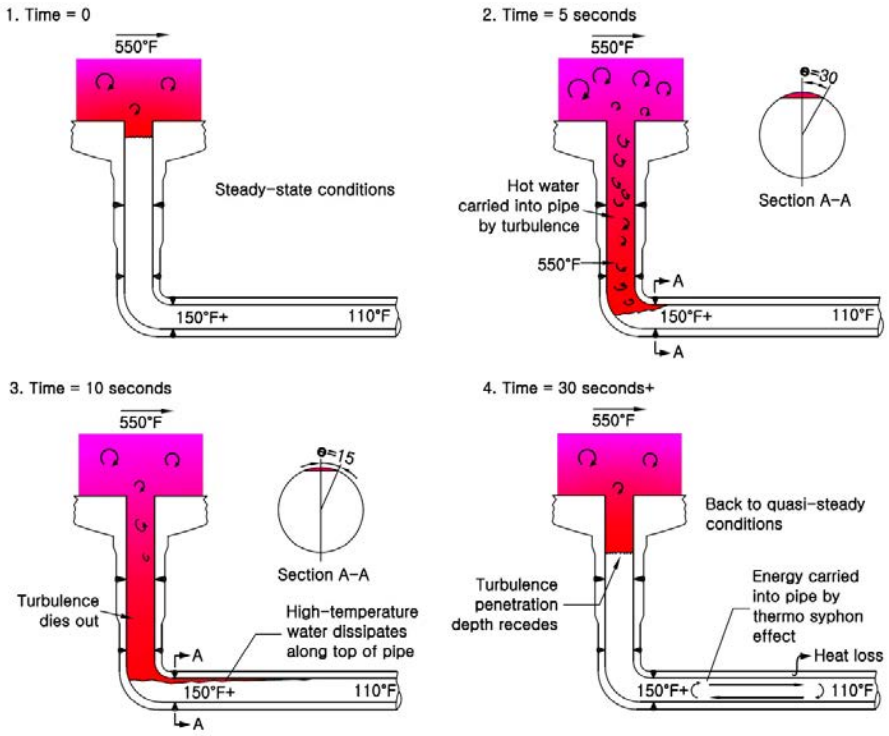

FIG. 29. Turbulence penetration (cavity flow type thermal stratification) [53].

— The potential accelerated growth of an identified defect due to reactor water environments.

The area of environmental fatigue is still evolving and is under considerable discussion in the technical community, code bodies and regulatory agencies.

Based on testing both in Japan and in the USA, the fatigue life in an LWR environment was determined to be adversely affected by certain water chemistries, strain amplitudes, strain rates, temperatures and material sulphur contents for ferritic steels. To determine the effect of the environment in operating NPPs during the current 40 years' licensing term and extended period of 20 further years, the Idaho National Engineering Laboratories (INEL) evaluated fatigue sensitive component locations and documented their results in NUREG/CR-6260 [57]. Continued research led to changes to the fatigue curves utilized in deriving the results presented in NUREG/CR-6260 [57]. The proposed environmental fatigue correlations are presented in NUREG/CR-6583 [58] for carbon and low alloy steels and in NUREG/CR-5704 [59] for austenitic stainless steels. The latest environmental fatigue correlations for reactor materials are presented in NUREG/CR-6909 Rev. 1 [60].

An evaluation of the implications of LWR environments on reducing component fatigue for 60 years plant life, documented in NUREG/CR-6674 [61], concluded that the environmental effects of reactor water on fatigue curves made an insignificant contribution to the core damage frequency for their plant design protection systems. However, the frequency of pipe leakage was shown to increase in some cases. More details on the technical aspects of environmental effects are given in Section 5.

4.2.2.9. Design configuration

The main fatigue failure cause can be considered in the design configuration on the basis of the information processed in Ref. [47]. This includes the original design of the system or component that did not properly account for steady state vibration loads. Design modifications to a system or component that result in fatigue failure are also included in this category. Some of the design modifications are due in part to replacement of components that appear to be the same but have slight differences that change the natural frequency of the component or system. Some of the typical fatigue failures that have been attributed to design configuration include [47]:

— *Heater drain pump sample line failure:* A leak was discovered in a BWR heater drain pump sample line on the valve side of the pipe at the toe of the bimetallic weld. The root cause of this event

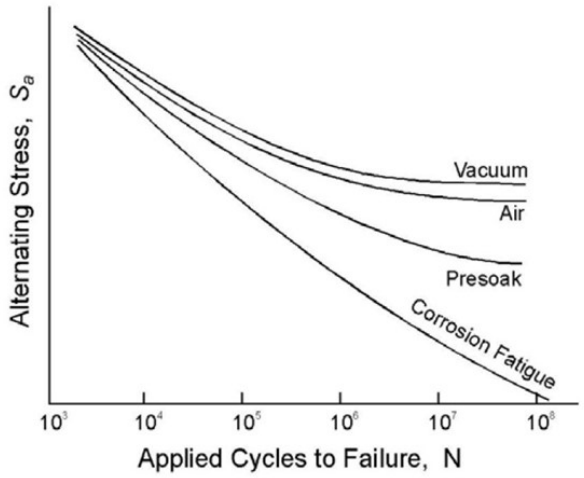

FIG. 30. Illustration of the effect of various environments on fatigue S–N curves [45].

was determined to be that the design of the piping components was inadequate for the operating conditions (susceptible to low stress HCF).

— *Main turbine electrohydraulic control (EHC) leak*: A leak was determined to be from a cracked piece of electrohydraulic control tubing on one of the turbine control valves. The root cause of this event was determined to be the design of the electrohydraulic control tubing that created a situation where operational vibrations led to the failure of the tubing. Subsequent analysis was performed, and all tubing socket welds were replaced with modified fillet welds that reduced the stresses in the socket welded joints.
— *Main steam line support*: This was caused by fatigue during normal plant operation at a Westinghouse type PWR. A section of the steel support had torn away from the remaining structure at the location of the welded bracket to a wire energy absorbing rope restraint. The loads on this support were finally attributed to FIV in the piping system due to the configuration of the main steam header located in the turbine building.
— *Extraction steam expansion joint failures*: Debris from the failure of an extraction joint at a Combustion Engineering type PWR caused condenser tube leaks. The two 457.2 mm expansion joints and their associated piping failed as a result of vibration induced HCF. Corrective actions included the installation of a new expansion joint design with natural frequencies that are different from the excitation frequencies.

The specific design of the piping system is also a critical factor in determining its susceptibility to thermal fatigue since the particular layout may promote thermal stratification and thermal striping. Introducing a definite slope and limiting stagnant horizontal lines is strongly recommended for mitigation of thermal mixing concerns. Design modifications that have been implemented to suppress thermal stratification in surge lines include a sloped section of the pressurizer surge line in place of the horizontal portion to mitigate the thermal loads caused by stratified flows [51].

The horizontal portion of the feedwater piping has a high potential for thermal fatigue cycling arising from thermal expansion, thermal shock, thermal stratification and thermal striping loading. The feedwater nozzle area represents the highest fatigue location in the horizontal piping, because besides having as severe a geometrical discontinuity as any other location in the horizontal section, it experiences the highest thermal transient stress from the shock of steam generator reflood flow when the feedwater flow is terminated.

EPRI has performed several thermal fatigue studies, which are described in greater detail in Section 4 of Volume 2 of Ref. [45]. These studies have, for the most part, focused on normally stagnant branch lines connected to the RCS. These branch lines fall into two categories:

— Top or side connected horizontal lines, such as safety injection lines;
— Bottom connected lines, such as drain and RHR suction lines.

The potential of mixing tee thermal fatigue related to RHR system operation has also been examined.

During initial plant design, it had been assumed that top or side connected horizontal lines would be kept at RCS temperature due to convection, and that the bottom connected line would be at containment temperature since they would not be warmed by convection from the RCS. In reality, RCS flow can penetrate into branch lines (swirl penetration), causing another source of thermal loading. Also, valve leakage in the top or side connected horizontal lines can provide an unexpected source of cold fluid for the swirl penetration to interact with.

The horizontal piping near the RCS can experience thermal stratification, with warmer water from the RCS on the top and colder water (stagnant water for the bottom lines, or leakage flow for top or side lines) on the bottom. Because the top of the pipe is expanding more than the bottom, stratification causes the piping to bend downward. This displacement is resisted at supports and anchor points, causing unanticipated forces and moments in the piping. Proper support configurations can eliminate these mechanically and thermally induced stresses.

Mitsubishi Heavy Industries has been involved in collecting information about field experience, domestically and abroad, on HC thermal fatigue on PWR piping, and in studying the radical measures which should be applied at the design stage of construction or remodelling of operating NPPs. It started an R&D programme in 2003 to develop a countermeasure against cavity flow type thermal stratification [50]. It has also focused on cavity flow characteristics which penetrate the branch line in the form of spiral vortex. Several structural candidates have been discussed and finally a vortex breaker was selected (see Fig. 31). It is installed in the branch line near the branch point from the main pipe and reduces the vortex energy significantly, forces the hot water to stop just downstream of the structure, and avoids the stratification and its fluctuation occurring at the elbow or bender. It is a mono-piece structure and has four vortex restriction fins inside.

4.2.3. Other potential fatigue issues

Although the endurance limit of carbon steel is lower than that of stainless steel, test data have indicated that some of the fatigue strength reduction factors of stainless steel are higher than carbon steel.

4.2.3.1. Construction, materials and fabrication

Construction is a cause of fatigue failure that occurs when the construction of the component or system has a defect (e.g. weld defect). Some of the typical fatigue failures that have been attributed to construction include [47]:

— A main generator hydrogen supply line leak was discovered in a PWR on a 63.5 mm nominal pipe size carbon steel socket weld. The crack initiation appears to be due to a combination of normal

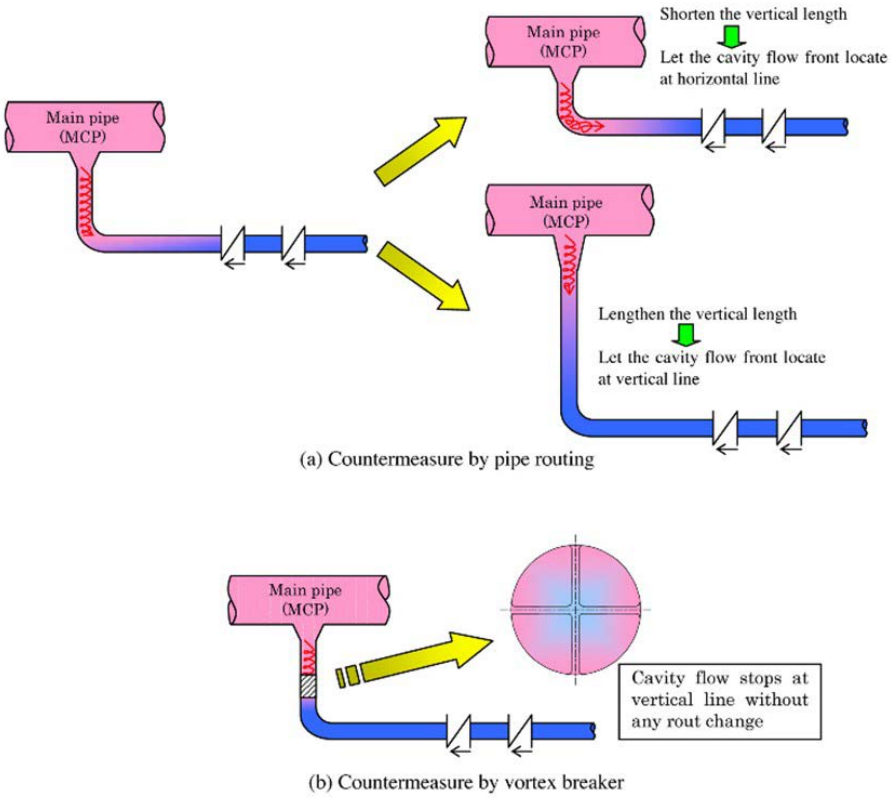

FIG. 31. Countermeasure concept for cavity flow type thermal stratification [50].

background turbine vibration, the design of the socket weld, and a weld defect in the root such as lack of fusion.

— A vent line socket weld failure occurred in the RCS of a PWR on a 19.05 mm vent line socket weld. The apparent cause of the crack was a construction groove, evident at the toe of the weld, which induced a stress riser. After several years of operation, the stress riser initiated a fatigue crack.
— A reactor recirculation sensing line socket weld failure at a BWR caused an increase in unidentified leakage. The root cause was attributed to HCF crack propagation resulting from severe FIV as a result of reactor recirculation pump operation at or near the sensing line natural frequencies, coupled with mechanical and welding induced residual pipe stresses.

A large variety of materials are used in major components potentially affected by fatigue: RCS piping and fittings — carbon steel, low alloy steel, stainless steel and cast austenitic stainless steel; reactor pressure vessel (applicable to both PWRs and BWRs); low alloy steel; wrought stainless-steel cladding; wrought nickel based penetrations; and various weld materials depending on the parent material used.

The ASME fatigue curves for stainless and carbon steel begin to diverge above 10^5 cycles. Although the endurance limit of carbon steel is lower than that of stainless steel, test data have indicated that some of the fatigue strength reduction factors for stainless steel are higher.

Structural or material discontinuities may indicate a high CUF. Components typically associated with high stress indices that result in multiplication of the stress relative to those that occur in most of the adjacent piping sections. For pipe to valve welds (or other changes of thickness) or bimetallic joints, high secondary stress ranges can occur even for slow transients. The metallurgical or geometric discontinuities at the toes of the welds (such as undercut or non-smooth transitions) promote a tendency for toe failure which greatly reduces fatigue life. By means of enhanced fit-up procedures it is possible to minimize residual stresses.

4.2.3.2. Effect of socket welds on vibrational fatigue life

Failures of small-bore piping connections occur frequently at NPPs in the USA, resulting in degraded plant systems and unscheduled plant downtime. Fatigue related failures are generally detected as small cracks or leaks before major pressure boundary ruptures occur. The critical component in small-bore piping (less than 51 mm nominal pipe size) with regard to HCF is the socket weld (socket welds are used extensively for small-bore piping and fittings). See Fig. 32 and Fig. 33 for socket welding fitting.

The fatigue failures in the socket welding flanges usually occurred as circumferential cracks in the pipe and began on the outside of the pipe near the toe of the fillet weld [62]. It is also found, contrary to the prior study by Markl et al. [62], that a significant number of the failures occurred in the root of the fillet weld rather than at its toe, but only in such cases which are associated with weld defects such as lack of penetration at the root of the weld. Lack of penetration at the weld root was found to have a very significant effect on failure initiation at the weld root [63].

EPRI started a socket weld testing programme [64] to improve socket weld design and fabrication practices to allow these welds to better resist against HCF. Analytical results have demonstrated that the socket weld leg configuration can have an important effect on its HCF resistance, with longer legs along the pipe side of the weld greatly increasing its predicted fatigue resistance. Other potentially important factors influencing fatigue life include residual stress, weld root and toe condition, loading mode, pipe size, axial and radial gaps and construction materials.

On the basis of testing, it was concluded that socket welds with a 2 to 1 (2 1) weld leg configuration (weld leg along the pipe side of the weld equal to twice the code required weld leg dimension) offer a significant HCF improvement over standard ASME Code socket welds. This weld design offers superior improvement in fatigue resistance over the replacement of socket welded fittings with butt welded fittings.

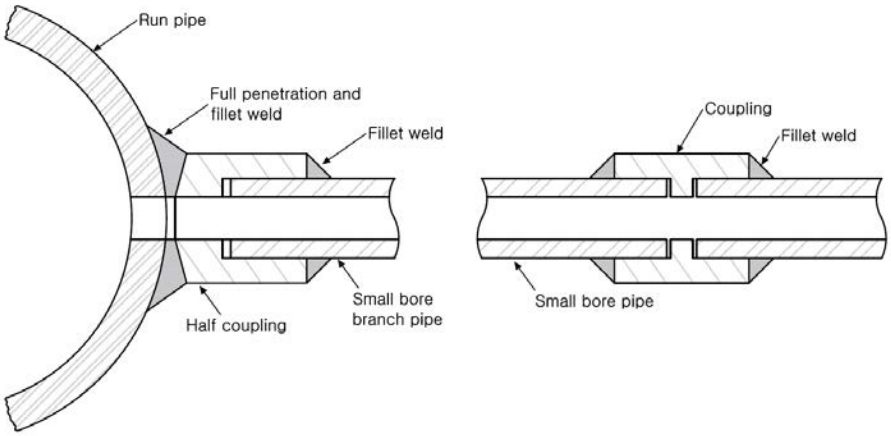

FIG. 32. Examples of socket welding fittings [45].

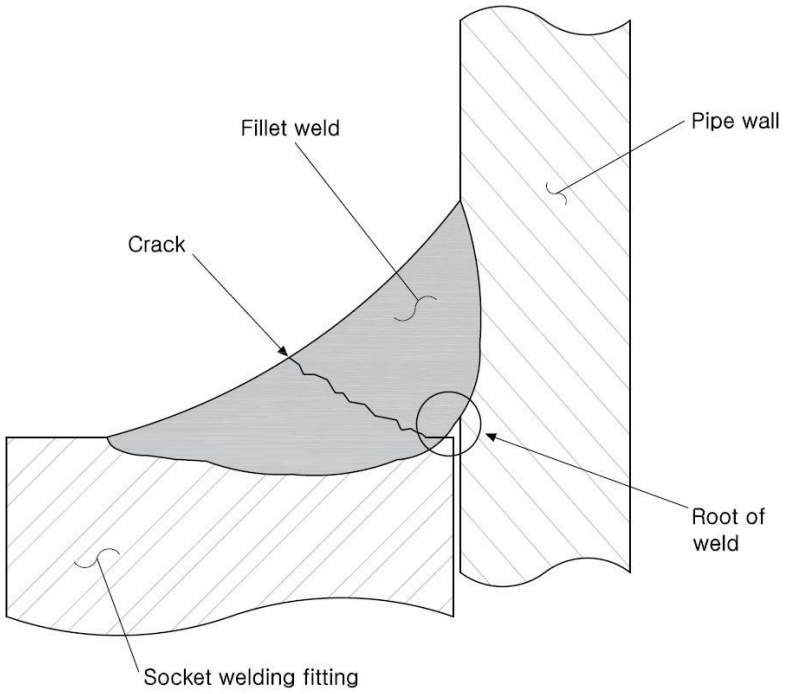

FIG. 33. Sectional view of cracked fillet weld [45].

4.2.3.3. Relief valve chattering

Piping fatigue can result from many sources, including equipment vibration, FIV, etc. One potential source of excessive fatigue loading on piping is liquid relief discharges that result in valve chatter [47] (opening and closing of the valves). The valves can be damaged due to the internal hydraulic loadings associated with the phenomenon of valve chatter. Relief valves are more susceptible to chatter (high frequency oscillation of the valve disc) when the valves lift under liquid conditions. The potential for chatter is higher for relatively colder water and for long inlet piping. During a chattering event, the relief valve inlet piping can be subjected to a large number of cycles with high pressure oscillations. These vibrations can also affect the welds of nearby attached piping.

4.2.3.4. Maintenance and testing

Maintenance is another cause of fatigue failure that occurs when a system or component fails after refurbishment or testing. Some of the typical fatigue failures that have been attributed to maintenance include the following [47]:

— High vibration levels on the reactor feed turbine pump were experienced after maintenance activity to balance the rotor. During startup of the pump the turbine experienced vibration levels higher than pre-balance activity levels.
— The diesel generator tripped on high turbocharger vibration while being loaded during the monthly operability surveillance test at PWR, and strong vibration occurred at the right bank turbocharger.

Pressure and tightness tests are usually carried out for NPP pressure retaining piping and components. These tests are defined by the design code and are carried out according to the NPP's procedures. The tests are in accordance with good practices. Pressure and tightness tests prove the functionality of the pressure retaining barrier. In some NPPs, the pressure and tightness tests are parts of the in-service inspection programme. When the tightness is compromised, then part of the repair procedure should be a root cause definition. If the root cause is an ageing effect, then it is necessary to use operational experience feedback in the ageing management programme.

4.3. AGEING MANAGEMENT APPLICATION ON FATIGUE

The task of managing plant ageing is assigned in most Member States to an engineering discipline called plant life management (PLiM), which applies a systematic analysis methodology to the ageing of structures, systems and components. Specifically, PLiM can be defined in one sentence as the integration of ageing and economic planning to maintain a high level of safety and optimize plant performance by addressing extended life ageing issues, maintenance prioritization, periodic safety reviews (PSRs), education and training [65]. In 2015, the IAEA issued a technical report, entitled Plant Life Management Models for Long Term Operation of NPPs, that addressed the various PLiM models for long term operation [65].

PLiM is part of ageing management and often consists of a special ageing management programme and preventive ageing measures. A special ageing management programme is a component related ageing management programme that limits the potential for radiological release to the environment in the case of an accident. Components are evaluated to ensure the proper operation of certain safety functions during the service life of the plant. Preventive ageing measures support lifetime management programmes and are applied to certain mechanical, electrical, I&C and civil structural SSCs within the plant.

Fatigue constitutes one relevant ageing mechanism. Within the scope of ageing management, the damaging process caused by fatigue mechanisms is of major concern. This results in the tightening of fatigue rules due to the consideration of EAF within the fatigue process. For the renewal of operating licences, PSRs, service life extensions, etc., different approaches are taken depending on the country or continent concerned. However, the goal is the same: to guarantee the safe operation of plants over the long term to an appropriate level of reliability [66].

These processes correspond to the main steps recommended by the IAEA [65]:

— Preliminary studies;
— Scoping and screening of components;
— Ageing management reviews by component;
— Implementation of solutions and new procedures [66].

The ageing management of NPP components is a major issue. As regards fatigue assessment of nuclear components, stringent safety standards require the consideration of new parameters within the framework of the fatigue analysis process:

— New design fatigue curves, consideration of EAF parameters;
— Stratification effects which might not have been considered in the original stress reports based on the design transients of plants.

In this context, the monitoring of operational loads as well as the storage of the acquired data should start at the beginning as part of a consolidated fatigue monitoring approach [67]. Detailed explanation on fatigue monitoring is given in Section 6. This includes a detailed discussion of applicable fatigue screening criteria [68].

4.3.1. Overview of fatigue screening criteria

Fatigue screening criteria are addressed both for thermal and vibrational fatigue in Ref. [68]. The screening process begins with a review of plant systems that have experienced fatigue problems in the past, based on prior industry records and an operating plant fatigue database. In this sense, the screening process is based on experience.

Thermal fatigue screening relies on previous thermal fatigue studies and operating experience. Plant systems where thermal fatigue problems have occurred are reviewed. Furthermore, simple 'system level' screening criteria are applied to other systems. All identified susceptible systems are evaluated with respect to more detailed criteria for screening individual components or pipe segments for typical thermal cyclic loading conditions. Based on the review of the operating NPP fatigue database it was revealed that thermal fatigue mechanisms that were not anticipated and therefore not addressed in the plant design process constituted a common source of thermal fatigue failures. These include thermal stratification, striping and unanticipated thermal cycling [68].

Similarly, vibrational screening relies on past experience concerning components and systems that have had a high incidence of vibrational fatigue failures. Other potentially susceptible components are identified, based on their geometry and proximity to sources of vibration. System walk downs are recommended for visual examination. Criteria are presented in the form of acceptable vibration amplitudes for such measurements [68].

Fatigue screening criteria and related fatigue monitoring locations are discussed in more detail in Section 6 and Ref. [68].

4.3.2. Overview on repair and replacement

Regarding the ASME Code, general rules and requirements for repair and replacement are part of article IWA-4000 and non-mandatory Appendix J of Section XI, and further referenced articles of Sections III and IX. Within the application scope of the ASME Code these rules have become the standard rules used for all in-service repairs, replacements and modifications to all ASME Code classes for NPP equipment. Methods covered include welding, brazing and metal removal [69]. Typical repair activities include:

— Removing weld or material defects;
— Reducing the size of defects to a size acceptable to the applicable flaw evaluation criteria;
— Addition of weld or braze material.

Typical replacement activities include:

— Spare and renewal components such as supports, parts, appurtenances, subassemblies, and material.

— Addition of components and modifications to a system (rerouteing of piping would be considered a system change).
— Reasons for replacement may include discrepancies detected during in-service inspection, change in regulatory requirements, design changes to improve equipment service, changes to improve reliability, damage, failure during service, personnel exposure, economics, end of service life or discrepancies detected during maintenance.

All repair/replacement activities are based on an individual programme and plan. These should include the following elements [69–71]:

— Applicable Code edition, addenda and Code cases of section XI (both those used for construction of the items being repaired or replaced and to be used for repair or replacement).
— For a repair, the description of the flaw and the NDE method used to detect it.
— For a repair, the methods used for flaw removal and measurement of the cavity resulting from the removal process. Also included are the requirements for reference points during and after the repair.
— Description of the work to be performed.
— Applicable procedures and requirements for welding, heat treatment, NDE, tests and material.
— Application examination, test and acceptance criteria to be used to verify acceptability.
— Intended life of the repair or of the item to be used for replacement (when less than the remainder of the design life of the item).
— For replacements, whether application of an ASME Code symbol stamp is required.
— Records to be maintained.

Further related issues are specification requirements, verification of acceptability, inspection, code applicability, material and welding requirements. Repairs by defect removal are regulated in ASME section XI [69].

4.3.3. Current regulatory fatigue issues

According to IAEA Safety Reports Series No. 57, Safe Long Term Operation of Nuclear Power Plants[19], the revalidation of safety analyses that involve time limited assumptions is documented in an update to the safety analysis report to demonstrate structural integrity against thermal and mechanical fatigue and assess structure and components from the point of view of fatigue damage.

5. ENVIRONMENTAL EFFECTS ON FATIGUE LIFE

5.1. OUTLINE OF PHENOMENA

There was a long-held view that the fatigue endurance of structural materials in the coolant of LWRs was not much different from that in the air atmosphere because of the use of high purity water. This view has been corrected by many studies on the fatigue behaviour of structural materials in a high temperature water environment, especially after landmark reports were published in the late 1980s and early 1990s [72, 73].

Many experiments have been carried out since then, resulting in a large quantity of experimental data which clearly show the reduction of fatigue lives in the high temperature water environments of LWR

[19] INTERNATIONAL ATOMIC ENERGY AGENCY, Safe Long Term Operation of Nuclear Power Plants, Safety Reports Series No. 57, IAEA, Vienna (2008).

plants, in comparison with fatigue lives in the normal air atmosphere at the same strain or stress range and temperature. All the materials constituting the pressure boundary, including austenitic and ferritic steels as well as a few types of Ni–Cr–Fe alloys, were found to be susceptible to this environmental effect to a larger or smaller extent.

Examples of fatigue data for the former two types of materials are shown in Fig. 34 and Fig. 35 shows the fatigue data taken in the air, whereas data taken in high temperature water environments are displayed in Fig. 36 and Fig. 37. The fatigue data in the air shown in these figures include those taken at room temperature as well as those at high temperatures up to 400°C, but the temperature dependency is not clear, at least within this temperature range, in both types of materials. This considered to be consistent with relatively stable monotonic tensile properties within this temperature regime.

On the other hand, a much larger variety of failure lives appears in the test data taken in the high temperature water, showing a clear trend of reduction of fatigue lives in comparison with the in-air data taken at the same strain range. A large variety in the lives also suggests the involvement of many factors, even if these data were taken in relatively similar environments representing plant conditions.

A factor of reduction from the best-fit curves for in-air data reaches about 50 points in the case of austenitic stainless steels and approximately 100 points in ferritic steels, but there are some data which do not exhibit significant life reduction. As will be shown later, temperature and strain rate are two important parameters that control the amount of life reduction, indicating that life reduction is basically aa thermally activated process likely related to the diffusion of certain atoms.

As expected from the nature of the environmental effect, the quality of water also influences the fatigue lives of all materials to a large or comparably smaller extent. In particular, the effect of oxygen content has been studied extensively as oxidation seems to play an important role in accelerating the process of fatigue damage, especially in the case of ferritic steels.

The main mechanism for environmental effects is oxidation and the resolution of slip bands formed near the specimen surface before crack initiation and near the crack tip during crack growth in the ferritic steels. The involvement of hydrogen atoms has also been pointed out in the case of austenitic stainless steels. The chemical compositions of the material are also known to influence the magnitude of environmental effects in some cases through involvement in relevant chemical reactions. These aspects also constitute an important factor controlling the amplitude of the environmental effects on fatigue characteristics.

Relevant test data on environmental effects on fatigue behaviour as well as the efforts for their modelling are reviewed and summarized in this section.

5.2. METHODS FOR ESTIMATING ENVIRONMENTAL EFFECTS

5.2.1. Basic principles

Fatigue lives are influenced by a number of factors so their effects need to be properly taken into account in evaluating the structural integrity of susceptible components. Past studies have identified the principal parameters that give a clear and strong influence on the life and their involvements have been quantified. In all the materials studied, temperature and the strain rate have a clear influence on the amplitude of life reduction. Dissolved oxygen content in the water was also found to give a non-negligible effect. It has also been shown that the fatigue lives show a systematic dependency on the sulphur content in the case of ferritic steels.

There are three or four parameters involved and thorough optimization of their effects with some interactions or a combination would not be an easy task. Therefore, some simplification assuming the absence of complex interaction or combined effects is required to develop the expressions which provide the amount of life reduction. As a result, life reduction is expressed by the simple products of functions of these selected parameters, including the strain rate and temperature as common parameters for all the materials of concern.

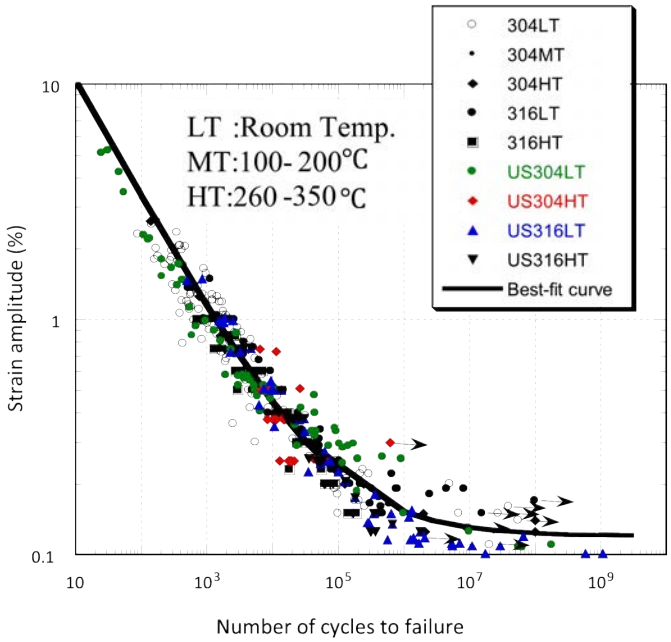

FIG. 34. Fatigue data in air — stainless steels [74].

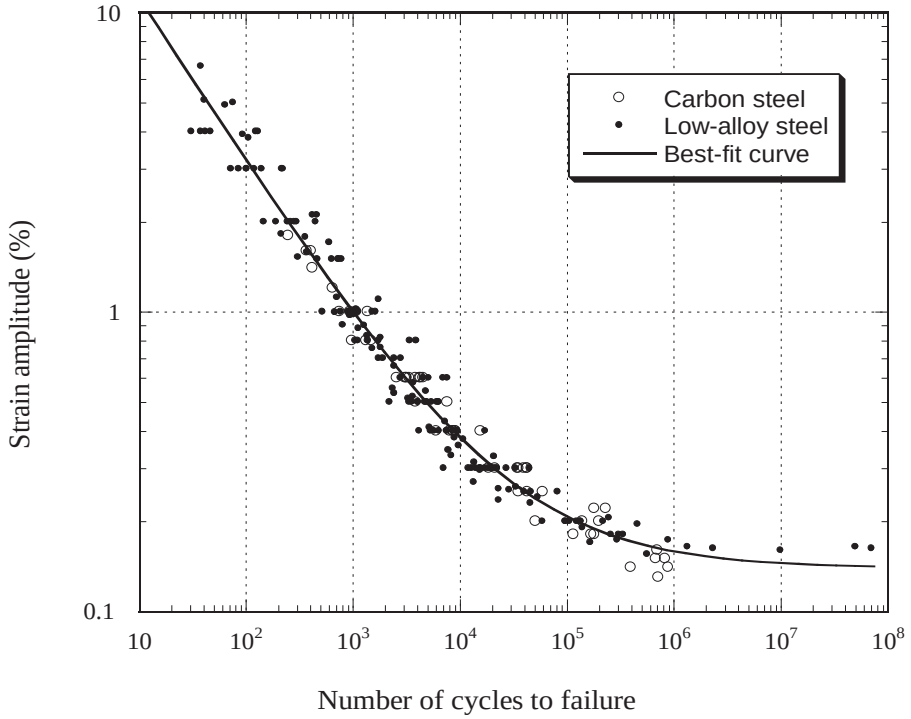

FIG. 35. Fatigue data in air — ferritic steels [74].

In many studies and guidelines, the amount of life reduction in high temperature water is commonly expressed by an environmental penalty parameter F_{en}, which is defined as a reciprocal of the ratio of the in-water life $N_{f,in-water}$ against the in-air life $N_{f,in-air}$, which represents the magnitude of life reduction and is expressed in Eq. (27).

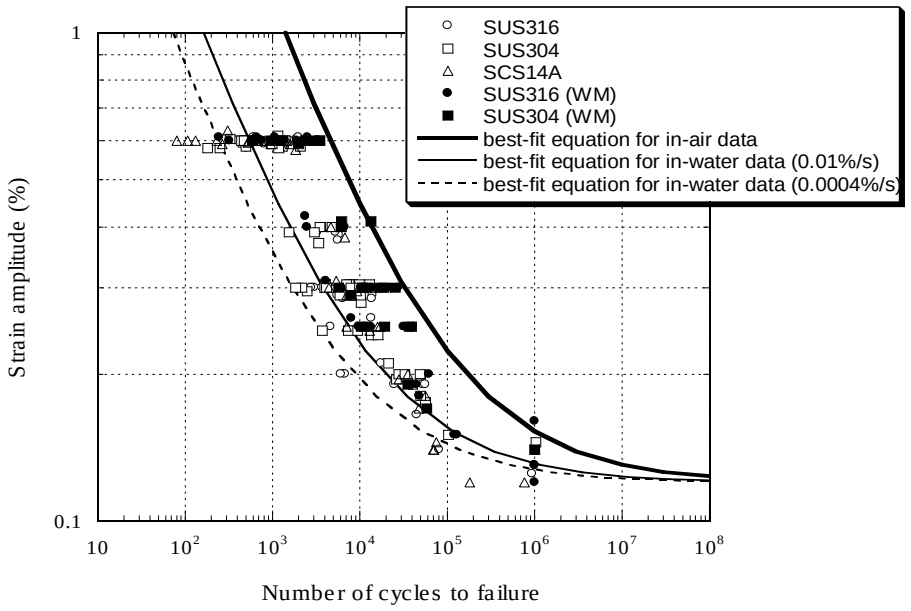

FIG. 36. Fatigue data in high temperature water — stainless steels [74].

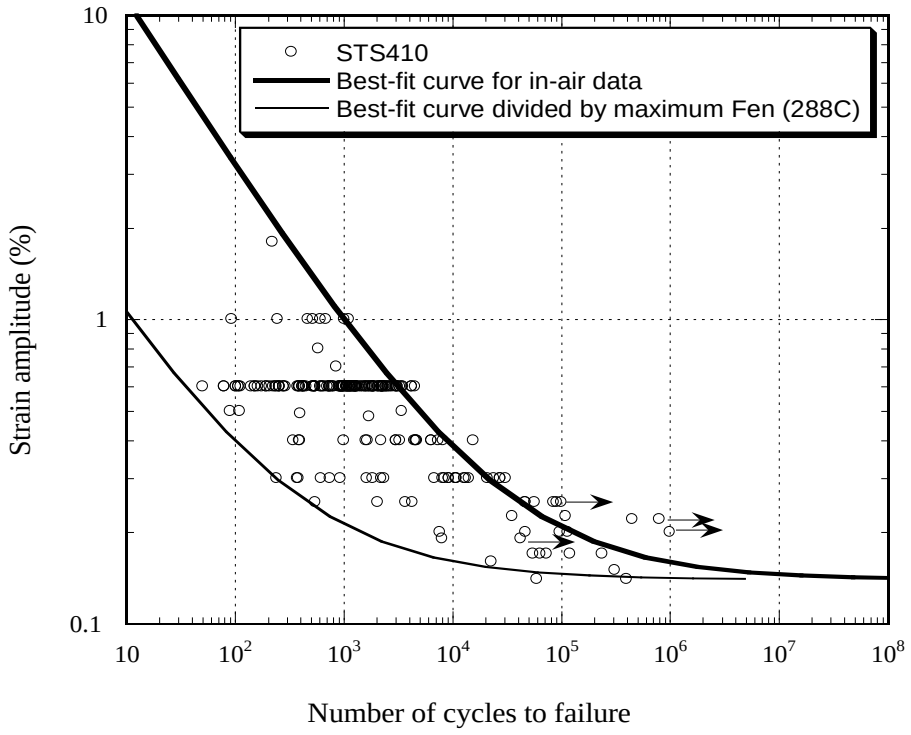

FIG. 37. Fatigue data in high temperature water — ferritic steels [74].

$$F_{en} = N_{\mathrm{f,in-air}} / N_{\mathrm{f,in-water}} \tag{27}$$

By definition, the value of F_{en} is generally larger than unity and changes with various parameters. In the most general form, F_{en} is expressed as a function of temperature T, strain rate $\dot{\varepsilon}$, dissolved oxygen content in the water DO, and sulphur content in the material S, and is expressed in Eq. (28).

$$F_{\text{en}} = f\left(T, \dot{\varepsilon}, DO, S\right) \tag{28}$$

Functional forms proposed for each element will be described in the following sections after a short discussion on the in-air fatigue curves, which are required as a basis for defining the values of F_{en}.

5.2.2. Reference in-air fatigue curves

In quantitatively expressing the effect of high temperature water environment on fatigue lives, it is necessary to define appropriate in-air fatigue properties free from environmental effects to be used as a reference in defining F_{en}. Equation (29), often called Stromeyer's equation, has been extensively used in many investigations.

$$\varepsilon_a = AN_{\text{f}}^{-\text{m}} + B \tag{29}$$

Or equivalently can be expressed by Eq. (30).

$$\ln(N_{\text{f}}) = \frac{\text{A} - \ln(\varepsilon_{\text{a}} - \text{B})}{\text{m}} \tag{30}$$

where

ε_a is the strain amplitude;

N_{f} is the number of cycles to failure;

and *A*, *m* and *B* are variables depending on materials.

Based on the statistical analyses of in-air fatigue data, mostly taken at room temperature, the equations listed in Table 5 have been derived for each material category used as a reference in the guidelines published by JSME [75], the NUREG report [76] and the German Nuclear Safety Standard (KTA) [77].

Fatigue curves generated by these equations are compared in Fig. 38 and Fig. 39. The reference curves of all the materials provided in JSME guidelines and the NUREG report are relatively similar to each other, except those for low alloy steels which have higher tensile strength than other materials. The JSME and NUREG equations developed for each material category give almost identical fatigue lives, suggesting the effect of the reference fatigue curves on the determination of F_{en} is insignificant. The KTA standard, on the other hand, provides two curves for use at temperatures lower and higher than 80°C for stabilized stainless steels of type 321 and 347. The curve for lower temperatures lies above the curves for conventional stainless steel, whereas the curve for higher temperatures is positioned somewhat below those.

5.2.3. Influence of strain rate

The effects of strain rate in high temperature water at normal operating temperatures in both PWRs and BWRs have been extensively studied on ferritic and stainless steels used in these plants. An example of relations obtained between the strain rate and fatigue life reduction in ferritic steels at a temperature of 289°C, a sulphur content of 0.015% and DO[20] > 0.7 ppm are shown in Fig. 40 [75] and Fig. 41 [76]. Both the test data and the estimations by the JSME and NUREG equations are given in these figures and the figures that follow. It can be seen first that F_{en} changes by an order of two magnitudes, reaching about

[20] Dissolved oxygen (DO) is a measure of how much oxygen is dissolved in the water.

TABLE 5. EXPRESSIONS OF REFERENCE IN-AIR FATIGUE CURVES

Code/Material	JSME S NF1-2009 [75]	NUREG/CR-6909 [76]	KTA 3201.2 [77]
Carbon steels	$\varepsilon_a = 25.71 N_f^{-0.490} + 0.113$	$\varepsilon_a = 28.0 N_f^{-0.506} + 0.113$	n.a.
Low alloy steels	$\varepsilon_a = 38.44 N_f^{-0.562} + 0.155$	$\varepsilon_a = 35.4 N_f^{-0.553} + 0.151$	n.a.
Stainless steel (type 304/316)	$\varepsilon_a = 23.0 N_f^{-0.457} + 0.110$	$\varepsilon_a = 36.2 N_f^{-0.521} + 0.112$	$\varepsilon_a = 36.2 N_f^{-0.521} + 0.112$
Ni–Cr–Fe Alloys	$\varepsilon_a = 19.0 N_f^{-0.450} + 0.118$		n.a.
Stainless steel (type 321/347)	n.a.	n.a.	$\varepsilon_a = 21.9 N_f^{-0.460} + 0.136$ $(T < 80C)$ $\varepsilon_a = 20.8 N_f^{-0.443} + 0.078$ $(T \geq 80C)$

Note: ε_a, N_f and T represent the strain amplitude, number of cycles to failure and temperature, respectively.

100 at the smallest strain rate employed in the test, i.e. 10^{-5} %/s, corresponding to a loading cycle of the order of a day. In this figure, the strain rate dependency in the whole range of strain rate is approximated by a combination of three regimes, i.e. the lower shelf, transient and upper shelf regimes. In the transient region, where F_{en} continuously increases with decreasing strain rate, variation of F_{en} can be fitted reasonably well by a power law function of the strain rate.

Fundamentally similar behaviour was observed for a few types of stainless steels and Ni–Cr–Fe alloys in terms of strain rate dependency, and similar fits have been made in the JSME and NUREG expressions, as shown in Fig. 42 and Fig. 43. In these materials, F_{en} in a PWR is a little higher than in a BWR, as opposed to the case of the ferritic steels. There is not a large difference between the life reduction in conventional grade 304 and low carbon nuclear grade — 316 nuclear grade.

Although there is some difference between the plots from the JSME and NUREG expressions, fundamental similarities can be seen in the figures, mainly because similar data have been commonly used in their development.

Figure 44 compares the variations of F_{en} with the strain rate for each material type in typical conditions according to the expressions in the JSME guidelines. Ferritic steels in BWR normal water chemistry (NWC) (assuming DO = 0.2 ppm) and stainless steels in PWRs and BWRs are characterized by higher F_{en}, reaching the maximum value of about 20 to 50, whereas relatively smaller values between 3 to 6 at maximum are provided for other cases (ferritic steels in PWR and Ni–Cr–Fe alloys in both conditions). This kind of comparison is very helpful in judging the importance of environmental effects in each combination of material and reactor type before going into more detail.

5.2.4. Influence of temperature

The temperature of the water also has a great influence on fatigue life even when tested at the same strain rate. Figures 45–47 show examples of the temperature dependency of life reduction at a relatively low strain rate of 0.001%/s, and with the same sulphur and DO content in the case of ferritic steels, as in Fig. 43. There is a clear trend of increasing F_{en} as the temperature rises, particularly in the range above 150°C. Reasonable fitting by exponential functions appears to be possible for the region exhibiting a clear temperature dependency. In this case, F_{en} at 289°C is about 20 times larger than that at 150°C, clearly indicating the significance of the temperature effect. There is a difference between the JSME and NUREG expressions in treating the temperature dependency below 150°C. Again, the proportional constant changes with other parameters, rendering temperature dependency smaller at higher strain rates.

The slope of F_{en} in PWRs is somewhat larger than that in BWRs for stainless steels and Ni–Cr–Fe alloys, suggesting that the difference in operating temperatures does not play a major role in the difference of F_{en} between the two conditions.

5.2.5. Influence of material composition and water chemistry

It was also found that the sulphur content in the material plays an important role in determining the extent of the reduction in the life reduction for ferritic steels, both carbon steel and low alloy steel. The effect of sulphur content at a fixed temperature, strain rate and dissolved oxygen is shown in Fig. 48. The effect seems to be comparably smaller than the effects of other parameters shown above, but systematic dependence can be seen. Predictions by the JSME and NUREG expressions differ largely in this figure and further study seems to be necessary. Since such a clear dependency of chemical composition has not been found for stainless steels and Ni–Cr–Fe alloys, any explicit consideration has not been made in these expressions.

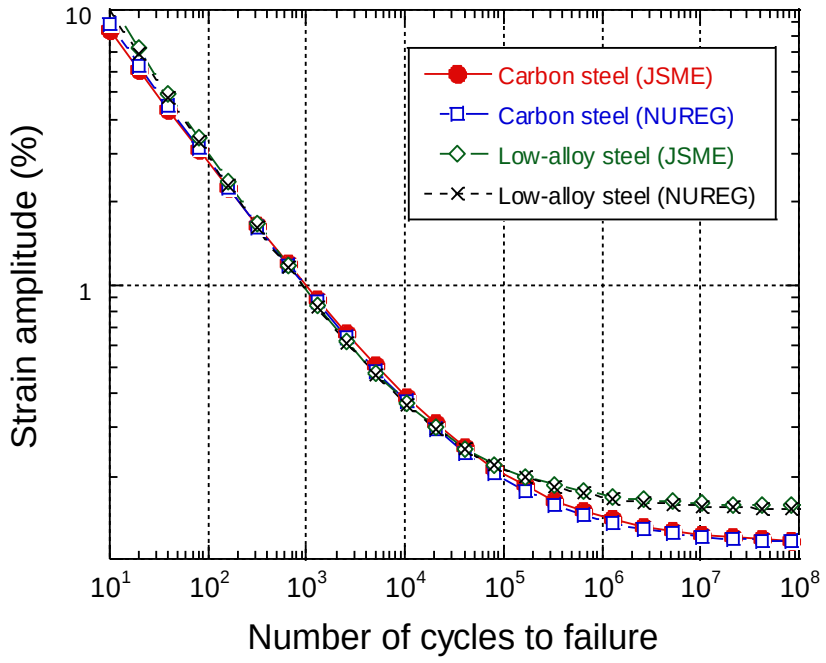

FIG. 38. Comparison of in-air reference fatigue curves — ferritic steels [75–77].

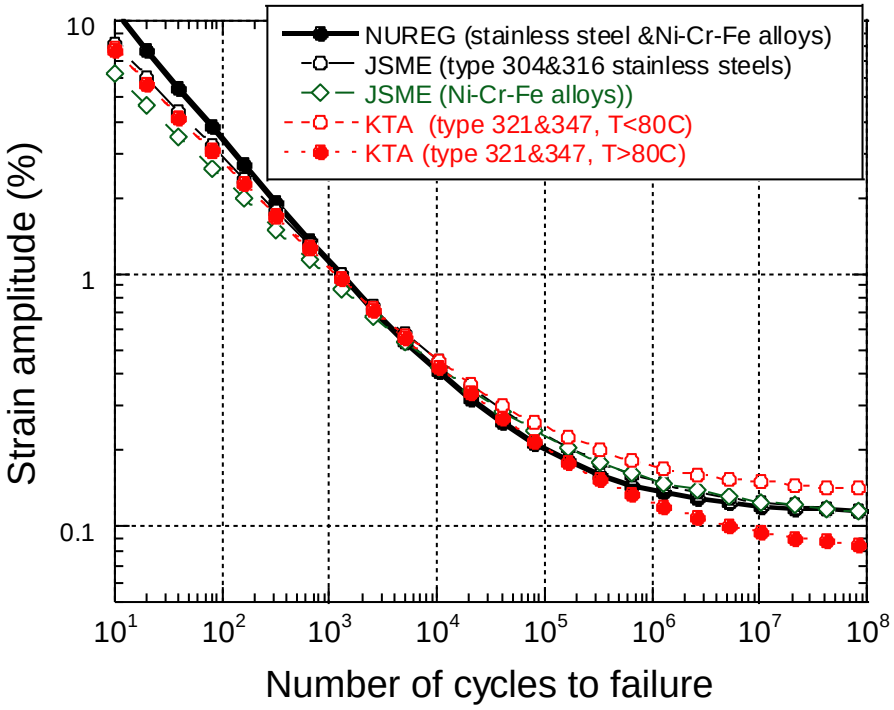

FIG. 39. Comparison of in-air reference fatigue curves — Ni–Cr–Fe alloys [75–77].

The water quality also has an influence. The effect of dissolved oxygen on the fatigue lives of ferritic steels at a temperature of 289°C, strain rate of 0.001%/s and sulphur content of 0.015% is shown in Fig. 49 (a). Again, a clear effect can be seen, and the general data trend can be separated into three regions, i.e. the upper shelf, the transient and the lower shelf regions, as in the strain rate dependency. The upper bound value obtained at DO > 0.5–0.7 ppm is about 20 times larger than the lower bound value attained at DO < 0.02–0.04 ppm. The quality of water alters the amplitude of life reduction also in stainless steels and Ni–Cr–Fe alloys. In contrast to an earlier expectation and the behaviour of ferritic steels, these materials showed a greater life reduction in PWR water than in BWR NWC water, as was already mentioned. Independent expressions have been developed for each water condition, rather than providing general expressions covering both conditions, because it is not clear which element has a dominating effect on life reduction.

5.2.6. Effect of strain amplitude

A parameter that plays a major role in fatigue assessment and may affect the fatigue life reduction in high temperature water is the amplitude of strain variation. In the plots shown in the figures in the foregoing sections, all the data obtained at various strain amplitudes have been plotted without any distinction. This has been done based on the observation that the effect of strain amplitude on the life reduction ratio, represented by F_{en}, does not show a clear dependence on the strain amplitude.

There have also been discussions regarding the existence of the strain thresholds below which the life reduction due to the environmental effect can be ignored. Although it is not easy to conduct an experimental investigation for such small strain amplitudes, strain thresholds have been introduced in both the JSME and NUREG guidelines. This is based on the idea that there is a minimum strain amplitude necessary for cracking the protective oxidation layer by cyclic loading for the environmental effect to appear. The values of the strain thresholds depend on the material type and guidelines, but they are approximately equal to the conventional strain thresholds in best-fit in-air fatigue curves or a little below them. Therefore, if the strain thresholds are applied to the best-fit curves, there is virtually no or very little effect on the total fatigue damage. On the other hand, if they are applied to design fatigue

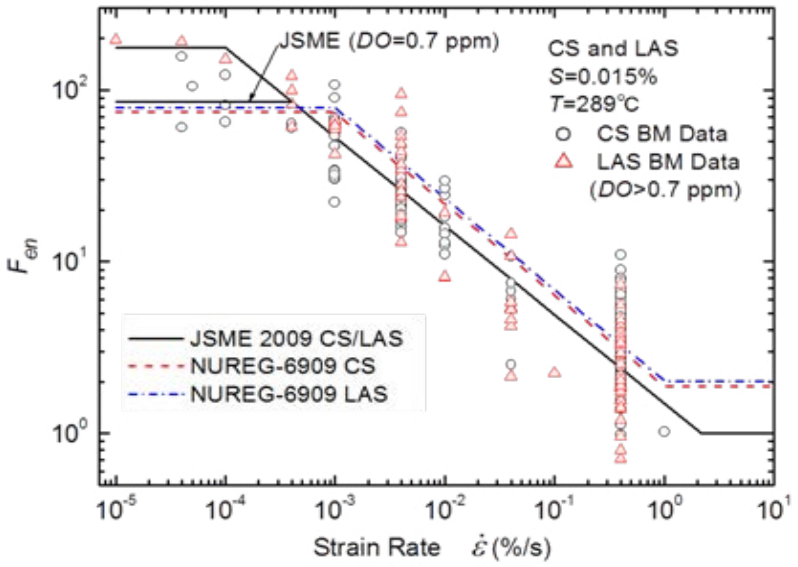

FIG. 40. Strain rate dependency of environmental life reduction factor, F_{en} in the JSME guidelines and NUREG report — ferritic steels in high DO water [75, 76].

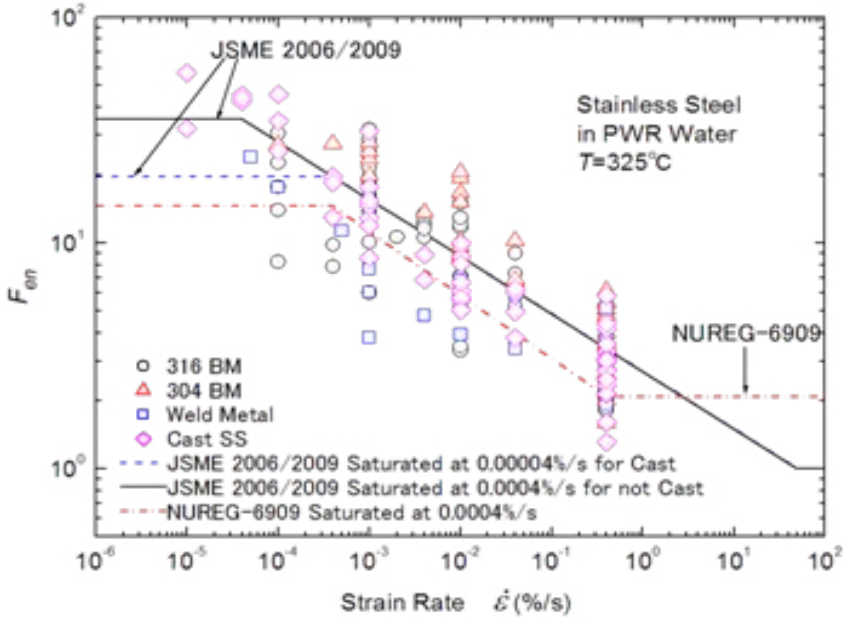

FIG. 41. Strain rate dependency of the environmental life reduction factor F_{en} in the JSME guidelines and NUREG report — stainless steels in typical PWR water [75, 76].

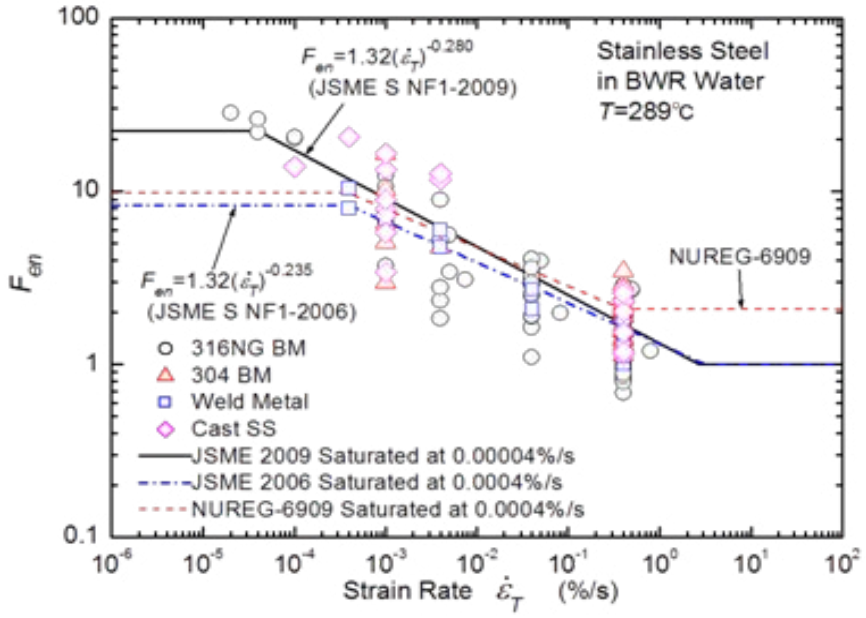

FIG. 42. Strain rate dependency of the environmental life reduction factor F_{en} in the JSME guidelines and NUREG report — stainless steels in typical BWR water [75, 76].

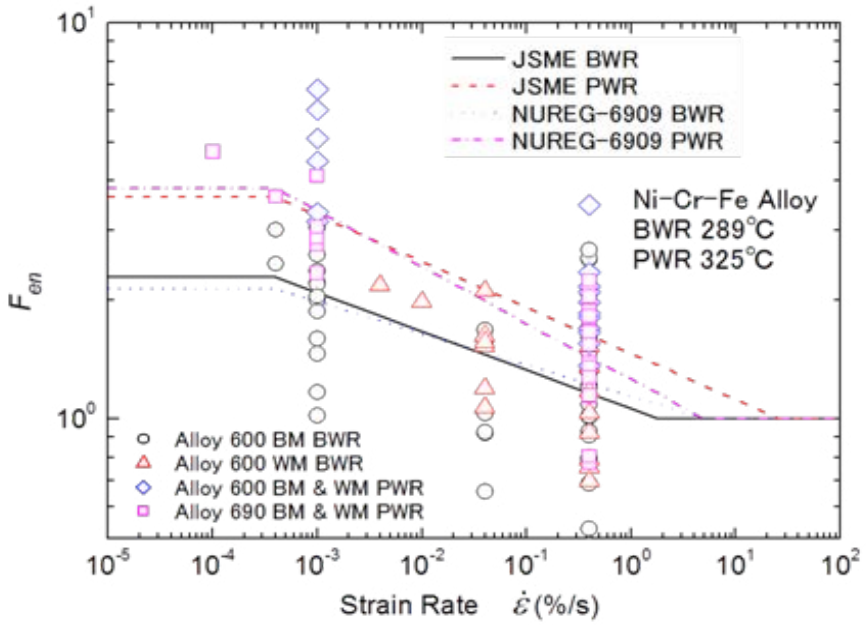

FIG. 43. Strain rate dependency of the environmental life reduction factor F_{en} in the JSME guidelines and NUREG report — Ni–Cr–Fe alloys [75, 76].

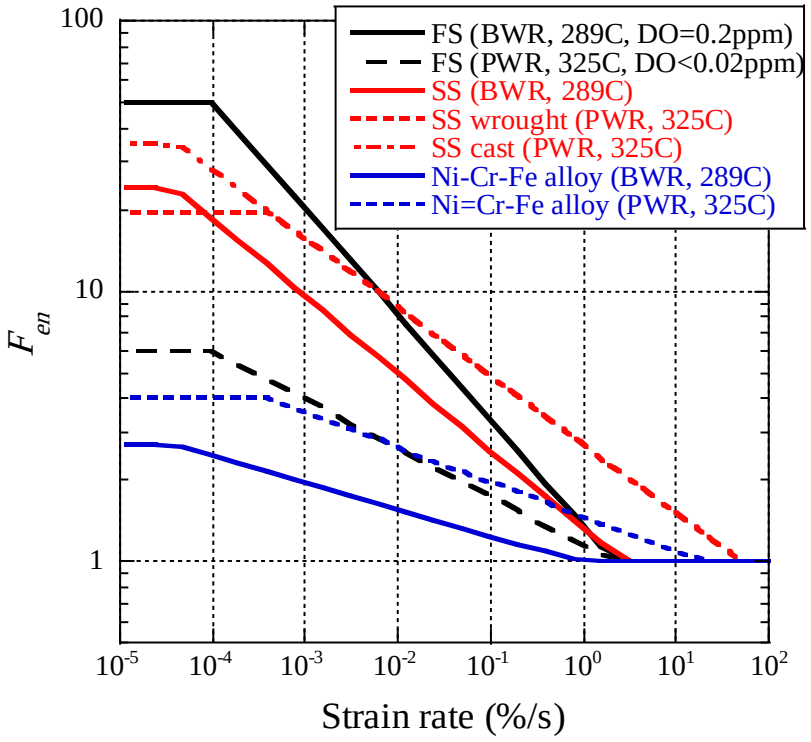

FIG. 44. Comparison of the strain rate dependence of F_{en} under isothermal sawtooth wave form conditions [75].

curves which are obtained by shifting the best-fit curves downwards by a factor of 2 or a little bit less, their consideration may reduce the fatigue damage to some extent. This indicates the importance of the reference fatigue curves even when the amount of life reduction due to environmental effect, rather than the total fatigue damage, needs to be known.

5.2.7. Existing formulas for F_{en}

As already mentioned, expressions for estimating F_{en} under various conditions have been proposed, first in Japan and later in the USA. As a large quantity of the data used for their development are common, they are nominally similar with each other in content as well as in functional forms.

Tables 6–8 summarize these expressions for each material category. They will be very useful in estimating the sensitivity to each parameter as well as obtaining a rough idea about the amount of life reduction that might be brought about by the environmental effect of high temperature water. It should be added, however, that these expressions are of an empirical nature and should be continuously updated with the accumulation of test data as well as the progress of understanding of the underlying physical mechanisms.

5.3. APPLICATION TO GENERAL LOADING CONDITIONS

Loading conditions in actual components are generally irregular and much more complex with varying temperature and strain rate during the cycle, as well as the presence of stress multiaxiality. In calculating the value of F_{en}, these aspects need to be processed. Stress multiaxiality is dealt with by

using the stress intensity range, which is based on the maximum shear stress criterion in determining the equivalent strain range. Two peaks constitute the stress intensity range, but no decision needs to be made concerning which is the tensile side and which is the compressive side in the case of conventional fatigue assessment, where the strain rate effect is ignored. However, as far as the strain rate effect on F_{en} is concerned, its sign needs to be determined as only the strain rate in a tension-going process is influential. Also, to be addressed is the variable temperature and strain rate during the tension-going

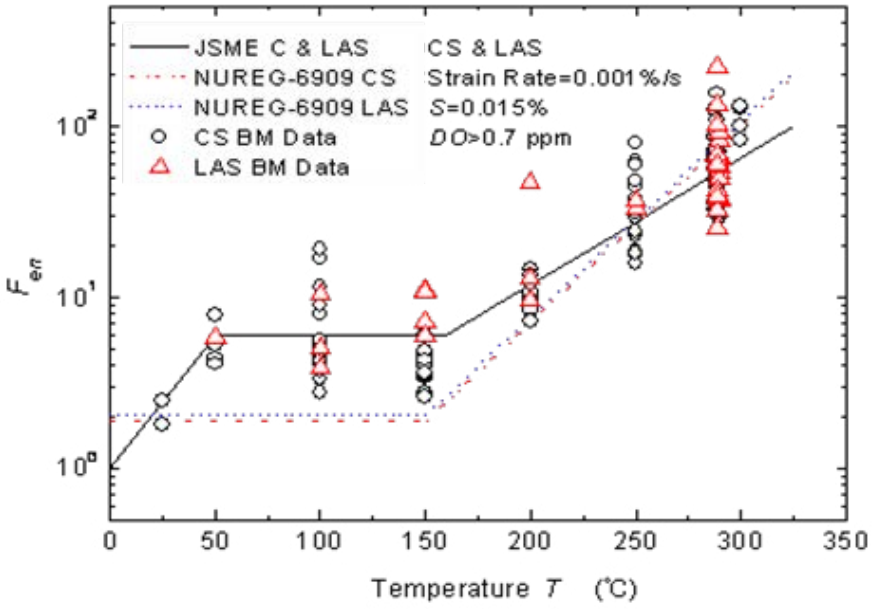

FIG. 45. Comparison of the temperature dependence of F_{en} in the JSME guidelines and NUREG report — ferritic steels in high DO water [75, 76].

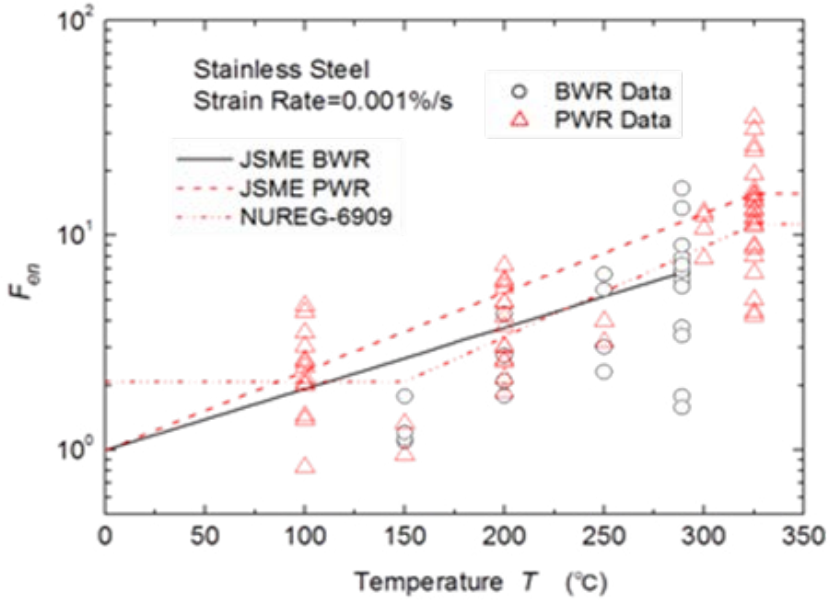

FIG. 46. Comparison of the temperature dependence of F_{en} in the JSME guidelines and NUREG report — stainless steels in BWR and PWR water [75, 76].

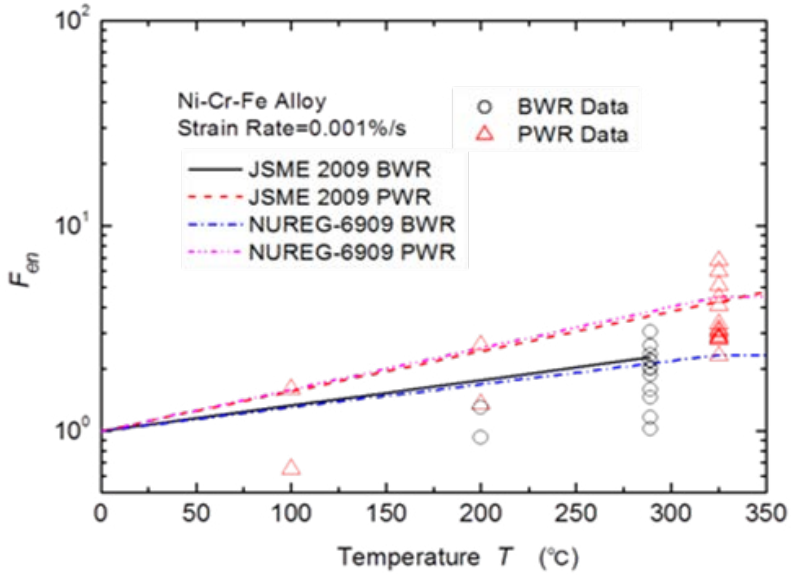

FIG. 47. Comparison of temperature-dependencies of F_{en} in JSME guidelines and NUREG report — Ni–Cr–Fe alloys in BWR and PWR water [75, 76].

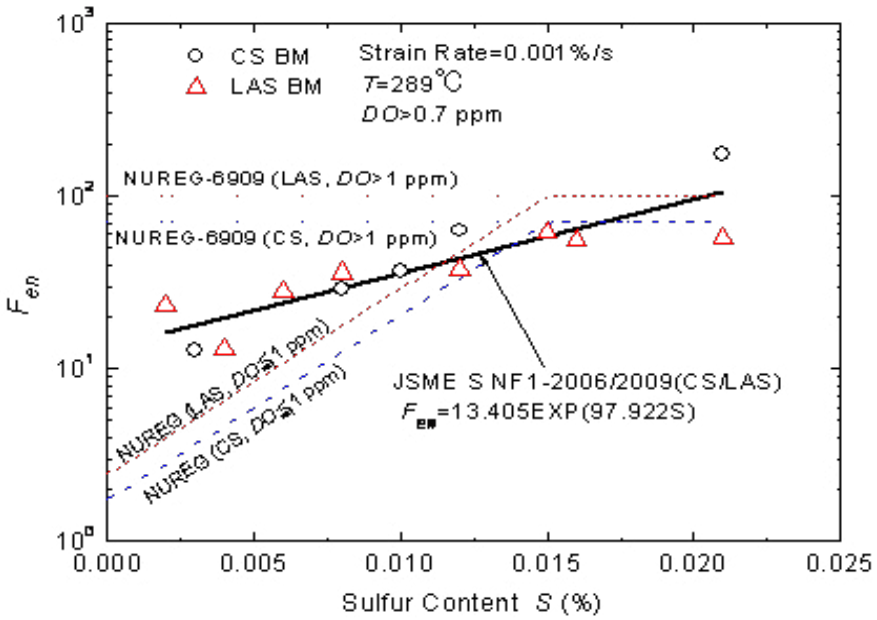

FIG. 48. Sulphur content dependence of F_{en} in ferritic steels [75, 76].

process. The simplest way is to employ the maximum (or average) temperature and average strain rate during the cycle of concern, but it may lead to too conservative an evaluation regarding the environmental effect. Therefore, an alternative, more sophisticated, approach that enables one to conduct a more realistic evaluation is expected to be developed.

There are two approaches, one is the simplified method using the average rate approach (see Fig. 49 (b)) and another is the detailed method using the integrated rate approach (see Fig. 50). In the case of the simplified method, often called the average rate approach for F_{en} determination, the average strain rate is calculated by dividing the strain range by the time between two peaks constituting the stress intensity

range (maximum shear stress range). An alternative way to determine F_{en} using the instantaneous strain rate instead of the average strain rate has also been proposed as the 'modified (or integrated) rate approach'. JSME guidelines [75] provided the technical detailed approaches.

5.4. REFLECTION IN DESIGN CODES AND REGULATIONS

5.4.1. Development in Japan (Thermal and Nuclear Power Engineering Society (TENPES)/JSME guidelines)

As stated earlier, studies have been conducted on environmental fatigue issues in Japan ever since the first report was issued in 1988 [72]. Guidelines for evaluating environmental effects were first issued by the Thermal and Nuclear Power Engineering Society (TENPES) in 2002 [78], as outlined in Ref. [79,

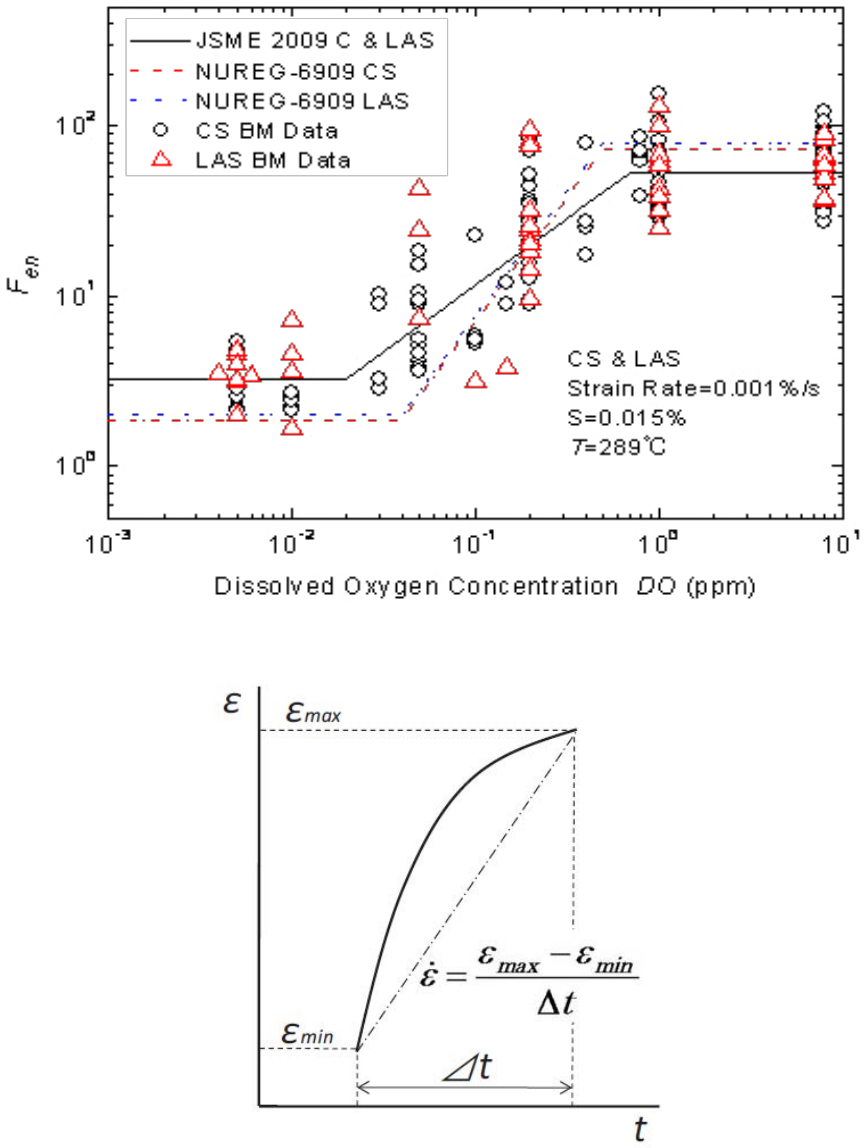

FIG. 49 (a). Dissolved oxygen dependence of F_{en} in ferritic steels (right) in the JSME guidelines and NUREG report [75, 76]. (b). Schematic illustrations of two procedures dealing with variable strain rate — simplified method [75].

80]. Updated guidelines were developed as a result of a long term study by the Nuclear Power Engineering Corporation and Japan Nuclear Energy Safety Organization (JNES) [81, 82]. Subsequently, guidelines were published as a JSME code and standard for power generation facilities [75, 83]. They were endorsed by the Nuclear and Industrial Safety Agency as one of the tools for PLiM, as reported in Refs [84, 85]. Introduction of the environmental effect in the design code as well as the update of design curves has been discussed [86, 87], but it has not yet been implemented in the design and construction code [88].

5.4.2. Development in the USA (NUREG report and ASME Code)

Following various publications from Japanese researchers, ANL in the USA started an investigation on this issue under contract to the NRC. This resulted in the publication of a series of ANL/NUREG reports [76, 89, 90]. In addition to the environmental effect factor F_{en}, the adequacy of the design fatigue curves was re-examined and updating was proposed in the reports. This included changes to the best-fit curves and the modification of adjustment factors that are used in deriving the design curve in order to deal with various uncertainties, such as surface finish, size effect and the scatter of fatigue property.

The modification of the best-fit curve for stainless steels and Ni–Cr–Fe alloys was proposed to make it more consistent with recent test data. With regard to the factors applied in deriving the design curve from the best-fit curve, a factor of 12 was recommended for the number of cycles instead of 20 employed in the ASME and other codes, leaving unchanged a factor of 2 for the strain amplitude

TABLE 6. F_{en} EXPRESSIONS FOR FERRITIC STEELS

JSME S NF1-2009	NUREG/CR-6909
$\ln(F_{en}) = 0.00822\,(0.772 - \dot{\varepsilon}^*)S^*T^*O^*$	$\ln(F_{en}) = 0.554 - 0.101S^*T^*O^*\dot{\varepsilon}^*$ (CS)
$\dot{\varepsilon}^* = \ln(2.16)$ ($\dot{\varepsilon} > 2.16\%$/s)	$\ln(F_{en}) = 0.898 - 0.101S^*T^*O^*\dot{\varepsilon}^*$ (LAS)
$\dot{\varepsilon}^* = \ln(\dot{\varepsilon})$(DO ≤ 0.7ppm, $0.0004 \le \dot{\varepsilon} \le 2.16\%$/s)	$\dot{\varepsilon}^* = 0$ ($\dot{\varepsilon} > 1\%$/s)
$\dot{\varepsilon}^* = \ln(\dot{\varepsilon})$(DO ≤ 0.7ppm, $0.0001 \le \dot{\varepsilon} \le 2.16\%$/s)	$\dot{\varepsilon}^* = \ln(\dot{\varepsilon})$ ($0.001 \le \dot{\varepsilon} \le 1$&/s)
$\dot{\varepsilon}^* = \ln(0.0004)$ (DO ≤ 0.7ppm, $\dot{\varepsilon} < 0.0004\%$/s)	$\dot{\varepsilon}^* = \ln(0.001)$ ($\dot{\varepsilon} < 0.001\%$/s)
$\dot{\varepsilon}^* = \ln(0.0001)$ (DO > 0.7ppm, $\dot{\varepsilon} < 0.0001\%$/s)	$T^* = 0$ ($T \le 150$°C)
$S^* = \ln(12.32) + 97.92$XS	$T^* = T - 150$ ($150 < T \le 350$°C)
$T^* = 0.0358$XT ($T < 50$°C)	$O^* = 0$ (DO < 0.04ppm)
$T^* = \ln(6)$ ($50 \le T \le 160$°C)	$O^* = \ln(\text{DO}/0.04)$ ($0.04 \le \text{DO} \le 0.5$ ppm)
$T^* = \ln(0.398) + 0.0170$XT($T > 160$°C)	$O^* = \ln(12.5)$ (DO > 0.5 ppm)
$O^* = \ln(3.28)$ (DO < 0.02 ppm)	$S^* = 0.015$ (DO > 1.0 ppm)
$O^* = \ln(70.79) + 0.7853$X ln (DO)	$S^* = 0.001$ (DO ≤ 1.0ppm & S ≤ 0.001%)
($0.02 \le$ DO ≤ 0.7 ppm)	S^* = S(DO ≤ 1.0 ppm & 0.001 < S ≤ 0.015%)
$O^* = \ln(53.5)$ (DO>0.7 ppm)	$S^* = 0.015$ (≤1.0 ppm & S > 0.015%)
$F_{en} = 1.0$ ($\varepsilon_a \le 0.042\%$ or in the case of an earthquake)	$F_{en} = 1.0$ ($\varepsilon_a \le 0.07\%$)

(fictitious stress amplitude). The resulting design fatigue curves are shown in comparison with the original ones for stainless and ferritic steels in Fig. 51. The new design curve for stainless steel is lower than the original curve in most of the strain amplitudes, as shown in Fig. 51 (a). The NRC now requires fatigue assessments in the design of new reactors [91]. It should be added that the F_{en} equations for austenitic and ferritic steels given in older NUREG reports [89, 90] can also be applied in licence renewal application to the NRC [92].

More recently, the ASME Code committee has also been engaged in the inclusion of the environmental effect in the design and construction codes, such as the BPVC, section III. As a result, two code cases have been issued to provide guidance in making fatigue assessments in consideration of environmental effects. One of them, Code Case N-792 [93], is very similar to NUREG/CR-6909 [76], including the same design curves and the formulas for F_{en}. They only differ regarding the treatment of F_{en} in the small strain amplitudes: the threshold assumed in NUREG/CR-6909 has not been implemented in Code Case N-792. Code Case N-761 [94] provides a set of design curves corresponding to different levels of strain rate. The equivalent values of F_{en} calculated from these design curves exhibit somewhat

TABLE 7. F_{en} EXPRESSIONS FOR STAINLESS STEELS

JSME S NF1-2009	NUREG/CR-6909
$\ln(F_{en}) = (C - \dot{\varepsilon}^*)T^*$	$\ln(F_{en}) = 0.734 - T^* O^* \dot{\varepsilon}^*$
(BWR)	
$C = 0.992$	$\dot{\varepsilon}^* = 0$ ($\dot{\varepsilon} > 0.4$%/s)
$\dot{\varepsilon}^* = \ln(2.69)$ ($\dot{\varepsilon} > 2.69$%/s)	$\dot{\varepsilon}^* = \ln(\dot{\varepsilon})$ ($0.0004 \leq \dot{\varepsilon} \leq 0.4$%/s)
$\dot{\varepsilon}^* = \ln(\dot{\varepsilon})$ ($0.00004 \leq \dot{\varepsilon} \leq 2.69$%/s)	$\dot{\varepsilon}^* = \ln(0.0004)$ ($\dot{\varepsilon} < 0.0004$%/s)
$\dot{\varepsilon}^* = \ln(0.00004)$($\dot{\varepsilon} < 0.00004$%/s)	$T^* = 0$ ($T \leq 150$°C)
$T^* = 0.000969T$	$T^* = (T - 150)/175$ ($150 \leq T \leq 325$°C)
(PWR)	$T^* = 1.0$ ($T \geq 325$°C)
$C = 3.910$	$O^* = 0.281$ (all DO levels)
$\dot{\varepsilon}^* = \ln(49.9)$ ($\dot{\varepsilon} > 49.9$%/s)	$F_{en} = 1.0$ ($\varepsilon_a \leq 0.10$%)
$\dot{\varepsilon}^* = \ln(\dot{\varepsilon})$ ($0.0004 \leq \dot{\varepsilon} \leq 49.9$%/s, wrought)	
$\dot{\varepsilon}^* = \ln(\dot{\varepsilon})$($0.00004 \leq \dot{\varepsilon} \leq 49.9$%/s, cast)	
$\dot{\varepsilon}^* = \ln(0.0004)$($\dot{\varepsilon} < 0.0004$%/s, wrought)	
$\dot{\varepsilon}^* = \ln(0.00004)$($\dot{\varepsilon} < 0.00004$%/s, cast)	
$T^* = 0.000782T$ ($T \leq 325$°C)	
$T^* = 0.254$ ($T > 325$°C)	
$F_{en} = 1.0$ ($\varepsilon_a \leq 0.11$% or in the case of earthquake)	

TABLE 8. F_{en} EXPRESSIONS FOR Ni–Cr–Fe ALLOYS

JSME S NF1-2009	NUREG/CR-6909
$\ln(F_{en}) = (C - \dot{\varepsilon}^*)T^*$	$\ln(F_{en}) = -T^*O^*\dot{\varepsilon}^*$
(BWR)	$\dot{\varepsilon}^* = 0$ ($\dot{\varepsilon} > 5.0\%$/s)
$C = 0.112$	$\dot{\varepsilon}^* = \ln(\dot{\varepsilon}/5.0)$ ($0.0004 \leq \dot{\varepsilon} \leq 5.0\%$/s)
$\dot{\varepsilon}^* = \ln(0.894)$ ($\dot{\varepsilon} > 0.894\%$/s)	$\dot{\varepsilon}^* = \ln(0.0004/5.0)$ ($\dot{\varepsilon} < 0.0004\%$/s)
$\dot{\varepsilon}^* = \ln(\dot{\varepsilon})$ ($0.00004 \leq \dot{\varepsilon} \leq 0.894\%$/s)	$T^* = T/325$ ($T < 325$°C)
$\dot{\varepsilon}^* = \ln(0.00004)$($\dot{\varepsilon} < 0.00004\%$/s)	$T^* = 1.0$ ($T \geq 325$°C)
$T^* = 0.000343T$	$O^* = 0.09$ (NWC BWR water)
(PWR)	$O^* = 0.16$ (PWR or HWC BWR water)
$C = 2.94$	$F_{en} = 1.0$ ($\varepsilon_a \leq 0.10\%$)
$\dot{\varepsilon}^* = \ln(19.0)$ ($\dot{\varepsilon} > 19.0\%$/s)	
$\dot{\varepsilon}^* = \ln(\dot{\varepsilon})$ ($0.0004 \leq \dot{\varepsilon} \leq 19.0\%$/s)	
$\dot{\varepsilon}^* = \ln(0.000)$($\dot{\varepsilon} < 0.0004\%$/s)	
$T^* = 0.000397T$	
$F_{en} = 1.0$ ($\varepsilon_a \leq 0.11\%$ or in the case of earthquake)	

Note: Hydrogenized water chemistry

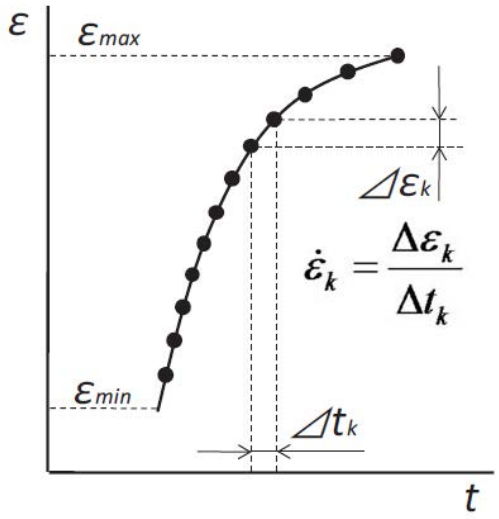

FIG. 50. Schematic illustrations of two procedures dealing with variable strain rate — detailed method [75].

different, more modest, temperature as well as strain rate dependences in comparison with the F_{en} values calculated by the NUREG/CR-6909 equations, as shown in Fig. 52 for the case of stainless steels.

At the same time, the design fatigue curve in the main design and construction code (section III of Ref. [95]) for the stainless steels has also been modified from that included in earlier editions [98] to that proposed in NUREG CR-6909 as reported in Ref. [96] to make them more consistent with recent test data. On the other hand, the design fatigue curve for the ferritic steels remains the same as that in older code, without the adaption of the new proposal in the design fatigue curves in ASME Code Case N-792 [97].

In addition, the so-called flaw tolerance approach in which structural integrity is addressed by crack growth analysis from a presumed initial crack is also being developed to provide a means of coping with instances where the UF exceeds 1 as a result of a large value of F_{en}, as reported in Ref. [99].

5.4.3. Development in France

In response to the proposals in Japan and the USA, studies on environmental effects in LWR coolant were also started in several European countries. In particular, EdF and AREVA NP in France have been conducting an experimental study on fatigue behaviour, including environmental effects, for type 304L stainless steel, which is a major piping material in their PWRs [100, 101]. In terms of the in-air best-fit

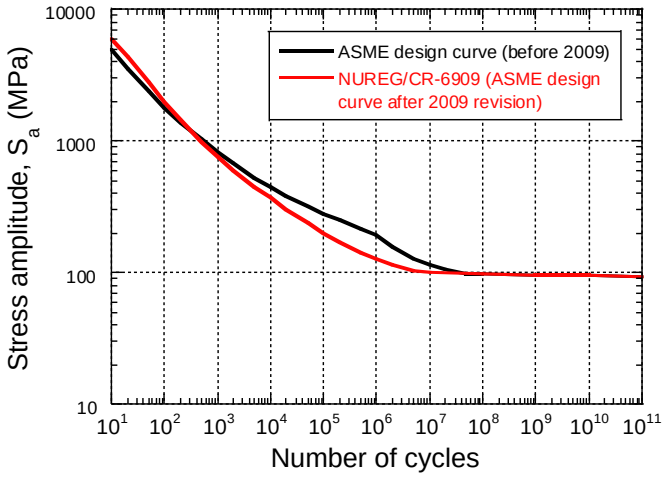

(a) Stainless steels

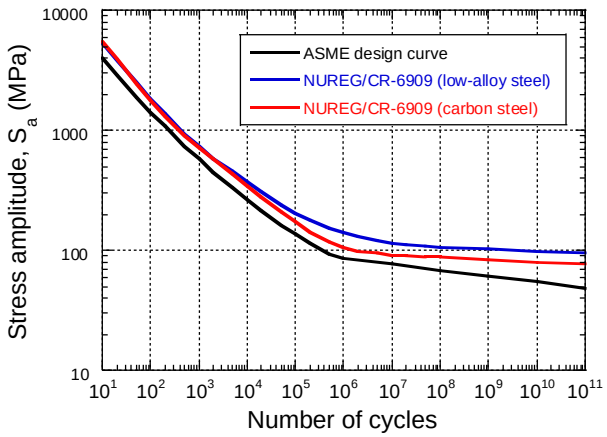

(b) ferritic steels

(FIG. 51. Comparison of design fatigue curves [76].

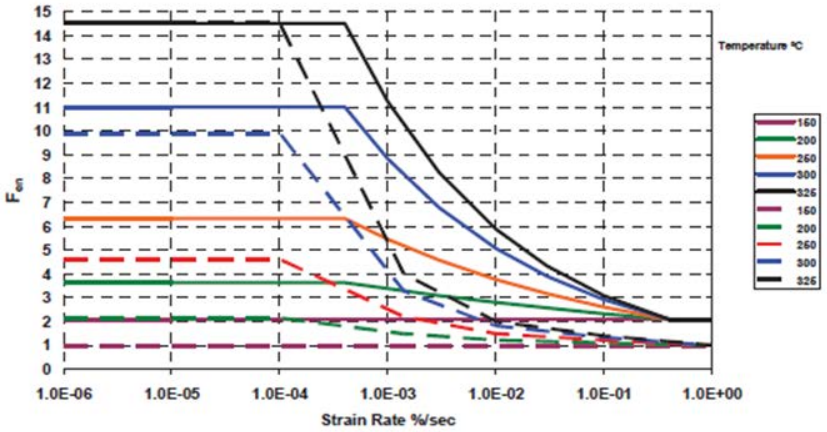

FIG.52. Comparison of the environmental factor in NUREG (solid lines) and equivalence in the ASME Code Case N-792 (in dashed lines) for stainless steels [96].

fatigue curve, their data, particularly at high temperatures such as 150°C and 300°C, were found to show good agreement with the NUREG curve for stainless steels, as shown in Fig. 53, so a new equation has not been developed. However, they found smaller scatter in their data and the reduction factor on strain amplitude applied in deriving the design curve, from 2.0 to 1.4, for instance, is under consideration for inclusion in French design code RCC-M [102].

In their tests conducted in PWR primary coolant conditions [101, 102], they used several strain waves, one of which was claimed to be more representative of the thermal transients in plants than those used in conventional tests with constant strain rate in testing specimens with both polihed and grounded surfaces, as shown in FIG. 54. Strain histories in the non-conventional wave tests were those constructed from the same pieces of strain waves in different orders, as shown in Fig. 54(a), so that even the integrated rate approach gives the same value for F_{en} of about 6 for all the cases. The results of these tests are plotted in Fig. 54(b) with various fatigue curves for austenitic stainless steels. Four test results on polished specimens showed the life reduction between 1.7 and 3.7, which is smaller than the value of F_{en} predicted by the NUREG equation. It was also found that specimens with grounded surfaces had shorter lives than polished specimens, but the life reduction was smaller than predicted by the NUREG equation in combination of the factor in the design codes used for monitoring the effect of surface finish. Efforts are in progress to develop a procedure to incorporate environmental effects into the design code in a less restrictive manner than the NUREG approach, mainly by treating the effects of surface finish and environmental effect together, rather than separately. This leads to Eq. (31) for the modified environment reduction factor as an alternative for the original F_{en}.

$$F'_{en} = \max\left(F_{en} / F_{en,\,allowable}, 1\right) \tag{31}$$

where $F_{en,allowable}$ is the maximum value of F_{en}.

$F_{en,allowable}$represents the maximum value of F_{en}, for which the consideration of environmental effects is not required because the life reduction is considered to be included in the margin of design fatigue curves. Based on the assumption that a factor of 5 is needed to cover the other uncertainties from the data scatter and size effect, the following expression has been derived.

$$F_{en,\,allowable} = \left(\frac{F_{en,\,test}}{5}\right)\frac{N_{f,\,test}}{N_{design}} \tag{32}$$

where

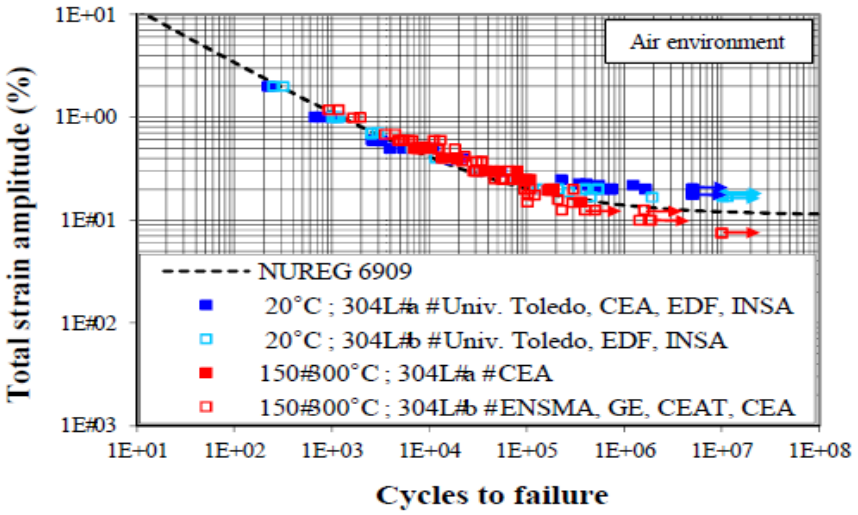

FIG. 53. Comparison of French in-air test data on 304L SS with NUREG best-fit curve for stainless steels [100].

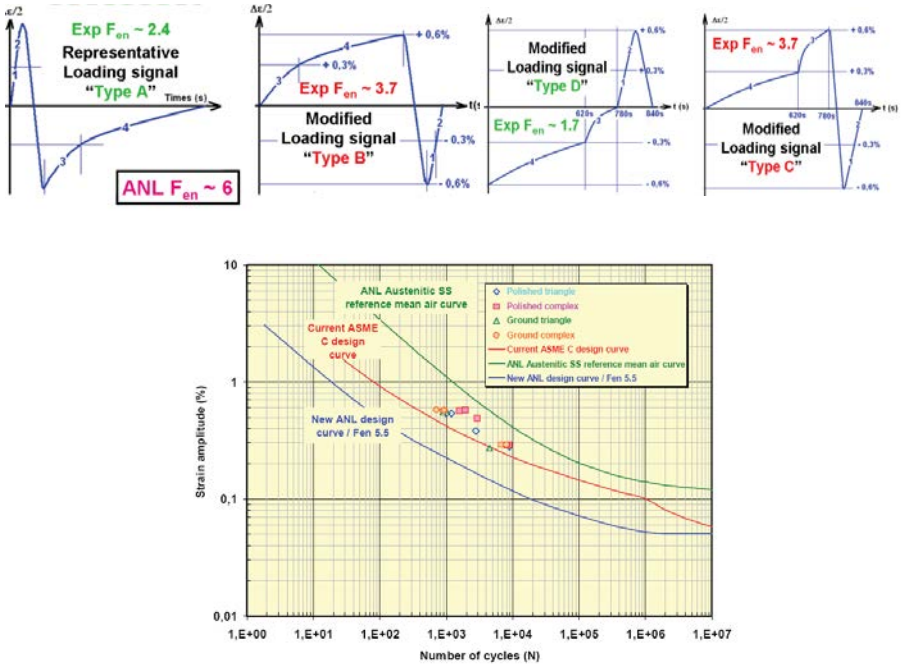

FIG. 54. Result of in-water fatigue tests on 304L stainless steel in AREVA NP [102]. (a) (top) Strain wave forms employed in non-conventional tests; (b) Comparison of failure lives with various fatigue curves.

$N_{f,test}$ is the actual number of cycles to failure obtained in the test;

N_{design} and $F_{en,test}$ are the number of cycles on the design curves;

and F_{en} is the value estimated for the test condition using the NUREG equation.

Values of $F_{en,allowable}$ obtained for each combination of loading condition and surface condition are summarized in Table 9 for the two design curves. By using these values with Eq. (31), a large relaxation value ranging from a factor of 3 to a factor of 7 is derived for the environmental factor.

TABLE 9. VALUES OF $F_{\text{en,allowable}}$ FOR EACH CONDITION AND DESIGN CURVE [102]

Industrial conditions	New ASME [97]	RCC-M [102] (Old ASME [98])
Ground components submitted to thermal ramps	3.5	3.0
Polished components submitted to thermal ramps	4.5	3.5
Ground components submitted to thermal shocks	5.5	4.0
Polished components submitted to thermal shocks	7.0	5.0

5.4.4. Development in Germany

Another independent study has been performed to investigate the fatigue property of niobium or titanium added 'stabilized' stainless steels (German grade 1.4541/1.4550; ASTM type 347/321) [103] in comparison with the NUREG equation, which has been developed principally based on the test data of conventional austenitic stainless steels such as type 304 and 316 and their low carbon variations. Based on this investigation, a large difference was found to exist between the fatigue strength of these materials at room temperature and the NUREG equation, as shown in Fig. 55. It was found, however, that these materials show gradual but more pronounced life reduction with increasing temperature, from 25°C to 325°C, even in the tests conducted in air. The design fatigue curves shown in Fig. 56 have been developed for these steels in the KTA code [77] from those for the 'conventional' stainless-steel grades. One of the two curves, applicable to room temperature only, is higher than the NUREG curve, but another curve for temperatures above 80°C is very similar to the NUREG curve.

In addition, independent studies are under way by AREVA regarding the fatigue life equations for austenitic stainless steels. As a first step, they compiled the literature test data of various kinds of stainless steels taken in air and derived a Langer type best-fit equation by analysing them [104]. They have also collected data from tests for the specimens with rough surfaces and examined the effects of surface condition, as shown in Fig. 57. As can be seen, results obtained by different sets of tests show different trends, some showing shorter lives, but others showing longer lives, in comparison with the smooth surface data. This occurs as a result of a combination of various factors, such as hardness increase and residual stress, in addition to surface morphology, but it is concluded that a factor of 2.5 proposed by ANL researchers is reasonable as the worst cases are covered by the factor.

As a follow-up of the study, they started to formulate a best-fit equation for fatigue behaviour under high temperature water of similar austenitic stainless steels and the following equations (33–36) have been proposed to express the fatigue endurance in a PWR environment [105].

$$N^{\text{PWR}} = N_{\text{Ref}}^{\text{PWR}} F_{\dot{\varepsilon}} F_{\text{T}} \tag{33}$$

where

$N_{\text{Ref}}^{\text{PWR}}$ represents the fatigue life in the PWR environment at the strain rate of a reference temperature of 300°C and reference strain rate of 0.4%/s and is given by Eq. (34) as a function of strain amplitude, ε_{a}.

$$N_{\text{Ref}}^{\text{PWR}} = 10^{\left\{4.18 - \log(\varepsilon_a - 0.085) - 1.35(\varepsilon_{\text{a}} - 0.085)^{0.35}\right\}} \tag{34}$$

Then, additional variables are used for expressing the effect of strain rate $\dot{\varepsilon}$ and the temperature T as

$$F_{\dot{\varepsilon}} = (\dot{\varepsilon} / 0.4)^{0.18} \tag{35}$$

and

$$F_{\mathrm{T}} = (\frac{0.28}{\varepsilon_{\mathrm{a}} - 0.105} + 1)^{\left(\frac{300-T}{150}\right)} \tag{36}$$

It should be noted that the dependency on strain amplitude was included in the expression for temperature dependence, unlike the expressions in the NUREG report and JSME guidelines. This brought about some improvement concerning the agreement between test data and predictions.

In terms of regulatory aspects, a concept known as 'threshold of attention values' was introduced to avoid unnecessarily detailed evaluations which were otherwise required. They represent the allowable UF (without F_{en}) below which no detailed evaluation considering the environmental effect is required. As a result of analyses of the difference between the design transients and actual thermal histories, a value of 0.4 is recommended as a part of the KTA code [106].

5.4.5. Development in Finland

Tests have also been carried out on high temperature water simulating PWR primary coolant on stabilized stainless steels in VTT, the technical research centre of Finland [107]. The effect of non-stressed high temperature holding introduced during fatigue tests was studied in addition to conventional fatigue tests. Those tests have demonstrated that these materials also show life reduction in water, in comparison with in-air lives, but the reduction is smaller than predicted by the NUREG F_{en} expression. A comparison of experimentally observed life reduction $F_{\mathrm{en,experiment}}$ with the prediction by the NUREG expression $F_{\mathrm{en,NUREG}}$ shown in Fig. 58(a) confirms this. The high temperature hold introduced during fatigue tests was found to be beneficial, rather than harmful, in prolonging the fatigue lives due to hardening caused during the holding, according to the authors' interpretation. There was also some discussion on the extraction of the real environmental effect $F_{\mathrm{en,water}}$ out of the total life reduction in high temperature

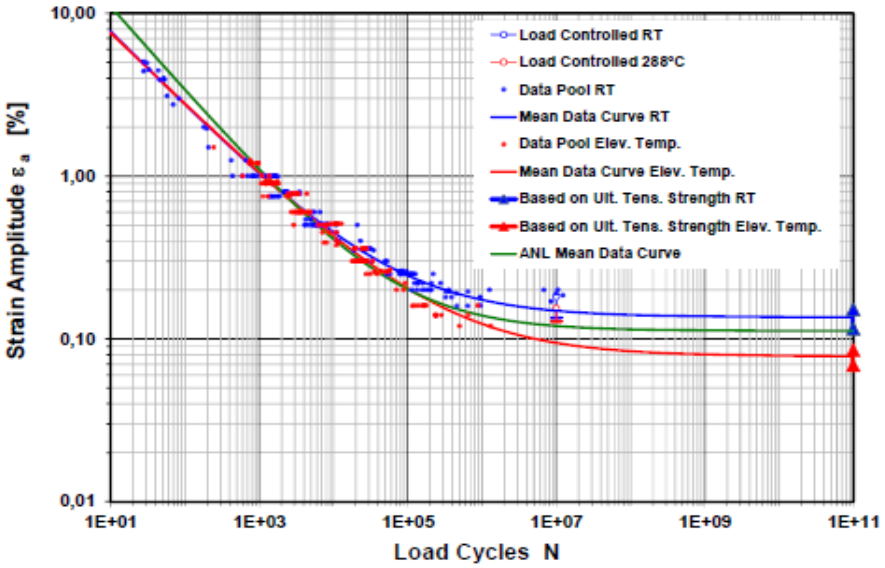

FIG. 55. Comparison of fatigue data on type 347/321 stainless steels and various fatigue curves including the ANL (NUREG) mean air curve [103].(b) high temperature.

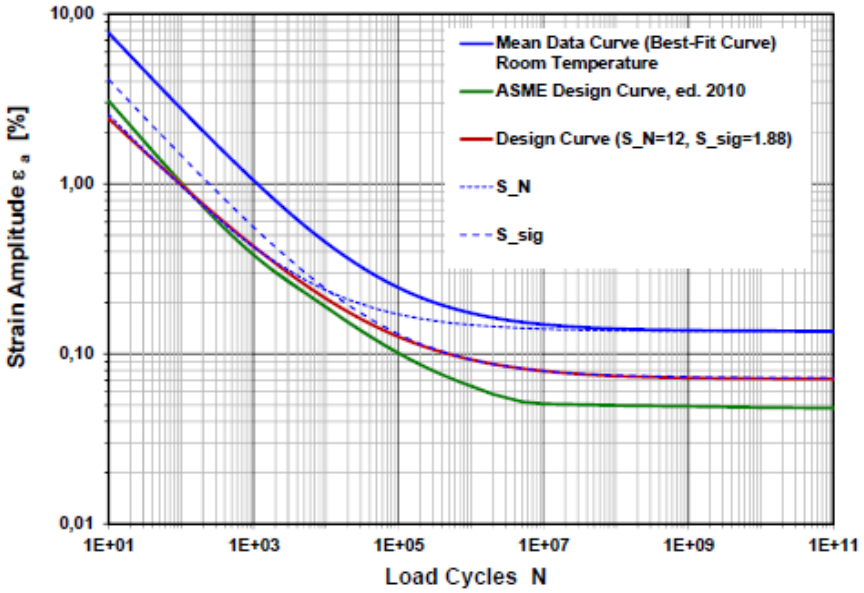

(a) room temperature

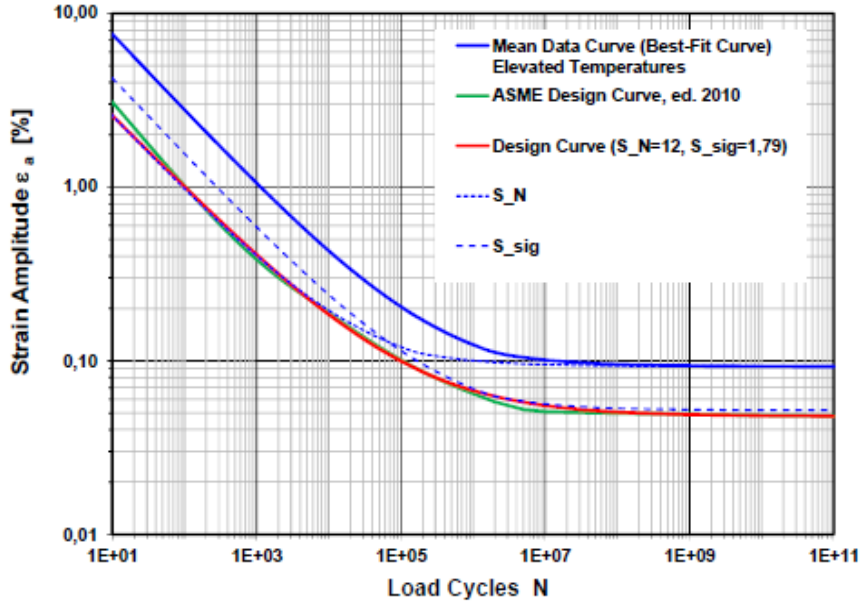

(b) high temperature

FIG. 56. Comparison of design fatigue curves for stabilized stainless steels using the KTA and NUREG curves [103] at (a) room temperature and (b) high temperature.

water $F_{\text{en,experiment}}$, as shown in Fig. 58(b) because these materials tended to show relatively large life reduction at high temperatures as against room temperature, even in air.

5.4.6. Summary

It is now commonly recognized by many organizations in a number of countries that the environmental effect should be borne in mind in evaluating structural integrity against fatigue mechanisms. However, simple treatment, such as dividing the allowable number of cycles on the design fatigue curves by the environmental factor, or multiplying it with the fatigue UF, often results in a judgement about

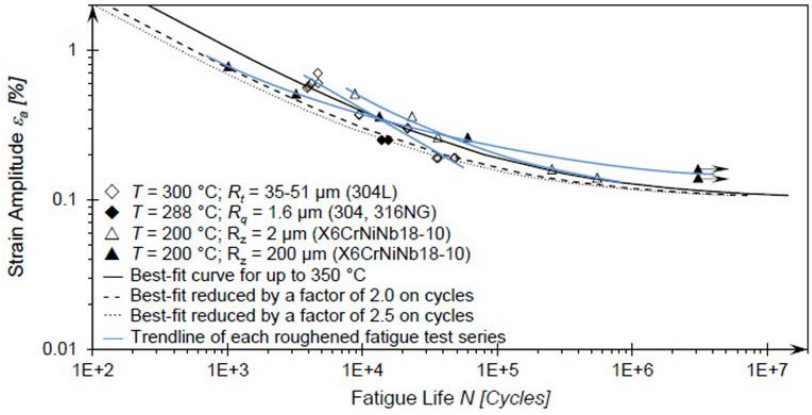

FIG. 57. Comparison of the AREVA reference curve with the NUREG curve [104].

the integrity that might seem too conservative because the design curves themselves already include a relatively large design transference factor for a conservative evaluation of various factors influencing the fatigue life.

A factor of 20 on life and a factor of 2 on strain amplitude are traditionally applied to the best-fit curves to obtain the design curves. However, simple superposition of environmental effects on such factors, as well as that of several subfactors, does not seem to have any rational justification, though such a thought has triggered efforts to re-examine the factors, as described above and listed in Table 10. Large discrepancies exist between these proposals, suggesting the need for more effort in establishing a commonly accepted procedure which is not excessively conservative.

5.5. ENVIRONMENTAL EFFECTS ON FATIGUE CRACK GROWTH

5.5.1. Outline

As stated in the first part of this section, the process of fatigue failure consists of the initiation and growth of cracks. Crack growth is also affected by environmental conditions; the effect of high temperature water on fatigue crack growth has been studied for the relevant materials. Codes and standards developed to address structural integrity when crack-like flaws are detected by ISI include a procedure for estimating fatigue crack growth in high temperature water as well as in the air environment using fracture mechanics [108–110]. This section summarizes the present status of these procedures, with special emphasis on the treatment of environmental effects.

5.5.2. Ferritic steels

The effect of high temperature water on fatigue crack growth in ferritic steels was recognized well before the recognition of that effect on fatigue endurance of plain bar specimens, and was reflected in the CGR equations in ASME B&PV code, section XI [108] and in other codes [109, 110]. The CGR in cycle da/dN in mm in-air environment is given in Eq. (37).

$$da/dN = 9.72\times10^{-8}\Delta K^{3.07}/(2.88-R)^{3.07} \quad (37)$$

Using the stress intensity factor range $\Delta K = Kmin_{max}$ in $\mathrm{MPa}\sqrt{m}$ and the stress ratio, $R = Kmax_{\min}$ is calculated from the maximum and minimum values of the stress intensity factors $K_{\max}$ and $K_{\min}$ experienced during the cycle to be evaluated.

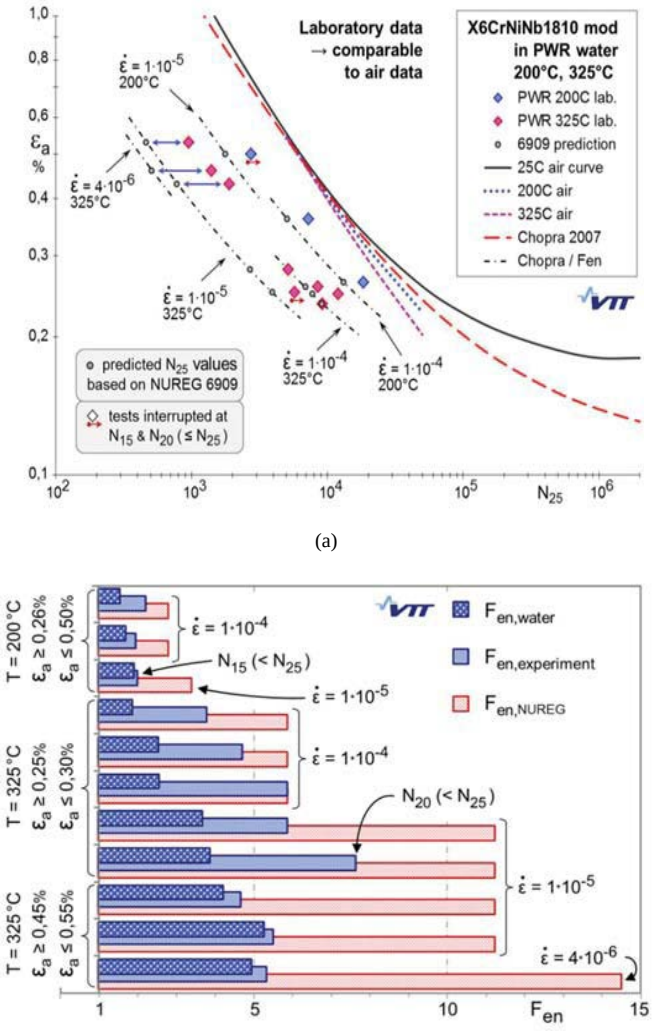

FIG. 58. Comparison of fatigue test data in simulated PWR water for stabilized stainless steels and various fatigue curves [107]. (a) Comparison of test results with the NUREG curve; (b) comparison of Fen from different methods.

An independent and more complicated equation is given for $R < 0$ in section XI but is not discussed here for simplicity. The effects of temperature or loading rate are not included. It is also assumed that crack growth does not occur when ΔK is smaller than the threshold calculated in Eq. (38).

$$\begin{aligned} &\Delta K = K\min_{\max} \\ &\text{MPa}\sqrt{m} \\ &R = K\max_{\min} \\ &\Delta K_{th} = 5.5 \text{ for } R < 0 \\ &= 5.5\left(1 - 0.8R\right) \text{ for } 0 \le R < 1.0 \end{aligned} \tag{38}$$

TABLE 10. SUMMARY OF SUBFACTORS AND TOTAL FACTORS RECOMMENDED FOR USE IN DERIVING DESIGN FATIGUE CURVES FROM BEST-FIT, IN-AIR CURVES

Code, etc./Sub factors	ASME III (2007) [98]	NUREG/CR-6909 [76]	Nomura et al [87]	RCC-M (in consideration [99])	KTA 3201 [77]	
					T<80°C	T>80°C
Material data scatter	2.0	2.1–2.8	2.7–3.4	2.5	1.27*	1.27*
Size effect	2.5	1.2–1.4	1.2–1.4	1.6	1.09*	1.09*
Surface finish (roughness)	4.0	2.0–3.5	2.0–3.5			
Loading history	—	1.2–2.0	—			
Mean stress	Separately	—	—	—	1.07*	1.05*
Total	20	6.0–27.4	6.6–16	5.2–7.2	—	—
Factor on life (recommended)	20	12	10–12	12	12	12
Factor on strain	2	2	1.9	1.4	1.88	1.79

* subfactors on strain, rather than life

where R is the stress ratio.

On the other hand, the following CGR equation in high temperature (HT) water, Eq. (39), has been developed based on the test results [111], and is included in section XI.

$$\frac{da}{dN} = Min\left\{ f_1(R)\Delta K^{5.95}, f_2(R)\Delta K^{1.95} \right\}$$
$$f_1(R) = 1.48\times10^{-11} \text{ for } R \le 0.25$$
$$= 1.48\times10^{-11}(26.9R - 5.725) \text{ for } 0.25 < R \le 0.65$$
$$= 1.74\times10^{-10} \text{ for } 0.65 < R \le 1 \qquad (39)$$
$$f_2(R) = 2.13\times10^{-6} \text{ for } R \le 0.25$$
$$= 2.13\times10^{-6}(3.75\,R + 0.06) \text{ for } 0.25 < R \le 0.65$$
$$= 5.33\times10^{-6} \text{ for } 0.65 < R \le 0.65$$

The same threshold as in the in-air environment is assumed to be present. However, many tests have been carried out after the proposal of this equation, and the existence of considerably greater acceleration, due to the HT environment, has been observed by many investigators [112–115]. The strong effect of sulphur content in the steels and the oxygen content in the water have been clarified, as well as the loading rate. Equations based on such information are now included in ASME Code Case N-643 [55]. N-643, which is applicable to the PWR primary water condition, now includes the effect of sulphur content and the time spent in the tension-going period, hereafter called rise time, in addition to the effect of R, unless environmental associated cracking is regarded as being negligible.

Figure 59 shows an example of the reference crack growth curves that are calculated by Code Case N-643 for three conditions, in comparison to the reference curve given in ASME section XI at the same value of *R*. Crack growth behaviour predicted by Code Case N-643 shows large dependence on the combination of the sulphur content and rise time. Sometimes it exceeds the section XI curve for in-water evaluation but becomes lower than in other cases. It should be added that the relation for a whole ΔK range cannot be expressed by a single power law, but different power law functions are applied to three regions based on the consideration of environmental associated cracking.

More recently, the effect of water chemistry was studied in more detail and a model that can be applied to different water chemistries, including BWR plants employing HWC as well as NWC, was developed, as shown in Fig. 60 [115].

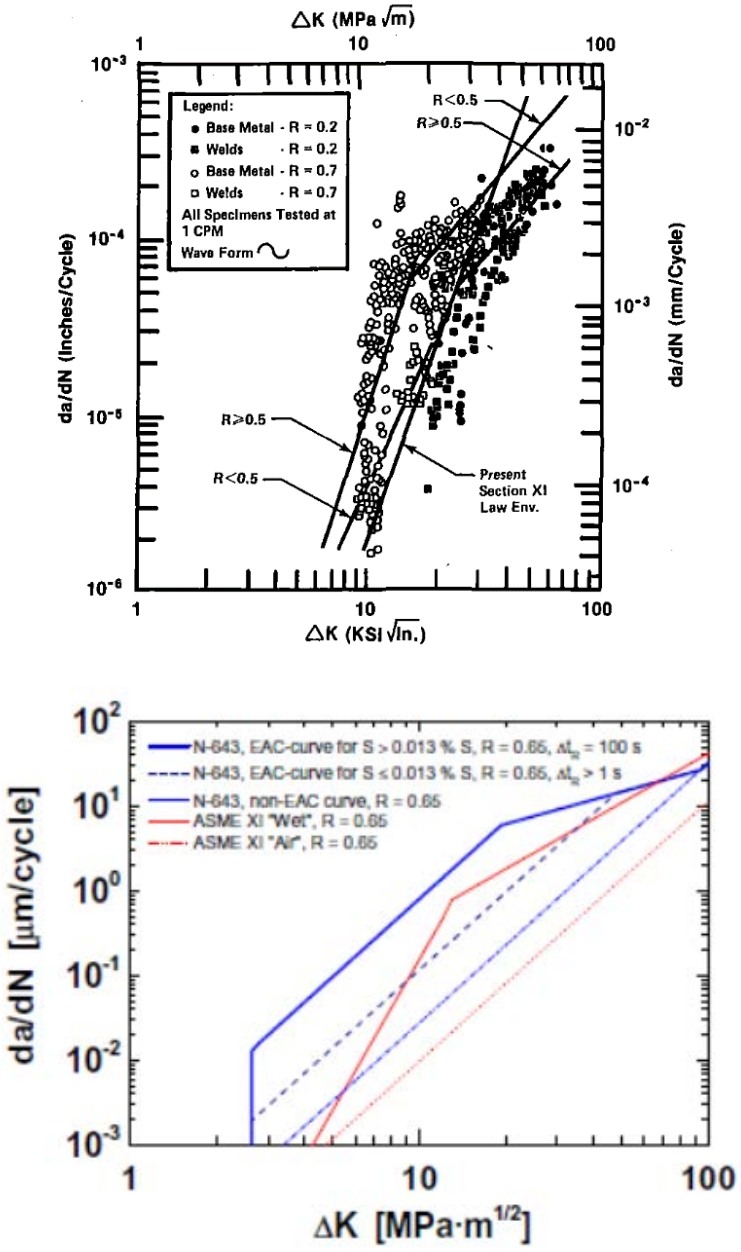

FIG. 59. Comparison of codified crack growth curves for ferritic steels [115].

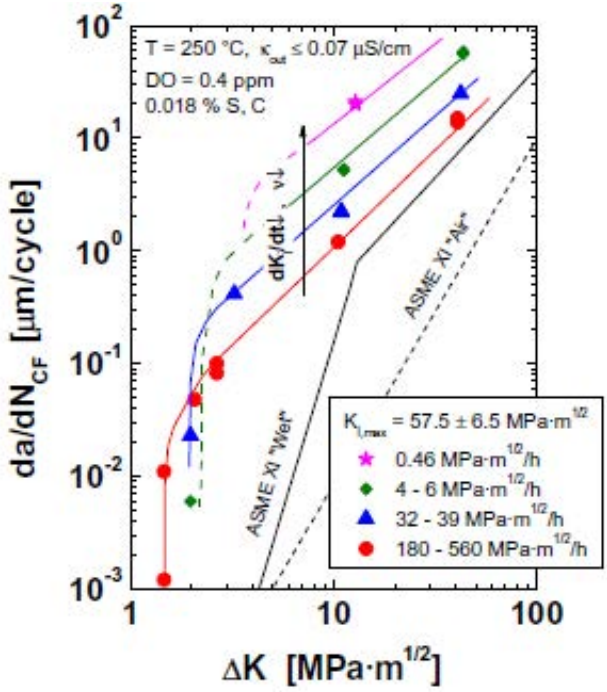

FIG. 60. CGR in high oxygenated water in comparison with ASME section XI curves for ferritic steels [115].

5.5.3. Austenitic stainless steels

For austenitic stainless steels, the following set of equations (40) is given for use in the assessment of fatigue crack growth in air environment in ASME Code section XI [108] and other codes [109, 110].

$$
\begin{aligned}
&Ada/dN = 18.61C(T)f(R)\Delta K^{3.3} \\
&C(T) = 10^{-9.984+1.337\times10^{-3}T-3.344\times10^{-6}T^2+5.949\times10^{-9}T^3} \\
&f(R) = 1 \text{ for } R \le 0 \\
&f(R) = 1+1.8R \text{ for } 0 < R \le 0.79 \\
&f(R) = 57.97R - 43.35 \text{ for } 0.79 < R \le 1
\end{aligned}
\qquad (40)
$$

The fatigue CGR in HT water is not given in ASME section XI, but the JSME code for fitness for service has the relevant equations for use in the assessment for PWR and BWR conditions [109], as shown in Table 11. In both equations, rise time is used as an additional parameter governing the extent of the environmental effects. For PWR conditions, the equation given in Table 11 was based on the test data [116]. The equations giving the upper bound of the test data exhibits a significant acceleration of CGR due to exposure to water environment.

Similar equations were developed for estimating CGR in BWR conditions [117], but temperature does not appear as an independent variable because most of the tests have been performed at the operating temperature of 289°C. Significant increase in CGRs due to environmental effects can be seen clearly as in the case of PWR condition. The ratios of CGRs in HT water against those in air decreases with the increase in the stress intensity factor range, but they are between about 20 and 120 at the longest rise time of 1000 s. The difference between PWR and BWR conditions appears to be relatively small.

ASME Code section XI has only the curve for the in-air condition, but Code Case N-809 [118], which includes the equations for reference CGRs in PWR water condition, has been developed and published

[119–121]. Some distinctions are given for the conventional grades of type 304 and 316 stainless steels and for their low carbon grades, as shown in Table 11. Comparison with JSME PWR curves revealed that while they are similar there is some difference, particularly at high *R* value, as shown in Fig. 61.

5.5.4. Ni–Cr–Fe alloys

Fatigue crack tests on some Ni–Cr–Fe alloys and their weldments have been conducted by ANL [119] and the equations of Alloy 600 both in air and in HT water have been developed and codified as part of a recent ASME Code for flaw assessment of this material [122]. The full equations (41) including all the influential parameters can be written as:

$$\begin{aligned} &da/dN = C_{\mathrm{T}} S_{\mathrm{R}} S_{\mathrm{ENV}} \Delta K^{4.1} \\ &C_{\mathrm{T}} = 4.835\times10^{-11} + 1.622\times10^{-13} T - 1.490\times10^{-15} T^2 + 4.355\times10^{-18} T^3 S_{\mathrm{R}} = \\ &1/(1-0.82R)^{2.2} \end{aligned} \tag{41}$$

where S_{ENV} is the factor expressing the effect of the environment by taking a unity in air and the value obtained by Eq. (42) in HT water.

$$S_{\mathrm{ENV}} = 1 + A_{\mathrm{E}} \left\{ Min\left(t_{\mathrm{r}}, 30\right) / C_{\mathrm{T}} S_{\mathrm{R}} \Delta K^{4.1} \right\}^{0.67} \tag{42}$$

Many tests have also been conducted in Japan on PWR conditions; the prediction of equations (41) and (42) was found not to be conservative. The alternative equations (43) and (44) were proposed for both in-air and in HT water characteristics by modifying them [123, 124]. The in-air CGR thus obtained is given by [123].

$$\begin{aligned} &da/dN = C_{\mathrm{T}} f\left(R\right) \Delta K^{4.1} \\ &C_{\mathrm{T}} = 1.30\times10^{-10} + 4.39\times10^{-13} T - 4.14\times10^{-15} T^2 + \\ &1.32\times10^{-17} T^3 \\ &f\left(R\right) = 1/(1-0.82R)^{2.2} \end{aligned} \tag{43}$$

whereas the average and upper bound CGR in HT water is described by [124]

$$\begin{aligned} &da/dN = 4.31\times10^{-11} T^{0.77} t_{\mathrm{r}}{}^{0.24} \Delta K^{3.25} / (1-R)^{1.34} \\ &da/dN = 1.16\times10^{-10} T^{0.77} t_{\mathrm{r}}{}^{0.24} \Delta K^{3.25} / (1-R)^{1.34} \end{aligned} \tag{44}$$

A large influence of the rise time on CGRs can be seen. Crack growth characteristics predicted by these equations are compared in Fig. 66 for two representative values of *R*. The ASME equations for HT water show unique characteristics deviating from a power law relation and converging into the in-air lines at a relatively small value of the stress intensity factor range, whereas the equations by Nomura et al. [123] provide more ‘ordinary’ or ‘normal’ behaviour following a power law relation as in other materials. The amount of acceleration of crack growth predicted by the equations by Nomura et al. also exhibits more natural behaviour than that estimated by the ASME equations, as can be seen in Fig. 62. The amount of acceleration is similar to that of stainless steels and much larger when compared with the maximum value of F_{en} specified for this class of material, which indicates that further study is required.

TABLE 11. COMPARISON OF CGR EQUATIONS FOR AUSTENITIC STAINLESS STEELS

Code	CGR equations
JSME PWR	$da/dN = 4.35\times10^{-10} T^{0.63} f(t_r) \Delta K^{3.0} (1-R)^{1.56}$ $f(t_r) = 1$ for $t_r < 1$s $= t_r^{0.33}$ for $1s \le t_r < 1000s$ $= 9.77$ for $t_r \ge 1000s$
JSME BWR	$da/dN = 8.17\times10^{-12} f(t_r) \Delta K^{3.0} (1-R)^{2.12}$ $f(t_r) = 1$ for t_r <1s $= t_r^{0.5}$ for $1s \le t_r < 1000s$ $= 31.6$ for $t_r \ge 1000s$
ASME Code Case for 304, 316 in PWR primary	$da/dN = CS_T S_R S_{ENV} \Delta K^{4.1}$ $C = 9.10\times10^{-6}$ for $\Delta K \ge 1.10$ $= 0$ for $\Delta K < 1.10$ $S_T = \exp\{-2516/(T+273.15)\}$ for 150°C < T < 343°C $= 3.39\times10^{5} \exp\{-2516/(T+273.15) - 0.0301(T+273.15)\}$ for 20°C < T < 150°C $S_R = 1+\exp\{8.02(R-0.748)\}$ for $0 \le R < 1$ $= 1.0$ for $R \le 0.0$ $S_{ENV} = t_R^{0.3}$
ASME Code Case for 304L, 316L in PWR primary	$da/dN = CS_T S_R S_{ENV} \Delta K^{4.1}$ $C = 1.39\times10^{-5}$ for $\Delta K \ge 1.10$ $S_T = \exp\{-2516/(T+273.15)\}$ for 150°C < T < 343°C $= 3.39\times10^{5} \exp\{-2516/(T+273.15) - 0.0301(T+273.15)\}$ for 20°C < T < 150°C $S_R = 1+1.5(R-0.7)$ for $0.7 \le R < 1$ $= 1.0$ for $R \le 0.7$ $S_{ENV} = t_R^{0.3}$

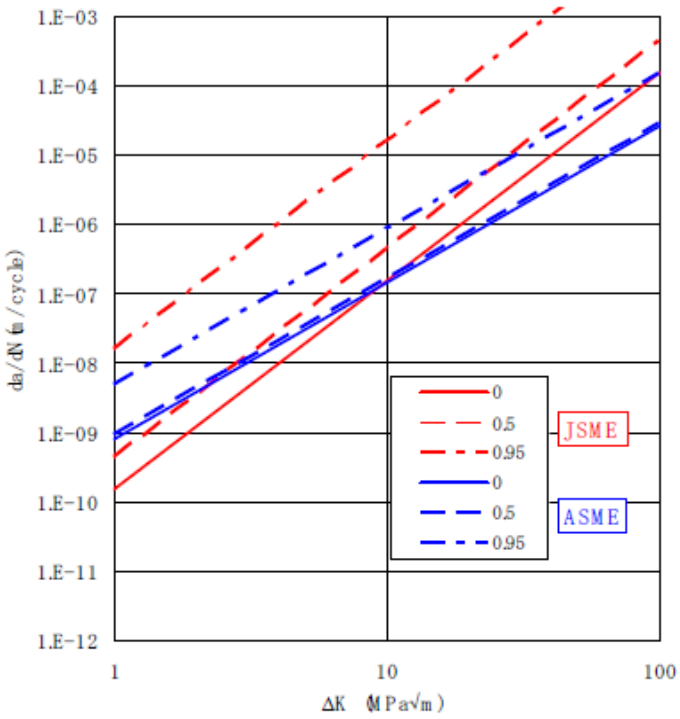

FIG. 61. Comparison of CGR properties for stainless steels for PWR conditions [119].

5.5.5. Comparison of crack growth equations for different materials

Fatigue CGRs in terms of the stress intensity factor range have been discussed for each material type in the above sections. They will be compared in this section to clarify the features of each material type. In the first step, fatigue crack growth properties in the air predicted by the representative codes for R = 0 and 0.9 are compared in Fig. 63(a). Ferritic steels and austenitic stainless steels show similar characteristics at R = 0, but the latter shows higher CGR when R becomes 0.9. It can also be seen that the Ni–Cr–Fe alloys shows a larger slope both at R = 0 and 0.9 compared with the other two types of material. On the other hand, in-water CGRs of three types of material calculated at 300°C and the rise time of 1000 s are compared in Fig. 63(b). In this case, three types of material show similar rates at R = 0, whereas larger differences appears at R = 0.9.

The ratio of the CGR in water to that in air obtained from these two plots is calculated and plotted in Fig. 64 as a function of the stress intensity factor range. In Fig. 64(a), where the rise time is fixed at 1000 s, the ratio remains unchanged for ferritic steels, whereas it decreases with the increase of the rise time, showing the load amplitude dependency of the environmental effect in the other two types of material. On the other hand, one can also compare the ratio at the same stress intensity factor rate $\dot{K}$, which is obtained simply by dividing ΔK by t_r. Crack growth equations (45) represented by the form of:

$$da/dN = A(T,R)t_r^{\,m}\Delta K^n \tag{45}$$

Crack growth equations (45) can be converted to an equivalent form as (46):

$$da/dN = A(T,R)\dot{K}^{-m}\Delta K^{m+n} \tag{46}$$

The ratio calculated at the fixed value of $\dot{K}$(=0.1 MPa m$^{0.5}$/s) is replotted as a function of ΔK in Fig. 64(b). It can be seen here that the variation of the ratio with the stress intensity factor range becomes smaller and it becomes almost constant even for the stainless steels. Although there is still a fairly large ΔK dependency in Ni–Cr–Fe alloys, the amplitude of the environmental effect is not dependent on the amplitude of cyclic loading when tested at the same loading rate, as already discussed in Section 5.2 on the fatigue life of initially uncracked bar specimens. It should also be added that the amount of life reduction in fatigue tests and the amount of crack growth acceleration in crack growth tests are approximately the same in ferritic and stainless steels.

Comparison of crack growth characteristics and fatigue life characteristics in terms of the environmental effect has also been performed in different ways. Seifert et al. [125] measured the time to

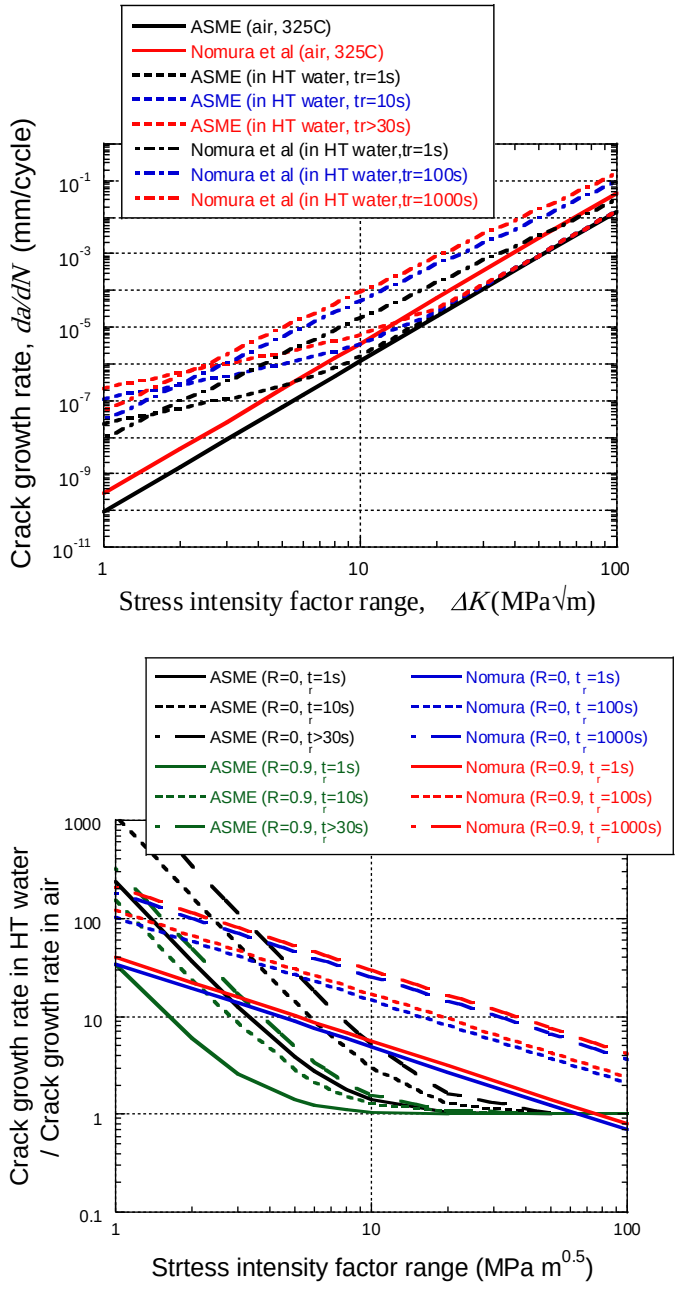

FIG. 62. Comparison of in-air and in-hot-water crack growth properties of Ni–Cr–Fe alloys [123].

crack initiation and the subsequent growth rate using the direct current potential drop method in sharply notched compact tension (CT) specimens of stainless steel. The acceleration due to environmental effects is compared with the value of F_{en} under the same environmental and mechanical conditions.

In an independent study by Kamaya [126], small crack growth behaviour in smoothed bar specimens was measured by the surface replication technique. It has been shown that the dependency of normalized crack rate on rise time is similar to that observed in more conventional crack growth tests using CT specimens and the fatigue life of such a specimen can be estimated using crack growth characteristics under specified conditions, as shown in Figs 64 and 65. This again demonstrates the existence of a strong correlation between fatigue life and fatigue crack growth characteristics. These observations clearly suggest the possibility of acquiring and improving the equations for the F_{en} factor from crack growth tests which do not require as much time as normal fatigue tests.

5.6. SUMMARY

Practices that take into account environmental effects on fatigue lives and fatigue crack growth have been reviewed in this section. Extensive work has been done on this crucial issue in fatigue assessments for LWRs over the last two decades. A great deal of progress has been made in understanding the material behaviour and developing procedures to deal with them. However, there are ongoing studies on this topic and more time is required to reach a consensus on the procedure to be applied for plant assessment. The following items are expected to play important roles as key ingredients of such a procedure:

Method of transformation from the mean material curves to design fatigue curves in air as well as in HT water. A probabilistic approach is worth exploring to avoid unduly conservative evaluation from deterministic treatment of many factors. It should also be added that the factors to be used for such a transformation are not necessarily the same in air and in HT water. For example:

— Incorporation of fatigue crack growth properties into fatigue damage assessment: Comparison of environmental factors in those two aspects provides an opportunity to reconsider one or both of them.
— Establishment of a flaw tolerance type approach as an alternative or complementary tool to the conventional fatigue damage approach: More emphasis is needed on the possibility of real failure evaluated through crack growth calculation, rather than initiation of crack in peak stressed area.

In order to further enhance the reliability of fatigue evaluation, including the environmental effect, it is necessary to devote more attention and effort to the following issues:

— Performance of welded joints;
— Influence of stress multiaxiality in terms of environmental effect. Higher stress triaxiality, or mean stress may bring about larger environmental effect than uniaxial push–pull condition.
— Undertaking of plant representative (environment and loading) feature testing for initiation and significant growth due to fatigue that can be used to benchmark improved analytical models.

6. FATIGUE MONITORING AND RELATED SYSTEMS

Fatigue monitoring delivers valuable information on operational fatigue loading. This is based on continuous measurement of thermal and mechanical loads locally or more globally using the standard plant instrumentation plus transfer functions. Local thermal loads are usually measured by measurement sections consisting of sets of thermocouples fixed on the outside locations of piping sections. LCF

loadings are reliably identified using this approach. The loads can be directly processed by identifying cycles or used for transient counting by comparison with cycles with transients already defined in stress reports. High cycle loadings, such as high cycle thermal fatigue and vibrational fatigue, are not within the scope of state of the art fatigue monitoring systems due to measurement restrictions. However, new systems still being developed may be helpful in overcoming this restriction [127, 128].

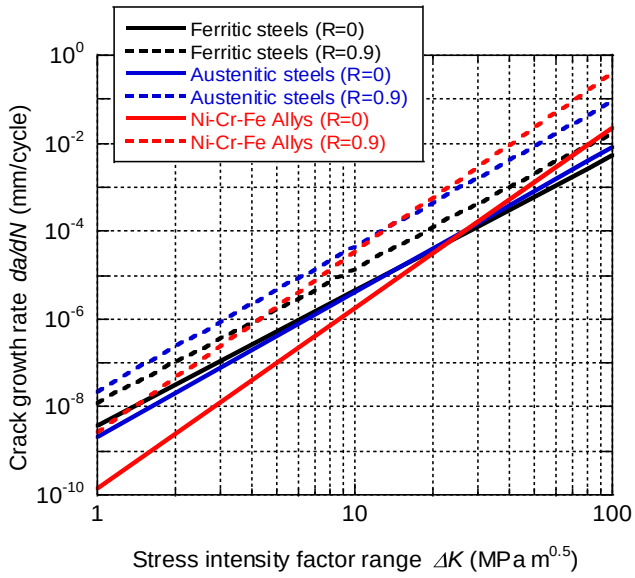

(a) In–air at room temperature

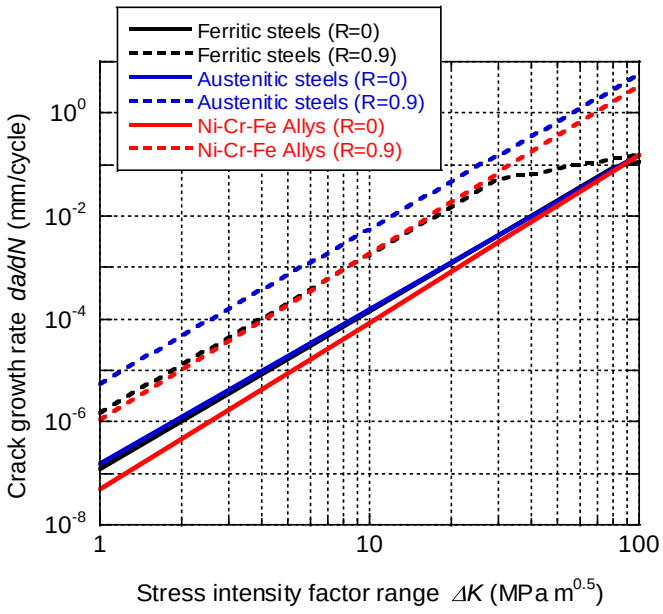

(b) In hot temperature water at 300°C (tr=1000 s)

FIG. 63. Comparison of crack growth properties for various materials (a) in-air at room temperature; (b) in hot water at 300°C (tr=1000 s) [125].

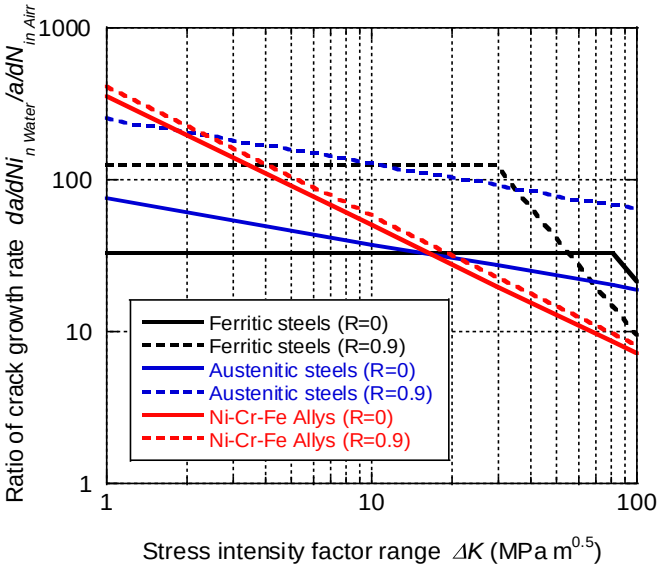

(a) At the same rise time (tr–1000 s)

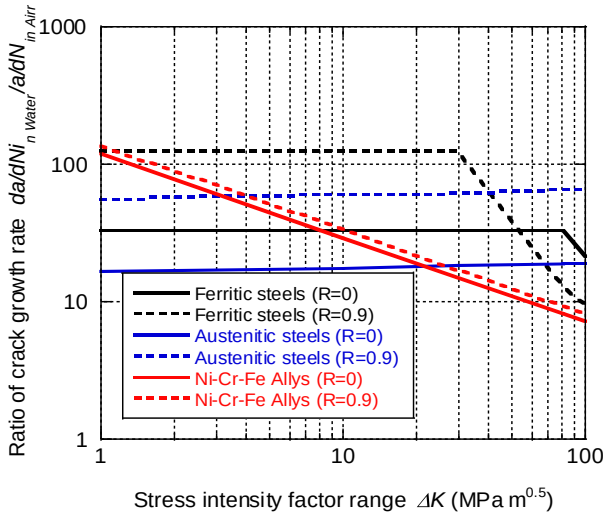

(b) At the same $\dot{K}$ (=0.1 MPa m$^{0.5}$/s).

FIG. 64. Variation of crack growth acceleration in various materials [125]. (a) At the same rise time (tr–1000 s) (b) At the same $\dot{K}$ (=0.1 MPa m$^{0.5}$/s).

6.1. FATIGUE MONITORING STRATEGIES AND TECHNOLOGIES

Plant cycle counting and fatigue monitoring in NPPs is indispensable for tracking design life as well as minimizing damage to important components, thus increasing safety [129]. Furthermore, there are associated regulatory requirements. For example, some form of fatigue tracking or cycle counting is required by the US NRC for operating NPPs to demonstrate that the ASME Code design basis has not been violated [129].

The following benefits of fatigue monitoring in the nuclear power industry are discussed in Ref. [129] and summarized in Ref. [130]:

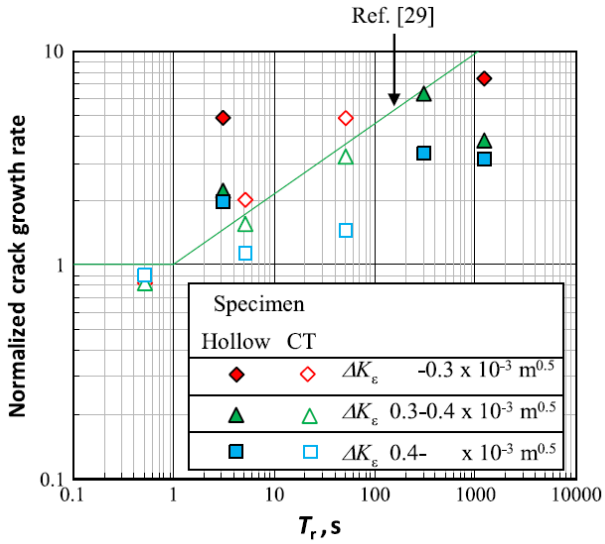

(a) Rise time versus the normalized CGR.

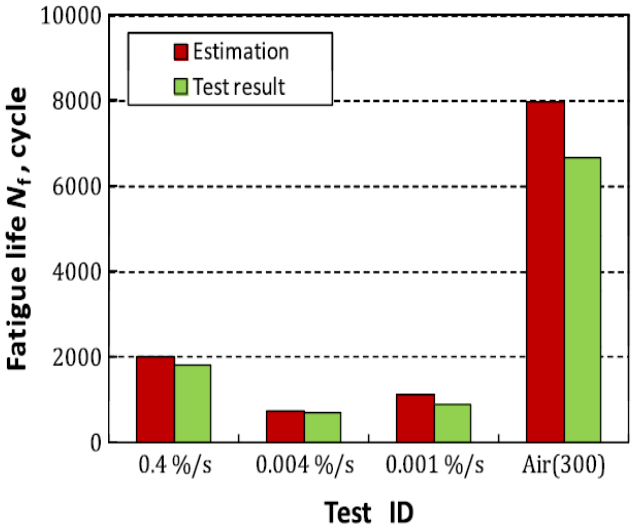

(b) Comparison of estimated life with the test result.

FIG. 65. Comparison of life predicted by crack growth evaluation with smooth specimen test data [126]. (a) Rise time versus the normalized CGR; (b) Comparison of estimated life with the test result.

— NRC requirements:
  - Responding to code and regulatory requirements and providing a technical basis for component life management;
  - Both final safety analysis reports (FSARs) and technical specifications may specify that records be kept of actual operating transients to ensure that the design bases are not violated;

— Component life management:
  - Screening of fatigue sensitive components;
  - Indication of the fatigue status of the specific component;
  - Results of fatigue monitoring correlated with ISI intervals and locations;

— Plant transient evaluation:
  - Identification of transients exceeding those considered in the original plant design process;

— Plant licence renewal for LTO:
  - Providing a strong technical basis for LTO beyond that considered in the original design;
  - Fatigue as a time limited ageing analysis, and thus the need for ageing management to support and prepare for LTO;
— Improved operating practices:
  - Understanding of fatigue mechanisms (e.g. stratification effects) in the feedwater nozzles [131].

Qualified fatigue monitoring systems are used:

— To log the real loads at the fatigue sensitive components;
— To establish a realistic basis of operating loads for fatigue analysis;
— To obtain strain rate history data for EAF calculation;
— To identify and optimize operating modes unfavourable to fatigue;
— To improve the design for availability in general and for LTO (if necessary).

The German Nuclear Safety Standard KTA 3201.4 [132] contains guidelines for operational monitoring (Section 9). Sections 9.2 and 9.2.1 state that to adhere to these fatigue monitoring requirements it is necessary to ensure:

> "that temporal and local temperature changes relevant to fatigue are monitored by a sufficiently dense net of measuring points of the standard instrumentation. When selecting the measuring points the effects of the mode of operation (little mass flows, indifferent pressure conditions, switching operations, temperature differentials) and the design (pipeline installation, isolating function of valves) shall be taken into account."

Where thermal stratification is expected to occur, the temperature measuring points should be located such that all relevant loading variables across the pipe cross-section and axially to the pipe run can be measured. The measuring results needs to be evaluated once per refuelling cycle and should be documented in a report.

As already stated, operating experience is very helpful because it enables utility engineers at operating NPPs to understand the fatigue failure mechanisms and, importantly, identify the specific components and locations susceptible to fatigue. Hence, the state of the art of transient and fatigue monitoring can help the utility engineer understand the options available and how to more effectively operate the plant to lessen fatigue damage. In this context, modern state of the art (mostly thermal) fatigue monitoring approaches gain in importance as part of the ageing management of NPP components.

Operators have to deal with demanding safety requirements to ensure the safe operation of power plants and to cope with LTO related issues. NPP applications require the qualified assessment of measured thermomechanical loads. The core challenge is the identification and qualified processing of realistic load-time histories. The related methodological requirements will be explained in detail.

In terms of the nuclear industry, the ageing management of NPP components is a major issue for all actors: regulatory agencies, operators, designers and suppliers. As regards the fatigue assessment of NPP components, stringent safety standards imply the consideration of new parameters in the framework of the fatigue analysis process:

— New design fatigue curves, consideration of EAF parameters;
— Stratification effects which might not have been considered in the original stress analysis reports based on the design transients of plants.

It should be noted that fatigue monitoring and fatigue assessment are closely related issues in the sense of determining operational loading conditions as realistically as possible (in the case of NPP

components, particularly thermomechanical loads) and using these load data as input for highly qualified fatigue assessment methods.

It is important to note that in the context of LTO, the monitoring of operational loads, as well as the storage of the acquired data, should start right at the beginning, i.e. in the commissioning phase for new NPPs. A later evaluation of these loads can be based on the available data. Note that in these cases, backward extrapolation should not be linear. Significant fatigue loads are characteristic for the commissioning phase and during early operation. Although fatigue monitoring is not requested everywhere or for every situation, the recommendation is to start monitoring critical locations as early as possible in an NPP's lifetime, for example, in the commissioning phase, which is characterized by particularly relevant fatigue loadings. Even if a complete fatigue monitoring system has not been implemented at fatigue critical locations, local instrumentation such as thermocouples and temperature measurement sections (even temporary and/or mobile) can be very useful.

As a consequence of the long operational lives, comprehensive solutions offered by vendors are preferable. The range of these solutions include monitoring of actual transient cycles and classifying and comparing them to previously evaluated design transients (cycle based fatigue), and fatigue usage assessment at control locations. Furthermore, there is a basic difference between the following:

— Cycle based fatigue (CBF):
  - Design basis CBF;
  - Partial CBF;
  - Stress history reconstruction CBF.
— Stress based fatigue (SBF):
  - Global fatigue monitoring;
  - Local fatigue monitoring.

Note that the identification of 'fatigue sensitive components' and 'locations susceptible to fatigue' is an important issue. Often, locations with a CUF < 1 in a standard fatigue analysis are considered not to be fatigue sensitive. However, if CUF > 1, additional analysis, normally using the finite element method (FEM), is usually needed. This usually reduces the CUF to a much lower value. Without going into the details of how the CUF was determined, the conclusion is that the second location is not fatigue sensitive, even though it might have been locations susceptible to fatigue in this system.

6.1.1. CBF

The determination of CBF relies on the set of design transients and their presumed frequency of occurrence during operation as part of the plant documentation and the technical specification in the final safety analysis report. Usually, these transients are conservative. Thus, the simplest way of implementing CBF is to count occurrences of the defined events.

This design basis cycle counting constitutes an explicit requirement for many operating plants and a transient fatigue monitoring system should be able to:

— Identify and track plant cycles;
— Compare actual and design base cycles;
— Deliver respective partial and CUFs.

Based on these design transients, fatigue analyses calculations are performed for the relevant components. During plant operation, events are compared with the design base events. In terms of partial CBF, additional analyses are performed with the aim of identifying the sensitivity of the key design transients in relation to the resulting stresses in a component [133, 134]. Stress history reconstruction CUF is used for situations where global plant conditions are fatigue relevant, where several types of plant events are superposed or where the order of events is important [130].

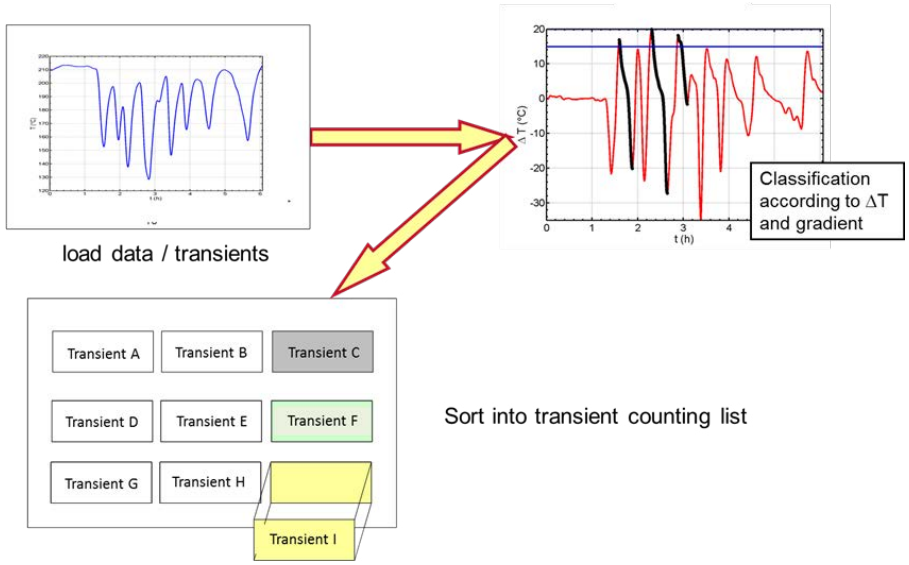

FIG. 66. CBF as a counting method [134, 135].

Additionally, a reanalysis of component fatigue usage can be based on actual plant transients. This constitutes an update of design transients. It can be concluded that thermomechanical loads are often connected to the term ‘transient’ or ‘thermal transient’. The terms ‘design transients’, ‘model transients’ and ‘operational loads’ are defined here for clarification:

— Design transients are usually specified in the commissioning phase, i.e. before operation. They are based on plant models and experience and are part of the licensing documents.
— Model transients are specified during operation. They are based on operational measurements and/or local measurements and cover the actual operational loading conditions in a conservative manner. Nevertheless, as these model transients are based on operational load information, they are usually significantly less conservative versions of design transients.
— Operational loads represent the measured load-time history.
— The related fatigue assessment methods are closely linked to the design code requirements of the fatigue check [135].

CBF is an easy counting method and is visualized in Fig. 66.
The advantages of CBF are:

— Easy to handle after initiation;
— Available automated tools allow for reliable transient identification;
— Can handle very large amounts of data;
— Direct information available on the number of actual/allowed transients.

The disadvantages are:

— The difficulty of EAF consideration;
— The conservativism of the approach;
— Lack of direct CUF state;
— Treatment of non-specified loads is not optimal condition.

A proposal to combine the advantages of cycle and SBF was made in Ref. [136]. The basic idea is a reduction of the gradient of the model transient. This can be selected based on the maximum stresses

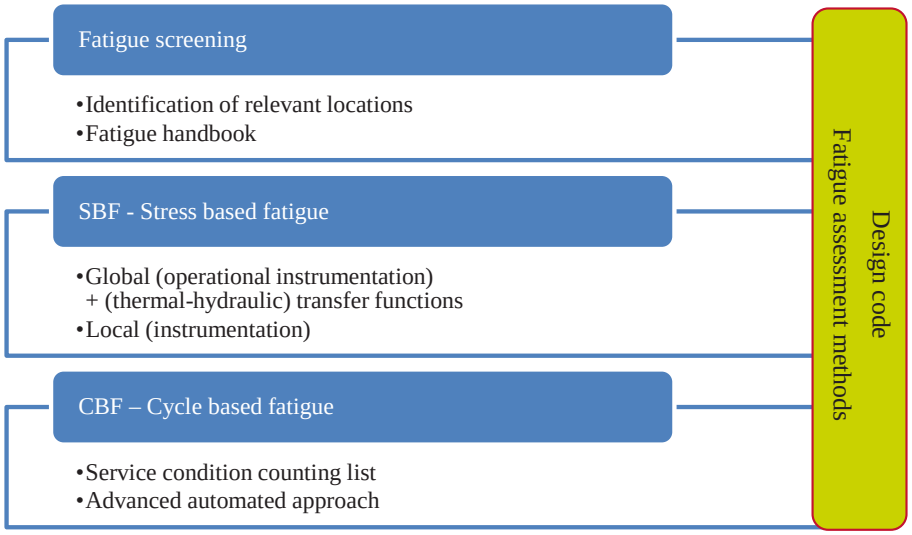

FIG. 67. Summary of fatigue monitoring methods.

instead of the maximum gradients in the measured temperature profile. The resulting model transient is more realistic and leads to lower, but still inclusive, usage factors.

6.1.2. SBF

SBF relies on the evaluation of operational plant data to determine the stress history at monitored locations. The processing of continuous operational load-time histories, or stress time histories, is characteristic of SBF. Within this fatigue monitoring approach, the related fatigue assessment conforming to design codes such as the ASME Code [137] or the German Nuclear Safety Standard [138] basically requires:

— The determination of the stress tensor (all six terms of total and linearized stresses) as a function of time;
— The application of a qualified cycle counting procedure for the determination of fatigue relevant cycles.

Appropriate methodology should be included to perform simplified elastic–plastic analysis if the primary plus secondary stress range is predicted to exceed 3*S*m. The result is a determination of the CUF at that point in time for the given location [129]. Figure 67 summarizes the fatigue monitoring process.

6.2. MONITORING LOCATIONS

In Refs [129, 130], the selection process of monitoring locations is based on the identification of plant components that exhibit the following characteristics:

— High CUF as documented in the stress report:
  - CUF = 0.5 for simplified elastic–plastic analysis type;
  - CUF = 0.25 for plastic analysis type;
— Severe temperature transients:
  - Fluid flows with large temperature differences that start and stop abruptly;
— Complex fluid flow conditions, such as surge-line flow;

— New physical phenomena not included in the design of a plant:
  - Thermal stratification;
  - Thermal striping;
  - Swirl penetration;
  - Rapid thermal cycling;
— Thermal sleeves;
— Locations where cracks have been discovered;
— Component heatups and cooldowns associated with startups, shutdowns and reactor trips;
— Sudden injections of cold water and reflooding of hot water:
  - Hot standby;
  - Safety injections;
  - Auxiliary spray;
  - Loss of letdown;
  - Charging flow.
— Thermal stratification in pressurizer surge and spray lines, and feedwater lines.

Potential sites for transient and thermal fatigue monitoring in PWRs and BWRs are listed in Ref. [129] and reproduced in Table 12 and Table 13.

TABLE 12. POTENTIAL SITES FOR TRANSIENT AND THERMAL FATIGUE MONITORING IN PWRS [129]

System	Components	Plant transients
Pressurizer	— Surge-line nozzle; — Spray line nozzle; — Water temperature instrument nozzle; — Shell; — Bottom head/support skirt.	Plant heatups and cooldowns, auxiliary spray injection, insurge/outsurge and primary leak tests
Steam generator	— Feedwater nozzle; — Auxiliary feedwater nozzle; — Girth welds; — Tubesheet; — Support skirt.	Hot standby, plant heatups and cooldowns
Reactor pressure vessel	— Inlet and outlet nozzles; — Closure studs.	Hydrostatic tests, plant heatups and cooldowns, boltup and unbolt
Reactor coolant piping	— Surge-line nozzle; — Charging nozzle; — RHR/ safety injection nozzle; — Cold leg spray nozzle.	Plant heatups and cooldowns, insurge/ outsurge, loss of letdown and charging, shutdown cooling, safety injection
Feedwater piping	— Auxiliary feedwater to main feedwater tee	Hot standby, plant heatups and cooldowns
Spray line piping	— Spray line; — Auxiliary spray line tee.	Auxiliary spray actuation
Reactor coolant pump	— Pump cover; — Pump nozzles.	Plant heat-up

TABLE 12. POTENTIAL SITES FOR TRANSIENT AND THERMAL FATIGUE MONITORING IN PWRS [129] (cont.)

System	Components	Plant transients
Reactor internals	— Lower core plate; — Lower support column; — Core barrel nozzle; — Upper core plate alignment pins; — Baffle former assembly bolts; — Core flooding nozzle; — Instrument tube nozzle.	Plant heatups and cooldowns

TABLE 13. POTENTIAL SITES FOR TRANSIENT AND THERMAL FATIGUE MONITORING IN BWRS

Component	Plant transients
Feedwater nozzle safe end	Turbine roll, hot standby, loss of feedwater heaters, scrams, turbine trips and loss of feedwater
Core spray nozzle	Loss of feedwater and inadvertent injections
Control rod drive return nozzle	(Capped in almost all plants)
Control rod drive penetrations	Scrams and loss of feedwater
Reactor pressure vessel support skirt	Heat-up, cooldowns and scrams
Reactor pressure vessel shroud support	Heat-up and cooldown
Reactor pressure vessel head flange	Heat-up and cooldown
Reactor pressure vessel head bolts	Boltup/unbolt
Recirculation inlet nozzle	Cold start transient
Reactor pressure vessel internal steam dryer support bracket	Heat-up and cooldown

It should be noted that these criteria give a rather rough guideline for the selection of monitoring locations. The determination of candidate locations is the subject of individual analyses between technical experts of the utility and the provider. Experience on system behaviour, fatigue, material and design are part of this process.

6.3. GENERAL STEPS FOR IMPLEMENTATION

6.3.1. Generic steps

The following generic steps are involved in the implementation of an integrated transient and fatigue monitoring system [130]:

— Review current requirements:
  - FSARs;
  - Technical specifications;
  - Other design documents;
  - Licensing commitments;
  - Current plant cycle counting procedures;
  - Check if HCF is relevant (mixing areas);
— Review stress reports and industry issues:
  - Stress reports;
  - Design specifications;
  - Industry findings related to new loadings;
— Selection of transients to track:
  - List of design basis transients;
  - Additional transients;
  - Exclusion of insignificant transients for actual plant operation.

6.3.2. Solutions for the cycle counting issue

As mentioned above, SBF monitoring strategies can be further classified in global and local fatigue monitoring. Both strategies require the resolution of the key items:

— The determination of the stress tensor (all six terms of total and linearized stresses) as a function of time;
— The application of a qualified cycle counting procedure for the determination of fatigue relevant cycles.

The methodology of SBF monitoring is comprehensively described in Ref. [139]. The determination of CUFs requires the application of appropriate cycle counting procedures. The peaks and valleys approach of ASME Code NB-3222.4 [137] is often applied for the determination of the required stress ranges. The largest stress ranges are usually determined from ‘outer combinations’ (e.g. load steps across different transients or events). The associated frequency of occurrence results from the actual number of cycles of the participating two events with the smaller number of cycles (see Fig. 68).

This event provides the associated contribution to the partial UF CUF_i. The summing up of all partial UFs according to Miner’s rule delivers the cumulated usage factor CUF.

In some applications the load history may be directly considered, and in this case a different cycle counting algorithm is necessary. One example is the hysteresis counting method according to Clormann and Seeger [140] for implementation of the widely accepted rain flow algorithm. This method is increasingly being introduced in design codes, including detailed procedural guidelines (e.g. ASME VIII [141] and EN13445-3, clause 18, appendix NB [142]).

However, there are also on-line monitoring fatigue assessment algorithms that capture stress cycles and process them according to the ASME Code section III methodology using some approximations that are adequate for the monitoring applications. For example, the EPRI methodology [139] adapts the conventional rainflow algorithm to three dimensional states of stress. Stress peaks and valley regions are first identified, based on the dominant principal stress ranges. These general areas of stress peaks and valleys are then used as the basis for identifying stress cycle pairs. However, ASME Code section III subarticle NB-3200 [137] procedures for computing stress intensity range, based on all six components of the stress tensor, are used, instead of the difference between one stress term at two different times (e.g. the EPRI EAF sample problem analyses [143]).

6.3.3. Using operational measurements

The global fatigue monitoring approach is based on the time histories of the existing operational signals in connection with applicable transfer functions. The corresponding operational signals could be fluid pressure, fluid temperature, mass flow, the position of valves, etc., measured at different parts of the systems. The existing plant computer data points (global data) are used with appropriate system models in order to predict the local loadings at the locations for evaluation. The system models can employ thermohydraulic relationships, logic mapping, empirical data and structural model relationships to transfer the effects of the global data to applied local loadings [135]. Such methodologies are discussed in detail in Refs [144–146] and shown in Fig. 69.

The obvious advantage is that local measurements are not needed, being replaced by the transfer function approach. Disadvantages may occur in regions with stratification effects (e.g. surge line), where the derivation of transfer functions may be difficult, requiring verification.

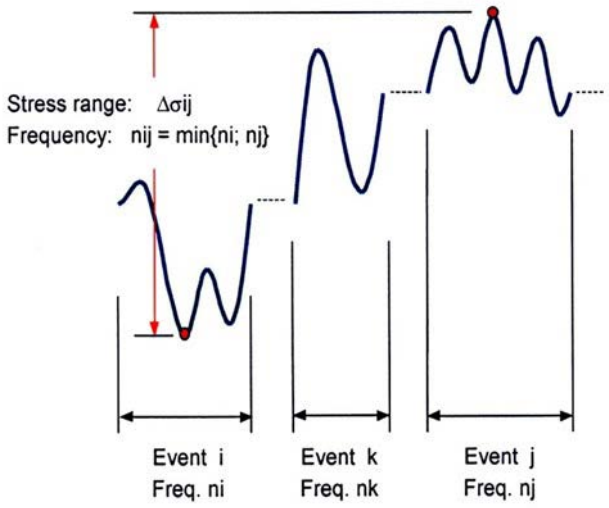

FIG. 68. Cycle counting according to ASME Code, section III [137].

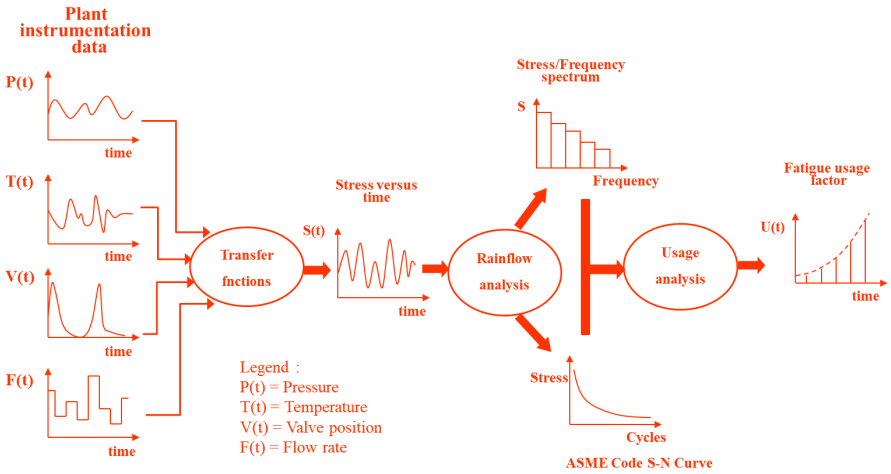

FIG. 69. Diagram of the SBF usage monitoring methodology [129].

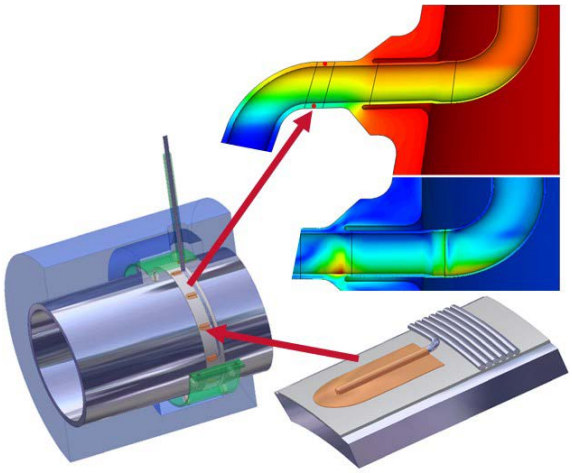

FIG. 70. Example of a local measurement section.

6.3.4. Using local measurements (local fatigue monitoring approach)

The local fatigue monitoring approach is based on existing operational signals and additional local instrumentation. For instance, the regulator in Germany requires thermal loading to be evaluated as realistically as is practical (see also the requirements of KTA3201.4 [77]), and thus additional instrumentation is typically added to measure the thermal response close to the monitored location. In this case, no transfer functions are required for the identification of the local thermal transient loads. Figure 70 shows the principle of local measurement and visualization.

6.4. COMMERCIALLY AVAILABLE FATIGUE MONITORING SYSTEMS

6.4.1. Description of different systems

Different fatigue monitoring systems are commercially available on an international scale. In the following, a short description of some of these systems is given.

6.4.1.1. AREVA fatigue concept (AFC) monitoring [135]

The AREVA fatigue concept (AFC) [135] monitoring methodology is discussed in Ref. [135]. The concept provides for a multiple step and multidisciplinary process against fatigue before and during the entire operation of NPPs. The central data logging system (FAMOSi Local Measurements) is the central data provider for the entire fatigue assessment process. In the case of unavailability of local measurements, this module may be replaced by a transfer functions approach for global fatigue monitoring. Subsequently, a qualified load evaluation by system engineering takes place and allows for the compilation of a model transients catalogue and an update of design transients. The core modules of the three step fatigue assessment methods of the AFC are shown on the righthand side of Fig. 75 (see Ref. [147]):

— *Step 1*: Simplified fatigue estimation. Simple estimations of fatigue relevance of real loads for components are based on thermal mechanical considerations using the equation of ideal thermally constrained strains. A basic decision about fatigue relevance (yes/no) for the monitored position is made. In the case of fatigue relevance, a further evaluation is proposed according to step 2;
— *Step 2*: Fast fatigue evaluation. A design code based CUF is calculated using an automated method based on the simplified elastic–plastic fatigue analysis route of relevant design codes, as in Refs [137, 138];

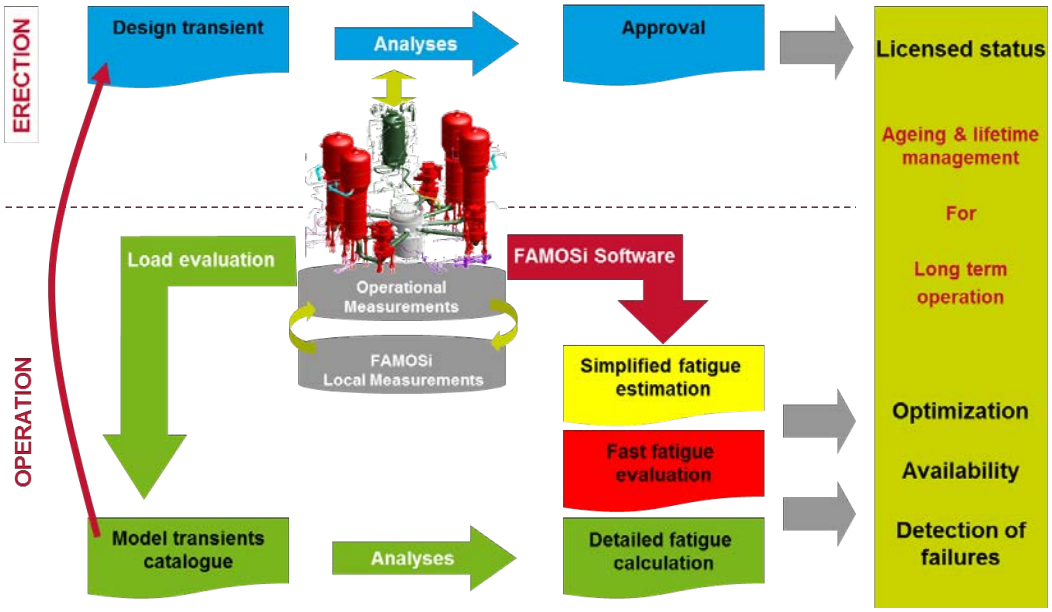

FIG. 71. General overview of the AREVA AFC [147].

— *Step 3*: Detailed fatigue calculation. Fatigue analysis is based on a set of model transients from a catalogue as shown in Fig. 71. The fatigue analysis for primary circuit components is based on design codes such as Refs [137, 138]. Fatigue calculations are usually carried out as elastic–plastic analyses based on appropriate material models. The ratcheting check is an additional design code requirement to be fulfilled. Related guidelines are found in Ref. [148]. It should be noted that EAF is considered in both the step 2 and step 3 approaches.

6.4.1.2. WESTEMS fatigue monitoring

Another example is the Westinghouse application of the WESTEMS diagnostic and monitoring system[21] for fatigue monitoring. In addition to employing system models to perform the transfer of global plant sensor data to local component loadings, it applies various methods to determine the associated stress component histories, including simplified closed form solution stress models for basic geometries as well as Green's function solutions for more complex geometries and/or loading situations. The models are developed based on the system and component design characteristics. System models also consider empirical data from available plant measurements. The stress models produce on-line stress and fatigue results from the calculated local loadings, consistent with the ASME Code fatigue rules [137].

In addition, the local component loadings used for on-line fatigue calculation are also recorded and can be used for additional detailed fatigue evaluation when required. These fatigue evaluations may be necessary to develop baseline fatigue estimates for initialization in an operating plant, or to perform more detailed elastic–plastic analysis, where necessary, to address extreme loading conditions. Such evaluations may also employ 'catalogued' model transients developed from the monitored loading data. This type of development is discussed in more detail in Refs [149, 150].

6.4.1.3. Structural Integrity Associates: FatiguePro 4.0 (FP4) fatigue monitoring

Another example is the FP4 fatigue monitoring system [139] implemented by the company Structural Integrity Associates. FP4 uses the SBF methodology developed by EPRI [139]. All implementations

[21] See WESTEMS Integrated Diagnostics and Monitoring Systems, https://www.westinghousenuclear.com/LinkClick.aspx?fileticket=uo6hKKcuEFw%3D&portalid=0.

of SBF have implemented the transfer function and Green's function approach, which uses existing plant instrumentation to infer the local temperature and pressure loading. This is because to date many utilities have not chosen to add local instrumentation. Further related issues are challenges concerning the reliability of thermocouples over the long term, competition for wires in containment penetrations, radiation shielding. quality assurance requirements for permanent instruments, etc.

In many cases, excessive conservatism is eliminated by using conservative transfer function methodology [151]. However, for NPPs that have experienced a large number of cycles, or those considering LTO to 80 years, more accurate measurement of loads using local instrumentation may be beneficial. With advances in technology, some of the aforementioned challenges are likely to be re-evaluated based on the cost–benefit to utilities and the eventual pursuit of LTO.

Given that for most critical locations there are no pre-existing local instruments to directly determine the loading, it is necessary to calculate local conditions based on remote sensor readings. In many cases, global readings are effectively the same as local conditions. This is generally true for pressures or for flows within a single piping line. In other cases, simple expressions can be used to obtain accurate predictions. The most difficult parameter to determine is local temperature. In some cases, switching from one temperature indication to another, based on the flow rate conditions, is sufficient and very conservative. In other cases, a relatively simple thermal-hydraulic model can reduce excess conservatism. To avoid the worst cases, more sophisticated modelling is required to produce both acceptable and conservative results.

A more conservative and simplified methodology — CBF — uses existing design fatigue analyses as input. This method of fatigue computation utilizes an event pairing table (either from the design stress report or developed from the stress results in design stress report) to compute fatigue usage. Correlations are developed between the transients defined in the stress report and the plant events identified by the cycle counting module. As plant events are identified, appropriate cycles of the stress report transients are counted. These counted cycles are used to construct an event pairing table. Fatigue usage is computed using allowable cycles from the design stress report table for each transient pair. This methodology produces conservative values of fatigue usage when fewer than the design basis number of plant events have been counted.

Plant cycle counting is required, at a minimum, for CBF monitoring. This methodology provides an automatic, rule based detection of plant events, such as those events identified in the Class 1 fatigue analysis that should be tracked by plant technical specification requirements. Automatic cycle counting operates on the principle that most plant events produce distinct patterns in the plant process variables. Therefore, plant events can be identified by detecting these distinct patterns. Design documents, operating history and plant data are reviewed to identify distinctive patterns for the initiation and termination of each plant event.

6.4.1.4. Electricité de France (EdF) Fatiguemètre system

Another system, called Fatiguemètre [129, 152], was developed by EdF. The initial installation of Fatiguemètre was at the Bugey-2 plant in 1985, followed by Dampierre-1 in 1988 [153]. Fatigue monitoring was identified as a key aspect of the optimization of PWR operation and maintenance as well as potential LTO [153]. The development and principle of a real time fatigue monitoring system by EdF is presented in Ref. [154]. It records plant operating parameters and calculates thermohydraulic conditions using simplified models, local stresses via Green's function and UFs resulting from each individual transient. The system allows automatic transient bookkeeping and UF assessment [154]. The goal is to facilitate on-line computation of the actual damage at critical locations of the primary circuit.

Some monitoring devices were nevertheless necessary to obtain correlations between in-service data, for instance, flow rate and thermal stratification distribution. Furthermore, after several measurement campaigns, EdF analysed that, despite interesting outcomes provided by the device, the uncertainty and scatter were too high for the fatigue meter results to be integrated in the decision process of maintenance management.

6.4.1.5. Stratimètres

Stratification and swirl instabilities were not accounted for in the initial transient files, but they were identified later as detrimental loadings. To assess these loadings in the concerned areas, EdF equipped several sections with thermocouples welded on the external wall of the relevant piping in the 1990s [152]. This monitoring campaign helped to identify the key characteristics of swirl penetration in dead legs and the stratification magnitude. Later, EdF developed another version of this monitoring device called stratimètres, associated with a numerical tool ORT (Outil de Reconstitution de la Température) dedicated to the reconstruction of the temperature of the internal wall.

— Stratimètre is composed of thermocouples fastened on the piping external wall with the help of a specific belt enabling quick and high-quality mounting/unmounting, providing robust data and minimizing operator exposure to radiation. Circular and longitudinal versions of stratimètres can be alternatively used, depending on the typology of the studied pipe. Stratimètres are available in a large diameter range, from 50.8 mm to 355.6 mm, the largest comprising 16 thermocouples so as to capture a precise description of azimuthal temperature variation in a section.
— Temperature variation of the piping internal wall is derived from the measurements on the external side with the help of a dedicated numerical tool ORT relying on data assimilation techniques. This tool has been developed by EdF in the framework of the Salome_Meca software platform [155].

6.4.1.6. NuFMS (Nuclear fatigue monitoring system) [156]

The nuclear fatigue monitoring system (NuFMS) [156] was developed by the Korea Hydro & Nuclear Power Co. (KHNP) in the Republic of Korea. It is an on-line system designed to perform stress and fatigue analysis, including EAF, for selected components, based on conventionally available plant process instrumentation. NuFMS performs fatigue monitoring using three stages: acquisition, processing and storage of the transient data. These data are received from the plant information system (a computer system which saves and manages data after receiving them from the main computer to analyse plant instrumentation data) on a regular basis and transfers the data received to NuFMS. In addition, all input/output data and fatigue evaluation results are saved in a database. Figure 72 shows the general system composition of NuFMS. The programme:

— Obtains and verifies transient data;
— Identifies the design basis set of transients (cycles) based on a stream of real plant input data;
— Evaluates fatigue effects by using a Green’s functions approach and the number of transient occurrences; and
— Saves input/output data and the information related to fatigue evaluation.

The system consists of three modules for the following functions:

(1) Intelligent cycle counting (ICC);
(2) CBF evaluation (CBE);
(3) SBF evaluation (SBE).

The ICC module determines whether a specific transient has occurred by using signals from the plant instrumentation as the main input data. In other words, ICC recognizes a transient (e.g. heat-up, loss of load) and records it in the database together with the key parameters that will characterize the severity of that event (e.g. heat-up rate, maximum pressure). These analysis results are also used as input data for the CBE.

Two primary methods are used to compute cumulative fatigue use: SBE and CBE. With the SBE method, each stress and stress intensity for selected plant components resulting from pressure, piping

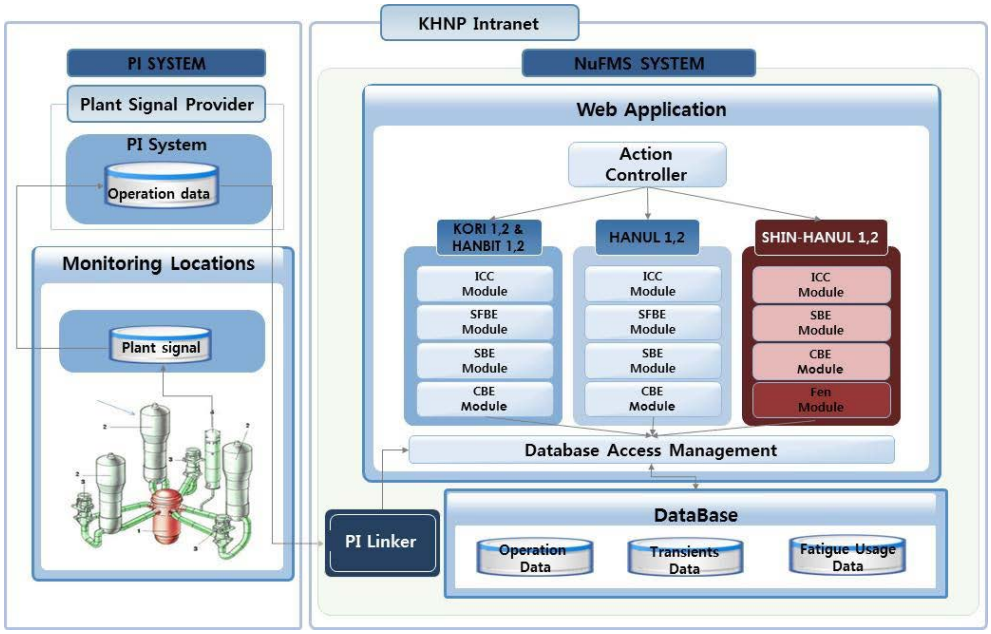

FIG. 72. Structure of the nuclear fatigue monitoring system [156].

loads and thermal expansion are computed using Green's functions and transfer functions, which convert instrumentation signals to stress. This method uses the plant instrumentation signals for temperature, pressure and flow (or velocity) of the target area as input data to calculate the stress time history. Then, based on the stress history, a rainflow cycle counting algorithm is used to determine the magnitude and the number of cycles for the alternating stress.

Finally, the calculated alternating stress is applied to the fatigue diagram to evaluate fatigue usage factors using the appropriate fatigue curve given in the ASME Code. SBE employs penalty factors for EAF using the technical rules provided in US NRC RG 1.207 [41] and NUREG/CR-6909 [38] for stainless steel, low alloy and carbon steel and Ni–Cr–Fe alloys, respectively. NuFMS is installed at NPPs under construction and operation in the Republic of Korea.

6.4.1.7. Fatigue usage monitoring system (FAMS)

In the 1990s, the Japanese PWR group developed an advanced transient and fatigue usage monitoring system (FAMS) [157] which can cope with the thermal stratification phenomenon and the change of inner surface heat transfer coefficient on the critical locations during plant operations. The system estimates the thermal transient changes making use of plant process data and calculates the stress versus time history and the CUF at the critical locations.

The Green's function approach of the FAMS software has been improved for use in the situation where the heat transfer coefficient changes with time on the inner surface of the critical location. The software uses a Green's function database assuming several different heat transfer coefficients and calculates thermal stress by interpolation of the Green's function database using the estimated heat transfer coefficient on the inner wall.

To calculate the static thermal stratification stress, the temperature distribution is classified into linear and non-linear components from self-balanced equations for the axial force and moment. The software has several inner surface temperature profiles normalized by the temperature difference between the maximum and minimum values on the cross-section and it has a stress database corresponding to each temperature profile. The thermal stress can be calculated by superimposing these stress components linearly. The system software logic was verified using measured data obtained from a PWR plant and conventional detailed computer simulations, such as three dimensional FE analyses.

6.4.1.8. DIALIFE

The DIALIFE [158] diagnostic system has been developed by the Institute of Applied Mechanics (IAM) in Brno, Czech Republic. The parts of the programme dealing with NPPs were designed in cooperation with the NPP Dukovany. The development of the DIALIFE program system is a natural continuation of the long term service which IAM has provided to the NPP Dukovany. The DIALIFE system is running at NPPs Dukovany, Temelin and Mochovce [158].

Based on the collected and measured data, DIALIFE determines the actual cumulative damage for selected components of the NPP and selected degradation mechanisms, typically LCF, crack growth and influence of the environment. The assessment procedure is divided into five parts:

— Settings of the input data;
— Stress calculation (or recognition of load cases);
— Enumeration of partial increase of damage;
— Calculation of cumulative damage;
— Prediction, trends and determining the time when operational limits will be exceeded.

DIALIFE has several different methods of evaluating cumulative damage based on stress/strains tensors. The most used is monitoring of load cycles during the time of operation and assigning corresponding partial increase of damage from the preprocessed database to each recognized load case. Values of the partial damage are mostly calculated using the transient FEM model outside the system. Alternatively, the artificial neural network, prepared stress databases and analytical equations can be used for stress determination for the next assessment using mechanisms of degradation.

The configuration of artificial neural network is transferred to DIALIFE. Then, the system can evaluate stress/strains in every load step by using the rainflow method from which the value of the partial damage increase is calculated. This method is used at the NPP Mochovce.

Analytical equations for stress/strains evaluation can be used only for the very simple geometry of the NPP component. These are also part of DIALIFE. A special module of DIALIFE is assessment of hypothetical defects according to British standard R6 [159]. This module uses the database of pre-evaluating values of stresses in each node of the FEM model for the unitary load and the entire spectrum of temperatures.

6.4.1.9. Computerized monitoring system of residual life (SACOR)

The computerized monitoring system of residual life — SACOR — was developed for equipment and pipelines of the primary circuit at VNIIAES (Moscow) and Gidropress (Podolsk), and implemented at water-water energetic reactor (WWER) 1000 and 1200 NPPs [160, 161].

There are two methods for monitoring fatigue damage accumulation in the metal of equipment and pipelines at Russian Federation NPPs. The first method is based on the requirements of the Russian standard STO 1.1.1.04.001.0143-2009 [32] according to which the number of realized design regimes of operation (loading cycles) for NPP equipment and pipelines should be recorded each year and the relevant analysis should be provided if necessary. The second method is based on application of the computerized monitoring system of fatigue damage accumulation of primary circuit components — SACOR [160].

The SACOR system is intended to monitor the accumulation of fatigue damage in reference points of the following equipment [160–162]:

— Reactor pressure vessel;
— Pressurizer;
— Steam generators;
— Main circulation pipes;
— Surge line;

— Pipe of the emergency core cooling system.

Evaluation of fatigue damage is carried out by the SACOR system according to the real thermal loading, which is provided by data obtained from standard sensors (pressure, temperature, flow, position of controllers and catches). The system provides a database with a history of thermal loading of equipment and pipelines during operation. In addition to standard sensors, additional sensors are used to collect information for the SACOR system [160].

Data obtained from the following sensors are used as an input for the SACOR system:

— Standard sensors of the SACOR system;
— Sensors of the in-core monitoring system;
— Sensors of the automated system of control over the operational processes (ASCOP);
— Sensors of displacement for shock absorbers [160].

Local thermal stresses caused by a non-uniform temperature field are defined by formulas based on Duhamel's integral [160].

6.4.1.10. Load evaluation application for fatigue

Load evaluation application for fatigue (LEAF) was developed by Nuclear Research and Consultancy Group (NRG) in the Netherlands. The system is a custom-built tool that monitors the fatigue status by validating the thermal load assumptions made in design fatigue analyses with respect to load monitoring data. This can be temperature data from a fatigue load monitoring system, but also data from the plant process instrumentation system. The fatigue status of the components is assessed by coupling load monitoring, transient counting and fatigue assessment in a sophisticated way [161]. The projected numbers of cycles are verified by load case counting. For the verification of the thermal transients, the CBF methodology described earlier is used. The tool evaluates temperature measurements and compares these to the design transients used in the fatigue analyses. Both uniform and stratified signals can be analysed. To ensure the quality of the assessment, the user always has full control over the settings and the choices that are made in the evaluation. Based on the results, the safety margins in the fatigue analyses are demonstrated and the actual fatigue status of the various reactor components can be monitored and reported. LEAF is currently used for the LTO fatigue management of the Borssele NPP in the Netherlands.

6.4.1.11. fatONE

The fatONE fatigue monitoring system has been developed by Innomerics. This software package has been installed in one BWR and is currently being installed at three PWR units in Spain. It is capable of evaluating fatigue usage based on two methodologies:

— SBF monitoring. Stress time histories are computed based on the time histories of the boundary conditions at all the components of interest. Boundary conditions, such as pressure, temperature and heat transfer coefficients, are computed from real time readings obtained from available plant instrumentation. Instead of using pre-existing process instrumentation for computing boundary conditions, fatONE can also be integrated with the innoSENSE family of smart sensors, specifically developed for the purpose of providing boundary condition time history data for fatigue monitoring. These non-invasive sensors can be placed directly on the components of interest, reducing the computational uncertainty associated with the use of readings from conventional process instrumentation. Furthermore, the use of local smart sensors is the most precise option for characterizing local phenomena, such as HCF damage induced by thermal mixing due to leakage or localized thermal stratification that can take place during certain plant transients.

— Cycle counting fatigue monitoring. This approach requires assigning a pre-defined sequence of stress peaks and valleys to each transient type defined in the licensing bases of the plant. Every time a transient takes place, it is automatically classified and assigned to one of the transient types found in the licensing bases, therefore generating a sequence of stress peaks and valleys at each of the monitored locations. Peak valley sequences are then combined into stress cycles using conventional rules. Transients can be automatically classified using the following algorithms:
  - Pattern recognition approach based on the dynamic time warping algorithm;
  - Rule based approach using rules and ad hoc models for each plant transient.

6.4.2. Comparison of different systems

Table 14 summarizes the features of the available fatigue monitoring systems.

TABLE 14. COMPARISON OF DIFFERENT SYSTEMS

System	On-line option	Basic approach	Remarks
AREVA AFC monitoring	Yes	— Local fatigue monitoring (alternatively global transfer functions approach); — SBF; — Green's functions approach for fast fatigue evaluation.	— Staged approach according to fatigue relevance; — CBF based on CONTARE tool.
WESTEMS fatigue monitoring	Yes	— Step change Green's functions; — Transfer functions; — SBF.	
Safety injection:FatiguePro 4.0 (FP4) fatigue monitoring	Yes	— Step change Green's functions; — Transfer functions; — SBF.	— Additional fatigue crack growth module.
EdF Fatiguemètre system	Yes	— Surge line and steam generator locations; — Stratification monitoring; — Existing plant; instrumentation + transfer function s + Green's function.	— Special local monitoring devices for stratification (stratimeter, Fatiguemètre).
NuFMS	Yes	— Step change Green's functions — Transfer functions — SBF	— CBE; — Signal feature based evaluation.
FAMS	Yes	— Green's function method; — SBF; — Thermal stratification and heat transfer coefficient monitoring.	— Improved Green's function method to be applied to the condition of a heat transfer coefficient change versus time.

TABLE 14. COMPARISON OF DIFFERENT SYSTEMS (cont.)

System	On-line option	Basic approach	Remarks
DIALIFE	Yes	— Stratification monitoring; — Existing plant instrumentation; — SBF; — The rapid stress determination by means of artificial neural network, prepared stress databases and mathematical approximation.	— Recording the changes of chemical concentration in the media (material damaged by corrosion cracking and corrosion fatigue); — Special temporary measurement: thermocouples and strain gauges used for local measuring near the critical spots (mostly damaged places).
SACOR	Yes	— Recording of realized loading cycles, e.g. CBF; — Computerized monitoring system of fatigue damage accumulation of primary circuit components, e.g. SBF; — Determination of local thermal stresses based on Duhamel's integral.	
AMTEC integrity management system monitoring	Yes	— Local monitoring of temperatures; — Identification of real loads including thermal stratification and internal leakages; — Local stress analysis for relevant loads.	— Detection of unspecified loads; — Immediate feedback for staff to optimize operational modes for mitigation of fatigue.
LEAF	Yes	— Local monitoring of temperatures; — Identification of real loads including thermal stratification and internal leakages.	— CBF
fatONE fatigue monitoring system	Yes	— SBF monitoring; — Cycle counting fatigue monitoring.	— Pattern recognition approach; — Rule based approach.

7. CONCLUSIONS AND GUIDANCE

A range of components in NPPs are subjected to fatigue relevant loadings during their lifetime. Fatigue is one of the major reasons for the structural deterioration that occurs from repeated stress/strain cycles caused by fluctuating mechanical and/or thermal loads. After repeated cyclic loading, if sufficient localized microstructural damage has occurred, crack initiation can occur at the most susceptible locations. Fatigue assessment of components in operating NPPs is an integral part of an ageing management strategy as one of the relevant ageing mechanisms, using TLAA, to calculate the residual lifetime of components. This residual life should be calculated with an appropriate margin that is relevant to the consequences of failure, where failure in the case of pressure boundary components is through-wall leakage.

The degradation mechanisms include the following features:

— HCF: The most classical fatigue related degradation mechanism is HCF, which involves a large number of stress cycles at relatively low stress amplitudes.
— LCF: The stress cycling that contributes to LCF is generally due to the combined effects of pressure and component loadings e.g. piping moments and local thermal stresses.
— Thermal fatigue: Thermal fatigue is due to cyclic stresses that result due to changing temperature conditions in a component or in the piping attached to the component.
— EAF: Environmentally assisted fatigue is the reduction in fatigue life in the reactor water environment compared with the in-air environment. EAF may enhance the other mechanisms mentioned above.

The characteristic of fatigue strength of material is represented by the relationship between stress or strain amplitude and the number of cycles to failure of the material. The equivalent stress amplitude of the component should be lower than the allowable stress amplitude of the fatigue curve, specifically the endurance limit. International codes and standards are useful in providing calculation methods for stress and strain amplitudes for fatigue analysis.

Usually, the fatigue damage process is divided into the crack initiation and crack propagation phases. Fatigue crack initiation and growth resistance is governed by a number of materials, structural and environmental factors. Cracks typically initiate at the locations of stress concentrations, such as welds, notches, surface roughness and structural discontinuities. The presence of an oxidizing environment or other deleterious chemical species can accelerate the fatigue crack initiation and propagation process.

The methodology of fatigue assessment for NPP components was summarized and the differences of the fatigue design requirements among different national structural design codes and standards were discussed. In the design and operating phase of NPPs, it is essential to consider the concurrent loadings associated with the design transients, thermal stratification, seismically induced stress cycles and all relevant loads due to the various operational modes to ensure structural integrity against fatigue damage according to structural design codes and standards.

Operating experience from NPPs is a very valuable source of information for design engineers and operators because they help to explain how design configuration, construction, materials, fabrication, operating conditions and operator practices such as maintenance, inspection and test can affect sensitivity to fatigue damage. This information can help to reduce operating costs, extend operating life and improve safety and reliability through the good practices of reporting, archiving and sharing between design engineers and operators. However, it should be recognized that when the number of NPPs is small, relative to the required target reliabilities for avoidance of fatigue failure, then operating experience alone is insufficient.

A large amount of test data has confirmed that fatigue lives become shorter and fatigue crack growth rates higher in HT water simulating coolants in PWR and BWR plants than in-air due to environmental effects. The expressions describing the amount of reduction or acceleration as a function of various factors, such as the temperature and loading rate, have been developed based on the test data obtained from small test specimens. Differences in terms of geometrical and loading conditions between test specimens and actual components and their consequences should be considered to avoid too conservative a judgement brought by a direct application of such expressions on the design fatigue curves.

Reconsideration of design fatigue curves and unification of environmental factors used in fatigue life estimation and crack growth assessment are also subjects requiring further investigation. In particular, this requires good quality plant representative testing that can be used to benchmark and validate the improved analytical methods. Ultimately, this would also enable the required margins for avoidance of fatigue failure to be applied in a quantified manner. Currently, the relevance of fatigue monitoring is steadily increasing. According to regulatory and design code requirements, particularly the growing need of consideration of EAF within the fatigue assessment procedure, qualified fatigue monitoring systems are needed to retrieve the strain rate data for EAF calculation, to identify and optimize operating modes, and to make design modifications such as future design improvements.

For fatigue monitoring, the fatigue relevant local load data are retrieved using standard operational measurements in connection with a global fatigue monitoring approach and local fatigue monitoring approach. The future of fatigue monitoring for operating NPPs will be a hybrid global–local approach based on specific needs and codes/standards to reduce the possibility of fatigue failures. Fatigue monitoring systems would be used for the various applications ranging from detecting and counting actual transient cycles for SBF comparing them with design transients at controlling locations for CBF. Thus, fatigue monitoring systems are assuming more important role in providing a strong technical basis for the LTO of NPPs.

Appendix I

SAMPLE FATIGUE EVALUATION OF VESSEL AND PIPING ACCORDING TO THE ASME CODE

I.1. FATIGUE EVALUATION FOR VESSELS

Fatigue evaluations are conducted for the direct vessel injection (DVI) nozzle of the reactor vessel and the primary head assembly of the steam generator. This sample analysis is provided to illustrate the application of ASME Code rules to a specific vessel but is not intended to illustrate all techniques for Class 1 vessels. The procedure and analysis consist only of the calculations of fatigue usage factors. The ASME NB-3200 Code [7] is used to determine the usage factors of the reactor vessel direct injection nozzle and primary head assembly of steam generator. Considered in fatigue evaluation are the loads which are generally applied to the vessel design for the NPPs such as seismic, pressure, thermal expansions and thermal transients. Figure 73 shows a typical procedure of calculating fatigue usage factors for a vessel in accordance with the ASME NB-3200 Code.

I.1.1. Direct vessel injection nozzles of reactor vessels

The DVI nozzles are attached to the reactor vessel for direct emergency coolant injection as a part of the safety injection system. The location of the DVI nozzle is above the cold leg nozzles and determined to avoid the interference with reactor vessel external nozzles and support structure as shown in Fig. 74. These provide cooling capability for the reactor during shutdown cooling and in the event of a loss of coolant accident. The nozzle is made of SA508 Gr. 3 Cl.1 and safe end is made of SA-182 F316LN. Material properties extracted from ASME Code, section II Part D, are used in this sample analysis.

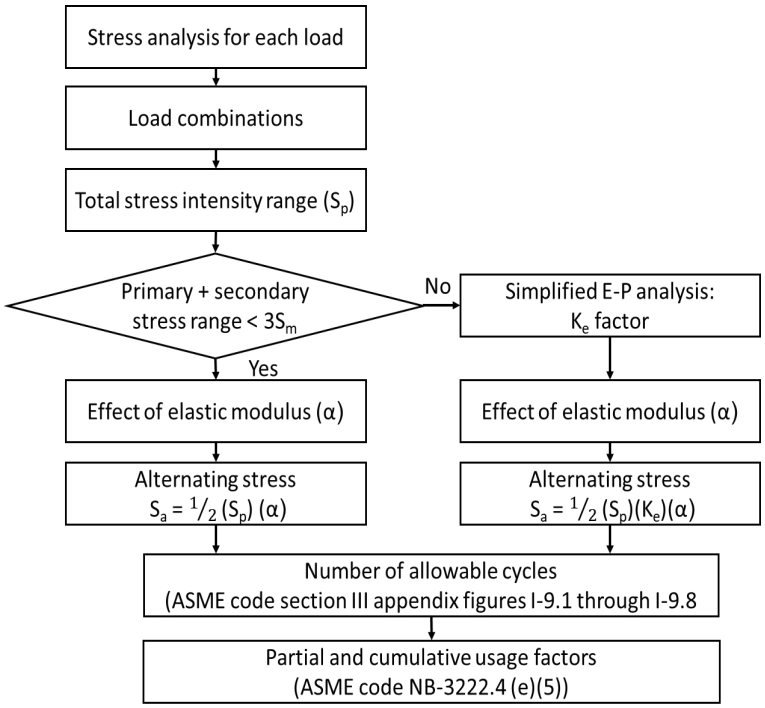

FIG. 73. Flow chart of the fatigue analysis procedure for vessels [7]; E-P— elastic–plastic.

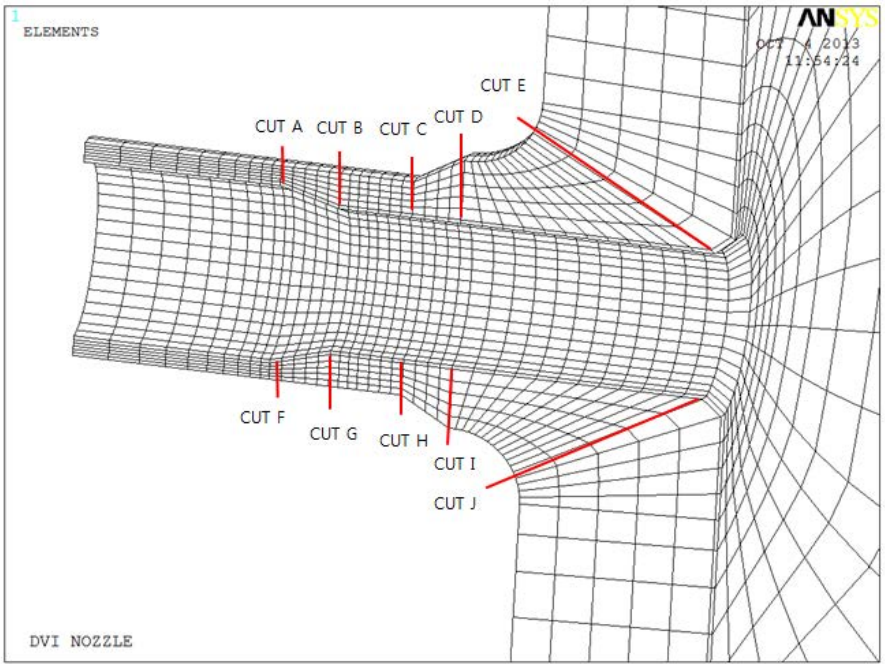

FIG. 74. DVI nozzles.

I.1.1.1. Loading conditions

The applicable design basis loads for the DVI nozzles are usually defined in the design specifications of reactor pressure vessel. Applied loading conditions which are thermal-hydraulic loads (pressure, thermal transient) and nozzle load are considered in this sample calculation. Nozzle loads such as seismic and IRWST load include the inertia and anchor movement loads. The transients evaluated include only those classified as Service Level A (normal), Service Level B (upset), and test conditions. Two groups of thermal data were used and designated as the cold leg and the DVI nozzles, respectively. It is noted that the sustained loads such as weights are not considered in these calculations because these kinds of loads do not contribute to fatigue UFs. The applied loading conditions to fatigue evaluations are summarized as follows:

— Pressure;
— Transient loads;
— Nozzle load:
  - Dead weight;
  - Thermal load;
  - IRWST discharge;
  - Seismic.

I.1.1.2. Stress analysis

The thermal transient analysis is performed by the ANSYS program[22]. ANSYS uses the wave front (or frontal) direct solution method for the system of simultaneous linear equations developed by the matrix displacement method. It produces a nodal temperature distribution for given input lists, including the nodal network descriptions, boundary conditions and material properties. The post-processing procedure generates an equivalent linear gradient from the actual radial temperature distribution. The temperature differences along with nodes at each area of interest are output for selected transient times.

[22] ANSYS is a large, finite element program for a broad range of analysis types.

In this analysis, the maximum and minimum pressures are considered in each transient as a conservative method. The transient time points were selected based on the maximum or minimum thermal gradients.

The FEM for structural analysis was used to analyse the reactor vessel direct injection nozzles. An elastic based analysis is performed by using the ANSYS computer program. The stresses in the components are produced by the internal pressure, thermal transient load and nozzle loads.

I.1.1.3. Fatigue evaluation

Total stresses are obtained by adding peak stresses to the primary plus secondary stresses. These peak stresses result from the effect of geometrical stress concentration at local structural discontinuities and from the non-linear potion of the radial (through-wall) thermal gradients. Several methods are used to calculate fatigue strength reduction factors or stress concentration factors at geometrically discontinuous locations. The methods are selectively used according to the geometry of each component. The alternating stresses intensities are derived per ASME Code NB-3216 and the cumulative fatigue UFs are calculated using ASME Code NB-3222.4:

— *Number of allowable cycles:* Since the alternating stress is calculated for each type of stress cycle which represents plant operating conditions, the actual number of cycles that a component will be subjected to at any particular range would be also known. Then the allowable number of cycles for specified alternating stress is determined from the Code fatigue curves.
— *Fatigue usage factors*: The partial usage factor for the *i*th stress cycle, U_i, can be calculated as follows (see Eq. (47) and (48)).

$$U_i = \frac{n_i}{N_i} \tag{47}$$

where

n_i is the number of cycles used for the stress cycle;

and N_i is the number of cycles allowable for the stress cycle.

Since most systems have many different operating conditions, multiple stress cycles will need to be defined. Therefore, there will be multiple stress intensity ranges which will have different magnitudes. The CUF U resulting from all stress intensity ranges and stress cycles should be accumulated to obtain the accumulated fatigue damage to a component expressed as:

$$U = \sum_i U_i = \sum_i \frac{n_i}{N_i} \tag{48}$$

The code stipulates that the value of the cumulated fatigue UF should not exceed 1.0. Table 15 shows the results of this sample calculation.

I.1.2. Primary head assembly of the steam generator

The primary head assembly of the steam generator (SG) consists of a spherical shell with an integral stay cylinder welded to the tube sheet. There is a divider plate in the primary head which forms two chambers. On the hot side, the primary side flow from the reactor vessel enters the SG through one primary inlet nozzle and is distributed to the evaporator tube circuits. On the cold side, the primary side flow leaves the SG through two primary outlet nozzles. The secondary side is bounded by the lower shell and economizer support cylinder.

The FEM of the assembly is shown in Fig. 75. Only the hot side is considered in this sample analysis. Several regions such as the nozzles, manways and divider plates are not presented here since

TABLE 15. THE RESULTS OF FATIGUE ANALYSIS AT CUT A LOCATION

Stress cycle	Number of cycles used, n	Range of primary plus secondary stress intensity, S_n (ksi)	Range of peak stress intensity, S_p (ksi)	Factor defined by NB-3228.5, K_e	Alternating stress intensity, S_{alt} (ksi)	Number of allowable cycles, N^g	Fatigue UF, U^h
1	30	71.68	119.03	1.0	67.64	8000	0.0037
2	30	67.93	112.13	1.0	63.72	10 212	0.0029
3	10	67.8	111.76	1.0	63.51	10 374	0.0010
4	80	58.77	94.53	1.0	53.72	23 587	0.0034
5	160	56.92	90.59	1.0	51.48	29 243	0.0055
6	140	55.06	84.5	1.0	48.02	41 574	0.0034
7	60	36.87	61.18	1.0	34.76	244 465	0.0002
8	20	30.13	49.51	1.0	28.13	1.02E+06	0.0000
9	220	25.91	43.49	1.0	24.71	1.54E+06	0.0001
10	15	24.73	41.01	1.0	23.3	1.86E+06	0.0000
11	125	23.39	40.9	1.0	23.24	1.88E+06	0.0001
12	300	19.35	33.76	1.0	19.18	4.19E+06	0.0001
13	360	12.18	23	1.0	13.07	INFINITE	0.0000
The remainder	—	—	—	—	—	INFINITE	0.0000
CUF, U =							0.0204

they are analysed separately. Figure 76 shows cut locations to be investigated. The cut locations include the geometric discontinuous regions and the centre lines of welding for in-service inspections. Material properties extracted from ASME Code, section II Part D, are used.

I.1.2.1. Loading conditions

The applicable design basis loads for the primary head assembly are usually defined in the applicable SG design specifications. Applied loading conditions that are thermal-hydraulic loads (pressure, thermal transient) are considered in this sample calculation. The dynamic load such as seismic load is insignificant in the primary head assembly of steam generation. Thus, there is no need to evaluate SSE loads in this calculation. The transients evaluated include only those classified as Service Level A (normal), Service Level B (upset), and test. Two groups of thermal data were used and designated as the primary side and the secondary side, respectively. It is noted that the sustained loads such as weights are not considered in these calculations because these kinds of loads do not contribute to fatigue usage factors. The applied loading conditions to fatigue evaluations are summarized as follows:

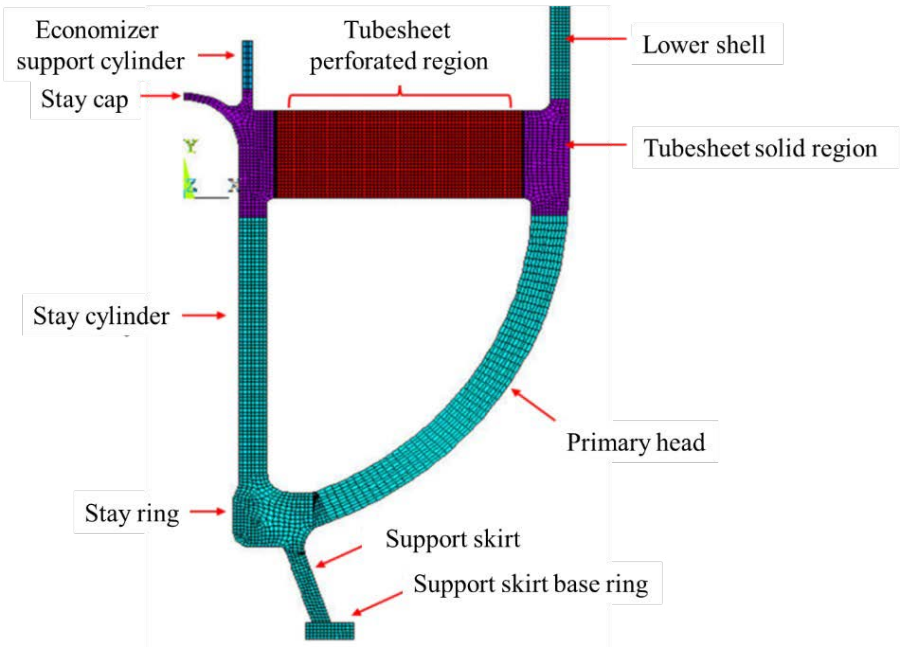

FIG. 75. Primary head assembly of the steam generator.

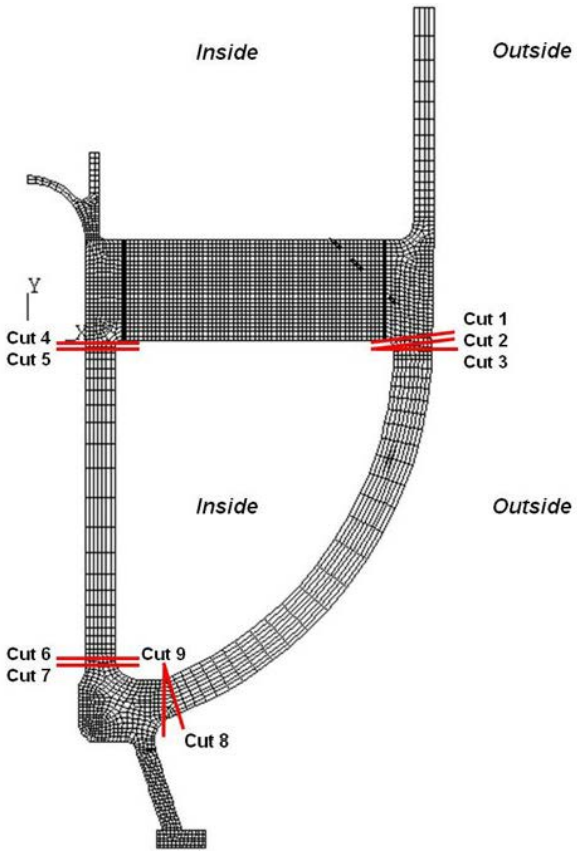

FIG. 76. Areas of interest in the primary head region.

TABLE 16. THE RESULTS OF FATIGUE ANALYSIS AT CUT 1 LOCATION

Stress cycle	load-set pairs, n	Range of primary plus secondary stress intensity, S_n (ksi)	Range of peak stress intensity, S_p (ksi)	Factor defined by NB-3228.5, K_e	Alternating stress intensity, S_{alt} (ksi)	Number of allowable cycles, N^g	Fatigue UF, U^h
1	15	83.64	109.29	1.18	78.42	1163	0.0129
2	15	81.06	105.75	1.05	67.58	1730	0.0087
3	20	80.72	104.14	1.03	65.48	1882	0.0106
4	80	72.93	94.75	1.0	57.78	2771	0.0289
5	20	68.38	91.97	1.0	56.08	3047	0.0066
6	40	68.37	91.89	1.0	56.03	3055	0.0131
7	110	67.98	91.03	1.0	55.5	3148	0.0349
8	300	42.52	52.96	1.0	32.29	17 394	0.0172
9	500	44.3	50.64	1.0	30.88	20 245	0.0247
10	300	39.8	49.34	1.0	30.09	21 922	0.0137
11	30	37.5	47.09	1.0	28.71	25 299	0.0012
12	30	14.32	18.25	1.0	11.13	INFINITE	0
The remainder	-	-	-	-	-	INFINITE	0.0000
CUF, U =							0.1725

— Transient load:
  - Pressure;
  - Thermal transient.

The following information should be provided for each event:

— P_t pressure versus time;
— P_t temperature versus time;
— Q_t flow rate versus time;
— Number of cycles.

I.1.2.2. Fatigue evaluation

The same method as the one described in Section I-1.1 was used for stress analysis and fatigue evaluation. Table 16 shows the results of this sample calculation.

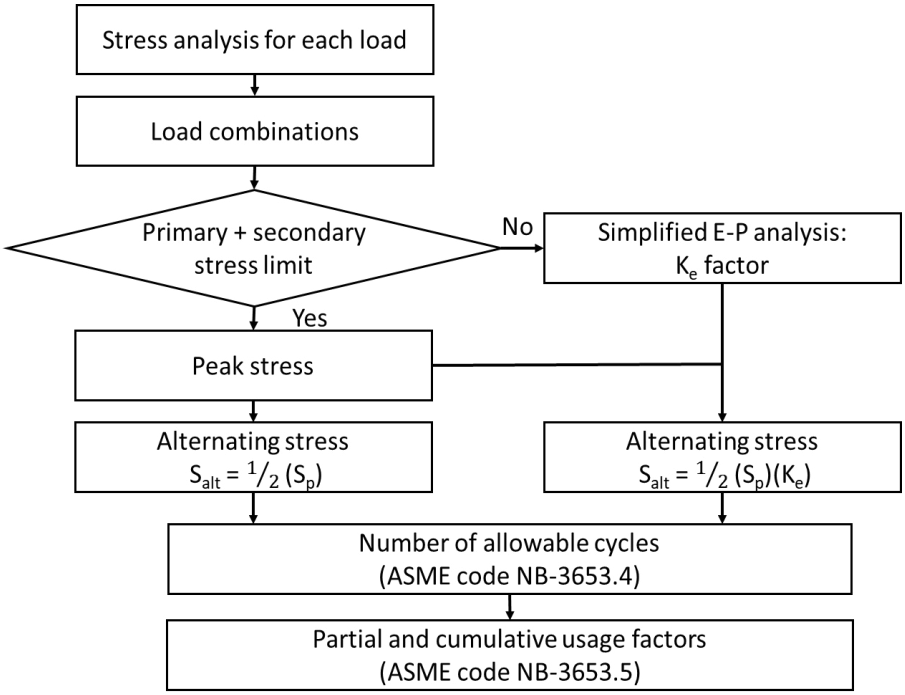

FIG. 77. Flow chart of fatigue analysis procedure for piping components [7].

I.2. FATIGUE EVALUATION FOR PIPING

Fatigue evaluations are conducted for Class 1 piping components in a PWR. This sample analysis is provided to illustrate the application of ASME Code rules to a specific piping system but is not intended to illustrate all techniques for Class 1 piping design. The procedure and analysis consist only of the calculations of fatigue UFs. The ASME NB-3600 Code [27] is used to determine the usage factors of the piping components. Considered in fatigue evaluation are the loads which are generally applied to the piping design for the NPPs, such as seismic, building filtered loads, pressure, thermal expansions, thermal transients and thermal stratifications. Figure 77 shows a typical procedure of calculating fatigue usage factors for a piping component in accordance with ASME NB-3600 Code.

I.2.1. Piping system

The typical piping component connected to the nozzle of a vessel or tank was selected for fatigue evaluations in which the weld between the safe end and pipe was taken as the location of evaluation, as shown in Fig. 78. This kind of location is a typical piping weld at a tapered transition. In NB-3600 based evaluations, the ‘a side’ is taken as the nozzle side of the weld that contains the thicker portion made of SA-182 F316LN. The ‘b side’ is on the other side of the weld that contains the straight pipe made of SA-312 TP316. Material properties extracted from ASME Code, section II Part D, are used in this sample analysis.

I.2.2. Loading conditions

The applicable design basis loads for all safety related piping systems are usually defined in the applicable piping system design specifications. Applied loading conditions such as seismic, building filtered load and thermal-hydraulic loads (pressure, thermal expansion and transient and thermal stratification) are considered in this sample calculation. Dynamic loads such as seismic and building filtered load include inertia and anchor movement loads. Thermal stratifications cause the additional

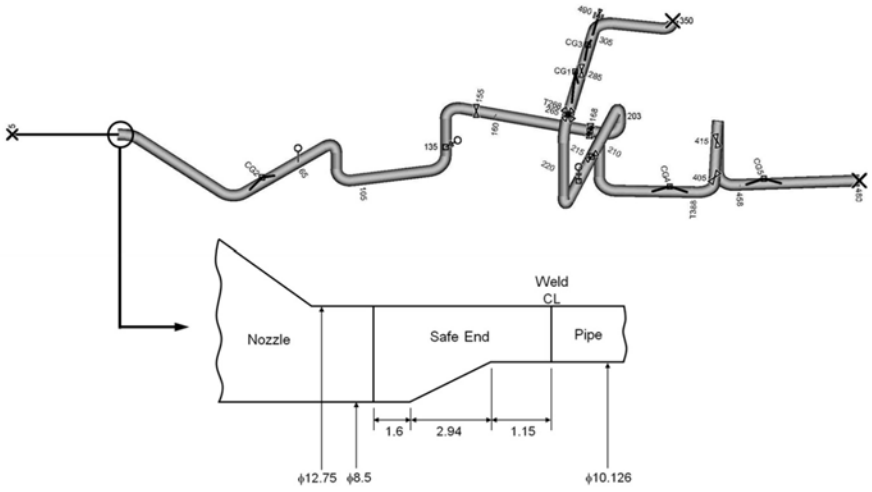

FIG. 78. Areas of interest in the piping system.

internal moments reflecting the bowing effects and local stress near the interface of the stratified flow due to large temperature gradients. Sustained loads such as weights are not considered in these calculations because these kinds of loads do not contribute to fatigue usage factors. The applied loading conditions to fatigue evaluations are summarized as follows:

— Seismic;
— IRWST as a building filtered load;
— Pressure;
— Thermal loads:
  - Thermal expansion, including thermal anchor movements;
  - Thermal transient;
  - Thermal stratification.

I.2.3. Stress analysis

I.2.3.1. Structural analysis

For the loads given earlier, except for thermal transients and stratifications, the full anchor to anchor piping models are used to calculate the moments of each piping component. The stress intensities by these loads and/or combined loads might be obtained by substituting the moments to the code equations given in Code NB–3650 with the known stress indices and cross–sectional geometries. In ASME NB–3600 evaluations, the stress intensity due to pressure could be directly calculated by using the code equations, and therefore additional detailed analysis is not required.

I.2.3.2. Thermal transient analysis

The heat transfer analysis for each thermal transient load is performed to determine the temperature distribution. The stress intensity stress is subsequently calculated by substituting the temperature distribution into the equations of $T_a - T_b$, ΔT_1 and ΔT_2 defined in ASME NB-3653.

I.2.3.3. Thermal stratification analysis

The thermal stratification stresses are composed of the thermal expansion, global bending and local stratification stress. The temperature distribution in the piping system is obtained from the thermal-hydraulic analysis, and then the bending moment due to the thermal expansion and global bending and local stresses are calculated from the sequential stress analysis.

I.2.4. Fatigue evaluation

I.2.4.1. Load sets

The operation of the piping system during the lifetime of the plant is the guideline for setting up the 'load sets', which are specific combinations of loads assumed to act simultaneously on a piping system at a given instant. The requirements of load combinations are usually prescribed in the design specification of a piping system, as follows:

$$\text{Pressure} + \text{Thermal Expansion} + [Seismic^2 + IRWST^2]^{1/2} + \left(T_a - T_b\right)_{\text{Stress}} + \Delta T_{\text{Stress}}$$

In this sample calculation the global bending and local stress due to thermal stratifications are included as the thermal expansion and T_{stress}, respectively.

I.2.4.2. Fatigue usage factors

The fatigue usage factor is calculated following the procedure described in Section I-1. Table 17 shows the results of this sample calculation.

TABLE 17. RESULTS OF FATIGUE ANALYSIS AT PIPING

Load-set pairs			Usage factors
1 (+ Seismic + IRWST)	32	125 527	0.05
2 (+ IRWST)	3	122 336	0.00
3 (+ IRWST)	5	116 750	0.01
4	25	116 565	0.03
5	235	93 567	0.15
6	30	67 264	0.01
7	60	63 853	0.01
8	30	63 509	0.01
9	5	62 446	0.00
10	30	57 798	0.00
11	85	55 865	0.01
12	30	55 632	0.00
13	30	53 931	0.00
14	30	53 332	0.00
15	30	51 982	0.00
16	95	48 334	0.01

TABLE 17. RESULTS OF FATIGUE ANALYSIS AT PIPING (cont.)

Load-set pairs			Usage factors
The remainder	630	45 130	0.04
CUF, *U* =			0.33

Appendix II

NATIONAL AND INTERNATIONAL RESEARCH ACTIVITIES TO MANAGE FATIGUE

II.1. INTERNATIONAL RESEARCH ACTIVITIES

Table 18 lists international research activities in the area of fatigue management.

TABLE 18. INTERNATIONAL RESEARCH ACTIVITIES TO MANAGE FATIGUE

Organization	Activity name	Objective (additional information)
EC	INCEFA+ (INcreasing safety in NPPs by covering gaps in environmental fatigue assessment) 2015–2019 HORIZON2020	INCEFA+ delivers new experimental data and new guidelines for assessment of environmental fatigue damage to ensure safe operation of European NPPs [163]
	AdFaM (Advanced Fatigue Methodologies for stainless steels in NPPs)	Advanced Fatigue Methodologies (AdFaM), a joint project of European research laboratories, vendors and plant operators was focused on empirical and mechanistic investigations to confirm the claimed effects of hold times on fatigue life. Strain-controlled fatigue tests incorporating accelerated hold times at temperatures between 290°C and 420°C were performed on stabilized and non-stabilized stainless-steel grades, which are used in Germany and the United Kingdom.
EPRI	MRP Thermal Fatigue Program	— MRP-146S, Revision 1, “Management of Thermal Fatigue in Normally Stagnant Non-Isolable RCSeactor Coolant System Branch Lines – Supplemental Guidance,” Product ID 300203264; — MRP-192, Revision 3, “Assessment of Residual Heat Removal Mixing Tee Thermal Fatigue in PWR Plants,” Product ID 300203266; — MRP-85, Revision 2,“Operating Experience Regarding Thermal Fatigue of Piping Connected to PWR Reactor Coolant,” Product ID 300203263; — MRP-433, “PWR Residual Heat Removal Mixing Tee Thermal Fatigue Guidance, Update: Current Experience, Selection of Modeling Tools, Input Data Identification, and Planned Approach,” Product ID 300201277.

II.2. NATIONAL R&D PROGRAMMES

Table 19 lists national research and development programmes in the area of fatigue management.

TABLE 19. NATIONAL R&D PROGRAMMES

Country	Activity name	Objective (additional information)
Korea, Rep. of	EAF experimental programme in KAIST	Environmental fatigue of metallic components of LWRs - supported by Korea Hydro and Nuclear Power Co. as an environmental fatigue project.
Russian Federation	The fatigue monitoring of equipment and pipelines at Russian NPPs	The monitoring of fatigue damage accumulation in metal of NPP equipment and pipelines must be carried out during operation (Russian Federation regulatory requirement). Two approaches are used: The first based on the number of realized design regimes of operation (loading cycles) and the second based on application of the computerized monitoring system of fatigue damage accumulation of primary circuit components — SACOR. SACOR was developed by specialists of research institute VNIIAES (Moscow) and the designer of WWER reactors OKB Gidropress (Podolsk) and implemented at nuclear power units with WWER-1000 and WWER–1200 [164, 165].
Czech Republic	MPO (MIT) project FR-TI1/423 Two R&D projects supported by Czech energy company ČEZ, performed by UAM Brno (Institute of Applied Mechanics, Brno)	Reliable and safe nuclear source of new generation for Czech power engineering, partly related to material problems of NPP primary circuit research — development of a new testing facility for simulation of EAF in ÚJV Řež. The first project (2010–2012) focused on base steel materials, which are used in the primary circuit of WWER-440. The second project (2013–2015) extended the suggested methodology to the additional area of welds. The output of both projects was to establish a draft normative text of the national standard for WWER NPPs (NTD, AME). The new LCF assessment in combination with corrosion environment (water of the primary circuit) was proposed as an alternative approach to F_{en} for WWER NPPs. [166, 167]
	Monitoring of fatigue lives of steam turbine blades	Problems with fatigue damage to turbine blades in the last stages. Measurements of all blade vibrations and resonant frequencies carried out by the blade tip timing (BTT) method. The equipment's residual fatigue life of blades, developed at VZÚ Plzeň, uses a procedure of processing output data from BTT up to fatigue lives of particular measured wheel blades [168].
	Mean stress effect on fatigue life and dislocation microstructures of 316L austenitic steel at high temperature in air and water environment	Unusual response of austenitic steels to mean stress data with more complex stress state and loading history in LWR environment. A series of load-controlled fatigue data have been obtained in the air and water environments to address the issue of mean stress influence on the fatigue behaviour of austenitic steel [169].
Switzerland/ Czech Republic	KORA_I (2006-8), KORA-II (2009-11), SAFE, projects sponsored by the Swiss Nuclear Safety Authority (ENSI)	Projects deal with ageing processes that affect steel components in the primary circuit in NPPs, focusing specifically on two processes: SCC and corrosion fatigue. SCC can cause long and thin branched fissures which cannot be detected with the naked eye. The influencing factors are mechanical stresses, the environment (water chemistry of the primary circuit) and material characteristics. Corrosion fatigue is a similar form of environment-induced fissure growth as the consequence of cyclic mechanical stress, e.g. due to vibrations. A series of load-controlled fatigue data have been obtained in the air and water environments to address the issue of mean stress influence on the fatigue behaviour of austenitic steel [169].

TABLE 19. NATIONAL R&D PROGRAMMES (cont.)

Country	Activity name	Objective (additional information)
Finland/ Switzerland	Safir 2014/ENVIS 2013 KORA_I (2006-8), KORA-II (2009-11), SAFE, projects sponsored by the Swiss Nuclear Safety Authority (ENSI)	Environmental influence on cracking susceptibility and ageing of nuclear materials. Fatigue of niobium stabilized austenitic stainless steel has been studied using specimens extracted from an NPP primary piping material batch (in air and in hot PWR water). The goal is the better transferability of laboratory data to fatigue assessment of NPP components. Projects deal with ageing processes that affect steel components in the primary circuit in NPPs, focusing specifically on two processes: SCC and corrosion fatigue. SCC can cause long and thin branched fissures which cannot be detected with the naked eye. The influencing factors are mechanical stresses, the environment (water chemistry of the primary circuit) and material characteristics. Corrosion fatigue is a similar form of environment-induced fissure growth as the consequence of cyclic mechanical stress, e.g. due to vibrations.
Hungary	EAF testing	EAF testing of cylindrical and CT specimens machined from Ti stabilized austenitic stainless steel (08Ch18N10T) and from its welds, started in 2016. Environmental influence on cracking susceptibility and ageing of nuclear materials.
Finland	DUF together with other research institutes (Safir) 2014/ENVIS 2013 (VTT and E.ON)	Fatigue of niobium stabilized austenitic stainless steel has been studied using specimens extracted from an NPP primary piping material batch (in air and in hot PWR water). The goal is the better transferability of laboratory data to fatigue assessment of NPP components.
France	EdF R&D Projects Domzone, Fatmav, Fatigue Thermique	There has been a continuous investment in R&D fatigue projects for more than 15 years in France. Some were conducted in the framework of the Institute Tripartite, which combines EdF, CEA and AREVA. A short description of the main outcomes of these projects is provided below. Previous R&D projects (DOMZOME, FATMAV, FATIGUE THERMIQUE EdF Projects): — Characterized experimentally thermal fluctuations in mixing zones and improved their modelling via large eddy simulations; — Derived a 1-D methodology for the screening of mixing zones sensitivity to thermal fatigue; Established the influence of several parameters on stainless-steel life thanks to extensive fatigue testing in air.

TABLE 19. NATIONAL R&D PROGRAMMES (cont.)

Country	Activity name	Objective (additional information)
	COFAT, MODERN	COFAT (completed in 2015) and MODERN (running till the end of 2019) EdF projects associated with the corresponding Institute Tripartite project: — Produce experimental data to increase the French fatigue data base including in air and environment and under multiaxial loading; — Feed the new RCC-M fatigue codification with experimental data and related statistical analysis; — Develop and qualify the stratimètre and the ORT tool (details in chapter 6) useful for the determination of piping internal temperature wall based on external wall measurement + mathematical reconstruction technique as well as new generation measurement techniques; — Maintains efforts of thermohydraulic simulation in order to enhance the temperature fluctuation in mixing zones and to predict the stratification and vortex instability in dead legs; — Develops and qualifies the FEM post-processing tool post-RCCM needed for industrial fatigue analysis including EAF; — Performed experimental fatigue crack propagation in the case of large scale plasticity.
Germany France	MPA Stuttgart AREVA GmbH EdF R&D Projects Domzone, Fatmav, Fatigue Thermique,	Environmental influences on the fatigue assessment of austenitic and ferritic steel components including welds. 1. Experimental investigations concerning the influence of loading parameters and EAF effects (LWR environment) on the fatigue strength of ferritic steels including weldments. 2. Experimental investigations concerning the influence of long hold times and the EAF effects on the fatigue strength of austenitic and ferritic steels. The results of the outlined experimental programme and published results will constitute the input for the proposal of an engineering fatigue assessment concept [170, 171]. There has been a continuous investment in R&D fatigue projects for more than 15 years in France. Some were conducted in the framework of the Institut Tripartite, which combines EdF, CEA and AREVA.

TABLE 19. NATIONAL R&D PROGRAMMES (cont.)

Country	Activity name	Objective (additional information)
Korea, Rep. of	Assessment of pipe design applicability under high temperature condition (Parts of Specific Design of BOP [balance of plant] System for Prototype Sodium-cooled Fast Reactor).	The main objectives of this activity are to develop detail design procedure of sodium fast reactor (SFR) balance of plant piping, which will be operated in a HT (500°C or higher) environment and to develop detail methodology to assess a fatigue and a creep fatigue by design by rule for piping for temperatures exceeding 500°C. Experimental investigations concerning the influence of loading parameters and EAF effects (LWR environment) on the fatigue strength of ferritic steels including weldments. Experimental investigations concerning the influence of long hold times and the EAF effects on the fatigue strength of austenitic and ferritic steels. The results of the outlined experimental programme and published results will constitute the input for the proposal of an engineering fatigue assessment concept [170, 171, 172].
	Development of technologies to manage environmental fatigue issues and environmental fatigue test (2003–2013, KHNP)	The main objectives of this activity were enriching environmental fatigue data of austenitic stainless steels in PWR water and examining the effects of varying strain rate on environmental fatigue life when considering actual transient conditions in operating plants. Equations to calculate F_{en} for stainless steels in PWR water and the modified rate approach method (strain based integral model) to predict environmental fatigue life under varying strain rate conditions were developed [172]. Major goals of this project were to resolve the EAF issues, as well as developing core technologies for the EAF design optimization for Class 1 components and piping for licensing Shin-Kori 3 and 4 units and its following NPPs. Major tasks are outlined as follows: environmental fatigue test for carbon steels, low alloy steels, austenitic stainless steels and Ni–Cr–Fe alloys, establishment of database on the fatigue test results, and optimization of design conservatism for EAF.
Japan/ USA	EFT (Environmental Fatigue Tests of Nuclear Power Plant Materials for Reliability Verification) Project, (1994 to 2006)	In this project, over a thousand fatigue tests were conducted for carbon, low alloy and austenitic stainless steels, as well as Ni–Cr–Fe alloys and their weld metals in simulated BWR and PWR water. Based on these test data, the following results were obtained: 1. Development of the new environmental fatigue life prediction model for Ni–Cr–Fe alloys; 2. Improvement of precision of existing environmental fatigue life prediction models for carbon, low alloy and stainless steels; 3. Confirmation of the strain rate threshold on environmental fatigue; 4. Development of an environmental fatigue life prediction method under the simultaneous conditions of varying strain rate, temperature and dissolved oxygen concentration; 5. Confirmation of the effects of water flow rate, strain holding and strain wave form on fatigue life for carbon, low alloy and stainless steels in BWR and PWR water. Development of an environmental fatigue evaluation method based on these results [172]. The main objectives of this activity were enriching environmental fatigue data of austenitic stainless steels in PWR water and examining the effects of varying strain rate on environmental fatigue life when considering actual transient conditions in operating plants. The equations to calculate F_{en} for stainless steels in PWR water and the modified rate approach method (strain based integral model) to predict environmental fatigue life under varying strain rate conditions were developed [172].

TABLE 19. NATIONAL R&D PROGRAMMES (cont.)

Country	Activity name	Objective (additional information)
Japan/USA	EFT (Environmental Fatigue Tests of Nuclear Power Plant Materials for Reliability Verification) Project, (1994 to 2006, Japan Power Engineering and Inspection Corporation, later known as JNES (Japan Nuclear Safety Organization) in 2003))	The objectives of this research are to obtain information for improving the fatigue integrity of welded structures fabricated from austenitic stainless steels. The effects on fatigue behaviour, such as residual stresses due to welding, concentrated stresses due to structural discontinuities, changes in material properties due to welding, environments and so on, are to be experimentally studied. In this project, over a thousand fatigue tests were conducted for carbon, low alloy and austenitic stainless steels, as well as Ni–Cr–Fe alloys and their weld metals in simulated BWR and PWR water.
	FDE subcommittee (Research on Fatigue Damage Evaluation Techniques in Nuclear Materials, 1997 to 2000, Strength of Stainless-Steel Welded Joints (1991 to 1994))	The aims of this research are to make clear effect of surface finish on fatigue strength and the relationships between fatigue CGR and fracture morphology. Experimental studies are being performed on carbon steel SGV410 and austenitic stainless-steel type SUS316NG, which are commonly used in Japanese NPPs. The objectives of this research are to obtain information for improving the fatigue integrity of welded structures fabricated from austenitic stainless steels. The effects on fatigue behaviour, such as residual stresses due to welding, concentrated stresses due to structural discontinuities, changes in material properties due to welding, environments and so on, are to be experimentally studied.
	FDE subcommittee (Research on Fatigue Damage Evaluation Techniques in Nuclear Materials (1997 to 2000))	The objectives of this research are to make clear HCF strength of a nuclear component material (SUS316NG) and effects of notch, mean stress and combination of them on the HCF strength. The aims of this research are to make clear the effect of surface finish on fatigue strength and the relationships between fatigue CGR and fracture morphology. Experimental studies are being performed on carbon steel SGV410 and austenitic stainless-steel type SUS316NG, which are commonly used in Japanese NPPs.
	GCF2 subcommittee (Research on High Cycle Fatigue Strength of Power Plant Component Material (2003 to 2006))	This project aims to confirm the reliability of the design fatigue curve for austenitic stainless steel in the HCF region, from 108 to 109 cycles, based on the test data. Discussions will be made on the effects of the work hardening and notches on the HCF strength of the austenitic stainless steel SUS316NG, with the modification of the HCF test method. The objectives of this research are to make clear the HCF strength of a nuclear component material (SUS316NG) and the effects of notch, mean stress and the combination of these on the HCF strength.

TABLE 19. NATIONAL R&D PROGRAMMES (cont.)

Country	Activity name	Objective (additional information)
	GCF3 subcommittee (Study on Evaluation of Giga-Cycle Fatigue (GCF) [Phase I] (2008 to 2011))	The objectives of this research are to ascertain the possibility of gigacycle fatigue and to evaluate the mechanism of fatigue strength properties in the very HC region for nuclear component materials. The materials selected for this study were carbon steel STPT370, low alloy steel SFVQ1A and austenitic stainless steel SUS304, and fatigue tests will be carried out up to around 108 cycles in air. Obtained data will contribute to assess the validity of design fatigue curve for more than 106 cycles. This project aims to confirm the reliability of the design fatigue curve for austenitic stainless steel in the HCF region, from 108 to 109 cycles, based on the test data. Discussions will be made on the effects of the work hardening and notches on the HCF strength of the austenitic stainless steel SUS316NG, with the modification of the HCF test method.
	LCF subcommittee (Study on Evaluation of Fatigue Strength Properties for Nuclear Component Materials Subjected Seismic Load (2008 to 2011))	The objectives of this research are to evaluate the fatigue strength properties for nuclear component materials subjected to very large load caused with plastic strain, such as seismic loading. 1. Expansion of data for the effect of cyclic pre-strain or cumulative mean strain on fatigue life 2. Investigation of the assessment of LCF strength and fatigue life based on fatigue damage
	MF I-III subcommittee (Research on Fatigue Properties under Multi-Axial State of Stress, Phase 1 to 3) (2002 to 2011))	The purposes of these projects are as follows: 1. Investigation of fatigue strength of the austenitic stainless steel, carbon steel and low alloy steel under combined loading. 2. Numerical simulation of fatigue crack growth under mixed mode loading condition. 3. Creation of fatigue crack growth equations under multiaxial stress. The objectives of this research are to evaluate the fatigue strength properties for nuclear component materials subjected very large load caused with plastic strain, such as seismic loading. 4. Expansion of data for the effect of cyclic pre-strain or cumulative mean strain on fatigue life. 5. Investigation of the assessment of LCF strength and fatigue life based on fatigue damage. 6. Integrity evaluation of component experienced with seismic loading.
	Material Ductile Fracture (MDF) subcommittee (Research on Ductile Fracture under Multi-Axial State of Stress for Component and Structure of Light Water Reactor (2010 to 2015))	The objectives of this project are as follows: 1. Experimental examinations of fracture behaviour and strength under cyclic combined loadings. 2. Numerical simulation of fracture behaviour under very low cycle combined loadings. The purposes of these projects are as follows: — Investigation of fatigue strength of the austenitic stainless steel, carbon steel and low alloy steel under combined loading. — Numerical simulation of fatigue crack growth under mixed mode loading condition.
	EPRI Actions: Thermal Fatigue Interim Guidance MDF subcommittee (2010 to 2015))	The objectives of this project are as follows: Experimental examinations of fracture behaviour and strength under cyclic combined loadings; Numerical simulation of fracture behaviour under very low cycle combined loadings.

TABLE 19. NATIONAL R&D PROGRAMMES (cont.)

Country	Activity name	Objective (additional information)
	EAF: Status in USAEPRI Actions: Thermal Fatigue Interim Guidance	Plants seeking Licence Renewal (and new plants) must meet existing EAF requirements (NUREG 6909); Most plants seeking licence renewal have met the requirements; Used more elaborate analytical techniques (FE analysis); Re-evaluating operating plant transient data; 10 to15 plants still need to apply for licence renewal and may exceed the CUF limit; Examining decay heat lines with cyclic operational outflow (June 2016); Accelerated exam of decay heat lines using 'Generic Analysis' (June 2016); Examination of vertical piping in decay heat lines (June 2016); NDE process improvements (October 2015); Good practice recommendations; Expand RHR mixing tee exam volumes to include upstream welds.
USA	EAF State of the Technology EAF: Status in USA	— Environmentally Assisted Fatigue Gap Analysis and Roadmap for Future Research (Dec 2012, Report ID 1026724): • Gap prioritization performed by industry expert panel; • 21 gaps identified as high priority — 7 hypotheses proposed to explain the apparent discrepancy between test data and field experience; — Plants seeking licence renewal (and new plants) must meet existing EAF requirements (NUREG 6909); — Most plants seeking licence renewal have met the requirements; — Used more elaborate analytical techniques (FE analysis); — Re-evaluating operating plant transient data: • 10 to15 plants still need to apply for licence renewal and may exceed the CUF limit.
	Material Reliability Programme Operation Experience regarding thermal fatigue of piping connected to PWR coolant systems (MRP-85 Rev.1)	— Driven by a complex fluid dynamic mechanism with inadequately understood sensitivities; — Generally unrecognized in original design and management programmes; — International management strategies are inconsistent; — Increasing component failure trends: • Management programmes have not met reliability expectations — Some thermal fatigue cracks have gone undetected Environmentally Assisted Fatigue Gap Analysis and Roadmap for Future Research (Dec 2012, Report ID 1026724)

Appendix III

SURVEY RESULT ON FATIGUE MONITORING AND ASSESSMENT

This appendix provides supporting information for Section 4.1. and contains the graphical representation of survey results. It contains additional and more detailed processing of survey results. The following questionnaire items and figures represent a short overview of experience with fatigue assessment in operating NPPs. The survey results on fatigue monitoring and assessment were processed based on 20 completely filled questionnaires from 11 different countries (South Africa, Brazil, Canada, Finland, China, Japan, Republic of Korea, Russian Federation, Slovakia, Sweden and USA). The possible answers on questionnaires are shown on the horizontal axis of the bar graphs. The number of positive responses to possible answers is located on the vertical axis.

III.1. CATALOGUE OF QUESTIONNAIRES

(1) How are the fatigue relevant NPP components or representative component locations selected for the plant fatigue monitoring? (Responses shown in Fig. 79.)
   (a) Selection based on the implementation of PLiM;
   (b) Based on design fatigue usage screening;
   (c) Based on the relative EAF sensitivity and feedback from similar plants;
   (d) Based on NUREG/CR-6260 recommendations;
   (e) Other criteria.

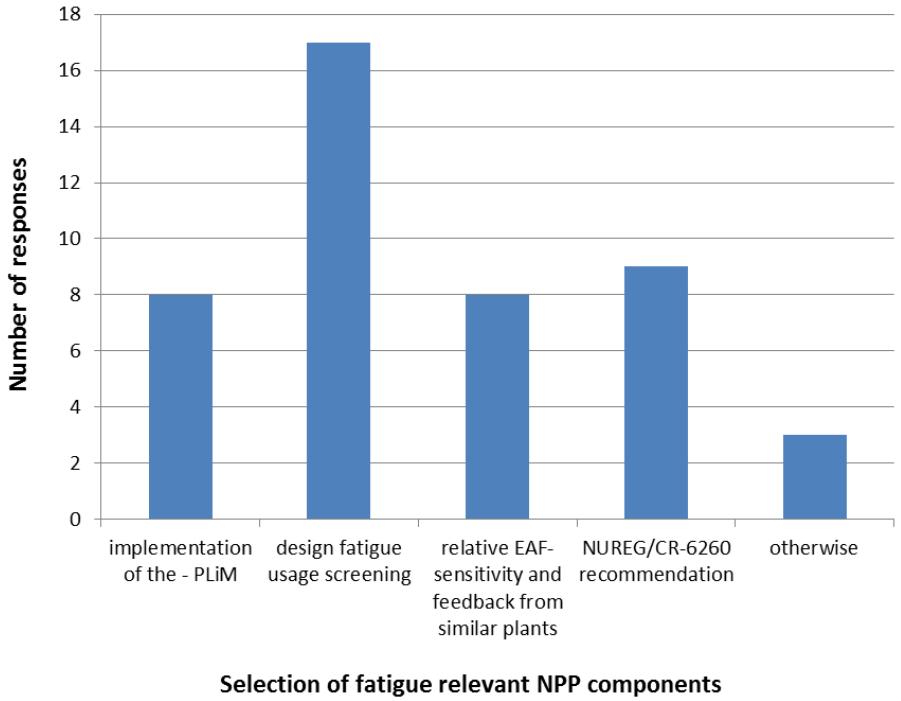

FIG. 79. Graphical representation of survey results to question 1.

(2) What codes and standards or guidelines are used for fatigue assessment (evaluation of CUF) and how is the assessment of crack growth due to fatigue realized? (Responses shown in Fig. 80.)
   (a) ASME;
   (b) RCC-M;
   (c) JSME;
   (d) KEPIC;
   (e) KTA;
   (f) Russian PNAE G;
   (g) Other codes.

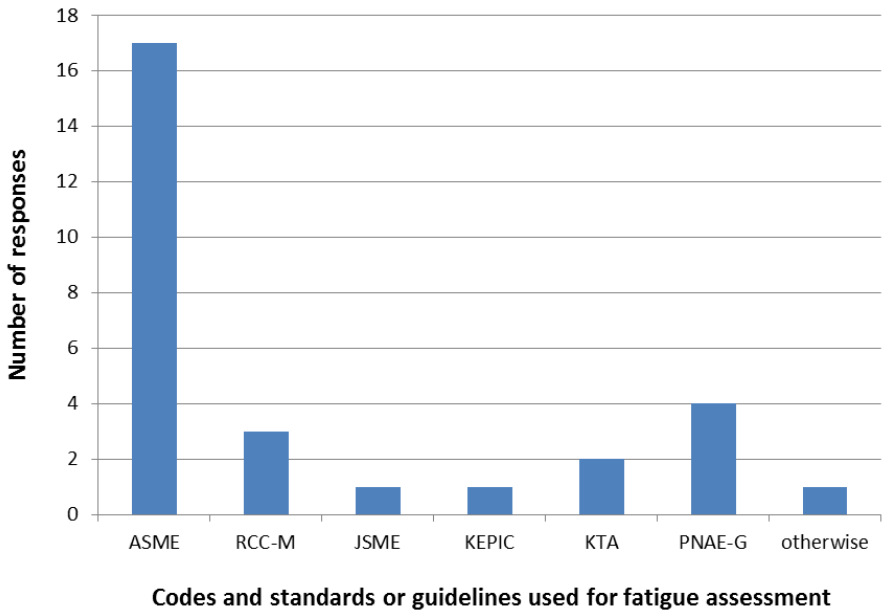

FIG. 80. Graphical representation of survey results to question 2.

(3) What kind of load data is used for the evaluation of the number of transient cycles and calculation of CUF? (Responses shown in Fig. 81.)
   (a) Design loads — design transient;
   (b) Realistic loads — real transients based on actual conditions measured during operation;
   (c) Combination of partial design transient and operating transient;
   (d) Another kind.

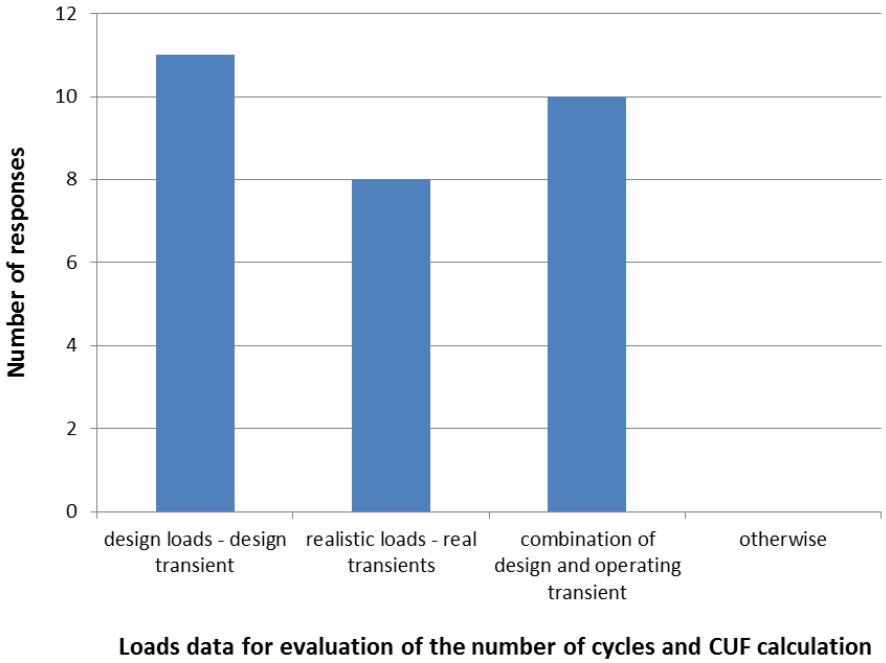

FIG. 81. Graphical representation of survey results to question 3.

(4) Is monitoring system installed for data acquisition, recording and storage of realistic operational load data measured continuously in the NPP for monitoring of real operating loads and subsequent use of measured data as an input for fatigue analyses by a fatigue monitoring system?
(a) Yes;
(b) No.

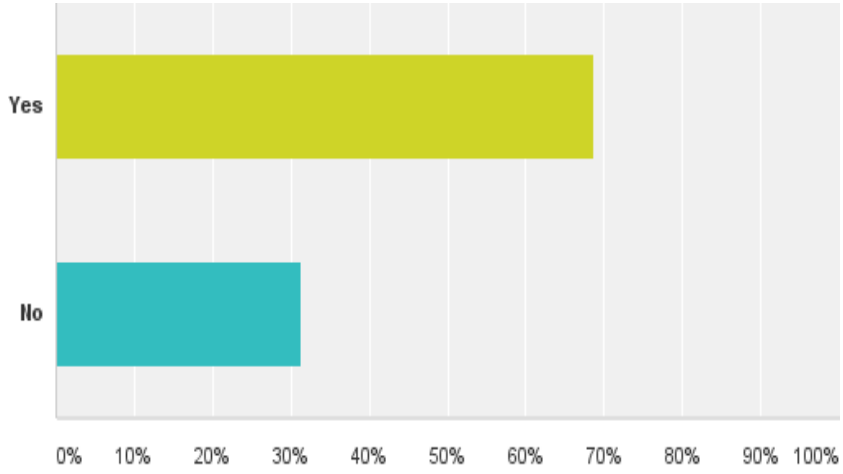

FIG. 82. Graphical representation of survey results to question 4.

(5) Is local data acquisition and monitoring of local loads at the fatigue relevant components implemented in order to get detailed information on the real component loadings during plant operation? (Responses shown in Fig. 83.)
(a) By permanent thermocouples;
(b) By temporary strain gauge measurement;

(c) None used
(d) Other.

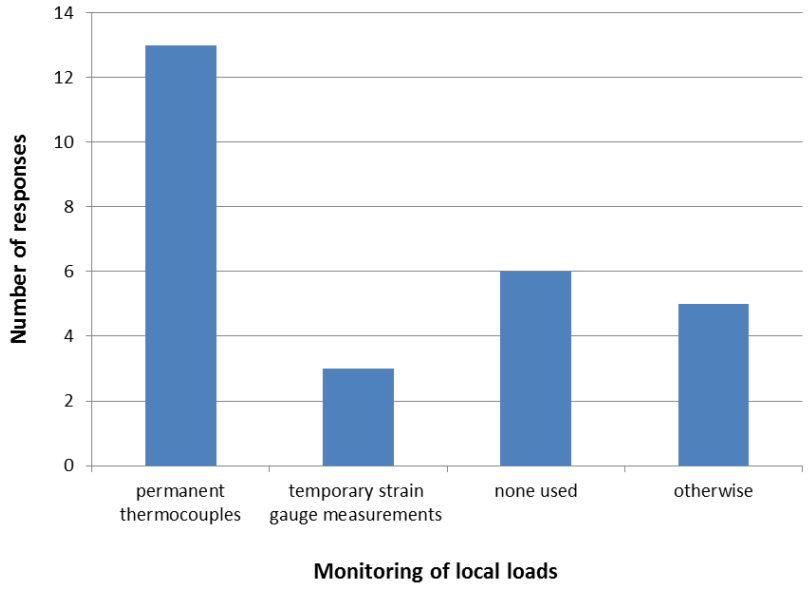

FIG. 83. Graphical representation of survey results to question 5.

(6) Evaluation period is dependent on the trend of fatigue damage on the basis of recorded measurement data. What is the periodicity of fatigue evaluation at your facility? (Responses shown in Fig. 84).
(a) Continuously on-line;
(b) Monthly;
(c) Yearly;
(d) Other.

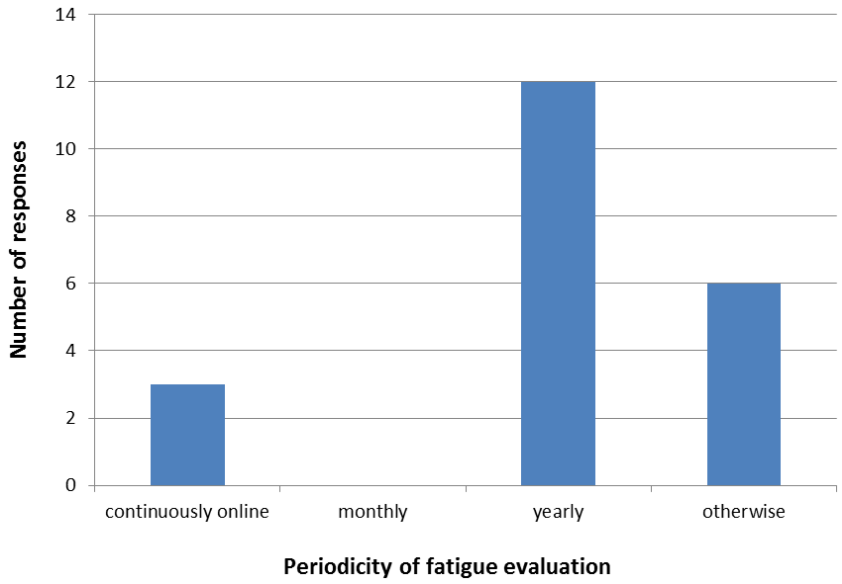

FIG. 84. Graphical representation of survey results to question 6.

(7) Do the methodology and requirements of PSR take into account the progress or improvement of stress calculation and fatigue evaluation methods according to the current state of knowledge? (Responses shown in Table 20).
(a) Yes;
(b) No.

TABLE 20. RESPONSE OF SURVEY RESULTS TO QUESTION 7.

Answer Choices	Responses
Yes	12/ 75.00%
No	4/ 25.00%
Total	16

(8) The NUREG report CR-6909 describes new environmental effects on the fatigue mechanism and gives rules for handling that influence in fatigue analysis. Is the influence of thermal conditions and chemical composition of the fluid inside the NPP components on allowable fatigue levels considered? (Responses shown in Table 21).
(a) Yes;
(b) No.

TABLE 21. RESPONSE OF SURVEY RESULTS TO QUESTION 8.

Answer Choices	Responses
Yes	12/ 75.00%
No	4/ 25.00%
Total	16

(9) Has an incident reporting system been implemented (any adverse event that occurs during operation contains a report describing the root causes and proposals for corrective action)? (Responses shown in Table 22).
(a) Yes;
(b) No.

TABLE 22. RESPONSE OF SURVEY RESULTS TO QUESTION 8.

Answer Choices	Responses
Yes	13/ 81.2%
No	3/18.7%

TABLE 22. RESPONSE OF SURVEY RESULTS TO QUESTION 8. (cont.)

Answer Choices	Responses
Total	16

(10) What is the dominant fatigue failure mechanism at your facilities? (Responses shown in Fig. 85.
- (a) Mechanical vibrations;
- (b) Flow induced vibrations;
- (c) Pressure pulsation;
- (d) Thermal fatigue;
- (e) None.

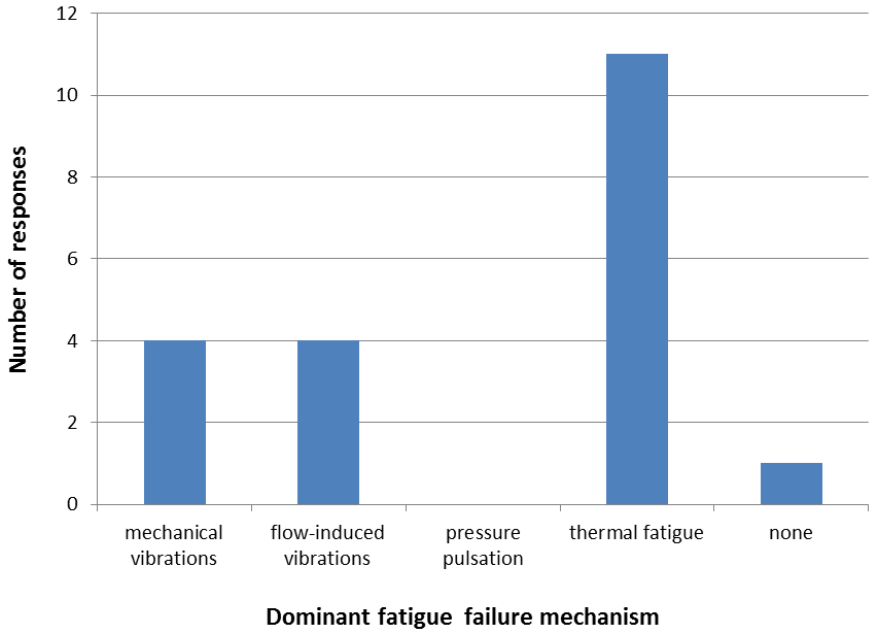

FIG. 85. Graphical representation of survey results to question 10.

(11) What are the components that have had occurrence of fatigue failure? (Responses shown in Fig. 86.)
- (a) Pipe;
- (b) Pumps;
- (c) Valves;
- (d) Heat exchangers/coolers;
- (e) Turbines;
- (f) Nozzles;
- (g) Other;
- (h) None identified.

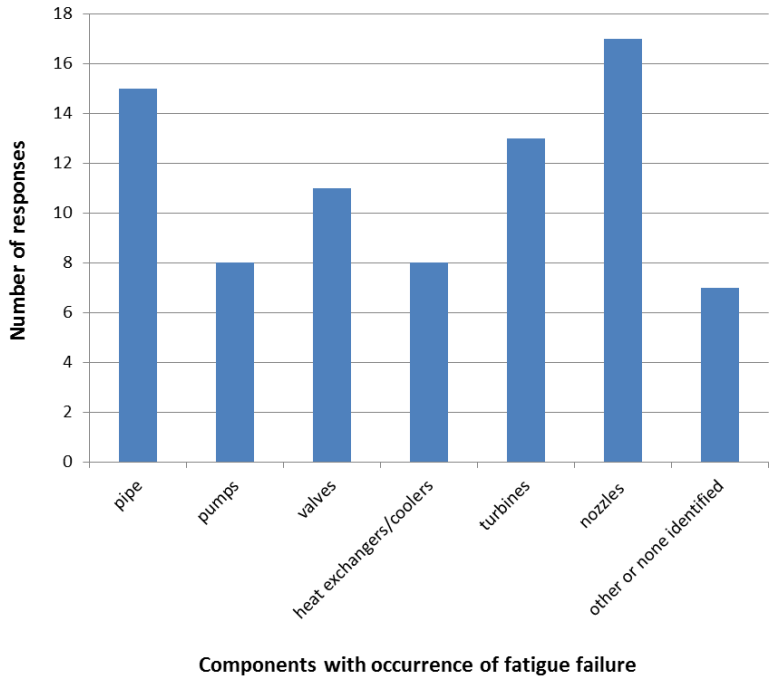

FIG. 86. Graphical representation of survey results to question 11.

The questionnaire responses are a compilation of contributions from members of an IAEA Technical Working Group on life management on their experience, general trends and issues. It contains the most frequent responses for the above questions which were typical for the specific region.

REFERENCES

[1] FORSYTH, P.J.E., Fatigue damage and crack growth in aluminium alloys, Acta Metall. 11 7 (1963) 703–715.

[2] CHU, S., Material Reliability Program: Fatigue Management Handbook, Rev. 1 Rep. MRP-235 with corrections, Electric Power Research Institute, Palo Alto, CA (2009).

[3] BASQUIN, O.H., The exponential law of endurance tests, Proc. ASTM 10 (1910) 625–630.

[4] COFFIN L.F., SCHENECTADY, N.Y., A study of the effects of cyclic thermal stresses on ductile materials, Trans. ASME 76, New York (1954).

[5] MANSON, S.S., Behaviour of Materials Under Conditions of Thermal Stress, NACA Tech. Note 2933, National Advisory Committee for Aeronautics, Hampton, VA (1955).

[6] LANGER, B.F., Design of pressure vessels for low-cycle fatigue, ASME J. Basic Eng. 84 (1962) 389–399.

[7] AMERICAN SOCIETY OF MECHANICAL ENGINEERS, “Sec III Div. 1, Subsection NB, NB-3228.5”, Boiler and Pressure Vessel Code, ASME, New York (2007).

[8] JAPAN SOCIETY OF MECHANICAL ENGINEERS, Codes for Nuclear Power Generation Facilities: Rules on Design and Construction for Nuclear Power Plants, S NC1-2008 (2007).

[9] ASSOCIATION FRANÇAISE POUR LES RÈGLES DE CONCEPTION, DE CONSTRUCTION ET DE SURVEILLANCE EN EXPLOITATION DES MATERIES DES CHAUDIERES ÉLECTRO-NUCLEAIRES, RCC-M Code, AFCEN, Courbevoie, France (2007) Paragraphs B 3234.3, B 3234.5 and B3234.6.

[10] KERNTECHNISCHER AUSSCHUSS, Komponenten des Primärkreises von Leichtwasserreaktoren Teil 2: Auslegung, Konstruktion und Berechnung , KTA, Salzgitter, Germany (2017), Rule 3201.2, Paragraph 7.8.4.

[11] ITOH, T., SAKANE, M., OHNAMI, M., SOCIE, D.F., Nonproportional low cycle fatigue criterion for Type 304 stainless steel, J. Eng. Mater. Technol. 117–3 (1995) 285–292.

[12] AMERICAN SOCIETY OF MECHANICAL ENGINEERS, “Subsection NB, NB-3222.4”, ASME Boiler and Pressure Vessel Code Sec III, Div. 1, ASME, New York (2007).

[13] AMERICAN SOCIETY OF MECHANICAL ENGINEERS, “Subsection NH-T-1413”, ASME Boiler and Pressure Vessel Code Sec III, Div. 1, ASME, New York (2007).

[14] AMERICAN SOCIETY OF MECHANICAL ENGINEERS, “Sec VIII, Div.3”, ASME Boiler and Pressure Vessel Code, ASME, New York (2007).

[15] ISHIBASHI, T., Prevention of Metallic Fatigue Failure and Fracture, Yokendo, Tokyo (1969).

[16] HEYWOOD, R.B., Design against Fatigue, Chapman and Hall, London (1962).

[17] MOSSONET, C., Relationship between fatigue limit and the diameter of the specimen, Proc. American Society for Testing and Materials (ASTM), Committee Report, Vol. 56, Proc. ASTM 56, New York (1956).

[18] NISHIJIMA, S., Statistical analysis of fatigue test data, J Soc. Mater. Sci, Japan 29 316 (1980) 24–29.

[19] LE DUFF, J.A., et al., “Effect of loading signal shape and surface finish on the LCF behavior of 304L stainless steel in PWR environment”, Proc. ASME 2010 Pressure Vessels and Piping Division/K-PVP Conf. Vol. 1, 2010, Bellevue, WA, ASME, New York (2010) 233–241.

[20] DE BAGLION, L., et al., “Influence of PWR primary water on LCF behavior of type 304L austenitic stainless steel at 300°C: Comparison with results obtained in vacuum or in air”, Proc. ASME 2012 Pressure Vessels and Piping Conf., Vol. 3, 2012, Toronto, ASME, New York (2012) 463–472.

[21] POULAIN, T., et al., Characterization of damage during low cycle fatigue of a 304L austenitic stainless steel as a function of environment (air, PWR environment) and surface finish (polished, ground), Proced. Engin. 160 (2016) 123–130.

[22] MANJOINE, M. J., “Fatigue damage models for annealed type 304 stainless steel under complex strain histories”, Structural Mechanics in Reactor Technology (SMiRT), Trans. 6th Int. Conf., Vol. L, 8/1, North Holland, Amsterdam (1981).

[23] SOLIN, J. P., “Fatigue of stabilized SS and 316NG alloy in PWR environment”, Proc. ASME Pressure Vessels and Piping/ICPVT-11 Conf. Vancouver, 2006, ASME, New York (2006).

[24] KOREA ELECTRIC ASSOCIATION, KEPIC MN, Nuclear Power Plant Components, 2005 Edition Including 2006, 2007, and 2008 Addenda, KEA, Seoul (2008).

[25] PARIS, P., ERDOGAN, F., A critical analysis of crack propagation laws, ASME Sep. J. Basic Eng. 85 4 (1963) 528–533.

[26] AMERICAN SOCIETY OF MECHANICAL ENGINEERS, Code Comparison Report for Class 1 Nuclear Power Plant Components, Rep. STP-NU-051-1, ASME, New York (2012).

[27] AMERICAN SOCIETY OF MECHANICAL ENGINEERS, “Section III, Division I, Rules for construction of nuclear facilities components”, Boiler and Pressure Vessel Code, 2007 Edition, ASME, New York (2007).
[28] ASSOCIATION FRANÇAISE POUR LES RÈGLES DE CONCEPTION, DE CONSTRUCTION ET DE SURVEILLANCE EN EXPLOITATION DES MATÉRIELS DES CHAUDIÈRES ÉLECTRO-NUCLÉAIRES, RCC-M Code, Design and Construction Rules for Mechanical Components of PWR Nuclear Islands, 2007 Edition, AFCEN, Courbevoie (2007).
[29] JAPAN SOCIETY OF MECHANICAL ENGINEERS, “Division 1, LWRs”, Rules on Design and Construction for NPPs, Rep. JSME S-NC-12008, JSME, Tokyo (2008).
[30] CANADIAN STANDARDS ASSOCIATION, General Requirements for Pressure-Retaining Systems and Components in CANDU Nuclear Power Plants/Material Standards for Reactor Components for CANDU Nuclear Power Plants, CSA Standard N285.0, CSA, Mississauga, Canada (2008).
[31] CANADIAN STANDARDS ASSOCIATION, Design Procedures for Seismic Qualification of Nuclear Power Plants, CSA Standard N289.3, CSA, Mississauga, Canada (2010).
[32] RUSSIAN FEDERATION NUCLEAR REGULATORY CODES, Norms for Strength Analysis of Equipment and Piping of Nuclear Installations, PNAGE G-7-002, Russiangost, Moscow (2007).
[33] INTERNATIONAL ATOMIC ENERGY AGENCY, Assessment and Management of Ageing of Major Nuclear Power Plant Components Important to Safety: PWR Pressure Vessels, IAEA-TECDOC-1120, IAEA, Vienna (1999).
[34] AMERICAN SOCIETY OF MECHANICAL ENGINEERS, Standards and Guides for Operation and Maintenance of Nuclear Power Plants, Rep. ASME OM-S/G-2007, ASME, New York (2007).
[35] NUCLEAR REGULATORY COMMISSION, Thermal Stresses in Piping Connected to Reactor Coolant System, Bulletin 88-08, NRC, Washington, DC (1988).
[36] JAPAN ELECTRIC ASSOCIATION, Technical Rule for Seismic Design of Nuclear Power Plants, Rep. JEAC 4601-2008, JEA. Tokyo (2008) (in Japanese).
[37] AMERICAN SOCIETY OF MECHANICAL ENGINEERS, Companion Guide to the ASME Boiler and Pressure Vessel Code, 3rd edn, ASME, New York (2007).
[38] NUCLEAR REGULATORY COMMISSION, Effect of LWR Coolant Environments on Fatigue Life of Reactor Materials (Final Report), Reps ANL-06/08, NUREG/CR-6909, NRC, Washington, DC (2007).
[39] ELECTRIC POWER RESEARCH INSTITUTE, Thermal Stratification, Cycling, and Striping (TASCS), Rep. 103581, EPRI, Palo Alto, CA (1994).
[40] ELECTRIC POWER RESEARCH INSTITUTE, Materials Reliability Program: Management of Thermal Fatigue in Normal Stagnant Non-Isolable Reactor Coolant System Branch Lines (MRP 146), Rep. 1011955, EPRI, Palo Alto, CA (2005).
[41] NUCLEAR REGULATORY COMMISSION, Guidelines for Evaluating Fatigue Analysis Incorporating the Life Reduction of Metal Components due to the Effects of the Light Water Reactor, Rep. R.G 1.207, NRC, Washington, DC (2007).
[42] NUCLEAR REGULATORY COMMISSION, Effect of LWR Coolant Environments on the Fatigue Life of Reactor Materials, NUREG/CR-6909, Rev. 1, NRC, Washington, DC (2005).
[43] STAIRMAND, J., et al., “Effect of Surface Condition on the Fatigue Life of Austenitic Stainless Steels in High Temperature Water Environments”, Proc. ASME Pressure Vessels and Piping Conf. Boston, 2015, ASME, New York (2015).
[44] COURTIN, S., et al., Modifications of the 2016 Edition of the RCC-M Code To Account for EAF, Proc. ASME Pressure Vessels and Piping Conf. Vancouver, 2016, ASME, New York (2016).
[45] ELECTRIC POWER RESEARCH INSTITUTE, Materials Reliability Program: Fatigue Management Handbook, Revision 1 (MRP-235 w/Corrections), EPRI, Palo Alto, CA (2009).
[46] LYDELL, B., Sigma-Phase Inc., “CODAP Project Operating Experience Insights Related to Fatigue Mechanisms”, Fatigue of Nuclear Reactor Components, Proc. 4th Int. Conf. Seville, 2015, OECD/NEA, Paris (2015).
[47] ELECTRIC POWER RESEARCH INSTITUTE, Materials Reliability Program: Fatigue Issues Assessment, Rep. MRP-138, EPRI, Palo Alto, CA (2005).
[48] FAIDY, C., “Thermal fatigue in mixing areas: Status and justification of French assessment method”, Fatigue of Reactor Components, Proc. 3rd Int. Conf., Seville, 2004, EPRI, Palo Alto, CA (2004).
[49] ELECTRIC POWER RESEARCH INSTITUTE, Thermal Stratification, Cycling and Striping (TASCS), Rep. TR-10358, EPRI, Palo Alto, CA (1994).
[50] SUZUKI, S., TANIMOTO, K., KONDOH, Y., “Prevention of piping high cycle thermal fatigue at design stage”, Ageing Issues in Nuclear Power Plants, Proc. Int. Symp. Dijon, 2005, French Nuclear Safety Authority, Paris (2005).
[51] INTERNATIONAL ATOMIC ENERGY AGENCY, Assessment and Management of Ageing of Major Nuclear

Power Plant Components Important to Safety: PWR Pressure Vessels: 2007 Update, IAEA-TECDOC-1556, IAEA, Vienna (2007).
[52] NUCLEAR REGULATORY COMMISSION, Pressurizer Surge Line Thermal Stratification, NRC Bulletin 88-11, NRC, Washington, DC (1988).
[53] ELECTRIC POWER RESEARCH INSTITUTE, Materials Reliability Program: Operating Experience Regarding Thermal Fatigue of Piping Connected to PWR Reactor Coolant Systems (MRP-85), EPRI, Palo Alto, CA (2003).
[54] FAIDY, C., et. al, "Thermal Fatigue in French RHR System, Fatigue of Reactor Components" PWSCC of Alloy 600 in PWRs, Proc. Int. Conf. St. Pete Beach, 2000, Electric Power Research Institute, Palo Alto, CA (2003).
[55] ELECTRIC POWER RESEARCH INSTITUTE, Materials Reliability Program: Operating Experience Regarding Thermal Fatigue of Piping Connected to PWR Reactor Coolant Systems, Rep. MRP-85, Rev. 1 to 1001006 (MRP-25), EPRI, Palo Alto, CA (2003).
[56] ELECTRIC POWER RESEARCH INSTITUTE, Materials Reliability Program: Management of Thermal Fatigue in Normally Stagnant Non-Isolable Reactor Coolant System Branch Lines (MRP-146 rev2), EPRI, Palo Alto, CA (2016).
[57] NUCLEAR REGULATORY COMMISSION, Application of NUREG/CR-5999 Interim Fatigue Curves to Selected Nuclear Power Plant Components, Rep. NUREG/CR-6260 (INEL-95/0045), NRC, Washington, DC (1995).
[58] NUCLEAR REGULATORY COMMISSION, Effects of LWR Coolant Environments on Fatigue Design Curves of Carbon and Low-Alloy Steels, Rep. NUREG/CR-6583 (ANL-97/18), NRC, Washington, DC (1998).
[59] NUCLEAR REGULATORY COMMISSION, Effects of LWR Coolant Environments on Fatigue Design Curves of Austenitic Stainless Steels, Rep. NUREG/CR-5704 (ANL-98/31), NRC, Washington, DC (1999).
[60] NUCLEAR REGULATORY COMMISSION, Effect of LWR Coolant Environments on the Fatigue Life of Reactor Materials, Rep. NUREG/CR-6909 Rev. 1 (ANL-12/60), NRC, Washington, DC (2014).
[61] UNITED STATES NUCLEAR REGULATORY COMMISSION, Fatigue Analysis of Components for 60-Year Plant Life, Rep. NUREG/CR-6674 (PNNL-13227), NRC, Washington, DC (2000).
[62] MARKL, A., GEORGE, H., "Fatigue tests on flanged assemblies", Pressure Vessel and Piping Design – Collected Papers 1927-1959, ASME, New York (1960) 91–101.
[63] HIGUCHI, M. et al., "Fatigue strength of socket welded pipe joint", Pressure Vessels & Piping Conf., Proc. 20th MPA Sem. Honolulu, 1995, ASME, Fairfield, NJ (1995).
[64] ELECTRIC POWER RESEARCH INSTITUTE, Vibration Fatigue Testing of Socket Welds, Rep. PWRMRP-07; TR-113890, EPRI, Palo Alto, CA (1999).
[65] INTERNATIONAL ATOMIC ENERGY AGENCY, Plant Life Management Models for Long Term Operation of Nuclear Power Plants, IAEA Nuclear Energy Series No. NP-T-3.18, IAEA, Vienna (2015).
[66] BERGHOLZ, S., HEINZ, B., RUDOLPH, J., Forward Alliance — AREVA's Initiative for NPP's LTO Projects, AREVA, Erlangen (2014).
[67] JOUAN, B., RUDOLPH, J., BERGHOLZ, S., "Fatigue monitoring approaches for power plants", Proc. Pressure Vessels and Piping Conf. Anaheim, CA, 2014, ASME, New York (2014).
[68] ELECTRIC POWER RESEARCH INSTITUTE, Materials Reliability Program: Fatigue Management Handbook, Revision 1 (MRP-235 w/Corrections), EPRI, Palo Alto, CA (2009).
[69] AMERICAN SOCIETY OF MECHANICAL ENGINEERS, "Section XI, Rules for Inservice Inspection of Nuclear Power Plant Components", ASME Boiler & Pressure Vessel Code, ASME, New York (2013).
[70] KERNTECHNISCHER AUSSCHUSS, Program of Standards, Standard No. 3201.4, Components of the Reactor Coolant Pressure Boundary of Light Water Reactors Part 4: In-service Inspections and Operational Monitoring, KTA, Salzgitter, Germany (2011).
[71] AMERICAN SOCIETY OF MECHANICAL ENGINEERS, "Section III Division 1 - Subsection NB: Class 1 components. Rules for construction of nuclear power plant components, ASME Boiler & Pressure Vessel Code, – ASME, New York (2013).
[72] HIGUCHI, M., IIDA, K., "An investigation of fatigue strength correction factor for oxygenated high temperature water environment", Pressure Vessel Technology, Proc. 6th Int. ICPVT Conf. Beijing, 1988, Pergamon Press, Oxford (1989).
[73] HIGUCHI, M., IIDA, K., Fatigue strength correction factors for carbon and low-alloy steels in oxygen-containing high-temperature water, Nuclear Eng. Design 129 (1991) 293–306.
[74] TAKAHASHI, Y., NAKAMURA, T., "Statistical analyses of in-air and in-water fatigue test data of austenitic stainless steels and ferritic Steels", Proc. Pressure Vessels and Piping Conf. Cleveland, 2003, ASME, New York (2003) 113-122.
[75] JAPAN SOCIETY OF MECHANICAL ENGINEERS, Code for Nuclear Power Generation Facilities, Environmental Fatigue EVALUATION Method for Nuclear Power Plants, Rep. JSME S NF1-2009, JSME, Tokyo (2009).

[76] CHOPRA, O.K., SHACK, W.J., Effects of LWR Coolant Environments on the Fatigue Life of Reactor Materials, Rep. NUREG/CR-6909, Final Report, Nuclear Regulatory Commission, Washington, DC (2007).
[77] KERNTECHNISCHER AUSSCHUSS, Components of the Reactor Coolant Pressure, KTA 3201, KTA, Salzgitter, Germany (2017).
[78] THERMAL AND NUCLEAR POWER ENGINEERING SOCIETY, Guidelines on Environmental Fatigue Evaluation for Nuclear Reactors, Thermal and Nuclear Power Engineering Society, Tokyo (2002) (in Japanese).
[79] HIGUCHI, M., SAKAGUCHI, K., NOMURA, Y. "Effects of strain holding and continuously changing strain rate on fatigue life prediction of structural materials in simulated LWR water", Proc. Pressure Vessels and Piping Conf. 2007, San Antonio, ASME, New York (2007).
[80] NAKAMURA, T., SAITO, I., ASADA, Y., "Guidelines on Environmental Fatigue Evaluation for LWR components", Proc. Pressure Vessels and Piping Conf. Cleveland, 2003, ASME, New York (2003).
[81] JAPAN NUCLEAR SAFETY ORGANIZATION, Environmental Fatigue Evaluation Method for Nuclear Power Generation Facilities, Rep. JNES-SS-0701, JNES, Tokyo, (2007) (in Japanese).
[82] HIGUCHI, M., SAKAGUCHI, K., NOMURA, Y., HIRANO, A., Final Proposal of Environmental Fatigue Life Correction Factor (Fen) for Structural Materials in LWR Water Environments, Proc. Pressure Vessels and Piping Conf. San Antonio, 2007, TX, ASME, New York (2007).
[83] HIGUCHI, M., NAKAMURA, T., SUGIE, Y., "Updated knowledge implemented to the revision of environmental fatigue evaluation method for nuclear power plants in JSME Code, Proc. Pressure Vessels and Piping Conf. Prague, 2009, ASME, New York (2009).
[84] IWASAKI, M., TAKADA, Y., NAKAMURA, T., "Evaluation of environmental fatigue in PWR PLM activities", Proc. Pressure Vessels and Piping Conf. Denver, 2005, ASME, New York (2005).
[85] NAKAMURA, T., MIYAMA, S., "Environmental fatigue evaluation in PLM activities of PWR plant", Japan Society of Mechanical Engineers, Tokyo (2010).
[86] NAKAMURA, T., IWASAKI, M., ASADA, S., "Optimization of environmental fatigue evaluation (Step 1)", Proc. Pressure Vessels and Piping Conf. San Antonio, 2007, ASME, New York (2007).
[87] NOMURA, Y., TSUTSUMI, K., INOUE, T., ASADA, S., NAKAMURA, T., "Optimization of environmental fatigue evaluation (Step 2)", Proc. Pressure Vessels and Piping Conf. Prague, 2009, ASME, New York (2009).
[88] JAPAN SOCIETY OF MECHANICAL ENGINEERS, Code for Nuclear Power Generation Facilities, Rules on Design and Construction for Nuclear Power Plants, Rep. JSME S NC1-2013, JSME, Tokyo (2014) (in Japanese).
[89] CHOPRA, O.K., SHACK, W.J., Effects of LWR Coolant Environments on Fatigue Design Curves of Carbon and Low-Alloy Steels, Rep. NUREG/CR-6583 (ANL-97/18), Nuclear Regulatory Commission, Washington, DC (1998).
[90] CHOPRA, O.K., Effects of LWR Coolant Environments on Fatigue Design Curves of Austenitic Stainless Steels, Rep. NUREG/CR-5704 (ANL-98/31), Nuclear Regulatory Commission, Washington, DC (1999).
[91] NUCLEAR REGULATORY COMMISSION, Guidelines for Evaluating Fatigue Analyses Incorporating the Life Reduction of Metal Components due to the Effects of the Light-Water Reactor Environment for New Reactors, NRC Reg. Guide 1.207, NRC, Washington, DC (2007).
[92] NUCLEAR REGULATORY COMMISSION, Standard Review Plan for Review of License Renewal Applications for Nuclear Power Plants, Final Report, Rep. NUREG-1800, Rev.2, NRC, Washington, DC (2010).
[93] AMERICAN SOCIETY OF MECHANICAL ENGINEERS, Fatigue Evaluation including Environmental Effects, Code Case N-792, ASME, New York, (2010).
[94] AMERICAN SOCIETY OF MECHANICAL ENGINEERS, Fatigue Design Curves for Light Water Reactor Environments, Code Case N-761, ASME, New York (2010).
[95] AMERICAN SOCIETY OF MECHANICAL ENGINEERS, "Section III, Division 1, Class 1 components, rules for construction of nuclear facility components", ASME Boiler and Pressure Vessel Code, Code year 2011, ASME, New York (2011).
[96] O'DONNELL, W.J., Code Design and Evaluation for Cyclic Loading — Sections III and VIII, Companion Guide to the ASME Boiler and Pressure Vessel Code, Volume 2, 3rd edn, ASME, New York (2009) Ch. 39.
[97] WATSON, C.T., The Background to Light Water Reactor Environment Fatigue Evaluation Methods for Austenitic Stainless Steel and Their Application To Sample Pressurised Water Reactor Components, Pressure Vessel and Piping, Proc Conf. Pressure Vessels and Piping, Baltimore, MD, 2011, ASME, New York (2011).
[98] AMERICAN SOCIETY OF MECHANICAL ENGINEERS, "Section III, Division 1, Class 1 components, rules for construction of nuclear facility components", ASME Boiler and Pressure Vessel Code, Code year 2007, ASME, New York (2007).
[99] DEWEES, D.J., ASME Section III Flaw Tolerance Sample Problem for Fatigue Design of Nuclear System Components, Proc. Pressure Vessels and Piping Conf. Anaheim, 2014, ASME, New York (2014).

[100] MÉTAIS, T., “French methodology proposal for environmentally assisted fatigue assessment”, Proc. Pressure Vessels and Piping Conf. Paris, 2013, ASME, New York (2013).
[101] COURTIN, S., LEFRANÇOIS, A., LE DUFF J.-A., LE PÉCHEUR, A., “Environmentally assisted fatigue assessment considering an alternative method to the ASME code case N-792”, Proc. Pressure Vessels and Piping Conf. Toronto, 2012, ASME, New York (2012).
[102] ASSOCIATION FRANÇAISE POUR LES RÈGLES DE CONCEPTION, DE CONSTRUCTION ET DE SURVEILLANCE EN EXPLOITATION DES MATÉRIELS DES CHAUDIÈRES ÉLECTRO-NUCLÉAIRES, RCC-M, Design and Construction Rules for Mechanical Components of PWR Nuclear Islands, AFCEN, Courbevoie, France (2012).
[103] SCHULER, X., HERTER, K.-H., RUDOLPH, J., “Derivation of design fatigue curves for austenitic stainless steel grades 1.4541 and 1.4550 within the German Nuclear Safety Standard KTA 3201.2”, Proc. Pressure Vessels and Piping Conf. Paris, 2013, ASME, New York (2013).
[104] WILHELM, P., STEINMANN, P., RUDOLPH, J., “Discussion of fatigue data for austenitic stainless steels”, Proc. Pressure Vessels and Piping Conf. Anaheim, ASME, New York (2014).
[105] WILHELM, P., STEINMANN, P., RUDOLPH, J., Fatigue strain-life behavior of austenitic stainless steels in pressurized water reactor environment, Proc. Pressure Vessels and Piping Conf. Boston, 2015, ASME, New York (2015).
[106] REESE, S.H., RUDOLPH, J., “Environmental assisted fatigue (EAF) rules and screening options in the context of fatigue design rules within German nuclear safety standards”, Proc. Pressure Vessels and Piping Conf. Boston, 2015, ASME, New York (2015).
[107] SOLIN, J., REESE, S., KARABAKI, H.E., MAYINGER, W., “Fatigue of stainless steel in simulated operational conditions: Effects of PWR water, temperature and holds”, Proc. Pressure Vessels and Piping Conf., Anaheim, 2014, ASME, New York (2014).
[108] AMERICAN SOCIETY OF MECHANICAL ENGINEERS, “Section XI”, ASME Boiler and Pressure Vessel Code, Rules for Inservice Inspection of Nuclear Power Plant Components, Code Year 2011, ASME, New York (2011).
[109] JAPAN SOCIETY OF MECHANICAL ENGINEERS, Code for Nuclear Power Generation Facilities, Rules on Fitness-for-Service for Nuclear Power Plants, Rep. JSME S NA1-2011, JSME, Tokyo (2011).
[110] ASSOCIATION FRANÇAISE POUR LES RÈGLES DE CONCEPTION, DE CONSTRUCTION ET DE SURVEILLANCE EN EXPLOITATION DES MATÉRIELS DES CHAUDIÈRES ÉLECTRO-NUCLÉAIRES, RSE-M Code. Rules for In-service Inspection of Nuclear Power Plant Components; 1997 Edition+1998, 2000 and 2005 Addenda, AFCEN, Courbevoie, France (1997).
[111] BAMFORD, W.H., Technical basis for revised reference crack growth rate curves for pressure boundary steels in LWR environment, J. Pressure Vessel Technol. 102 (1980).
[112] VAN DER SLUYS, W.A., EMANUELSON, R.H., Cyclic crack growth behavior of reactor pressure vessel steels in light water reactor environments, J. Eng. Mater. Technol. 108 (1986).
[113] ERNEST, D., et al., Modeling of fatigue crack growth rate for ferritic steels in light water reactor environments, Nucl. Eng. Design 184 (1998).
[114] ERNEST, D., et al., Fatigue crack growth rate of medium and low sulfur ferritic steels in pressurized water reactor primary water environments, J. Pressure Vessel Technol. 125 (2003).
[115] SEIFERT, H.P., RITTER, S. Corrosion fatigue crack growth behaviour of low-alloy reactor pressure vessel steels under boiling water reactor conditions, Corrosion Sci. 50 (2008).
[116] NOMURA, Y., “Fatigue crack growth curve For austenitic stainless steels in PWR environment, Proc. Pressure Vessels and Piping Conf. San Diego, 2004, ASME, New York (2004).
[117] ITATANI, M., OGAWA, T., NARAZAKI, C., SAITO, T., “Re-evaluation of fatigue crack growth curve for austenitic stainless steels in BWR environment, Proc. Pressure Vessels and Piping Conf. 2012, Toronto, ASME, New York (2012).
[118] CIPOLA, R.C., BANFORD, W.H., “Technical basis for Code Case N-809 on reference fatigue crack growth curves for austenitic stainless steels in pressurized water reactor environments, Proc. Pressure Vessels and Piping Conf. Boston, 2015, ASME, New York (2015).
[119] BANFORD, W.H. CIPOLA, R.C., UDYAWAR, A., GRUNT, N.L., “Example analysis for environmental fatigue crack growth in austenitic stainless steel piping using Code Case N-809, Proc. Pressure Vessels and Piping Conf. Boston, 2015, ASME, New York (2015).
[120] AMERICAN SOCIETY OF MECHANICAL ENGINEERS, Code Case N-809, Fatigue Crack Growth Rate Curves for Austenitic Steels in PWR Water Environment, ASME, New York (2015).

[121] SEIFERT, H.-P., RITTER, S., Environmentally Assisted Cracking in Austenitic Light Water Reactor Structural Materials, Final Rep. KORA-I Project 2003, PSI Rep. 09-03, Paul Scherrer Institute, Villigen, Switzerland (2009).
[122] BAMFORD, W., CIPOLLA, R., RUDLAND, D., BOO, G.D., "Technical basis for revisions to Section XI Appendix C for alloy 600/82/182/132 flaw evaluation in both PWR and BWR environments, Proc. Pressure Vessels and Piping Conf. Chicago, 2008, ASME, New York (2008).
[123] NOMURA, Y., KANASAKI, H., "Fatigue crack growth rate for nickel-based alloys in PWR environment, Proc. Pressure Vessels and Piping Conf. Chicago, 2008, ASME, New York (2008).
[124] NOMURA, Y., SAKAGUCHI, K., KANASAKI, H., "Fatigue crack growth rate curve for nickel-based alloys in PWR environment", Proc. Pressure Vessels and Piping Conf. San Antonio, 2007, ASME, New York (2007).
[125] SEIFERT, H.P., RITTER, S., LEBER, H.J., Corrosion fatigue crack growth behaviour of austenitic stainless steels under LWR conditions, Corrosion Sci. 55 (2012).
[126] KAMAYA, M., Environmental effect on fatigue strength of stainless steel in PWR primary water: Role of crack Growth Acceleration in Fatigue Life Reduction, Int. J. Fatigue 55 (2013).
[127] SORICH, A., SMAGA, M., EIFLER, D., Fatigue monitoring of austenitic steels with electromagnetic acoustic transducers (EMATs), Mater. Perform. & Charact. 4 (2015).
[128] ALTPETER, I., Early Detection Of Damage In Thermo-Cyclically Loaded Austenitic Materials, Studies in Applied Electromagnetics and Mechanics Vol. 36, IOS Press, Amsterdam (2012).
[129] WARE, A.G., "A survey of fatigue monitoring in the nuclear industry", Proc. Pressure Vessels and Piping Conf. New Orleans, 1992, ASME, New York (1992).
[130] ELECTRIC POWER RESEARCH INSTITUTE, Materials Reliability Program: Fatigue Management Handbook, Revision 1 (MRP-235 w/Corrections), EPRI, Palo Alto, CA (2009).
[131] SHVARTS, S., GERBER, G.A., HOUSE, K.A., HIRSCHBERG, P., Development of methodology for evaluating and monitoring steam generator feedwater nozzle cracking in PWRs, Proc. Pressure Vessels and Piping Conf. Minneapolis, 1994, ASME, New York (1994).
[132] KERNTECHNISCHER AUSSCHUSS, Components of the Reactor Coolant Pressure Boundary of Light Water Reactors Part 4: In-service Inspections and Operational Monitoring Standard No. 3201.4 (2010-1011), KTA, Salzgitter, Germany (2011).
[133] GOSSELIN, S.R., SIEGEL, E.A., "A method for monitoring and evaluating thermal transient fatigue usage in a nuclear power plant, Proc. Pressure Vessels and Piping, Conf. San Diego, 1987, ASME, New York (1987).
[134] SANTANDER, J.H., GOSSELIN, S.R., Analysis and Program to Extend the Design Life of The Charging Nozzle in a First Generation Nuclear Power Plant, Proc. Pressure Vessels and Piping Conf. New Orleans, 1992, ASME, New York (1992).
[135] GILMAN, T., GRAY, M., RUDOLPH, J., HEINZ, B., Fatigue Monitoring and Assessment: Different Approaches Combined for Lifetime Extension Challenges, Proc. Pressure Vessels and Piping Conf. Boston, 2015, ASME, New York (2015).
[136] HEINZE, C., RUDOLPH, J., BERGHOLZ, S., JOUAN, B., REITHINGER, M., Advanced Cycle Based Fatigue – A Stress and Temperature Based Synthesis of Existing Basic Approaches, VGB Power Tech, Essen, Germany (2012).
[137] AMERICAN SOCIETY OF MECHANICAL ENGINEERS, "Class 1 Components, rules for construction of nuclear power plant components", Boiler & Pressure Vessel Code, ASME, New York (2013) Section III Division 1: Subsection NB.
[138] KERNTECHNISCHER AUSSCHUSS, Components of the Reactor Coolant Pressure Boundary of Light Water Reactors, Part 2: Design and Analysis, KTA Standard No. 3201.2, KTA, Salzgitter, Germany (2011).
[139] ELECTRIC POWER RESEARCH INSTITUTE, Stress-Based Fatigue Monitoring: Methodology for the Fatigue Monitoring of Class 1 Nuclear Components in a Reactor Water Environment, EPRI, Palo Alto, CA (2011).
[140] CLORMANN, U.H., SEEGER, T., Rainflow HCM, ein Zählverfahren für Betriebsfestigkeitsnachweise auf Werkstoffmechanischer Grundlage, Stahlbau 55 (1986).
[141] AMERICAN SOCIETY OF MECHANICAL ENGINEERS, ", Alternative Rules for Construction of Pressure Vessels", Boiler & Pressure Vessel Code, ASME, New York (2013) Section VIII, Division 2.
[142] RUDOLPH, J., BAYLAC, G., WILHELM, P., WINTLE, J., BUENNAGEL, E., "Recent amendments of EN13445-3, clause 18 and related annexes: Detailed assessment of fatigue life, Proc. Pressure Vessels and Piping Conf. Anaheim, 2014, ASME, New York (2014).
[143] ELECTRIC POWER RESEARCH INSTITUTE, Guidelines for Addressing Environmental Effects in Fatigue Usage Calculation, EPRI, Palo Alto, CA (2012).
[144] CRANFORD, E.L., GRAY, M.A., SAHGAL, S., Predicting Steam Generator Auxiliary Feedwater Nozzle Thermal

Stratification Transients and Fatigue Effects in Complex Systems, Proc. Pressure Vessels and Piping Conf. Denver, 2005, ASME, New York (2005) 17–21.
[145] CRANFORD, E.L., GRAY, M.A., Simulation of a PWR residual heat removal system for component fatigue monitoring, Trans. SMiRT 19 (2007).
[146] MEIKLE, T.L., JOHNSON, E.D., GRAY, M.A., GLUNT, N.L., BURR, J.D., Simulation and evaluation of thermal stratification in a sloped surge nozzle correlated with plant measurements, Proc. Pressure Vessels and Piping Conf. Baltimore, 2011, ASME, New York (2011).
[147] RUDOLPH, J., BERGHOLZ, S., HEINZ, B., JOUAN, B., AREVA Fatigue Concept — A Three Stage Approach to the Fatigue Assessment of Power Plant Components, InTech, Rijeka, Croatia (2012)
[148] GILMAN, T., WEITZE, B., RUDOLPH, J., WILLUWEIT, A., KALNINS, A., Using nonlinear kinematic hardening material models for elastic-plastic ratcheting analysis, Proc. Pressure Vessels and Piping Conf., Boston, 2015, ASME, New York (2015).
[149] GRAY, M.A., CRANFORD, E.L., Evaluation of Thermal Stratification in PWR Pressurizers, Proc. Pressure Vessels and Piping Conf., Boston, 2015, ASME, New York (1999).
[150] DWIVEDY, K.K., SHAH, N.J., GRAY, M.A., Life cycle management of PWR pressurizer, Trans. SMiRT 17 (2003).
[151] EVON, K., GILMAN, T., WALTER, M., Fatigue monitoring of BWR feedwater nozzles, Proc. Pressure Vessels and Piping Conf., Paris, 2013, ASME, New York (2013).
[152] NAUDIN, C., VIDARD, S., Evaluation of the Stratification Loads with the EDF Fatigue Assessment Device, Proc. Pressure Vessels and Piping Conf., Paris, 2013, ASME, New York (2013).
[153] BIMONT, G., CORDIER, G., A new approach for NSSS fatigue life assessment, Trans. SMiRT 10 (1989).
[154] AUFORT, P., et al., On-line fatigue meter: A large experiment in French nuclear plants, Nucl. Eng. Design 129 (1991).
[155] ARGAUD J.P, BOURIQUET B., COURTOIS M., LE ROUX J.C, Reconstruction by data assimilation of the inner temperature field from outer measurement in thick pipe, Proc. Pressure Vessels and Piping Conf., Vancouver, 2016, ASME, New York (2016).
[156] BOO, M.-H., LEE, K.-S., OH, C.-K., KIM, H.-S., "Fatigue monitoring system for NPP in KHNP", Proc. 4th Int. Conf. on Fatigue of Nuclear Reactor Components, Seville, Spain, 2015, OECD Nuclear Energy Agency, Paris (2015).
[157] SAKAI, K., HOJO, K., KATO, A., UMEHARA, R., On-line fatigue-monitoring system for nuclear power plant, Nucl. Eng. Design 153 (1994).
[158] VINCOUR, D., Application of DIALIFE system for residual life time assessment on nuclear power plants, Trans. SMiRT 17 (2003).
[159] BRITISH ENERGY GENERATION, Assessment of the Integrity of Structures Containing Defects, Revision 4, Central Electricity Generating Board, London (2004).
[160] RUBTSOV, V.S., KORABLEVA, S.A., "Fatigue monitoring of equipment and pipelines at Russian NPPs", Proc. 4th Int. Conf. on Fatigue of Nuclear Reactor Components, Seville, Spain, 2015, OECD Nuclear Energy Agency, Paris (2015).
[161] HANNINK, M.H.C., et al., Fatigue Management during LTO of Nuclear Power Plant Borssele, Proc. Pressure Vessels and Piping Conf. Vancouver, 2016, ASME, New York (2016).
[162] BERKOVICH, V.Y., BOGACHEV, A.V., DRANCHENKO, B.N., SEMISHKIN, V.P., "Ageing management with application of the system of automated monitoring of residual service life (SAKOR), Proc. 20th Int. Conf. on Structural Mechanics in Reactor Technology, Espoo, Finland, 2009, VTT, Espoo (2009).
[163] MOTTERSHEAD, K., et al., "INCEFA-PLUS (increasing safety in NPPs by covering gaps in environmental fatigue assessment), Proc. Int. Conf. on Fatigue of Nuclear Reactor Components, Seville, Spain, 2015, OECD Nuclear Energy Agency, Paris (2015).
[164] BERKOVICH, V.Ya., BOGACHEV, A.V., DRANCHENKO, B.N., SEMISHKIN, V.P., "Ageing management with application of the system of automated monitoring of residual service Life (SAKOR), Proc. 20th Int. Conf. on Structural Mechanics in Reactor Technology, Espoo, Finland, 2009, VTT, Espoo (2009).
[165] RUBTSOV, V.S., KORABLEVA, S.A., "Fatigue monitoring of equipment and pipelines at Russian NPPs, Proc. Int. Conf. on Fatigue of Nuclear Reactor Components, Seville, Spain, 2015, OECD Nuclear Energy Agency, Paris (2015).
[166] VLCEK, L., "The current status of new Czech corrosion fatigue evaluation proposal for WWER nuclear power plants", New Methods of Damage and Failure Analysis of Structural Parts, Elsevier, Amsterdam (2014).
[167] VLCEK, L., ERNESTOVA, M., ERTL, J., "Corrosion fatigue evaluation: Czech proposal for WWER-440 nuclear power plants", Proc. Int. Conf. on Fatigue of Nuclear Reactor Components, Seville, Spain, 2015, OECD Nuclear Energy Agency, Paris (2015).
[168] BALDA, M., ČERNÁ, O., Residual fatigue lives of steam turbine blades, Appl. Mech. Mater. 827 (2016) 121–124.
[169] SPÄTIG, P., SEIFERT, H.P., HECZKO, M., KRUML, T., "Mean stress effect on fatigue life and dislocation

microstructures of 316L austenitic steel at high temperature in air and Water Environment, Proc. Int. Conf. on Fatigue of Nuclear Reactor Components, Seville, Spain, 2015, OECD Nuclear Energy Agency, Paris (2015).
[170] ROTH, A., et al., “Environmental influences on the fatigue assessment of austenitic and ferritic steel components including welds”, Proc. Pressure Vessels and Piping Conf. Anaheim, 2014, ASME, New York (2014).
[171] HERTER, K.-H., KAMMERER, M., RUDOLPH, J., SCHULER, X., WILHELM, P., “Experimental investigations on environmentally assisted fatigue of ferritic and austenitic materials including dissimilar metal welds”, Proc. 41st MPA Sem., Stuttgart, Germany (2015).
[172] MAKOTO H., “Comparison of environmental fatigue evaluation methods in LWR water”, Proc. Pressure Vessels and Piping Conf. Chicago, 2008, ASME, New York (2008).

ABBREVIATIONS

AFC	AREVA fatigue concept
ALWR	advanced light water reactor
ASME	American Society of Mechanical Engineers
BPVC	boiler and pressure vessel code
BWR	boiling water reactor
CBE	cycle based fatigue evaluation
CBF	cycle based fatigue
CSA	Canadian Standards Association
CC	component cooling
CODAP	component operational experience, degradation and ageing programme
CRISM	Central Research Institute of Structural Materials
CT	compact tension
CUF	cumulative usage factor
DVI	direct vessel injection
EAF	environmentally assisted fatigue
EdF	Électricité de France
EPRI	Electric Power Research Institute
ERV	electrometric relief valve
FIV	flow induced vibration
FE	finite element
FEM	finite element method
HCF	high cycle fatigue
HT	high temperature
ICC	intelligent cycle counting
IRWST	in-containment refuelling water storage tank
JSME	Japan Society of Mechanical Engineers
KEA	Korea Electric Association
LEAF	load evaluation application for fatigue
LCF	low cycle fatigue
LWR	light water reactor
KEPCI	Korea Electric Power Industry Code
MDF	Material Ductile Fracture
MRP	materials reliability programme
NDE	non-destructive examination
NIKIET	Research and Design Institution for Energy Technology
NPP	nuclear power plant
NWC	normal water chemistry
PLiM	plant life management
PSR	periodic safety review
PWR	pressurized water reactor
RCS	reactor coolant system
RHR	residual heat removal
SBE	stress based fatigue evaluation
SBF	stress based fatigue
SCC	stress corrosion cracking
SSCs	system, structure and components
SSE	safety shutdown earthquake

UF	usage factor
VHCF	very high cycle fatigue
VMS	vibration monitoring system
WWER	water-water energetic reactor

CONTRIBUTORS TO DRAFTING AND REVIEW

Álvaro Fernández, M.	TECNATOM, Spain
Arganis Juarez, C.	Instituto Nacional de Investigaciones Nucleares, Mexico
Bakirov, M.	CMSLM Ltd., Russian Federation
Baladia, M.	CNAT, Spain
Bergholz, S.	AREVA, Germany
Boylan, P.	AREVA, Germany
Chapuliot, S.	AREVA, France
Chen, Y.	Research Institute of Nuclear Power Operation, China
Cicero González, R.	INESCO Ingenieros, Spain
De Baglion, L.	AREVA, France
De Bont, C.G.	NRG, Netherlands
Döring, R.	Swiss Federal Nuclear Safety Inspectorate, Switzerland
Eom, S.	Canadian Nuclear Safety Commission, Canada
Ertl, J.	ČEZ, Czech Republic
Fayard, J.L.	CEA, France
Fernandez Bugna, J.	Nucleoelectrica Argentina, Argentina
Franz, M.	AREVA, Germany
Fuchs, T.	AREVA, Germany
Garcia, T.	IDOM, Spain
Gauter, K.	AREVA, Germany
Gendebien, A.	BELV, Belgium
Gorrochategui, I.	IDOM, Spain
Gourdin, C.	CEA, France
Grebenyuk, Y.	State Nuclear Regulatory Inspectorate of Ukraine, Ukraine
Haddadi, M.	Atomic Energy Organization of Iran, Islamic Republic of Iran
Hannink, M.	NRG, Netherlands
Jiroušek, J.	State Office for Nuclear Safety, Czech Republic
Kang, S.Y.	KEPCO Engineering & Construction, Republic of Korea
Kruglov, V.	South Ukrainian Nuclear Power Plant, Ukraine

Le Roux, J.C.	EdF RandD, France
Lienau, W.	SVTI, Switzerland
Liendo, M.	Nucleoelectrica Argentina, Argentina
Lopos, I.	Nuclear Research Institute, Slovakia
Magnusson, R.	Ringhals, Sweden
Malekian, C.	Tractebel Engineering, Belgium
Mei, J.	Suzhou Nuclear Power Research Institute, China
Miesen, P.	AREVA, Germany
Nakane, M.	Hitachi-GE Nuclear Energy, Japan
Pistora, V.	ÚJV Řež, Czech Republic
Prompt, N.	EdF SEPTEN, France
Quist, P.	NV EPZ Nuclear Power Plant Borssele, Netherlands
Radu, V.	Institute for Nuclear Research, Romania
Raunio, V.	Radiation and Nuclear Safety Authority, Finland
Romanov, S.	State Scientific and Technical Centre for Nuclear and Radiation Safety, Ukraine
Romanova, A.	CMSLM, Russian Federation
Roth, A.	AREVA, Germany
Rudolph, J.	AREVA, Germany
Ruiz López, P.	Mexican Nuclear Regulatory Body, Mexico
Salnikova, T.	AREVA, Germany
Samarska, G.	Zaporizhzhya Nuclear Power Plant, Ukraine
Schuler, F.X.	University of Stuttgart, Germany
Shen, X.	Shanghai Nuclear Engineering Research and Design Institute, China
Shrivastav, V.	Bhabha Atomic Research Centre, India
Sun, H.	Nuclear and Radiation Safety Centre, China
Takahashi, Y.	Central Research Institute of Electric Power Industry, Japan
Thibault, A.	Autorité de Sûreté Nucléaire, France
Vincenc-Obona, J.	Slovenské Elektrárne, Slovakia
Vincour, D.	ČEZ, Czech Republic
Vlček, L.	Institute of Applied Mechanics Brno, Czech Republic
Wang, C.	Nuclear and Radiation Safety Centre, China

Wilhelm, P.	AREVA, Germany
Wright, K.	Rolls-Royce, United Kingdom
Živko, T.	Slovenian Nuclear Safety Administration, Slovenia

Consultants Meeting

Vienna, Austria: 20–23 May 2014, 6–8 July 2015,

14–15 December 2016, 26–28 April 2017

Technical Meeting

Erlangen, Germany: 6–8 July 2016

Structure of the IAEA Nuclear Energy Series*

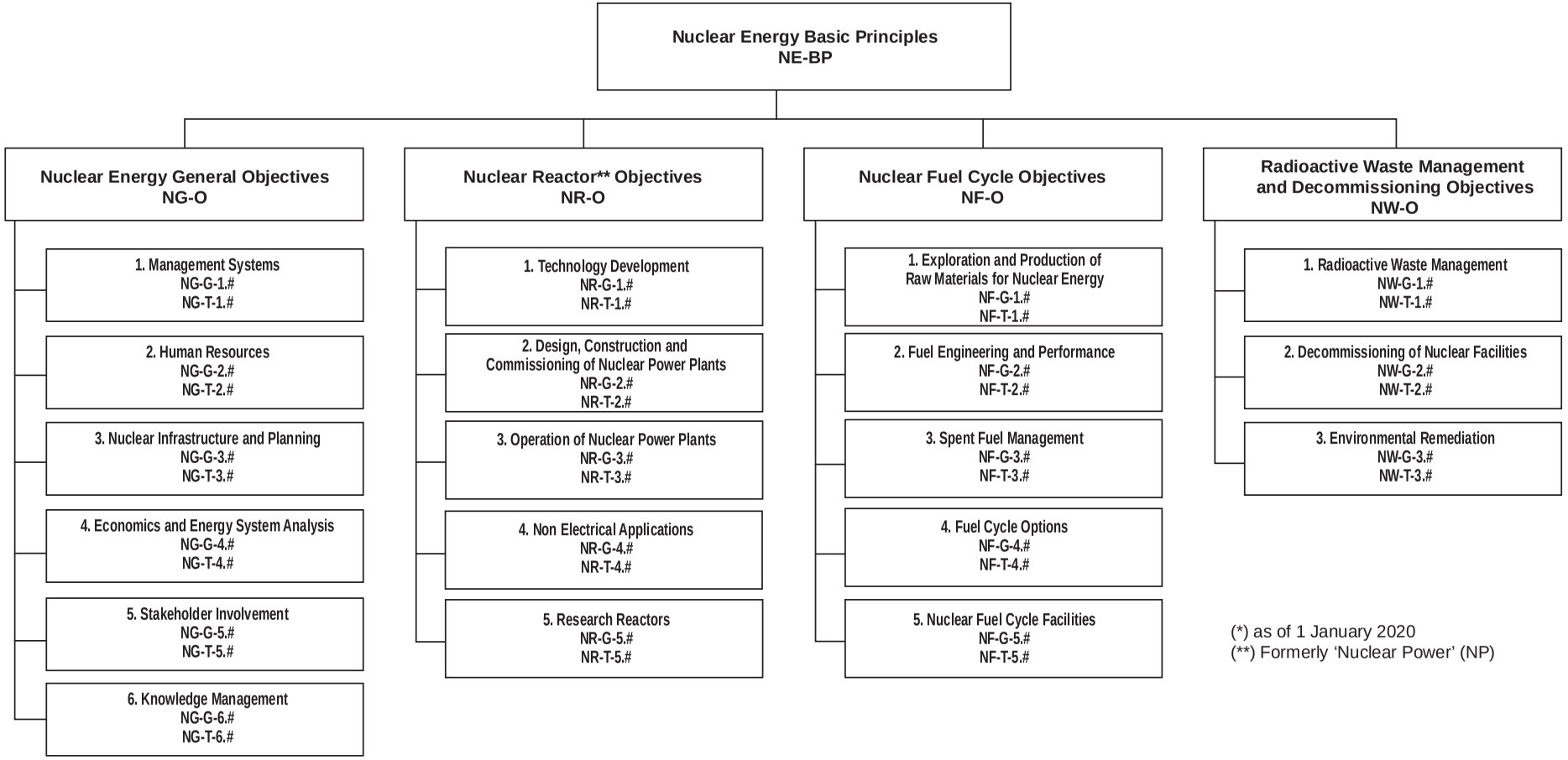

(*) as of 1 January 2020
(**) Formerly 'Nuclear Power' (NP)

Key

BP:	Basic Principles
O:	Objectives
G:	Guides and Methodologies
T:	Technical Reports
Nos 1–6:	Topic designations
#:	Guide or Report number

Examples

NG-G-3.1:	Nuclear Energy General (**NG**), Guides and Methodologies (**G**), Nuclear Infrastructure and Planning (topic **3**), **#1**
NR-T-5.4:	Nuclear Reactors (**NR**), Technical Report (**T**), Research Reactors (topic **5**), **#4**
NF-T-3.6:	Nuclear Fuel (**NF**), Technical Report (**T**), Spent Fuel Management (topic **3**), **#6**
NW-G-1.1:	Radioactive Waste Management and Decommissioning (**NW**), Guides and Methodologies (**G**), Radioactive Waste Management (topic **1**) **#1**

IAEA
International Atomic Energy Agency

No. 26

ORDERING LOCALLY

IAEA priced publications may be purchased from the sources listed below or from major local booksellers.

Orders for unpriced publications should be made directly to the IAEA. The contact details are given at the end of this list.

NORTH AMERICA

Bernan / Rowman & Littlefield

15250 NBN Way, Blue Ridge Summit, PA 17214, USA
Telephone: +1 800 462 6420 • Fax: +1 800 338 4550

Email: orders@rowman.com • Web site: www.rowman.com/bernan

REST OF WORLD

Please contact your preferred local supplier, or our lead distributor:

Eurospan Group

Gray's Inn House
127 Clerkenwell Road
London EC1R 5DB
United Kingdom

Trade orders and enquiries:

Telephone: +44 (0)176 760 4972 • Fax: +44 (0)176 760 1640
Email: eurospan@turpin-distribution.com

Individual orders:

www.eurospanbookstore.com/iaea

For further information:

Telephone: +44 (0)207 240 0856 • Fax: +44 (0)207 379 0609
Email: info@eurospangroup.com • Web site: www.eurospangroup.com

Orders for both priced and unpriced publications may be addressed directly to:

Marketing and Sales Unit
International Atomic Energy Agency
Vienna International Centre, PO Box 100, 1400 Vienna, Austria
Telephone: +43 1 2600 22529 or 22530 • Fax: +43 1 26007 22529
Email: sales.publications@iaea.org • Web site: www.iaea.org/publications

INTERNATIONAL ATOMIC ENERGY AGENCY
VIENNA